UNIVERSITÉ SAVOIE MONT BLANC

THÈSE

Pour obtenir le grade de

DOCTEUR DE L'UNIVERSITÉ SAVOIE MONT BLANC

Spécialité : **Physique Théorique**

Arrêté ministériel : 25 Mai 2016

Présentée par

Felipe FIGUEROA VILAR DEL VALLE

Thèse dirigée par **Luc FRAPPAT** et
codirigée par **Piotr TOURKINE**

préparée au sein du **Laboratoire d'Annecy-le-Vieux de Physique Theorique**
dans **l'École Doctorale de physique de Grenoble**

Dual Models revisited: A bootstrap perspective from QCD to String Theory

Thèse soutenue publiquement le **10 Décembre 2024**
devant le jury composé de :

Francesco RIVA
Associate Professor at the University of Geneva, Rapporteur
Balt C. VAN REES
Professor at École Polythecnique, Rapporteur
Björn HERRMANN
Professor at the Université Savoie Mont Blanc, Président
Yifei HE
Chargée de recherche à l'École Normale Supérieure, Examinatrice
Alexander ZHIBOEDOV
Permanent staff member at CERN, Examinateur


UNIVERSITÉ
SAVOIE
MONT BLANC

Abstract

Dual model amplitudes are weakly coupled (tree-level) amplitudes involving the exchange of infinitely-many higher spin states. They are the staple of tree-level string theory, with the Veneziano and Virasoro-Shapiro amplitudes being their most famous representatives, but they also appear in the large N limit of gauge theories as QCD, which becomes a weakly coupled theory of baryons and glueballs in the limit where the number of colors goes to infinity. While they were first discovered in the 60s in the context of the Hadronic S-matrix Bootstrap program and subsequently led to the discovery of String Theory and its proposal as a theory for Quantum Gravity, there is still a lot to learn about their basic properties and this is the central theme of this thesis. Unveiling their secrets would shed light on the structures of both String Theory and QCD via its large N limit.

The main body of the thesis is divided in two parts. In the first one I study this class of amplitudes from a bootstrap perspective, namely using the requirements of analyticity, crossing symmetry and unitarity to constrain, or in some cases even derive, dual model amplitudes. I start by an introduction to the S-matrix bootstrap and its application to tree-level amplitudes. Then, I apply this framework to study the Coon amplitude, a solution to the dual model amplitude bootstrap constraints known since the late 60s but whose main properties remained largely unknown. I describe our new results concerning their unitarity properties and critical dimension, and introduce a generalization of the method used to originally derive the Coon amplitude. I continue by an elementary introduction to Regge theory, and I use it as a tool to study dual model amplitudes. In particular, I use these techniques to show that dual model amplitudes require infinitely many Regge trajectories to be consistent. Finally, I end the first part by introducing a numerical bootstrap method based on Regge theory to obtain solutions to the bootstrap constraints on dual amplitudes. I make use of this method to obtain for the first time consistent dual model amplitudes with bending Regge trajectories, a feature expected from the ones corresponding to large N gauge theories.

The second part of this thesis is devoted to the study of three-point amplitudes between physical 1-particle states of arbitrary mass and spin in String Theory, a basic object missing in the literature that has various applications ranging from building higher point amplitudes of arbitrary external states to exploring high energy string scattering and its connection to black holes. A crucial part of the problem is imposing the physical state condition, and we do so by using the lightcone gauge formalism to restrict to the physical Hilbert space at the cost of manifest Lorentz invariance. After a short introduction on the lightcone quantization of String Theory, I present our novel method to build full SO(25) 1-particle states from lightcone gauge oscillators, and I show how to bootstrap full "trajectories" of physical states. Next, I explain the method to compute scattering amplitudes in this formalism and use it to compute three-point amplitudes between infinite classes of 1-particle states, and show how to covariantize the resulting lightcone gauge amplitudes. The thesis concludes with an overall discussion of the results presented as well as of future research directions.

Résumé

Les amplitudes du modèle dual sont des amplitudes faiblement couplées (au niveau de l'arbre) impliquant l'échange d'un nombre infini d'états de spin supérieur. Elles sont la base de la théorie des cordes au niveau de l'arbre, les amplitudes de Veneziano et de Virasoro-Shapiro étant leurs représentants les plus célèbres, mais elles apparaissent aussi dans la limite de grand N des théories de jauge comme la QCD, qui devient une théorie faiblement couplée de baryons et de glueballs lorsque le nombre de couleurs tend vers l'infini. Découvertes dans les années 60 dans le cadre du programme du Bootstrap de la matrice S hadronique, ces amplitudes ont conduit à la découverte de la Théorie des Cordes et à sa proposition comme théorie de la Gravité Quantique. Malgré ces avancées, leurs propriétés fondamentales restent à explorer, et cela constitue le thème central de cette thèse. Les dévoiler permettrait d'éclairer les structures de la Théorie des Cordes et de la QCD dans la limite de grand N.

Le corps principal de la thèse est divisé en deux parties. Dans la première, j'examine cette classe d'amplitudes en utilisant les conditions d'analyticité, de symétrie de croisement et d'unitarité pour contraindre ou dériver les amplitudes du modèle dual. Je commence par une introduction au bootstrap de la matrice S et à son application aux amplitudes au niveau de l'arbre. Ensuite, j'applique ce cadre à l'étude de l'amplitude de Coon, une solution aux contraintes du bootstrap connue depuis les années 60 mais dont les propriétés principales restaient inconnues. Je présente nos résultats sur leurs propriétés d'unitarité, leur dimension critique, et j'introduis une généralisation de la méthode utilisée pour dériver l'amplitude de Coon. Je poursuis par une introduction à la théorie de Regge, utilisée ici pour étudier les amplitudes du modèle dual. En particulier, je montre que ces amplitudes nécessitent une infinité de trajectoires de Regge pour être bien définies. Enfin, je termine par une méthode numérique de bootstrap basée sur la théorie de Regge pour obtenir des solutions aux contraintes de bootstrap sur les amplitudes duales, obtenant ainsi pour la première fois des amplitudes avec des trajectoires de Regge courbées, une caractéristique attendue des théories de jauge à grand N.

La deuxième partie de cette thèse est consacrée à l'étude des amplitudes à trois points entre des états physiques à une particule de masse et de spin arbitraires dans la théorie des cordes. Ces amplitudes, absentes de la littérature, ont diverses applications allant de la construction d'amplitudes à points plus élevés à l'exploration de la diffusion de cordes à haute énergie et de sa connexion avec les trous noirs. Une partie cruciale du problème consiste à imposer la condition d'état physique, ce que nous faisons en utilisant le formalisme de jauge du cône de lumière, en se restreignant à l'espace de Hilbert physique au prix d'une invariance de Lorentz manifeste. Après une introduction sur la quantification du cône de lumière, je présente notre méthode pour construire des états complets de 1 particule SO(25) à partir d'oscillateurs de jauge du cône de lumière, amorçant des « trajectoires » complètes d'états physiques. Ensuite, j'explique comment calculer les amplitudes de diffusion dans ce formalisme pour des classes infinies d'états à une particule et comment rendre covariantes les amplitudes résultantes. La thèse se termine par une discussion générale des résultats ainsi que des directions de recherche futures.

Contents

Abstract **3**

Résumé **5**

Foreword **11**

I Bootstrapping Dual Model Amplitudes **13**

The rise and fall (and rise again) of Dual Models **15**

1 S-matrix bootstrap for Dual Models **23**
1.1 Introducing the S-matrix . . . 23
1.2 The S-matrix fundamentals: Analitycity, Crossing Symmetry and Unitarity . 25
1.2.1 Analyticity . . . 26
1.2.2 Crossing Symmetry . . . 27
1.2.3 Unitarity . . . 28
1.3 Bootstrapping with the right tools . . . 30
1.3.1 Partial Wave Expansion . . . 30
1.3.2 Dispersion Relations . . . 32
1.4 Leveraging consistency: The bootstrap philosophy . . . 33
1.4.1 Primal approach . . . 34
1.4.2 Dual approach . . . 35
1.5 Bootstrap constraints for Dual Model Amplitudes . . . 37
1.5.1 Unitarity for Dual Models . . . 37
1.5.2 The structure of the residues . . . 38
1.5.3 Color ordering, dispersion relations and channel duality . . . 40

2 The Coon amplitude: A case study **45**
2.1 The Coon amplitude . . . 46
2.2 Characterization of the Coon amplitude . . . 49
2.2.1 Positivity of the amplitude . . . 49
2.2.2 Low energy expansion and EFT-hedron . . . 55
2.2.3 Impact parameter representation of the Coon amplitude . . . 59
2.3 Attempting to extend Coon's method . . . 61
2.3.1 Brief review of Coon's derivation of the Coon amplitude . . . 61
2.3.2 Generalization to double-pole products . . . 64
2.3.3 The differential equation in the double-pole product ansatz . . . 66
2.3.4 Inconsistent numerator function . . . 69
2.3.5 Why can Coon's method can fail? . . . 70
2.4 Outlook and current status of the Coon amplitude . . . 70

3 Regge Theory for Dual Models **73**
3.1 Froissart-Gribov projection of the partial wave coefficients . . . 74
3.2 Regge Theory basics . . . 77
3.3 Ruling out dual model amplitudes with finitely many trajectories . . . 80
3.3.1 Case without subtractions . . . 81
3.4 Discussion . . . 88

4 Numerical bootstrap scheme for Dual Model Amplitudes **91**
4.1 Mandelstam-Sommerfeld-Watson transform . . . 96
4.2 Lessons from the Veneziano amplitude . . . 100
4.2.1 Extraction of the Regge poles . . . 100
4.2.2 Super-unitarity . . . 102
4.2.3 Validity of the Mandelstam-Regge pole expansion . . . 103
4.3 The Bootstrap method . . . 106
4.3.1 The truncated Mandelstam-Regge ansatz . . . 106
4.3.2 Unitarity . . . 107
4.3.3 Crossing . . . 108
4.3.4 Setting up the optimization problem: Choosing observables to optimize 110
4.3.5 Comment on the numerics . . . 110
4.4 Results . . . 111
4.4.1 Linear trajectories . . . 111
4.4.2 Bending trajectories . . . 113
4.4.3 Asymptotic linearity . . . 116
4.5 Discussion . . . 117
4.5.1 Numerics, precision and convergence of the results . . . 117
4.5.2 Scope of the method . . . 117

II Three-point amplitudes in String Theory **121**

5 String three-point amplitudes from the light-cone **123**
5.1 String Theory in the light-cone gauge . . . 126
5.1.1 The classical string . . . 126
5.1.2 The quantum string . . . 130
5.1.3 Light-cone quantization . . . 133
5.2 Building one-particle states from light-cone oscillators . . . 136
5.2.1 Some warm-up examples . . . 137
5.2.2 General method . . . 143
5.2.3 Validity of the results in arbitrary frames . . . 146
5.3 Amplitudes in the light-cone gauge formalism . . . 147
5.3.1 The tachyon vertex operator . . . 148
5.3.2 Covariantizing the amplitudes: The case of the massive spin 2 state at level 4 to two tachyons . . . 151
5.3.3 Covariant tachyon-leading Regge trajectory amplitudes . . . 155
5.3.4 Excited vertex operators . . . 156
5.4 Discussion and future directions . . . 158

Conclusions **161**

A Finite Energy Sum Rules (FESRs) **165**

B Regge residues of the Veneziano amplitude **167**

C Details on the numerics of chapter 4 **169**

D Open string one-particle states **171**
D.1 Level 5 171
D.2 Level 6 172
D.3 Level 7 172
D.4 Level 8 173

Bibliography **175**

Foreword

The following thesis presents most of the research work I have conducted during the course of my PhD in the last three years, whose leitmotiv has been the analysis of a class of weakly interacting higher spin theories dubbed Dual Models through the eyes of the modern S-matrix bootstrap approach. Higher spin theories are fundamental for a full description of nature, as not only do higher spin particles exist as resonances and composite states in particle and nuclear physics, but it is expected that any reasonable quantum theory of gravity, whether it is String Theory or not, will involve higher spin states. Yet, interacting theories of particles of spin greater than 2 are complicated beasts, and making them compatible with the general principles that we expect from any consistent quamtum theory is a complicated task.

Dual models are a concrete realization of consistent higher spin theories born in the 60s, in the context of the seminal studies on hadronic interactions in an attempt to describe the ever increasing content of higher spin resonances found in hadronic scattering experiments at the time. They are weakly coupled theories and therefore they have a simple analytic structure, yet they probe non-perturbative phenomena such as confinement and reggeization, and provide a unique example of how the infinitely many higher spin degrees of freedom can conspire to make a theory consistent. While famously this approach was superseded by QCD as the dominant description of hadronic interactions, it was understood that dual models could provide a consistent way of introducing massless spin 2 interactions at the quantum level, giving birth to String Theory as a candidate theory for quantum gravity. Moreover, a dual string-like description of hadronic scattering is expected to exist, which should correspond to a dual model in the limit in which the number of colors is large.

Despite being almost 60 years old, Dual Models are far from over, and the aim of this thesis is to analyze them using the tools and philosophy of the S-matrix bootstrap, an approach to the study of quantum theories in which the focus is put on the consistency of the observables with the basic principles of unitarity, analyticity and crossing symmetry that any quantum theory should satisfy, rather than on a concrete microscopic description in terms of a Lagrangian. In fact, this approach was born hand in hand with dual models during the 60s, but in the recent it years has recieved a new wave of attention and has proved to be an extremely useful tool to probe quantum theories. The main novelty of the modern S-matrix bootstrap with respect to its original version is a philosophical shift in which the attention is put on understanding the space of possible theories consistent with the mentioned set of principles rather than on the expectation of finding *the* unique theory describing our universe. This approach has shown to be very powerful, and together with modern numerical techniques it has provided a plethora of new, non-perturbative information on quantum field theories.

In this thesis we use this framework to try to answer the question of what is the space of Dual Models, and what are the features that define it. We do so by the means of both analytical and numerical tools, and by analyzing the structure of Dual Models in general as well as focusing on concrete examples. The presentation of the thesis is organized in two

main parts: In the first one I present the bulk of my PhD research done in collaboration with my supervisor Piotr Tourkine and partly in collaboration with Christopher Eckner, in which we attack the question of building general consistent Dual Model amplitudes from various points of view. The second, shorter part presents preliminary results of an on-going project in collaboration with Bruno Bucciotti and Guilherme Pimentel on the dual model for excellence: bosonic String Theory.

The results presented on the first part of this thesis are largely based on the following works:

- [1] F. Figueroa and P. Tourkine, Unitarity and Low Energy Expansion of the Coon Amplitude, Phys. Rev. Lett. 129 (2022), arxiv: 2201.12331.
- [2] C. Eckner, F. Figueroa and P. Tourkine, The Regge bootstrap, from linear to non-linear trajectories, arxiv: 2401.08736.
- [3] C. Eckner, F. Figueroa and P. Tourkine, On the number of Regge trajectories for dual amplitudes, arxiv: 2405.21057.

The second part corresponds to work in progress, and the results presented are entirely up to now unpublished.

Part I.

Bootstrapping Dual Model Amplitudes

The rise and fall (and rise again) of Dual Models

We start this journey with a quick historical introduction of one the main players throughout most of this thesis: Dual Model amplitudes, and their intimate connection with the boostrap program since its inception. For this we will need to take a detour into the state of high energy physics during the 60s, before the advent of Quantum Chromodynamics as the Quantum Field Theory of strong interactions.

Back then, the community was both amazed and puzzled by the ever increasing number of unstable massive particles with high spin being discovered as resonances in scattering experiments between hadrons. This was very different from the situation arising in the case of the electromagnetic and weak forces, which had been quite recently found to be succesfully described using the framework of perturbative Quantum Field Theory (QFT) developed in the previous decade, and which consisted of only a few fundamental fields with spins not greater than 1. The large number of hadronic resonances suggested that it was unlikely that they could all be fundamental fields appearing in the Lagrangian of strong interactions[1]. Even if they were, the corresponding field theory would be untractable with the time's tools, as the couplings between hadrons were large and thus a pertubative approach was not possible. To make things worse, the modern Effective Field Theory point of view was not available yet, and the idea at the time was that only renormalizable Quantum Field Theories were good candidates to describe nature. The fact that higher spin interactions are power-counting non-renormalizable added one more element to the list of reasons that caused the high energy theorists of the time to not take the idea of a Quantum Field Theory for strong interactions as a viable option.

Instead, the chosen approach was to give up on the quest for a microscopic Lagrangian for strong interactions and to focus on observable quantities that could be measured in experiments and didn't required necessarily a field theory description. After all, what one can actually determine through scattering experiments is not the Lagrangian itself but cross-sections between the different particles, which can in turn be computed by squaring the scattering matrix (from now on S-matrix) element between the given external states. The hope was that the set of basic requirements imposed on the S-matrix by demanding that it is consistent with Quantum Mechanics and Special Relativity was so rigid that, complemented with experimental input, it could be used to obtain the hadronic S-matrix directly, bypassing the field theory construction. This approach was called the S-matrix bootstrap, and became the predominant strategy to deal with the strong interactions [4]. As we will explain, nowadays it is clear that these expectations were too optimistic and the old S-matrix bootstrap didn't succeed in its goal of providing the S-matrix for hadronic

[1] Even though the idea that hadrons could be treated as bound states of fundamental fields -the quarks- already existed in the 60s, these constitutents were seen mostly as mathematical entities to keep track of the flavor group representations, and were not taken seriously from a physical point of view until the deep inelastic scattering experiments that were performed at the end of the decade.

interactions. However, this was not the end of the bootstrap philosophy. In the following decades, this approach was further developed in the case of Conformal Field Theories in what is called the conformal bootstrap, allowing to access non-perturbative information about this class of theories. Moreover, a modern take on the old idea of bootstrapping the S-matrix has recently been revived and proved to be a very powerful tool to study quantum theories in general. This modern approach to the S-matrix bootstrap will be a main theme in this thesis, but before getting there let's continue looking at the early days of hadronic physics a bit longer.

The set of constraints imposed on the S-matrix by requiring that it stems from a consistent relativistic, quantum theory are the requirements of analitycity, crossing symmetry and unitarity. They are respectively related to the causality of the interactions, their invariance under charge, parity and time-reversal transformations and the probabilistic interpretation of Quantum Mechanics, and we will spend a good part of the next section discussing them in detail. Let us now, however, address some of the experimental features of the hadronic scattering amplitudes observed in the 1960s accelerators.

Consider an elastic scattering process involving incoming particles of momenta p_1 and p_2, and outgoing particles of momenta p_3 and p_4, such that momentum conservation is $p_1+p_2=p_3+p_4$. Throughout this thesis we will use the the mostly plus signature convention for the metric $\{-+\cdots+\}$, meaning that the mass of particle i is $m_i^2=-p_i^2$, and we define the Mandelstam variables as

$$s=-(p_1+p_2)^2, \quad t=-(p_1-p_3)^2, \quad u=-(p_1-p_4)^2, \tag{0.1}$$

which satisfy $s+t+u=\sum m_i^2$, and thus only two out of the three Mandelstam variables are independent.

In scattering experiments, unstable particles manifest themselves as bumps or *resonances* in the cross-section corresponding to poles in the scattering amplitude at complex values of s. Near the mass of the resonance, this behavior of the scattering amplitude $A(s,t)$ is well aproximated by the Breit-Wigner distribution [4, 5]

$$A(s,t)\sim\frac{m_r R(t)}{m_r^2-s-im_r\Gamma}, \quad s\sim m_r^2, \tag{0.2}$$

were Γ is the width of the resonance and is proportional to the inverse of its lifetime τ, m_r^2 is the mass of the unstable particle and $R(t)$ is the residue at the resonance pole, of which we will have more to say later.

In low energy experiments, namely with s of the order of a few GeV, it was observed that hadronic scattering amplitudes were well described by a sum of Breit-Wigner amplitudes corresponding to the exchange of unstable hadrons. These resonances had the right quantum numbers to be created in the s-channel, and their spin increased with the energy. Actually, they could be organized in families called *Regge trajectories* defined by the relationship between their spin and their mass squared $J=\alpha(M^2)$. Moreover, this relationship was experimentally found to be very well aproximated by a line:

$$J=\alpha(s)=\alpha_0+\alpha' s, \quad s=M^2. \tag{0.3}$$

An an example of this behavior is given by the ρ-meson trajectory in Figure 1.

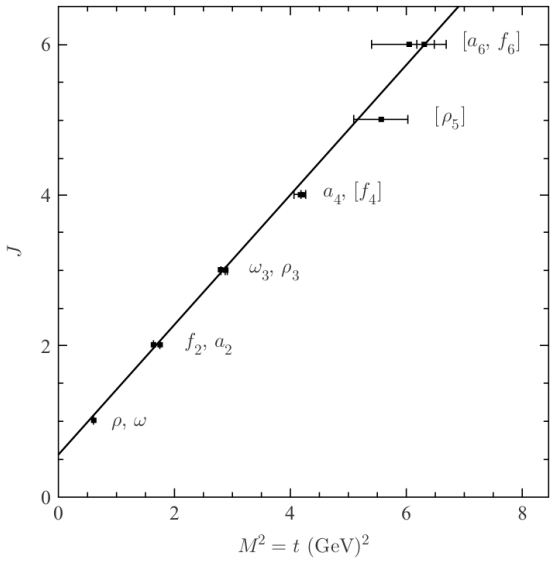


Figure 1.: Trajectory of the ρ-meson, fitted by the line $J = 0.55 + 0.86(\text{GeV})^{-2}t$. Image taken from [6].

On the high energy side, most of the available experimental results probed the Regge limit of the scattering process, in which $s \gg t$, $t \leq 0$, corresponding to forward scattering. In this regime, it was found that the cross-section -and thus the scattering amplitude- decayed at large s in a way that was very well fitted by

$$A(s,t) \sim s^{\alpha(t)}, \tag{0.4}$$

where $\alpha(t)$ was the *same* Regge trajectory function as the one determined by the spectrum in Eq. (0.3). This decay of the amplitude at large energies and the connection between the low energy spectrum and its high energy behavior couldn't be explained from a field theory point of view, but was a precise prediction of Regge theory, which will be introduced in upcoming sections.

The ever increasing masses and spins in the hadronic spectrum and the soft behavior of the amplitudes at high energies had very important implications. These two features could only be compatible if there exists an infinite number of hadrons of arbitrarily high masses and spin exchanged in the process. To see why this is the case, consider the $2 \to 2$ scattering of scalar particles exchanging a spin J intermediate state of mass m^2 in the t-channel at tree level. The contribution from this process to the scattering amplitude is

$$A(s,t) \supset -g^2 \frac{P_J(\cos\theta)}{t - m^2}, \tag{0.5}$$

where g is the coupling between the scalar and the spin J particles, θ is the scattering angle and $P_J(\cos\theta)$ is the Legendre polynomial of degree J that signals the exchange of a spin J state. At large s and fixed t, $\cos\theta \sim s$, and thus the contribution from the exchange of a spin J particle in the t channel in the Regge limit grows as s^J.

As said before, the known hadronic spectrum consisted of many particles of increasingly large spin, and therefore the t-channel contribution from these states at large energies would

be of the form

$$A(s,t) \supset \sum_J -g_J^2 \frac{(-s)^J}{t-m_J^2}, \tag{0.6}$$

where now the couplings and masses depend on the specific state exchanged.

From this expression it is clear that if there existed a maximum spin $J_{\max}$ in the spectrum, then the asymptotic behavior of the amplitude would simply be $s^{J_{\max}}$, in clear contradiction with the observed behavior shown in Eq. (0.4). One might complain that the strong interaction is *strong* and therefore a tree-level approximation is not enough to correctly describe its dynamics, but even in this case quantum corrections are unlikely to tame such a wild high energy behavior. A way out, however, is to consider an infinite number of terms in the sum. In this case, it is possible to imagine that cancellations could occur in such a way as to give a high energy behavior for the amplitude that is softer than each of the individual terms.

Moreover, accepting an infinite number of higher spin states has another consequence: It allows for the amplitude to be expressed as a sum over infinitely many poles on a single channel, instead of simultaneously including s and t-channel singularities explicitly as one would do in a standard Quantum Field Theory computation. The reason for this is that crossing symmetry implies that the amplitude should be invariant under the exchange of s and t, and therefore a truncated sum of terms as the ones in Eq. (0.6) would require the addition of the corresponding s-channel poles to be consistent. However, for an infinite sum it is concievable that with the appropriate choice of masses and couplings the singularities in the other channel could be generated by the divergence of the series and not by explicit poles written in the sum, very much differently from the field theory case.

In fact, even though this was unnoticed at the time, we will see later that the equivalence between the s and t-channel expansions is not just a possibility but a necessary consequence of the analytic properties of the amplitude and its soft behavior at high energies. Back then, however, this property was introduced on the grounds of experimental evidence by Dolen, Horn and Schmid, and became known as the *channel duality hypothesis*, seen mostly as an empirical fact that could be used as an extra requirement to bootstrap hadronic amplitudes [7]. This is how attempting to build models satisfying channel duality on top of the axioms of analyticity, unitarity and crossing symmetry -that is, *Dual Models*- became a very active topic, building up on what could nowadays be thought of as the first wave of the S-matrix bootstrap program.

Less than a year after the article by Dolen, Horn and Schmid, Veneziano proposed an explicit solution that implemented channel-duality, had the right behavior in the Regge limit, and satisfied crossing symmetry[2] [8]. The famous expression for the Veneziano amplitude is

$$A(s,t) = \frac{\Gamma\left(-\alpha(s)\right)\Gamma\left(-\alpha(t)\right)}{\Gamma\left(-\alpha(s)-\alpha(t)\right)} = B(-\alpha(s),-\alpha(t)), \tag{0.7}$$

where $\Gamma(x)$ is the Euler gamma function, $\alpha(s) = \alpha_0 + \alpha' s$, and $B(x,y)$ is the Euler beta function $B(x,y) = \frac{\Gamma(x)\Gamma(y)}{\Gamma(x+y)}$.

[2] The amplitude proposed by Veneziano is only symmetric under the exchange of s and t, but not fully s,t,u symmetric. This can be understood by considering the amplitude as a color-ordered amplitude between scalar particles transforming in the adjoint representation of a gauge group. A fully symmetric amplitude is obtained trivially by summing the different contributions $A(s,t) + A(t,u) + A(s,u)$.

The function $B(x,y)$ has simple poles at $x,y=-n$, with n non-negative integer, and therefore the Veneziano amplitude has infinitely many equidistant poles at real values both in the s and t channels. The residue at the $\alpha(s)=n$ pole is

$$\lim_{\alpha(s)\to n}(\alpha(s)-n)A(s,t)=-\frac{(\alpha(t)+1)(\alpha(t)+2)\dots(\alpha(t)+n)}{n!}, \tag{0.8}$$

and naturally a converse equation holds for the t-channel poles. Moreover, the Euler beta $B(x,y)$ function has the property that it can be expanded as an infinite sum over poles in *either* variable, which implies that the Veneziano amplitude satisfies the desired channel duality property. More specifically, we have

$$A(s,t)=-\sum_{n=0}^{\infty}\frac{1}{n!}\frac{(\alpha(t)+1)\dots(\alpha(t)+n)}{\alpha(s)-n}=-\sum_{n=0}^{\infty}\frac{1}{n!}\frac{(\alpha(s)+1)\dots(\alpha(s)+n)}{\alpha(t)-n}. \tag{0.9}$$

Furthermore, to see that it has the right Regge behavior it suffices to use the Stirling approximation for $\Gamma(x)$ at large x,

$$\Gamma(x)\sim\sqrt{2\pi}x^{x-1/2}e^{-x},\quad x\to\infty. \tag{0.10}$$

Substituting this into Eq. (0.7) at fixed t we immediately obtiain

$$A(s,t)\sim-\Gamma(-\alpha(t))(-\alpha(s))^{\alpha(t)}, \tag{0.11}$$

which precisely matches the form (0.4).

The fact that the Veneziano amplitude satisfied all these requirements in such a simple way sparked a lot of enthusiasm. The first fruit of the S-matrix bootstrap program was out there, and physicist hurried to try to compare it with experiments or find modifications and extensions of the model. The only drawback at the theoretical level was that having only real poles, it corresponded to a *narrow width* or tree-level amplitude and therefore it could not satisfy unitarity completely but only its tree-level incarnation, as will be explained in the next section. This was not seen as too much of a problem, as quantum corrections were expected to generate widths on the masses of the resonances and restore unitarity.

The upcoming years witnessed the development of dual models, with a plethora of new discoveries taking place in a very short amount of time. The generalization of the Veneziano amplitude to higher multiplicities was quickly discovered [9, 10], and Lovelace, Shapiro and Virasoro proposed other examples of dual model amplitudes with different phenomenological features [11–14]. Soon after, it was understood that the model proposed by Veneziano described the quantum dynamics of a relativistic string, with the Veneziano amplitude corresponding to the $2\to2$ scattering between open string groundstates and the one discovered by Virasoro and Shapiro to the analog process for closed strings [15, 16]. It was found how to introduce fermions into dual models via supersymmetry [17], as well as the mysterious fact that the model could only be free of negative norm states in 26 spacetime dimensions in the case of the bosonic theory, or in 10 dimensions when including fermions [18]. Unitarity required also that the value of the Regge intercept α_0 was 1 for the open string and 2 for the closed string, implying from Eq. (0.3) the existence of massless spin 1 and spin 2 particles in the spectrum.

What was not found, however, was a way of using these dual models to correctly describe hadronic interactions. Apart from the fact that the predicted massless hadrons were not found in nature, in the late 60s and early 70s high energy scattering experiments probed the previously unexplored *fixed angle* regime, when $s \to \infty$, $t \to -\infty$, with $1 + 2\frac{s}{t} = \cos\theta$ fixed [19]. In this region, hadronic scattering amplitudes were found to decay as power laws, while the Veneziano amplitude decays exponentially as

$$A(s,t) \sim F(\theta)^{-\alpha' s}, \tag{0.12}$$

in stark disagreement with experiments. The ultimate reason for this was the failure of dual models to reproduce the parton behavior of strong interactions that was responsible of the fixed-angle power-law decay of hadronic amplitudes. Furthermore, it was seen that at these energies the strong interaction becomes weaker, opening the door to the perturbative Quantum Field Theory techniques that had not been accessible until then. These developments allowed for a new description of the strong interaction to be formulated in the early 70s, Quantum Chromodynamics (QCD), which succesfully accounted for these features [20–22]. This way the original question that motivated dual models found a different answer, in a sense putting an end to the first days of the S-matrix bootstrap program.

However, this was not the end of dual models. Not much after the advent of QCD as a field theory for the strong interactions, it was realized that dual models could have a different, unexpected purpose. Identifying the massless spin 2 particle present in the dual model spectrum as the graviton and the massless spin 1 as a Yang-Mills gauge boson, Scherk and Schwarz put forward the tantalizing idea that dual models could be used as a way of providing a unified theory of quantum gravity and particle physics, where the higher spin states characteristic of dual models played the role of unitarizing the non-renormalizalbe interactions that arise when one tries to directly quantize General Relativity as a field theory of a massless spin 2 field [23]. This was the beginning of String Theory as we know it today, with dual model amplitudes corresponding to the tree-level scattering between different excitations of the string. The study of scattering amplitudes in bosonic String Theory as a theory of quantum gravity will be the subject of the second part of this thesis.

An important point that should be appreciated is the fact that despite the failure of dual models and the old S-matrix bootstrap to obtain the hadronic S-matrix, there was nothing *wrong* with the underlying ideas of the program. Not only did dual models find a new home as the most promising theory for unifying gravity with quantum mechanics, but the stringy dynamics managed to reproduce at least at a quantitative level many of the characteristic features of hadronic interactions. The reason for this is that string-like excitations such as the chromoelectric flux tubes between quarks inside mesons and baryons do exist and are very relevant for the dynamics of the strong interaction at low energies. It is not a coincidence that String Theory was accidentally discovered when trying to understand hadronic phyisics: the cartoon picture of a meson being made up of two quarks joined by a string-like confining flux tube is not so far from reality. In fact, at the same time that QCD was rising as the dominant description for the strong interactions, it was proposed by t'Hooft that there should exist a dual description in terms of strings that would become weakly coupled in the limit in which the number of colors was sent to infinity, and thus describable in terms of dual model amplitudes [24]. This putative string theory description for hadrons is still unknown, but continues to be an active research topic that recieved renewed interest since the discovery of holography, as this opened the possibility of describing four-dimensional gauge theories from a dual higher-dimensional string theory [25–29].

To conclude this introduction let us jump back to the present. Nowadays we understand that even if the basic ideas of the early S-matrix bootstrap were correct, the goal of completely determining the hadronic S-matrix from consistency conditions only was too naive. The main difference between the attempts in the 60s and the modern S-matrix bootstrap approach is -apart from the ubiquity of powerful computers- a philosophical shift. Since the seminal papers that renewed the interest in the S-matrix bootstrap [30–33], and inspired by important developments in the conformal bootstrap [34–37], the expectation is no longer to find *the* one-and-only, consistent S-matrix of the world, but rather the idea that the constraints of analyticity, crossing symmetry and unitarity determine a space of allowed theories, and that by asking the right questions we can explore and chart this space, often finding relevant theories living at special points where they can be examined in detail. Probably the most famous example of this fact is the bootstrap associated to the three-dimensional Ising model in the context of Conformal Field Theories, which gave the current best determination of its critical exponents [38]. This way of looking at quantum theories has been very fruitful, and recent years have seen lots of applications of the S-matrix bootstrap ranging from bounding the Wilson coefficients of Effective Field Theories and the study of confinement and flux tubes in gauge theories to the implications of non-invertible symmetries on the space of allowed S-matrices, passing through bounding the interactions in higher dimensional supergravity theories, to provide a not at all exhaustive list. More details on modern applications will be given in the following section.

In the light of all these recent developments, and considering the fact that the S-matrix bootstrap and dual models have been joined since their inception, with the Veneziano amplitude arguably being the first object to ever be constructed from bootstrap principles only, it is somewhat surprising that by the time I started my PhD in 2021 there was little attention paid to dual model amplitudes as natural objects to be studied with the modern bootstrap approach, with some remarkable exceptions [39, 40]. Applying this philosophy to dual model amplitudes was the quest that occupied the majority of my research during my PhD, and the output of these investigations makes up the bulk, and the first part of this thesis. This work is my -and my collaborator's- attempt to shed some light on this old yet far from fully understood topic.

It is important to say, however, that since 2021 this situation has certainly changed, and apart from the results presented in this thesis an important number of works attempting to bootstap this class of amplitudes from different approaches came out. The main research directions have been to provide new ways of explicitly constructing dual model amplitudes satisfying all the bootstrap constraints and the study of their properties [41–58], trying to bootstrap the dual model corresponding to large N QCD by locating it in the space of low energy Wilson coefficients [59–64], bootstrapping tree-level string theory from an EFT point of view [65–68], or bounding the space of dual-model amplitudes with linear Regge trajectories [69, 70].

Part 1 of this thesis is organized as follows:

- Chapter 1 corresponds to an introduction to the S-matrix bootstrap and its modern uses, as well as its application to dual model amplitudes.
- In chapter 2 I introduce the Coon amplitude, a deformation of the Veneziano amplitude known since the 60s but whose main features remained unknown. I present the first characterization of its unitarity properties and EFT expansion, in what can be thought of as a case study in which the concepts introduced in chapter 1 are applied. I also

investigate an extension of the method originally used to derive the Coon amplitude. Part of the results presented in this chapter follow the work in [1].

- In Chapter 3 I give a review on Regge theory of complex angular momentum, and I explain how it can be used to study dual model amplitudes. As an example of the power of Regge theory, I prove a theorem stating that consistent dual model amplitudes require having infinitely many Regge trajectories. The proof of this theorem is based on the results in [3].
- In chapter 4 I present a new bootstrap approach based on Regge theory that allows to construct consistent dual model amplitudes with customizable Regge trajectories. This method is implemented numerically to construct for the first time dual model amplitudes with bent Regge trajectories, mimicking the fixed-angle behavior of QCD amplitudes. This chapter is based on [2].

Chapter 1.

S-matrix bootstrap for Dual Models

In this chapter we will review the basic tools of the S-matrix bootstrap, and then specialize them to the study of dual model amplitudes. Since most of this is standard material, we will only go through the most relevant concepts and refer the reader to the standard reference [71] or to the more recent paper [72] for more details on general S-matrix theory, while we will spend a bit more time on the aspects that are specific to dual model amplitudes. Throughout this chapter and the whole first part of this thesis we will restrict to four spacetime dimensions, and use the mostly plus convention for the Minkowski metric.

1.1. Introducing the S-matrix

It is hard to overstate the importance that scattering experiments have for our understanding of the world. The basic idea is very simple: to understand a desired object, we throw another object at it, and we infer the properties of the first one by how the second one bounces off the target. Humanity has been carrying out this type of experiments since immemorial times, with Nature's own photon detectors -the eyes-. In the last century, the resolution required to study physics at ever-decreasing distances demanded new sorts of scattering experiments. In 1909, Geiger, Marsden, and Rutherford carried out the first man-made scattering experiment by firing alpha particles at a thin gold foil, leading to the discovery of the atomic nucleus. Since then, countless scattering experiments have revealed the fundamental particles that make up the physical world. This journey of discovery reached a milestone in 2012 with the detection of the Higgs boson at the Large Hadron Collider, filling the last gap in the Standard Model of particle physics as a self-consistent theory for fundamental interactions (excluding gravity, of course).

The relevant object that one needs to compute in order to study scattering in a quantum theory is called the S-matrix, $\mathcal{S}$. Its construction is based on the notion that interactions decay fast enough at large distances as to consider the initial and final states to be essentially free, stable particles when far enough from the interaction. These *asymptotic states* form two different Fock spaces, one for the incoming and one for the outgoing states, and the S-matrix is the unitary operator that relates the set of incoming and outgoing states.

Each of these Fock spaces can be endowed with an orthonormal basis where the basis elements are labeled by the number of particles it contains and their individual momenta, as well as other possible quantum numbers that these particles might carry such as spin, charge, etc. Collectively calling these quantum numbers by lettes a, b, c..., this basis satisfies

$$ {}_{\text{in}}\langle a|b\rangle_{\text{in}} = \delta_{ab}, \quad \sum_c |c\rangle_{\text{in}}\langle c|_{\text{in}} = \mathbb{1}, \tag{1.1} $$

and the same for the ougoing states, while the orghogonality and completeness relations for momentum eigenstates are

$$\langle q|p\rangle = (2\pi)^3 2p_0\delta^{(3)}(q-p), \tag{1.2}$$

$$\mathbb{1} = \int_q d\text{LIPS}_q |q\rangle\langle q|, \tag{1.3}$$

$$d\text{LIPS}_q = \frac{d^4q}{(2\pi)^4}\delta(q^2-m^2)\theta(q_0), \tag{1.4}$$

where $p=(p_0,\vec{p})$ and $q=(q_0,\vec{q})$ are on-shell momentum vectors satisfying $p^2=-m^2$, and we defined the *Lorentz invariant phase space* (LIPS) integration measure.

As said before, the S-matrix is the operator that relates the states between these Fock spaces by mapping a state in the incoming Fock space into the outgoing. More concretely, if we consider a scattering experiment between particles prepared in a given initial state $|\alpha\rangle_{\text{in}}$ and we want to compute the probability of observing a given final state $|\beta\rangle_{\text{out}}$, we need the overlap ${}_{\text{out}}\langle\beta|\alpha\rangle_{\text{in}}$, related to the S-matrix by

$${}_{\text{out}}\langle\beta|\alpha\rangle_{\text{in}} = {}_{\text{in}}\langle\beta|\mathcal{S}|\alpha\rangle_{\text{in}} = \mathcal{S}_{\beta\alpha}, \tag{1.5}$$

where $\mathcal{S}_{\beta\alpha}$ is defined as the S-matrix element between the initial and final states. The probability of observing the state $|\beta\rangle_{\text{out}}$ as a final state of the scattering process given the initial state $|\alpha\rangle_{\text{in}}$ is obtained by taking the modulus squared of the S-matrix element $\mathcal{S}_{\beta\alpha}$. From now on, the subscripts in/out will be supressed and will be understood that we are always mapping states between the incoming and outgoing Fock spaces when computing S-matrix elements.

It is standard to separate the trivial or non-interacting part of the S-matrix by defining the interacting piece $\mathcal{T}$ by

$$\mathcal{S} = \mathbb{1} + i\mathcal{T}. \tag{1.6}$$

The $n\to m$ scattering amplitude $\mathcal{M}_{mn}$ is defined as the matrix element of the interacting part $\mathcal{T}$ taken between the n-particle initial state $|n\rangle$ and the outgoing m-particle state $|m\rangle$, factoring out a momentum-conserving delta function:

$$i\langle m|\mathcal{T}|n\rangle = i(2\pi)^4\delta^4\left(\sum_{i\in n}p_i - \sum_{j\in m}p_j\right)\mathcal{M}_{mn}. \tag{1.7}$$

Throughout this thesis we will consider only $2\to 2$ scattering amplitudes, and therefore we shall omit the subscript and simply refer to it as $\mathcal{M}(p_1,p_2,p_3,p_4)$. Moreover, except in the last part of this thesis we will deal exclusively with amplitudes where the external particles are scalars. In this case the scattering amplitude itself will also be a scalar, and the Lorentz invariance of the theory requires it to be a function of Lorentz invariant combinations of the external momenta, namely the Mandelstam variables defined in Eq. (0.1). Specializing the

previous equation to the $2 \to 2$ case, we have

$$i\langle p_3, p_4|\mathcal{T}|p_1, p_2\rangle = i(2\pi)^4\delta^4\left(p_1 + p_2 - p_3 - p_4\right)\mathcal{M}(s,t), \tag{1.8}$$

where we omitted the dependence on u because it can be expressed as $u = \sum_i m_i^2 - s - t$, as was explained in the previous section.

In the case of identical scalars we have $s + t + u = 4m^2$, and physical s-channel processes correspond to the range of values

$$s \geq 4m^2, \quad (4m^2 - s) \leq t \leq 0, \quad (4m^2 - s) \leq u \leq 0. \tag{1.9}$$

This can be determined most easily by writing the Mandelstam variables in the center of mass frame, where $p_1 = (E, \vec{p})$ and $p_2 = (E, -\vec{p})$ (see Fig. 1.1):

$$\begin{aligned} s &= 4E^2 = 4(m^2 + \vec{p}^2), \\ t &= -2\vec{p}^2(1 - \cos\theta), \\ u &= -2\vec{p}^2(1 + \cos\theta). \end{aligned} \tag{1.10}$$

Demanding that the scattering angle is a real number gives the above physical s-channel kinematical region. En passant, we can determine a useful expression for $\cos\theta$ in the s-channel in terms of the Mandelstam variables:

$$\cos\theta = 1 + \frac{2t}{s - 4m^2} = -1 - \frac{2u}{s - 4m^2}. \tag{1.11}$$

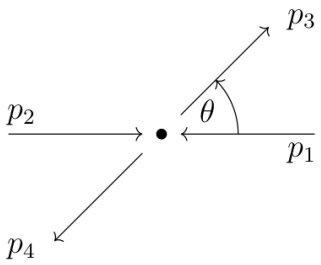


Figure 1.1.: Kinematics of a $2 \to 2$ scattering process in the center of mass frame.

1.2. The S-matrix fundamentals: Analitycity, Crossing Symmetry and Unitarity

As mentioned in the previous chapter, the S-matrix must satisfy the principles of analyticity, crossing symmetry and unitarity, which we will be introduced in what follows. These are the basic requirements that arise from the assumption that the S-matrix describes the dynamics of a relativistic, quantum theory, and lie at the core of all bootstrap applications.

1.2.1. Analyticity

In the previous section we defined the S-matrix and the $2 \to 2$ scattering amplitude $\mathcal{M}(s,t)$ for momenta that correspond to real physical processes in the s-channel. However, a crucial step forward in S-matrix theory was the realization that physical scattering amplitudes can be regarded boundary values of analytic functions of the Mandelstam invariants seen as complex variables, as this puts the wealth of tools coming from complex analysis at our disposal . For $2 \to 2$ scattering, this is

$$\mathcal{M}(s,t) = \lim_{\epsilon \to 0} \mathcal{M}(s + i\epsilon, t), \tag{1.12}$$

where s and t are real and belong to the physical s-channel kinematical region.

Elucidating in full generality the domain of $(s,t) \in \mathbb{C}^2$ in which a scattering amplitude between arbitrary external states is analytic is a formidable task of which we have still only partial understanding despite decades of work. As will be explained soon, unitarity implies the existence of branch-cut singularities along the real axes, and the existence of finite domains of analyticity for complex values of s,t can be determined as a consequence of causality: The starting point to prove the different theorems on the analyticity of the scattering amplitude is to use the LSZ prescription to express the scattering amplitude in terms of position-space correlation functions. Causality plays a crucial role in the requirement that commutators between local operators must vanish at space-like separated points, and this fact is the basic ingredient to prove the analyticity of the scattering amplitude in a given complex variable. While we will not derivate them in this thesis, we present for completeness a summary on the existing non-perturbative results on the analyticity of the scattering amplitude:

- For fixed $t \in [-t_0, 0]$, the amplitude $\mathcal{M}(s,t)$ is an analytic function of s with two branchcuts along the real axis at $s > 4m^2$ and $s < -t$ and possible poles corresponding to light bound states of mass lower than $4m^2$. In the case of scattering between identical scalars, $t_0 = 28m^2$ [73].
- For a fixed, real $s \geq 4m^2$, the amplitude $\mathcal{M}(s,t)$ as a function of the scattering angle $\cos\theta$ is analytic within an ellipse (known as the Lehmann ellipse) with foci at $\theta = \pm 1$ and whose semi-major axis depends on the details of the theory and scattering process [74].
- When both s and t are complex, the proven analyticity domain for elastic scattering between identical scalars is $|st| < 256m^2$, with both s and t away from the cuts in the real axis [75, 76].
- By incorporating unitarity, the domain of analyticity can be further expanded. For identical scalars, the enlarged region is $|t| < 4m^2$, $s \in \mathbb{C}$, away from the cuts in the real axis [77].

There exists also the notion of *maximal analyticity*, in which the amplitude $\mathcal{M}(s,t)$ is assumed to be analytic in the full domain $s,t \in \mathbb{C}^2$, except for the singularities predicted by unitarity on the real s, t, u axes. While maximal analyticity in the case of lightest particle scattering does not contradict any known results and is consistent with what is known from perturbation theory, this property has never been proven, and in the case in which the external states are not the lightest particle in the spectrum this assumption is known to fail due to the presence of anomalous thresholds. However, as we will see soon, in the case of dual model amplitudes the combination of unitarity and weak coupling restricts the possible

singularities of the amplitude to single poles along the real axis only, and thus the property of maximal analyticity is realized by the class of amplitudes that we will be concerned with.

1.2.2. Crossing Symmetry

The next property that we require from the S-matrix is crossing symmetry. Up to now, when considering physical processes we have restricted to the s-channel. Taking as a reference a scattering process as in figure (1.1), this considering particles 1 and 2 to be in the initial state and 3 and 4 in the final state, represented as $1\,2 \to 3\,4$. However, we can consider *crossed* processes in which a particle in the initial state is transformed into an antiparticle in the final state, or vice-versa. Restricting to $2 \to 2$ scattering, this allows us to consider the t and u-channel processes $1\,\bar{3} \to \bar{2}\,4$ and $1\,\bar{4} \to \bar{2}\,3$, where the bar means that we consider the corresponding antiparticle. The center of mass energy of these processes is $\sqrt{t}$ and $\sqrt{u}$, and their corresponding physical kinematical regions are

$$t \geq 4m^2, \quad (4m^2 - t) \leq s \leq 0, \tag{1.13}$$

for the t-channel and

$$u \geq 4m^2, \quad (4m^2 - u) \leq s \leq 0, \tag{1.14}$$

for the u-channel. The physical regions in all three Mandelstam variables intersected with the on-shell condition $s + t + u = 4m^2$ in $\mathbb{C}^3$ are nicely visualized in the diagram in figure (1.2). The three physical regions are shown in blue, while in red is the so called *Mandelstam triangle*, a region where the amplitude is free of branch-cut singularities, though poles due to bound states can exist.

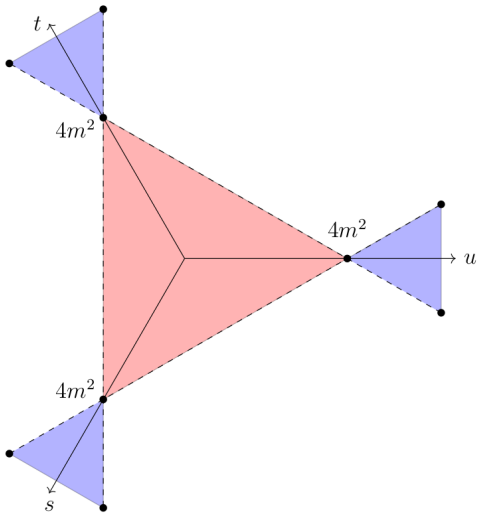


Figure 1.2.: In blue: physical channels of the $2 \to 2$ scattering amplitude. In red: Mandelstam triangle.

The different processes $1\,2 \to 3\,4$, $1\,\bar{3} \to \bar{2}\,4$ and $1\,\bar{4} \to \bar{2}\,3$ correspond to completely different interactions, and so *a priori* one would expect that each of them would be associated

to a different scattering amplitude. However, crossing symmetry is the statement that the physical scattering amplitudes for the three processes are boundary values of the *same* complex function $\mathcal{M}(s,t)$. Moreover, if we consider the scattering of identical particles, then the s, t and u-channel processes are the same. This implies that the scattering amplitude is symmetric under any permutation of the Mandelstam variables, namely

$$\mathcal{M}(s,t) = \mathcal{M}(t,s) = \mathcal{M}(s, 4m^2 - s - t). \tag{1.15}$$

1.2.3. Unitarity

The third basic property of the S-matrix that will form the basis of the bootstrap approach is unitarity. This requirement is simply the validity of the probabilistic interpretation of Quantum Mechanics, which implies the sum over the probabilities of all possible outcomes of a given process adds up to 1. For a given initial state $|i\rangle$, this is

$$1 = \sum_f |\langle f|\mathcal{S}|i\rangle|^2 = \sum_f \mathcal{S}^*_{if}\mathcal{S}_{fi} \implies \mathcal{S}^\dagger\mathcal{S} = \mathbb{1}, \tag{1.16}$$

where the sum over f scans the full Fock space of outgoing states.

If we look at the implications of unitarity for the interacting part of the S-matrix projected onto the $2 \to 2$ sector, we obtain

$$\frac{1}{i}\langle p_3 p_4|\mathcal{T} - \mathcal{T}^\dagger|p_1 p_2\rangle = \langle p_3 p_4|\mathcal{T}\mathcal{T}^\dagger|p_1 p_2\rangle. \tag{1.17}$$

Factoring out the momentum conserving delta function, the left hand side is the imaginary part of the scattering amplitude $\mathcal{M}(p_1 p_2 \to p_3 p_4) = \mathcal{M}(s,t)$. Inserting a complete set of states in the right hand side, we obtain

$$\begin{aligned} 2\mathrm{Im}\mathcal{M}(p_1 p_2 \to p_3 p_4) = \sum_{q_i}\prod_i \int \mathrm{LIPS}_{q_i} \mathcal{M}^*\left(p_3 p_4 \to \{q_i\}\right)\mathcal{M}\left(p_1 p_2 \to \{q_i\}\right) \\ \times (2\pi)^4 \delta^{(4)}(p_1 + p_2 - \sum_k q_{i,k}), \end{aligned} \tag{1.18}$$

where the sum $\sum_{\{q_i\}}$ runs over all possible on-shell states with arbitrary number of particles, as well as over all the extra quantum numbers (helicity, isospin, etc) that the intermediate state can have consistently with the external states.

On physical grounds we should expect that the expression in eq. (1.18) is valid when the momenta p_1, p_2, p_3 and p_4 are such that the amplitude is evaluated in the physical s-channel region $s \geq 4m^2$, as this is where it can be related to real, physical scattering. However, assuming that eq. (1.18) holds in the range $0 < s < 4m^2$ is usually refered to as *extended unitarity*.

A given term in the sum over on-shell states in the right hand side of eq. (1.18) will only contribute if s is large enough as to produce this state. In particular, in the absence of bound states and assuming that we are scattering the lightest state in the spectrum, there are no terms contributing to the sum when $s < 4m^2$, and thus the amplitude is real below this value.

This implies that $\mathcal{M}(s,t)$ satisfies the *real analyticity* condition

$$(\mathcal{M}(s,t_0))^* = \mathcal{M}(s^*,t_0), \quad t_0 \text{ fixed}, \tag{1.19}$$

and thus we can relate the imaginary part of the amplitude to its discontinuity along the real s axis by

$$\text{Im}\mathcal{M}(s,t) = \frac{1}{2i}\text{Disc}_s\mathcal{M}(s,t), \quad s \geq 4m^2. \tag{1.20}$$

Eq. (1.18) becomes then a statement about the singularity structure of the scattering amplitude, showing the existence of a discontinuity above the $s = 4m^2$, 2-particle threshold. Naturally, crossing symmetry implies the existence of discontinuities at $u \geq 4m^2$ and $t \geq 4m^2$ corresponding to the 2-particle threshold in the other channels. At higher energies more thresholds appear associated to the exchange of higher number of particles (e.g. the 3-particle threshold at $s,t,u = 9m^2$), giving rise to a complicated, multi-Riemann sheet structure for the amplitude in the complex plane.

Unitarity not only predicts the existence of discontinuities, but also puts severe restrictions on their behavior, requiring that the discontinuities of the amplitude have certain positivity properties. The simplest of them is the so-called *optical theorem*, in which we consider the forward limit of the $2 \to 2$ scattering amplitude, namely when the initial and final states are the same. Noting that the term $\mathcal{T}\mathcal{T}^\dagger$ on the right hand side of eq. (1.17) is a positive semi-definite matrix, and thus

$$\langle\alpha|\mathcal{T}\mathcal{T}^\dagger|\alpha\rangle = |\mathcal{T}^\dagger|\alpha\rangle|^2 \geq 0, \quad \forall\,|\alpha\rangle. \tag{1.21}$$

With $|\alpha\rangle = |p_1p_2\rangle$ this implies the positivity of the imaginary part of the scattering amplitude in the forward limit $\mathcal{M}(p_1p_2 \to p_1p_2) = \mathcal{M}(s,0)$

$$2\text{Im}\mathcal{M}(s,0) = \sum_{q_i}\prod_i \int \text{LIPS}_{q_i}(2\pi)^4\delta^{(4)}(p_1+p_2-\{q_i\})|\mathcal{M}\left(p_1p_2 \to \{q_i\}\right)|^2 \geq 0. \tag{1.22}$$

To fully exploit the constraints imposed by unitarity on the S-matrix its convenient to diagonalize it by going to the partial wave basis, i.e. the basis of eigenstates of energy angular momentum that we shall introduce shortly. However, let us before present another important feature of the S-matrix determined by unitarity: lower-point factorization.

For this, lets consider the following example. Extending unitarity to values of $s < 4m^2$ allows to use eq. (1.18) to analyze the consequences of the existence of stable bound states with mass M^2 below the 2-particle threshold[1]. Inserting the 1-particle state associated to this bound state on the right hand side of the unitarity equation and performing the phase space integration gives

$$2\text{Im}\mathcal{M}(p_1p_2 \to p_3p_4) = \pi\delta(s-M^2)\sum_\sigma \mathcal{M}_\sigma(p_1p_2 \to p)\mathcal{M}^*_\sigma(p_3p_4 \to p) + \ldots, \tag{1.23}$$

with $p = p_1 + p_2 = p_3 + p_4$, and the dots represent the multiparticle contributions. The sum over σ denotes the sum over all possible the possible quantum numbers of the bound state, such as polarizations in the case of a spinning particle.

[1] The same analysis could be carried out for stable particles with masses $M^2 > 4m^2$, but in this case we would in principle have contributions both from the 1-particle and multiparticle intermediate states.

The delta function $\delta(s-M^2)$ in eq. (1.23) implies that when s hits the mass of the bound state this term diverges and thus becomes the dominant contribution to the amplitude. Using the distributional identity $\frac{1}{x+i\epsilon} = PV(\frac{1}{x}) - i\pi\delta(x)$, where PV denotes the Cauchy principal value, we see that

$$\lim_{s\to M^2} \mathcal{M}(p_1p_2 \to p_3p_4) = -\sum_\sigma \mathcal{M}_\sigma(p_1p_2 \to p)\frac{1}{p^2-M^2}\mathcal{M}^*_\sigma(p_3p_4 \to p). \tag{1.24}$$

As is clear from this equation, when s takes the value of a mass in the spectrum the amplitude diverges as a simple pole, and the residue of the amplitude factorizes into the product of on-shell three-point amplitudes between the external states and the 1-particle state exchanged at the pole. This fact will be of great importance when we consider dual model amplitudes, as the weak coupling assumption will require that these simple poles are the only possible singularities.

1.3. Bootstrapping with the right tools

In the previous chapter it was described how the idea of bootstrapping the hadronic S-matrix came about during the 60s. As was explained, the hope back then was that the constraints of analyticity, crossing symmetry and unitarity would be so constraining that they would determine the unique S-matrix that described nature. Nowadays, we know that this was a bit too ambitious. There exist infinitely many S-matrices consistent with these principles, and the goal of the modern incarnation of the S-matrix bootstrap is to chart the space of allowed theories compatible with them. The expectation is that understanding the allowed space of physical theories could provide insights into the structure of QFT itself. Moreover, there are numerous examples in which physically relevant theories lie in special points located at the boundary of this region, and this fact can be used to probe the details of these specific theories. However, to achieve this goal we must harness the power of the bootstrap constraints. Two crucial tools that allow one to do this are the partial wave expansion and dispersion relations, that we introduce in this section.

1.3.1. Partial Wave Expansion

To fully exploit the constraints arising from unitarity, it is useful to diagonalize the S-matrix by going to a basis of states that furnish an irreducible representation of the Lorentz group[2]. These states are labeled by their energy and angular momentum in the center of mass frame, with these two quantum numbers being enough to characterize a state in the case of 2-particle states. This gives

$$\langle p_1p_2|p,J,m\rangle = \sqrt{\frac{E_{\vec{p}}}{|\vec{p}|E_{\vec{p_1}}E_{\vec{p_2}}}}\delta^4(p-p_1-p_2)Y^m_J(\hat{p}_1), \tag{1.25}$$

where $p^2=E^2$, m is the component of the angular momentum along the $\hat{z}$ direction, the Y^m_J are spherical harmonics and $\hat{p}_1$ denotes the angular direction defined by p_1 in the center of mass frame.

[2] Note that 2-particle states are not an irreducible representation

Since we are considering the scattering of scalar particles, the scattering process is symmetric with respect to rotations around the scattering axis and therefore the dependence on m drops. The S-matrix elements in this basis are referred to as the partial wave coefficients $f_J(p^2)$, given by

$$f_J(p^2) \propto \langle p, J, m|\mathcal{T}|p, J, m\rangle, \tag{1.26}$$

with a convention-dependent factor independent of p and m.

Inserting a complete set of states $|p, J, m\rangle$ into the definition of the $2 \to 2$ scattering amplitude we can express it as a sum over partial wave coefficients in the following way:

$$\mathcal{M}(s,t) = 16\pi \sum_J (2J+1) f_J(s) P_J(\cos\theta), \tag{1.27}$$

where the $P_J(\cos\theta)$ are Legendre polynomials and correspond to the *partial waves* representing the angular dependence of the amplitude arising from the exchange of all states with spin J.

To extract the partial wave coefficients $f_J(s)$ from the amplitude, we can use the fact that the Legenedre polynomials satisfy the following orthogonality relation:

$$\frac{1}{2}\int_{-1}^{1} dz P_J(z) P_{J'}(z) = \frac{\delta_{JJ'}}{2J+1}, \tag{1.28}$$

and therefore

$$f_J(s) = \frac{1}{32\pi}\int_{-1}^{1} dz\, P_J(z)\, \mathcal{M}(s, t(s,z)), \quad z = \cos\theta = 1 + \frac{2t}{s-4m^2}. \tag{1.29}$$

One of the greatest virtues of the partial wave expansion is that the unitarity constraint eq. (1.18) also diagonalizes, and instead of mixing amplitudes with different number of particles in the external states the unitarity equation becomes a separate condition for each partial wave coefficent. Inserting the necessary complete sets of states into the unitarity equation and performing some algebra steps, we arrive at the simple condition

$$2\mathrm{Im} f_J(s) \geq \sqrt{\frac{s-4m^2}{s}}\, |f_J(s)|^2, \tag{1.30}$$

for all non-negative integer J. This equation, completely equivalent to eq. (1.18), turns out to be much more useful to enforce unitarity on candidate S-matrices and is a central ingredient in most bootstrap approaches. Adding back the non-interacting part of the S-matrix to its partial wave expansion, eq. (1.30) can be recasted as

$$|S_J(s)| \leq 1, \quad \text{with } S_J(s) = 1 + i\sqrt{\frac{s-4m^2}{s}} f_J(s), \tag{1.31}$$

explicitly becoming the statement that the probability for the scattering process in each spin sector must be bounded by one.

Another important use of the partial wave expansion of the amplitude is the continuation of the scattering amplitude into complex values of the angular momentum. This is the topic of Regge Theory, which provides a valuable tool to study scattering, as will be explained later. Moreover, the partial wave expansion is the basic ingredient to prove the famous Froissart

bound [78], a non-perturbative upper bound on the asymptotic growth of the amplitude as a function of the energy in the case of a gapped spectrum:

$$|\mathcal{M}(s,t)| \leq \text{const} \times s \log^2 s, \quad s \to \infty, \, t\text{fixed}. \tag{1.32}$$

1.3.2. Dispersion Relations

Another fundamental technique for the S-matrix bootstrap are dispersion relations. They rely on the analyticity properties of scattering amplitudes introduced previously to express the full amplitude in terms of its discontinuities, relating the real and imaginary parts of the amplitude as well as its high and low energy regimes.

We consider still the $2 \to 2$ scattering of scalar particles of mass m^2 as a function of s for fixed $t < 0$. Assuming the existence of a stable bound state with mass $m_b^2 < 4m^2$, the analytic structure of the scattering amplitude in the complex s plane corresponding to the physical sheet is the one shown in figure (1.3): The function is analytic away from the real axis, while over the real axis there are a pair of simple poles at $s = m_b^2$ and $s = \bar{m}_b^2 = 4m^2 - m_b^2 - t$ corresponding to the exchange of the bound state in the s and u-channels, and branch cuts at $s \geq 4m^2$ and $s \leq -t$ corresponding to the s and u-channel multiparticle cuts.

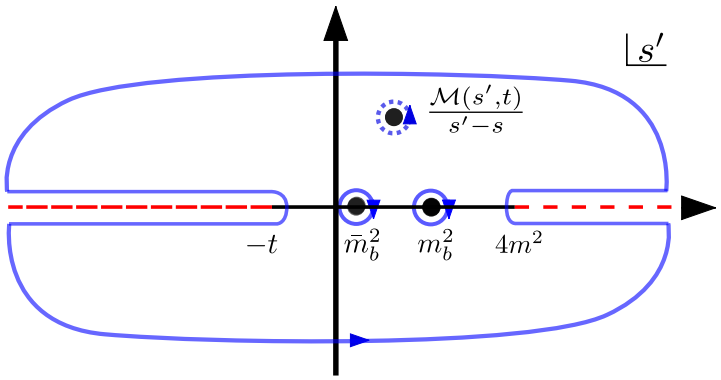


Figure 1.3.: Singularity structure of the scattering amplitude on the physical sheet and integration contours used to derived the unsubtracted despersion relation.

Dispersion relations can be derived simply by aplying Cauchy theorem in the s-plane. Consider the identity

$$\mathcal{M}(s,t) = \oint_{\mathcal{C}} \frac{ds'}{2\pi i} \frac{\mathcal{M}(s',t)}{s'-s}, \tag{1.33}$$

where s is any point in the s-plane where the amplitude is analytic and $\mathcal{C}$ is a small contour around it. These are represented in figure (1.3) by the dashed contour. The analyticity of the scattering amplitude as a function of s for fixed t allows us to blow up the contour, picking up contributions from the poles and discontinuities along the real axis, as well as from the arc at $|s| \to \infty$.

The simplest kind dispersion relation, referred to as an *unsubtracted* dispersion relation, can be derived in the case in which the amplitude decays when $|s| \to \infty$ in all directions in the complex plane, namely when $\lim_{|s|\to\infty} \frac{\mathcal{M}(s,t)}{s} = 0$. In this case we can drop the arc at

infinity, to have

$$\mathcal{M}(s,t) = \frac{R_s(t)}{s-m_b^2} + \frac{R_u(t)}{u-m_b^2} + \int_{4m^2}^{\infty} \frac{ds'}{2\pi i} \frac{\text{Disc}_{s'}\mathcal{M}(s',t)}{s'-s} + \int_{-\infty}^{-t} \frac{ds'}{2\pi i} \frac{\text{Disc}_{s'}\mathcal{M}(s',t)}{s'-s}. \quad (1.34)$$

The power of this result is the fact that, while unitarity in principle determines the imaginary part of the amplitude for $s \geq 4m^2$, we can use analyticity in the form of dispersion relations to obtain from it also the real part, and therefore these combined requirements can be used to devise a self consistent bootstrap.

To derive eq. (1.34) we assumed that the amplitude decays at large energies, but this is often not the case. To deal with the scenario in which this requirement is not satisfied, we can use *subtracted* dispersion relations, in which we simply add to the Cauchy kernel $(s-s')^{-1}$ enough factors of s^{-1} as to be able to drop the arc at infinity. A k-subtracted dispersion relation would be of the form

$$\begin{aligned} \frac{\mathcal{M}(s',t)}{(s'-s_1)\dots(s'-s_k)} &= \sum_{i=1}^{k} \frac{\mathcal{M}(s_i,t)}{s-s_i} \prod_{j=1,\, j\neq i}^{k} (s_i-s_j)^{-1} + \\ \int_{4m^2}^{\infty} \frac{ds'}{2\pi i} \frac{\text{Disc}_{s'}\mathcal{M}(s',t)}{(s'-s_1)\dots(s'-s_k)(s'-s)} &+ \int_{-\infty}^{-t} \frac{ds'}{2\pi i} \frac{\text{Disc}_{s'}\mathcal{M}(s',t)}{(s'-s_1)\dots(s'-s_k)(s'-s)}, \end{aligned} \quad (1.35)$$

omitting the terms related to the bound state. The effect of the subtractions is rendering the integrals along the discontinuity finite at the cost of introducing k unkown terms, the values of the amplitude at the various subtraction points.

As was mentioned when introducing the partial wave expansion, the Froissart bound eq. (1.32) puts an upper bound on the growth of the amplitude at high energies and thus implies that we can always get away with dispersion relations with at most two subtractions. However, in practical cases there are sometimes reasons to assume a softer behavior at high energies, giving room to once-subtracted or unsubtracted dispersion relations. Moreover, it is worth it to mention that while gravity evades the assumptions of the Froissart bound by the presence of the massless graviton, it can still be shown to satisfy dispersion relations with two subtractions. For a recent discussion, see [79].

1.4. Leveraging consistency: The bootstrap philosophy

After introducing the bootstrap axioms of analyticity, crossing symmetry and unitarity, as well as the fundamental tools needed to exploit them, we are finally ready to see some examples of the bootstrap in action, in which the consistency with these basic principles can be used to extract information on the allowed space of QFTs.

There exist two main approaches to bootstrap methods: The *primal* and *dual* bootstrap. The primal bootstrap is a constructive approach. Its primary objective is to find explicit examples of S-matrices that satisfy the fundamental physical constraints. In this framework, one typically parameterizes the scattering amplitude and then imposes the constraints of unitarity, crossing symmetry, and analyticity, trying to solve for the coefficients in the parametrization such as to find an amplitude that satisfies these constraints. In this way, one can explore the space of allowed theories form the inside, constructing explicit examples of amplitudes that live at a given point in parameter space.

The dual bootstrap on the other hand is focused on excluding unphysical solutions rather than constructing explicit ones. In this approach, the goal is to prove that certain regions of parameter space are not allowed by the bootstrap constraints. This is typically done by constructing functionals that act on the space of scattering amplitudes and test whether a given amplitude violates any of these constraints.

In numerical applications, both approaches typically require solving linear or semidefinite optimization problems, in which one tries to extremize a given parameter that caracterizes the amplitude subject to the bootstrap constraints, in an attempt to find the boundary of the space of consistent amplitudes. In what follows, we review briefly the main features of both approaches and give examples of recent applications.

1.4.1. Primal approach

Modern implementations of primal S-matrix bootstrap problems are based on different parametrizations of the amplitude. A widely used choice is the one introduced in [32], usually referred to as the ρ ansatz, which we will briefly review as an example of primal bootstrap. The idea is simply to expand the amplitude in a convenient basis of functions that implement the right analytic properties of the amplitude and crossing symmetry by construction, and then impose unitarity on the ansatz as a constraint on the expansion's coefficients.

Assuming the existence of a single stable bound state of mass m_b^2, the ansatz is given by

$$\mathcal{M}(s,t,u) = -\frac{g^2}{s-m_b^2}\frac{g^2}{s-m_b^2}\frac{g^2}{s-m_b^2} + \sum_{a,b,c} \alpha_{abc}\, \rho_s^a \rho_t^b \rho_u^c\,, \quad \rho_x = \frac{\sqrt{4m^2-s_0}-\sqrt{4m^2-x}}{\sqrt{4m^2-s_0}+\sqrt{4m^2-x}}, \tag{1.36}$$

where the map $x \mapsto \rho_x$ maps the cut complex x plane $\mathbb{C}\setminus(4m^2,\infty)$ into the unit disk, with the upper side of the cut mapping to the upper boundary of the disk, and the bottom to the lower boundary. Therefore, the ansatz in eq. (1.36) has the expected analytic structure in each Mandelstam variable assuming maximal analyticity, namely it is analytic in the full complex plane except for the discontinuities at $s,t,u \geq 4m^2$ associated to unitarity. Crossing symmetry is also ensured by construction by choosing the coefficients α_{abc} to be completely symmetric in $\{abc\}$, and s_0 is an arbitrary number that corresponds to the value of s that is mapped to the center of the unit disk. Note that the relation $s+t+u=4m^2$ implies that the ρ variables also satisfy a polynomial equation.

Apart from solving crossing and analyticity explicitly, the power if this ansatz lies on the fact that *any* function of (s,t,u) obeying the analyticity constraints on the surface $s+t+u=4m^2$ can be extended to a function on Disk^3, and thus can be expanded as in (1.36). Using the partial wave projection (1.29), the unitarity constraints (1.30) become an infinite set of constraints on the ansatz parameters g^2 and $\{\alpha_{abc}\}$, and the primal problem becomes finding the possible sets of parameters satisfying unitarity.

Naturally, to deal with this problem numerically one must truncate the infinite sum in eq. (1.36) at a finite value $N_{\max}$, and then check that the obtained results converge as $N_{\max}$ increases. Similarly, unitarity is imposed on a grid of values of s and up to a maximum spin

$J_{\max}$. In terms of the $S_J(s)$ it can be recast as the positive semi-definiteness condition

$$\begin{pmatrix} 1 & S_J(s) \\ S_J(s) & 1 \end{pmatrix} \succcurlyeq 0, \quad J = 0, \ldots, J_{\max}. \tag{1.37}$$

This set of equations is linear in the ansatz parameters and defines a positive-semidefinite program that can be solved numerically to find a consistent scattering amplitude at any given truncation[3].

Moreover, it is natural to not just want to solve the bootstrap constraints but to extremize some physical observable to explore the boundaries of the allowed parameter space. Different choices exist in the literature depending on the problem at hand, and they tipically involve the value of the amplitude and its derivatives around a given value of the Mandelstam variables. Figure (1.4) shows as an example the first result ever derived with this method, in which the authors of [32] maximized the value of g^2 as a function of the mass of the bound state.

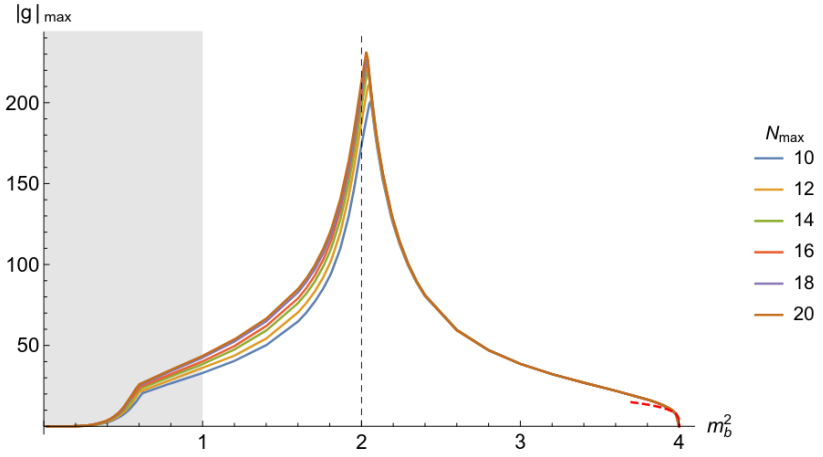


Figure 1.4.: Largest cubic coupling as a function of m_b^2. Plot taken from [32].

Since this first application in the context of the modern S-matrix bootstrap the primal approach has proven to be extremely flexible, both in its ρ ansatz implementation and in other formulations, and it has been used succesfully to obtain a plethora of interesting results. An incomplete list of recent achievements of the primal S-matrix bootstrap is the derivation of non-perturbative bounds on various couplings [31, 32, 81–88], bounding the Wilson coefficients of different EFTs (such as flux tubes, goldstone bosons, photons, etc) [89–92], the study of pion scattering in QCD [93–95], and locating string theory in the space of EFTs with supergravity [96, 97], as well as being improved to include the information about form factors in addition to the constraints on amplitudes [98–100].

1.4.2. Dual approach

The primal approach, despite being very powerful and flexible, suffers from the disadvantage that the bounds that it produces are generally non-rigorous in the sense that they rely on

[3] The semidefinite optimization software that has became the standard of the bootstrap community is called SDPb, and was originally developed in the context of the CFT bootstrap [80].

numerical optimization of a specific parameterization of the scattering amplitude, which may not exhaustively explore the entire space of possible solutions. As a result, there is a risk that certain regions of parameter space might not be fully explored, and the found bounds might be suboptimal or leave gaps in the allowed space of amplitudes. This lack of rigor can be seen as a disadvantage because the primal approach might fail to capture the sharpest possible bounds on observables or miss valid solutions that lie outside the numerically explored region.

The dual approach, on the other hand, focuses on excluding regions of parameter space that correspond to S-matrices that violate the bootstrap assumptions rather than constructing explicit solutions that satisfy them. This way the allowed space of amplitudes is *carved out* from the outside rather than built from the inside, and the bounds obtained by dual methods are always rigorous, meaning that no consistent amplitude can ever lie outside them.

To achieve this, the most direct approach is the use of dual functionals, in which functionals that act on the space of possible scattering amplitudes are designed to detect violations of the bootstrap constraints. If a functional finds a violation in a certain region of parameter space, it proves that no valid S-matrix can exist in that region. This was the method originally pioneered for CFTs in [34], and is widely used in the study of positivity constraints for Effective Field Theories, where the dual functionals correspond to dispersion relations and null constraints relating the different Wilson coefficients. In this context, the dual bootstrap approach has been used to carve out the space of allowed low energy Wilson coefficients in various theories, both gravitational and not [59–63, 65–68, 101–112].

Another dual approach which actually corresponds to what *dual* means in the convex optimization terminology consists on the dualization of a primal problem. This procedure, standard in the convex optimization literature, involves reformulating the original optimization program, where one seeks to find scattering amplitudes that satisfy physical constraints, into a dual problem using a Lagrangian function, where the constraints from the primal problem are incorporated into the Lagrangian via Lagrange multipliers [113]. This creates a new objective function (referred to as the dual function), and the dual problem is to extremize it with respect to the Lagrange multipliers instead of the original variables, effectively optimizing over functionals that test for violations of the constraints. This approach was first introduced in the S-matrix bootstrap context in [83] for the 2d case and further improved in various works [82, 114–116]. Apart from producing rigorous bounds, this method has the advantage that it does not necessarily require the assumption of maximal analyticity and can be set up as to only use the regions of analyticity that are rigorously proven, as first introduced in [116]. Examples of recent developments based on this method are the study of various non perturbative aspects of QCD such as confining flux tubes, glueball couplings and pion scattering [95, 99, 117, 118] and the constrain of the coefficients of higher dimensional operators in Higgs boson self interactions [84, 119].

Nonetheless, a disadvantage of dual approaches is the fact that while approaching the allowed amplitude space from the outside ensures rigorous bounds, there is no guarantee that the amplitudes living on the boundary determined by dual methods actually correspond to consistent amplitudes. This fact can lead to the existence of a *duality gap*, namely a separation between the boundaries of the allowed space carved out by dual methods and the one built from the inside with primal methods. For this reason both approaches are complementary, and one can claim to have achieved an optimal bound when both primal and dual bounds match.

1.5. Bootstrap constraints for Dual Model Amplitudes

After introducing the main ingredients necessary for the S-matrix bootstrap and a short review on its modern applications, we can finally focus on using it to investigate Dual Model amplitudes. A good review on the subject dating back to the Dual Model days can be found in [120].

As was explained in the previous chapter, Dual Model amplitudes are characterized for corresponding to weakly coupled processes in which intermediate heavy states of increasingly high spin are exchanged. Importantly, the weak coupling aspect of these models modifies the constraints imposed on the amplitude by analyticity and unitarity.

1.5.1. Unitarity for Dual Models

By weakly coupled amplitudes we mean amplitudes that constitute the leading term in the Born expansion in some small coupling constant. Considering a typical Lagrangian with interaction terms schematically of the form $\mathcal{L}_{\text{int}} \sim g\phi_i\phi_j\phi_k$, where g is the cubic coupling between the generic fields ϕ_1, ϕ_2 and ϕ_3, it is easy to see using perturbative computations that the leading term in powers of g in a $2 \to 2$ amplitude is of order 2, namely

$$\mathcal{M}(s,t) = g^2\mathcal{M}_0(s,t) + g^4\mathcal{M}_1(s,t)\dots, \tag{1.38}$$

where $\mathcal{M}_0(s,t)$ is the leading or *tree-level* contribution to the scattering amplitude, $\mathcal{M}_1(s,t)$ is the *one-loop* correction and so on. The statement that Dual Model amplitudes are weakly coupled simply means that we will truncate this expansion and consider only the leading term $\mathcal{M}_0(s,t)$.

This elementary fact has non-trivial consequences on the bootstrap axioms. If we plug this expansion in powers of g into the unitarity equation (1.17) we obtain

$$g^2\text{Im}\mathcal{M}_0(s,t) + g^4\text{Im}\mathcal{M}_1(s,t)\cdots = \frac{1}{2}\sum\!\!\!\!\!\!\int_X \mathcal{M}(p_1\,p_2 \to X)\mathcal{M}^*(p_3\,p_4 \to X), \tag{1.39}$$

where $\sum\!\!\!\!\!\!\int_X$ denotes the sum over the full on-shell multiparticle phase space.

To be consistent with the weak coupling assumption we need to truncate this expansion and keep only the $\mathcal{O}(g^2)$ terms. However, it is simple to check by perturbative computations that the leading contribution to an amplitude corresponding to a $2 \to n$ process is of order g^{n-2}, and thus the only terms in the sum over on-shell states on the right hand side that gives a contribution at order $\mathcal{O}(g^2)$ are those in which X corresponds to a single particle state. Therefore, unitarity applied to the Dual Model amplitude setting reads

$$\text{Im}\mathcal{M}_0(s,t) = \frac{1}{2}\sum\!\!\!\!\!\!\int_X \mathcal{M}_0(p_1\,p_2 \to p)\mathcal{M}_0^*(p_3\,p_4 \to p), \tag{1.40}$$

with $p = p_1 + p_2 = p_3 + p_4$. This is precisely the same situation that we found when analyzing the factorization of the scattering amplitude at a pole, and as was explained then it implies that $\mathcal{M}_0(s,t)$ has a simple pole at $s = p^2$ whose residue corresponds to the sum over polarizations of the product ot two three-point amplitudes. However, in that case this expression was only valid near the pole and contributions to the discontinuity from

multiparticle processes are expected to be relevant away from it, while when truncating the unitarity constraint at order g^2 multiparticle processes don't contribute, and therefore the imaginary part of the amplitude is strictly zero except when s matches the mass of a particle in the spectrum. This in turn means that the *only* singularities required by unitarity are simple poles at every mass in the spectrum, and removes the branch cuts associated to multiparticle thresholds.

The previous argument shows that Dual Model amplitudes do not posses the complicated multi-Riemann sheet structure of non-perturbative amplitudes, and can be defined in a single sheet -the phyisical one-. Their only singularities are then the simple poles dictated by unitarity, and thus Dual Model amplitudes satisfy maximal analyticity.

Moreover, the fact that only three-point amplitudes contribute to the right hand side of the unitarity equation eq. (1.18) has another consequence: unitarity no longer implies an upper bound on the partial wave coefficients. The reason for this is that schematically the non-perturbative unitarity equation says that the imaginary part of the $2 \to 2$ amplitude is equal to its modulus squared plus the positive multiparticle contributions. Since a complex number whose imaginary part is bigger than its modulus squared must belong to the disk of radius $1/2$ centered at $z = i/2$, this implies an upper bound on the scattering amplitude in the partial wave basis. However, this restriction disappears when we consider Dual Model amplitudes, as the weak coupling version of the unitarity equation eq. (1.40) does not relate the imaginary part and the modulus of the $2 \to 2$ amplitude, but rather the imaginary part of the $2 \to 2$ amplitude to products of three-point amplitudes. As we will see in the next section, unitarity in the case of Dual Models only implies the positivity of the couplings between the scattered particles and the intermediate states exchanged at the poles.

1.5.2. The structure of the residues

Not only does unitarity constrain Dual Model amplitudes to be meromorphic functions of the Mandelstam invariants, it also dictates the specific functional form that the residues at the poles must have. In fact, unitarity and invariance under Lorentz transformations dictate that the residue of the amplitude corresponding to the exchange of an on-shell spin J intermediate state must be proportional to $P_J(\cos\theta)$, the Legendre polynomial of order J, and the proportionality coefficient must be positive.

To see this, lets go back to the factorization of the $2 \to 2$ amplitude at the pole at $s = M^2$. Eq. (1.23) shows that the residue of the amplitude is given by

$$\operatorname*{Res}_{s=M^2} \mathcal{M}(s,t) = -\sum_{\sigma} \mathcal{M}_\sigma(p_1 p_2 \to p)\mathcal{M}^*_\sigma(p_3 p_4 \to p), \tag{1.41}$$

with $p = p_1 + p_2 = p_3 + p_4$, and the sum over σ corresponds to tracing over all the quantum numbers of the intermediate state.

In the case in which the intermediate state is a particle of spin J and assuming for simplicity that this is the only relevant quantum number, we have

$$\operatorname*{Res}_{s=M^2} \mathcal{M}(s,t) = -\sum_{\lambda=-J}^{J} \mathcal{M}^{\lambda}(p_1 p_2 \to p)\mathcal{M}^{-\lambda}(p_3 p_4 \to p), \tag{1.42}$$

where now λ corresponds to the helicity of the massive spin J particle, and we used the fact that taking the complex conjugate of the amplitude reverses the sign of the helicity.

The sum over helicities can be computed thanks to the simplicity of the three-point amplitudes caused by the fact that at three points there are no Lorentz invariant combinations of the momenta equivalent to the Mandelstam variables. To see this, note that for a generic three point scattering with $p_i^2 = -m_i^2$, $i = 1, 2, 3$ and $p_1 + p_2 = p_3$, we have that $2p_i \cdot p_j = (p_i + p_j)^2 - p_i^2 - p_j^2 = p_k^2 - p_i^2 - p_j^2 = m_i^2 + m_j^2 - m_k^2$. This together with the fact that the polarization tensor of the spin J particle must be transverse to its momentum completely fix the three-point amplitude between two scalars and a spin J particle to be

$$\mathcal{M}^{\lambda}(p_1 p_2 \to p) = g\,(p_1 - p_2)^{\mu_1} \dots (p_1 - p_2)^{\mu_J} \epsilon^{\lambda}_{\mu_1 \dots \mu_J}(p), \tag{1.43}$$

where $\epsilon^{\lambda}_{\mu_1 \dots \mu_J}(p)$ is the polarization tensor and g is an undetermined constant that measures the coupling strength between the scalars and the spin J particle. Unitarity imposes that g must be real, as can be seen by the fact that the amplitude (1.43) would be generated by an interaction term in the Hamiltonian schematically as $g\phi\,\partial_{\mu_1} \dots \partial_{\mu_J} \phi\, \sigma^{\mu_1 \dots \mu_J}$, where ϕ and σ are the scalar and spin J fields respectively. If g was complex then the Hamiltonian would be non-hermitian, and therefore the theory would be non-unitary.

Using the form (1.43) for the three-point amplitudes, the polarization sum in the residue of the four-point amplitude becomes

$$F(k, q) \equiv \sum_{\lambda} k^{\mu_1} \dots k^{\mu_J}\, q^{\nu_1} \dots q^{\nu_J} \epsilon^{\lambda}_{\mu_1 \dots \mu_J} \epsilon^{-\lambda}_{\nu_1 \dots \nu_J}, \tag{1.44}$$

where $k^{\mu} \equiv (p_1 - p_2)^{\mu}$ and $q^{\nu} \equiv (p_3 - p_4)^{\nu}$.

This sum over polarizations is the one that generates the Legendre polynomials. A possible way to see this is to use polarization completeness relations to evaluate the sum. For example, for $J = 1$ we have that

$$\sum_{\lambda} \epsilon^{\lambda}_{\mu}(p) \epsilon^{-\lambda}_{\nu}(p) = g_{\mu\nu} - \frac{p^{\mu} p^{\nu}}{m^2}, \tag{1.45}$$

and thus

$$\sum_{\lambda} (p_1 - p_2)^{\mu} (p_3 - p_4)^{\nu} \epsilon^{\lambda}_{\mu}(p) \epsilon^{-\lambda}_{\nu}(p) = (M^2 - 4m^2) \cos\theta, \tag{1.46}$$

which can be most easily seen by performing the contractions in the center of mass frame. Since $P_1(x) = x$, we find that indeed the residue at the pole corresponding to the exchange of a spin 1 particle of mass M^2 is

$$\operatorname*{Res}_{s = M^2} \mathcal{M}(s, t)\Big|_{J=1} = -g^2 (M^2 - 4m^2) P_1(\cos\theta). \tag{1.47}$$

The generalization to higher spins is straightforward, but the tensor structures appearing in the polarization sums become more and more involved. A more efficient way of obtaining this result for arbitrary J is as follows: Consider the polarization sum (1.44) in the center of mass frame, where the polarization tensors and k^{μ} and q^{ν} have only spatial components, and the scattering angle is given by $\cos\theta = \vec{k} \cdot \vec{q} / |\vec{k}||\vec{q}|$. This allows us to write the polarization

sum as

$$F(\vec{k},\vec{q}) = \sum_{\lambda} k^{i_1}\dots k^{i_J}\, q^{j_1}\dots q^{j_J}\epsilon^{\lambda}_{i_1\dots i_J}\epsilon^{-\lambda}_{j_1\dots j_J} \equiv |\vec{k}|^J|\vec{q}|^J F(\cos\theta). \tag{1.48}$$

The next step is noting that the polarization tensors must be fully symmetric and traceless in all pairs of indices, and this implies that $F(\vec{k},\vec{q})$ satisfies the Laplace equation

$$\nabla^2_k F(\vec{k},\vec{q}) = 0, \tag{1.49}$$

whose solution is

$$\frac{1}{|\vec{k}-\vec{q}|} = \frac{1}{\sqrt{|\vec{k}|^2 - 2|\vec{k}||\vec{q}|\cos\theta + |q|^2}} = \frac{1}{|\vec{q}|}\sum_{\ell=0}^{\infty}\left(\frac{|\vec{k}|}{|\vec{q}|}\right)^{\ell} P_\ell(\cos\theta). \tag{1.50}$$

Simply matching the powers of $\vec{k}|$ in (1.48) and (1.50) we get $F(\cos\theta) = P_J(\cos\theta)$. Since $|\vec{k}| = |\vec{q}| = \sqrt{M^2-4m^2}$, we find that the polarization sum for spin J is

$$F(k,q) = (M-4m^2)^J P_J(\cos\theta), \tag{1.51}$$

and therefore the residue of the amplitude is proportional to a Legendre polynomial:

$$\operatorname*{Res}_{s=M^2}\mathcal{M}(s,t) = -g^2(M^2-4m^2)^J P_J(\cos\theta). \tag{1.52}$$

More generically it can also happen that various particles of different spin are exchanged at the same pole, as is the case in tree-level string theory. Naturally, in this case the residue will be a sum over terms like (1.52), one for each spin. Moreover, since for physical kinematics the factor depending on the masses and the spin of the resonance is positive and we had established that unitarity required the coupling constant g to be real, we see that the most general residue will be a positive sum of Legendre polynomials:

$$\operatorname*{Res}_{s=M^2}\mathcal{M}(s,t) = -\sum_J c_{M^2,J}\, P_J(\cos\theta), \quad c_{M^2,J}\geq 0. \tag{1.53}$$

A negative c_{nJ} would imply $g^2<0$, which signals a breakdown of unitarity in which the spin J state propagating at the pole corresponds to a negative norm state or *ghost*. Moreover, locality of the interactions requires that at any given pole at finite energy the maximum spin exchanged must be finite, as unbounded spin would correspond to an interaction term with infinitely-many derivatives in the Lagrangian. This is a clear signature of a non-local theory, as can be seen simply by considering a non-local interaction term such as $\phi(x)\phi(x+a)$ and Taylor expanding around x.

1.5.3. Color ordering, dispersion relations and channel duality

As was explained in the first chapter, the feature that gives their name to Dual Models is called channel duality, which requires that the amplitude admits a representation as an infinite sum over poles in a single channel, with the singularities in the crossed channel encoded in the divergence of this infinite series and accesible by its analytical continuation. As was also mentioned, this property is not an independent assumption from the bootstrap axioms

applied to tree-level amplitudes, and can instead be derived as a consequence of the analytic structure of dual model amplitudes if one assumes a behavior soft enough at high energies.

Before showing this fact, let us introduce the notion of *color-ordered* amplitude. Lets consider still the scattering between massive scalars, but now we assume that they transform in the adjoint representation of a Lie group that we refer to as the color group to follow the standard terminology, even if it is not necessarily related to the SU(3) group of QCD. In this case, the "color" quantum numbers of the ith external scalar are specified by a color matrix λ_i, and the scattering amplitude will be a sum over color traces with non-equivalent orderings of the λ matrices:

$$\mathcal{M}(s,t) = \mathrm{Tr}(\lambda_1\lambda_2\lambda_3\lambda_4)\mathcal{A}[1234] + \text{permutations of } (234), \tag{1.54}$$

where the coefficients $\mathcal{A}[1234]$, $\mathcal{A}[1243]$, etc of each color trace are called color-ordered amplitudes, and correspond to different orderings of the external particles.

The dependence on the ordering of the external states will cause the individual color-ordered amplitudes to not be fully crossing symmetric, even if their combination into the full amplitude $\mathcal{M}(s,t)$ is. However, they do retain some crossing symmetric properties. For instance, if we consider the amplitude $\mathcal{A}(1243)$, we note that the fact that the term $\mathrm{Tr}(\lambda_1\lambda_2\lambda_4\lambda_3)$ is invariant under the cyclic permutation $1243 \to 2431$ implies that the color-ordered amplitude should be invariant under $p_1p_2p_3p_4 \to p_2p_4p_1p_3$, which amounts to $s \leftrightarrow t$, but not to the full symmetry under permutations of s, t, u.

Moreover, the color stucture can forbid that a given color-ordered amplitude exchanges physical states in a given channel. To simplify the analytical structure of the amplitudes that we consider, we will often work with the color-ordered amplitude that is symmetric under $s \leftrightarrow t$ but not under permutations involving u, denoted by $\mathcal{A}(s,t)$ in contrast to $\mathcal{M}(s,t)$, the fully crossing symmetric amplitude. We will also assume that $\mathcal{A}(s,t)$ has only singularities in s and t, but is free of u-channel poles.

Let us now go back to the derivation of channel duality for the color-ordered amplitude $\mathcal{A}(s,t)$. The only extra input we need is the assumption that the amplitude decays at large energies. As was mentioned in the last chapter, this is only possible if the amplitude is made up of an infinite number of poles, as any individual term in the sum grows at large energies and thus only by cancellations among infinitely many terms one can get a decaying amplitude.

Under this assumption, the amplitude satisfies an unsubtracted, fixed t dispersion relation as described in the previous section, except that in this case there are no u-channel singularities, and the s-channel cut is replaced by an infinite number of simple poles.

Using the integration contours shown in figure (1.5), we can obtain an expression for the amplitude in terms of its poles:

$$\mathcal{A}(s,t) = \oint \frac{ds'}{2\pi i}\frac{\mathcal{A}(s',t)}{s'-s} = \sum_{n=0}^{\infty}\frac{\mathcal{R}_n(t)}{s-m_n^2}, \quad \text{with } \mathcal{R}_n(t) = \operatorname*{Res}_{s=m_n^2}\mathcal{A}(s,t), \tag{1.55}$$

where we used that the contribution from the arc at infinity varishes due to the asymptotic decay of the amplitude. This representation of the amplitude is manifestly channel-dual, as no t-channel poles are included in the sum. We see this way that channel duality is simply a consequence of the assumption that the only singularities of the amplitude are simple poles and that it decays as $|s| \to \infty$.

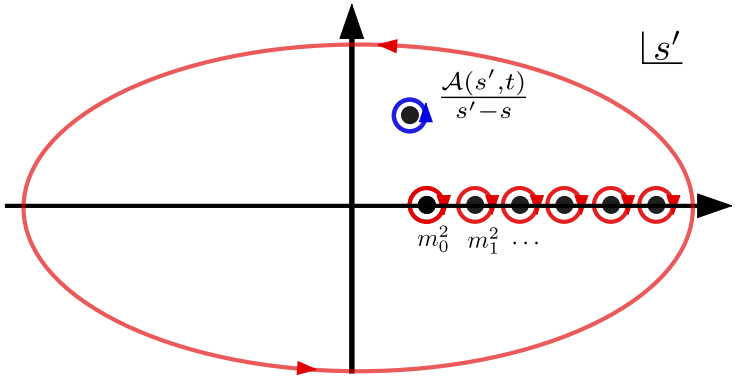


Figure 1.5.: Unsubtracted dispersion relation for the color-ordered amplitude $\mathcal{A}(s,t)$.

Using the Legendre decomposition of the residues introduced in the previous section, we see that the amplitude can be written as[4]

$$\sum_{n,J} c_{nJ} \frac{P_J\left(1+\frac{2t}{m_{n,J}^2-4m_0^2}\right)}{s-m_{n,J}^2}, \tag{1.56}$$

and thus is entirely specified by the spectrum $\{m_{n,J}^2\}$ and the set of coefficients $\{c_{nJ}\}$.

Naturally, since crossing symmetry requires the existence of the corresponding t-channel poles, the s-channel expansion of the amplitude shown in eq. (1.55) can only be a good representation of the amplitude for $t < m_0^2$, with m_0^2 the first t-channel singularity. As we will see later when we introduce Regge theory this is indeed the case, and as $t \to m_0^2$ the asymptotic behavior of the amplitude goes to a constant and therefore integral along the contour at infinity diverges, giving rise to the leading t-channel singularity.

Because the amplitude is invariant under $s \leftrightarrow t$ we can obviously perform the same manipulations at fixed s, giving

$$\sum_{n,J} c_{nJ} \frac{P_J\left(1+\frac{2s}{m_{n,J}^2-4m_0^2}\right)}{t-m_{n,J}^2}, \quad s < m_0^2. \tag{1.57}$$

When both s and t are below the first singularity the expansions in the two channels are simultaneously good representations of the amplitude, which allows us to recast channel duality as the condition

$$\sum_{n,J} c_{nJ} \left(\frac{P_J\left(1+\frac{2t}{m_{n,J}^2-4m_0^2}\right)}{s-m_{n,J}^2} - \frac{P_J\left(1+\frac{2s}{m_{n,J}^2-4m_0^2}\right)}{t-m_{n,J}^2} \right) = 0, \quad s,t < m_0^2, \quad c_{nJ} \geq 0. \tag{1.58}$$

This condition is an extremely hard constraint that the spectrum and couplings of an amplitude consistent with channel duality must satisfy and is strongly reminiscent of the

[4] Recall that the scattering angle in the s-channel is given by $\cos\theta_s = 1 + 2t/(s-4m^2)$, while in the t-channel it is $\cos\theta_t = 1 + 2s/(t-4m^2)$.

OPE crossing equation from the CFT bootstrap, which has proven to be extremely powerful to derive constraints on the allowed CFTs.

In the face of this crossing equation it is natural to ask what the space of allowed masses and couplings compatible with channel duality is, and if it is possible to apply methods analogous to those used in the conformal bootstrap to chart this space and/or obtain new examples of dual model amplitudes. An immediate issue is the fact that to apply numerical methods to probe eq. (1.58) one is forced to truncate the infinite sum, and differntly from what happens with the OPE crossing equation in CFTs, the convergence of (1.58) is extremely slow. Therefore, naively applying the machinery of dual functionals designed to deal with the analog case in CFTs doesn't give convergent results in general. However, as will be explained in following chapters, there are ways around this difficulty and it is indeed possible to devise numerical bootstrap approaches to obtain spectra and couplings that solve eq. (1.58).

Chapter 2.

The Coon amplitude: A case study

This chapter is devoted to the characterization from an S-matrix bootstrap point of view of the Coon amplitude, a solution to the dual model bootstrap constraints known since short after the discovery of the Veneziano amplitude [121–123]. We chose this object as a case study of the S-matrix bootstrap constraints applied to dual models, since at the moment in which this work was done it was the only explicitly known solution to the channel duality constraints departing from the linear, Veneziano-like Regge trajectories, making it a very relevant data point for the S-matrix bootstrap. Yet, its main properties such as the conditions under which it is unitary and its low energy expansion remained unknown.

Moreover, the Coon amplitude has very interesting features: It has non-linear Regge trajectrories, it depends on a continuous parameter that allows to interpolate between string and field theory, and it possesses an accumulation point in its spectrum of resonances. This fact resonates[1] with the recent observation that the allowed space of Wilson coefficients for gravitational EFTs is populated by amplitudes with accumulation points as one moves away from the small island where known physical theories live [124], making the Coon amplitude an explicit example of such an object. Furthermore, it was recently pointed out by Maldacena and Remmen that scattering amplitudes for open strings attached to a D-brane in AdS also exhibit an accumulation point which is approached as energy increases in a similar way as for Coon, as well as the fact that the Coon amplitude has the same high energy/fixed angle behavior as the open strings in this setting. This suggested the possibile realization of the Coon amplitude by some string background [125, 126].

Finally, the Coon amplitude was originally derived using a simple bootstrap method devised by Coon in an attempt to generalize the back then recently discovered Veneziano amplitude, and thus it is natural to wonder if this technique can be extended to obtain new solutions to the S-matrix bootstrap constraints combined with channel duality.

This chapter is structured as follows: First we introduce the Coon amplitude and its main features, as well of a review of the results presented in the chapter. Then, we proceed to its characterization and derive the conditions of positivity and the low energy expansion of the amplitude. Later we review Coon's method to produce the amplitude and attempt to generalize it, finding that our generalized method still only provides the Coon amplitude as a consistent solution (and the Veneziano amplitude as a limiting case). While sections on the unitarity and low energy expansion are based on [1], the extension of Coon's method is unpublished work. We end the chapter with a discussion of these results and the current status of the Coon amplitude.

[1] Pun intended

2.1. The Coon amplitude

We start by reviewing some facts about the Coon amplitude. The Coon amplitude was found just months after the discovery of the Veneziano amplitude as an attempt to generalize it to non-linear Regge trajectories. It is defined in terms of a parameter q, with $q \leq 0 \leq 1$, and therefore the Coon amplitude really corresponds to a continuous one-parameter family of dual model amplitudes[2]. In $\alpha' = 1$ units, it is defined by the infinite-product expression

$$A_q(s,t) = (q-1)q^{\frac{\log(\sigma)}{\log(q)}\frac{\log(\tau)}{\log(q)}} \prod_{n=0}^{\infty} \frac{(\sigma\tau - q^n)\,(1-q^{n+1})}{(\sigma - q^n)\,(\tau - q^n)} \tag{2.1}$$

with

$$\sigma = 1 + (s-m^2)(q-1), \quad \tau = 1 + (t-m^2)(q-1) \tag{2.2}$$

where s, t are the Mandelstam variables (0.1).

As defined in (2.1), it describes a color-ordered scattering amplitude between lightest scalars of mass m^2, and interpolates between string and field theory in the sense that at $q = 0$ it reduces to tree-level scalar amplitude, while at $q = 1$ it gives back the Veneziano model:

$$\lim_{q\to 0} A_q(s,t) = \frac{1}{s-m^2} + \frac{1}{t-m^2} - 1, \tag{2.3}$$

$$\lim_{q\to 1} A_q(s,t) = A^V(s,t) = -\frac{\Gamma(-s+m^2)\Gamma(-t+m^2)}{\Gamma(-s-t+2m^2)}, \tag{2.4}$$

with intermediate values of q defining a continuous set of amplitudes connecting both theories.

The spectrum of the amplitude can be read from eq. (2.1) and is shown in figure (2.1). It has single poles located at $\sigma = q^n$ which correspond to [3]

$$s = m_n^2 \equiv m^2 + \frac{q^n - 1}{q-1}. \tag{2.5}$$

For $q < 1$, these poles build up an accumulation point as $n \to \infty$,

$$s_* = m^2 + \frac{1}{1-q}\,, \tag{2.6}$$

somewhat reminiscent of the ionization threshold of the hydrogen atom for instance.

At the accumulation point starts a cut, coming from the non-meromorphic prefactor $q^{\frac{\log(\sigma)}{\log(q)}\frac{\log(\tau)}{\log(q)}} \sim q^{\log s \,\log t}$ in eq. (2.1). As we explain below, this prefactor is crucial to ensure polynomial residues as required to have an amplitude generated by local interactions. Analogies with atomic physics of such an analytic structure were drawn in [127] but never made precise. Even though this makes this amplitude depart from the strictly tree-level case corresponding to the standard definition of dual models, the machinery developed in the

[2] The Coon amplitude with $q > 1$ can be defined and was in fact the first case studied, but it was soon realized that it inevitably has negative residues and therefore violates unitarity. For this reason, we restrict to the $q \leq 1$ case.

[3] Note that $\frac{q^n-1}{q-1}$ is also known as a q-deformed integer, sometimes denoted $[n]_q$. When $q \to 1$, it reduces to ordinary numbers, $[n]_q \to n$ and we recover the spectrum of the Veneziano model.

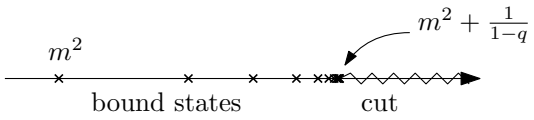


Figure 2.1.: Spectrum of resonances of the Coon amplitude. The poles are situated at $s = m_n^2 = m^2 + \frac{q^n-1}{q-1}$, and accumulate to the point $m_\infty^2 = m^2 + \frac{1}{1-q}$ as $n \to \infty$, below which there is a branch cut.

previous chapter can still be applied for energies below the accumulation point. This would certainly be sensible if we interpreted this accumulation point as some sort of UV cutoff beyond which the amplitude stops giving a good description of the scattering process.

On a given pole $s = m_n^2$, the non-meromorphic q-factor reduces to τ^n and cancels an inverse factor τ^{-n} coming from the denominator and the residue of the amplitude reduces to a polynomial of degree n in t, corresponding to the exchange of particles of spins 0 to n, which reads

$$\text{Res}(A_q(s,t))\Big|_{s=m_n^2} = \prod_{j=0}^{n-1} \left(\frac{\tau - q^{j-n}}{1 - q^{-j-1}} \right). \tag{2.7}$$

To see this directly from eq. (2.1) one needs to treat carefully the infinite product, in which each of the terms is made up of factors that do not define a convergent infinite product by themselves[4]. This leads to subtleties when computing the residues, and this led to the non-meromorphic prefactor being missed in the original papers and the more recent reference [128], and we rediscovered it by analyzing the non-local version of the amplitude anf realizing how it should be fixed.

A better way of dealing with this fact is to switch to an equivalent representation of the amplitude where factors of σ and τ appear in the denominator of q^n , obtained by simply dividing both the numerator and denominator by $\sigma\tau$. In this way, we obtain a representation for the Coon amplitude in which each piece of the infinite product is convergent by itself:

$$A_q(s,t) = (q-1) q^{\frac{\log(\sigma)}{\log(q)}\frac{\log(\tau)}{\log(q)}} \prod_{n=0}^{\infty} \frac{\left(1 - \frac{q^n}{\sigma\tau}\right)}{\left(1 - \frac{q^n}{\sigma}\right)\left(1 - \frac{q^n}{\tau}\right)} (1 - q^{n+1}). \tag{2.8}$$

In this way, if we remove the non-meromorphic factor the residue corre- sponding to the infinite product is $(1\breve{}q^n/\tau)$ and it is obvious that without τ^n coming from the q-factor, this residue would not be a polynomial in t.

This aspect of the Coon amplitude indicates that accumulation points are a clear sign of tension between weak-coupling (meromorphy) and locality. This tension also suggests a physical rationale as to why amplitudes with accumulation points evade the general expectation that dual model amplitudes should posses Regge trajectories that become asymptotically linear at large, positive energies [39].

[4] Namely, $\prod_n(\sigma\tau - q^n)$, $\prod_n(\sigma - q^n)$ and $\prod_n(\tau - q^n)$ don't converge as infinite products.

The Regge and fixed-angle regimes can be extracted from eq. (2.8). In the Regge regime, where $s \gg -t$ and t fixed, $1/\sigma$ vanishes and the amplitude behaves as

$$A_q(s,t) \sim f(t) s^{\alpha(t)}, \quad \alpha(t) = \frac{\log((t-m^2)(q-1)+1)}{\log(q)} \tag{2.9}$$

where $f(t) \sim \prod(1 - q^n/\tau)$. Since $q < 1$, the amplitude is *suppressed* at physical negative t for $m^2 \geq 0$. In particular, all bounds on couplings derived assuming standard twice-subtracted dispersion relations are expected to hold, as they use a stronger condition of Regge boundedness $\frac{A(s,t)}{s^2} \to 0$ at large s. We plot $\alpha(t)$ in figure (2.2) for a fixed value of the mass.

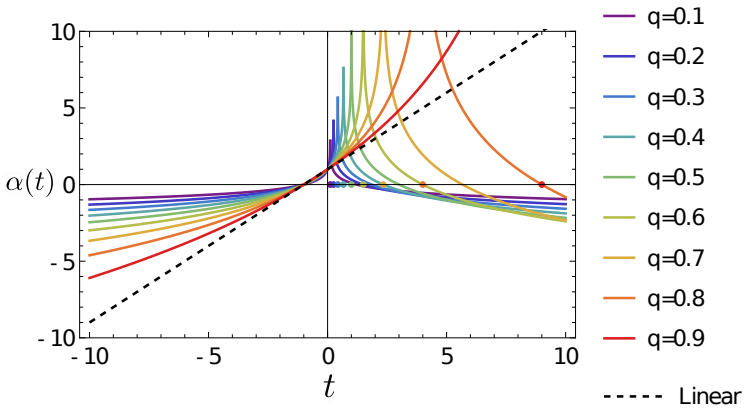


Figure 2.2.: Plot of the real part of $\alpha(t)$ for different values of q. As $q \to 1$, the trajectories unbend and approach the linear trajectory of the Veneziano amplitude. Past the accumulation point $t = t_*$ (depicted by a dot of the same color as the corresponding curve on the x-axis), $\alpha(t)$ diverges and then acquires a constant imaginary part. Increasing values of the mass simply translate the plot to the right.

In the fixed angle regime, $\frac{s}{-t}$ fixed, both $1/\sigma$ and $1/\tau$ vanish, therefore we get

$$A_q(s,t) \sim e^{\log(s)\log(-t)/\log(q)} \sim s^{\log(s\cos(\theta))/\log(q)}\,. \tag{2.10}$$

Finally, as will be expanded on later, we also worked out the impact parameter transform of the amplitude at large impact parameter b (and $q < 1$), which reads

$$\hat{A}_q(s,b) \sim \left(\frac{b}{\sqrt{t_*}}\right)^{-\frac{\log s}{\log q}} e^{-b\sqrt{t_*}}, \quad t_* = m^2 + \frac{1}{1-q}\,. \tag{2.11}$$

It is similar to the Yukawa potential of a single particle of mass $m = \sqrt{t_*}$, dressed by power corrections. When $q \to 1$, these resum to the Gaussian behaviour of string theory amplitudes [129]. Taking the analogy with atomic physics further and interpreting the Coon amplitude as representing the scattering of bound states with ionization threshold at the accumulation point energy, this allows to define an effective size for the Coon bound state that grows with q, and is well approximated by the functional form

$$\ell_C \simeq \ell_0 + q\sqrt{\log(s)}. \tag{2.12}$$

Since this expression grows linearly with q it provides a possible physical interpretation for the parameter q as the effective length of the Coon particle.

The main results presented in this chapter are the following: Firstly, we map the positivity region of the amplitude (q, m^2)-space, see fig. 2.3. For each value of (q, m^2) we determine the maximal dimension in which no negative norm states are exchanged as intermediate states. This generalizes the known $d = 26$ critical dimensions of bosonic string theory for $m^2 = -1$ and $d = 10$ for superstring theory with $m^2 = 0$. Our results show the existence of two regimes separated by a critical value of the parameter q_c. In the first one, with q below q_c, we prove that the amplitude is ghost-free in all dimensions. While this goes against intuition from standard string theory, null strings are known to possess similar features [130–134]. In the other regime, we determine numerically the positivity surface, which interpolates from infinite critical dimensions to the standard critical dimensions of string theory. Along the way, we found that the Coon and thus Veneziano amplitudes can be extended to positive $m^2 \to 1/3$, with critical dimension $d \simeq 6.3$ for the latter. Beyond this value of the mass, the amplitudes are plagued with ghosts in all dimensions. While this fact about intercepts allowed to be negative with bound –1/3 might have been known in the old days of dual models, we have not been able to find a trace of it.

Secondly, we compute some low energy couplings of the Coon amplitude in terms of q-polylogarithm values, which generalize the known zeta-values of the string low-energy expansion and suggest the possible existence of a q-deformed worldsheet theory where we relate q to the Coon parton in eq. (2.12). We compute explicitly the first coefficients $g_2(q), g_3(q), g_4(q)$ and map their location in the space of couplings, comparing to [101]. We also comment on the connection to the notion of low-spin dominance (LSD) of [105].

Finally, we generalize the original method to derive the Coon amplitude by allowing higher order terms in the infinite product ansatz used by Coon to this end. Following this strategy we obtained that the spectrum must be determined by a new equation involving the Weierstrass $\wp$-function, so that the poles of the amplitude $m_n^2 := p_n$ are given by $p_n = c_0 + c_1 \wp(n, g_2, g_3)$, with c_0, c_1, g_2 and g_3 arbitrary coefficients. While this solution would bevery exotic because the spectrum would be either periodic or densely populate the (positive) real line, we found that for generic values of the coefficients the amplitudes obtained are inconsistent, and the only cases that work correspond to degenerate values that yield the Veneziano and Coon amplitudes, as expected.

2.2. Characterization of the Coon amplitude

2.2.1. Positivity of the amplitude

We present now our results on the unitarity of the Coon amplitude, i.e. the conditions under which no negative-norm states, or *ghosts*, decouple. Ghosts are characterised by negative residues on single poles, or more precisely by negative coefficients in the partial wave expansion of the amplitude's residues. Recall that near a resonance of mass m_n^2 in the s-channel, the amplitude takes the form

$$A(s,t) \sim \frac{\mathrm{Res}_n(t)}{s - m_n^2}\,, \quad s \to m_n^2. \tag{2.13}$$

As explained in section (1.5), Lorentz invariance and locality imply that $\text{Res}_n(t)$ is a polynomial whose degree corresponds to the highest spin among the modes of mass m_n being exchanged, and that in 4 dimensions it can be further decomposed into Legendre polynomials. Since in this chapter we will be working on generic spacetime dimension d, we will use the generalization of this fact and expand the residues into Gegenbauer polynomials $\mathcal{P}_J^{(d)}$, which are angular eigenfunctions in dimension d and descend to the Legendre polynomials when $d = 4$. They are defined in terms of hypergeometric functions as

$$\mathcal{P}_J^{(d)}(z) = {}_2F_1\left(-J, J+d-3, \frac{d-2}{2}, \frac{1-z}{2}\right). \tag{2.14}$$

Therefore, in generic dimension d the residues can be expressed as

$$\text{Res}_n(t) = -\sum_{J=0}^{n} c_{nJ}\mathcal{P}_J^{(d)}(\cos(\theta)), \tag{2.15}$$

with $\cos(\theta) = 1 + \frac{2t}{m_n^2 - 4m^2}$ and where each term in the sum corresponds to a different particle of mass m_n and spin J being exchanged. The amplitude amplitude is then free of ghosts if at every pole we have $c_{nJ} \leq 0$, for every J and n, and the c_{nJ} can be extracted from each residue using the orthogonality of the Gegenbauer polynomials. This formula is a generalization of the one for Legendre polynomials in $d = 4$ given in eq (1.28), and following the conventions of [72] is given by

$$\frac{1}{2}\int_{-1}^{1} dz(1-z)^{\frac{d-4}{2}}\mathcal{P}_J^{(d)}(z)\mathcal{P}_{J'}^{(d)}(z) = \frac{\delta_{JJ'}}{\mathcal{N}_d n_J^{(d)}}, \tag{2.16}$$

with

$$\mathcal{N}_d = \frac{(16\pi)^{\frac{2-d}{2}}}{\Gamma(\frac{d-2}{2})}, \quad n_J^{(d)} = \frac{(4\pi)^{\frac{d}{2}}(d+2J-3)\Gamma(d+J-3)}{\pi\Gamma(\frac{d-2}{2})\Gamma(J+1)}. \tag{2.17}$$

In the case of string theory, the no-ghost theorem [18, 135] guarantees that such negative norm states decouple from all scattering amplitudes in $d \leq 26$ or 10. At the level the Veneziano amplitude, a recent paper showed that residues should all be positively expandable on Gegenbauer polynomials [136] in $d \leq 6$. It would still be desirable to be able to bridge the gap to $d = 10$ or 26 and maybe the Coon amplitude in its $q \to 1$ limit could be useful for this.

Regarding Coon, the authors of [137] investigated the presence of ghosts in the amplitude in $d = 4$, and observed numerically that some regions in the q, M^2 parameter space are ghost-free. While their (numerical) method finds ghosts in $d = 4$, we do not, for any values of q. This is because our set-up is different: for them, the mass of the external particles M^2 is distinct from m^2 (the first pole of the amplitude), while for us, $M^2 = m^2$. The subsequent work [128] also studied the problem (while being unaware of [137]), but was inconclusive. Overall, before the present work, nothing was known on the critical dimensions of the Coon amplitude.

To find the regions in the (q, m^2) parameter space where the Coon amplitude is ghost-free, we need a way of proving the positivity of all the infinitely-many $c_{nJ}(q, m^2)$ coefficients corresponding to the expansion into Gegenbauer polynomials of the residues of the Coon amplitude (2.7). Moreover, since the Gegenbauer polynomials depend on the spacetime dimension d, the positivity of a given residue is a dimension-dependent statement, and it is

possible that the Coon amplitude defined at a given value of (q, m^2) is ghost-free in a range of dimensions, but becomes non-unitary beyond some critical dimension $d(q, m^2)$.

A first approach to this question could be to check the sign of the residues numerically. However, it is clear that this will require truncating at some finite number of poles, and therefore it would be desirable to have some analytical handle on this issue.

2.2.1.1. Bound on the mass

To begin, we show that requiring that the residues are positive immediately puts an upper bound on the mass of the external particle: if $m^2 > \frac{1}{3}$, the Coon amplitude exhibits ghosts at all values of q and d. This can be seen straightforwardly by the direct computation of the first low lying Gegenbauer coefficients of the Coon amplitude. For instance, the $c_{1,1}$ coefficient corresponding to the vector exchanged at level 1 reads

$$c_{1,1} = \frac{(1 - 3m^2)}{2} q, \tag{2.18}$$

which is manifestly negative for $m^2 > 1/3$ and $q > 0$. The fact that it is independet of the dimension is not surprising: the $J = 1$ Gegenbauer polynomial is simply $\mathcal{P}_1^{(d)}(z) = z$ for any d.

Differently, there is no such strict lower bound for the mass of the Coon amplitude. However, for masses $m^2 < -1$, the Veneziano amplitude is known to *not* be unitary (corresponding to intercepts greater than 1). For the Coon amplitude, a related statement holds : for $m^2 < -1$, there is a ghost at scalar mass-level 2 for $q > \frac{2}{m^2-1}$. For $q < \frac{2}{m^2-1}$, this state becomes a positive-norm state. We gathered solid numerical evidence that there exists a unitarity range similar to the one described above, for all masses $m^2 \to -\infty$. However, to keep a smooth $q \to 1$ limit to string theory we restricted ourselves to $m^2 \geq -1$, but the $m^2 < -1$ regime might contain some physics worth studying.

All in all, in what respects to the mass we restrict ourselves to the range

$$-1 \leq m^2 \leq 1/3\,. \tag{2.19}$$

2.2.1.2. Unitarity in all dimensions: $q < q_c(m^2)$

Having set the range of m^2, we proceed to show that there exists an m^2-dependent critical value of q below which the Coon amplitude is ghost-free in all dimensions. This critical value q_c is given by

$$q_c(m^2) = \frac{m^2 - 3 + \sqrt{9 + 2m^2 + m^4}}{2m^2} \tag{2.20}$$

To see this, we start by the simple observation that a polynomial with only positive coefficients also has a completely positive expansion into Gegenbauer polynomials. This is

implied from the positivity of each monomial z^n, which follows from the identity

$$\int_{-1}^{1} z^{n+2\rho}(1-z^2)^{\frac{d-4}{2}}\mathcal{P}_n^{(d)}(z)dz = 2\frac{\Gamma\left(\frac{d-2}{2}\right)\Gamma\left(\rho+\frac{1}{2}\right)\Gamma(n+2\rho+1)}{2^{n+1}n!\Gamma(1+n)\Gamma(2\rho+1)\Gamma(n+\rho+\frac{d-1}{2})} > 0, \quad (2.21)$$

for $\rho \geq 0$ integer. When n and J do not have the same parity, $\int_{-1}^{1} z^n \mathcal{P}_J^{(d)}(1-z^2)^{\frac{d-2}{2}}$ vanishes.

The next step is to write the residues of the Coon amplitude as a function of $x = \cos(\theta) = 1 + \frac{2t}{m_n^2-4m^2}$. The expression resulting from simply substituting x into eq. (2.7) can be massaged into

$$\text{Res}A(s,t)\Big|_{\sigma=q^n} = b_n \prod_{j=0}^{n-1}(x - x_{j,n}), = b_n \sum_{k=0}^{n} p_{n,k}x^k, \quad (2.22)$$

where $b_n = \prod_{j=0}^{n-1}\left(\frac{1+3m^2(q-1)-q^n}{2(1-q^{-j-1})}\right)$, and

$$x_{j,n} = \frac{3+m^2(q-1)-2q^{j-n}-q^n}{1+3m^2(q-1)-q^n}. \quad (2.23)$$

From (2.21), if all the coefficients $p_{n,k}$ in the expansion of the residue into powers of x are positive, we are guaranteed to have a positive decomposition into Gegenbauer polynomial and therefore a ghost-free amplitude. It is important to note, however, that this is a sufficient but not necessary condition, and therefore it allows to determine a range of parameters in which the amplitude is unitary, but not to exclude the region of parameters outside this range.

The residue has all of its coefficients $p_{n,k}$ positive if and only if all of its roots are positive, thus we want to study the domain in the (q, m^2) parameter space where $x_{j,n} \leq 0$ for all j and all n. Firstly, note that if $m^2 < 1/3$ the roots are ordered: since $q < 1$, if $j < j'$, then $x_{j,n} < x_{j',n}$. Hence, a necessary and sufficient condition for all the roots to be positive (at fixed n) is that $x_{n-1,n} \leq 0$.

Moreover, the $x_{n-1,n}$ increase monotonically with n, and therefore if we manage to ensure that the limit $n \to \infty$ of $x_{n-1,n}$ is negative, we can conclude the same for all roots with finite n. The $n \to \infty$ limit amounts to setting $q^n \to 0$ in $x_{n-1,n}$, giving

$$\lim_{n\to\infty} x_{n-1,n} = \frac{3+m^2(q-1)-2q^{-1}}{1+3m^2(q-1)}. \quad (2.24)$$

Demanding this to be negative leads us to the constraint

$$q < \frac{m^2-3+\sqrt{9+2m^2+m^4}}{2m^2} \equiv q_c(m^2) \quad (2.25)$$

which defines the critical value $q_c(m^2)$ below which the residue is a polynomial with only positive coefficients. This implies that the amplitude is ghost-free in all dimensions in this region of parameter space.

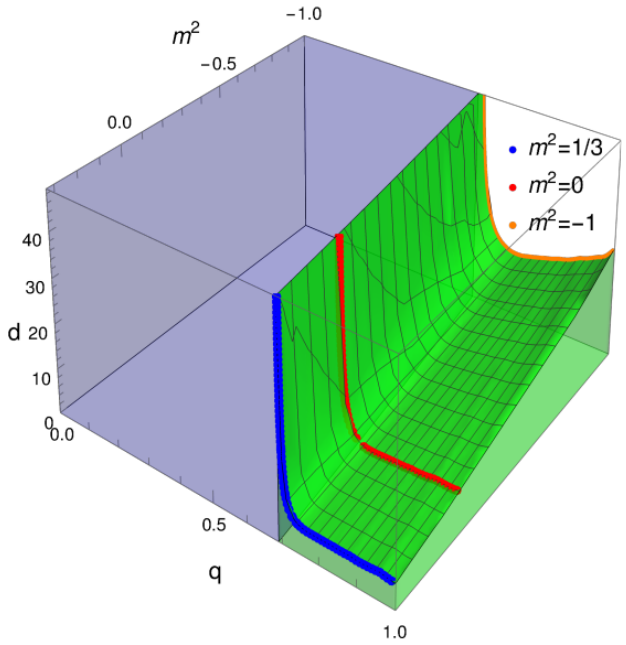


Figure 2.3.: Green surface: Numerical boundary of the unitary region. Blue shaded region: Unitary region determined by $q \leq q_c(m^2)$.

2.2.1.3. Determination of the critical dimensions: $q > q_c(m^2)$

For values of q above $q_c(m^2)$, we proceeded to an extensive numerical evaluation by computing the Gegenbauer coefficients for the first 50 resonances and all spins $J \leq 50$ for a grid of values of $m^2 \in [-1, \frac{1}{3}]$ and $q \in [0; 1]$ varying the spacetime dimension d in the range $[3, 50]$. In this regime the situation is very different, and we found that at each value of (q, c) there existed a critical dimension above which the amplitude developed negative residues. This is in consonance with the natural expectations from String Theory, and we indeed observed that in the limit $q \to 1$ we recover the expected critical dimensions $d = 26$ for the bosonic string and $d = 10$ for the superstring when setting $m^2 = -1$ and $m^2 = 0$ respectively.

By performing a numerical bisection in this region of parameters we can determine the critical surface $d(q, m^2)$ that separates the unitary and non-unitary regions. These results are shown in figure (2.3), with an accuracy of 1%.

As expected, the critical dimension computed numerically diverges as we approach the critical value $q_c(m^2)$. In different colors we show also the curves of fixed m^2 corresponding to the mass of bosonic and fermionic string theory, as well as the one corresponding to the maximum value of the mass allowed by unitarity, $m^2 = 1/3$. In the limit in which $q \to 1$, the critical dimension is $d \approx 6.3$. Despite the fact that this non-integer value of the dimension seems a bit exotic, it would be interesting to know more about the extremal amplitude living in this corner of parameter space.

A curious observation that emerged from the numerical study of the residues is that the scalar ghost sector seems to always define the unitarity surface. While we were not able to prove this fact in general, an argument showing that this must be the case in at large dimensions is at follows:

Consider the pole at $\sigma = q^n$. We want to relate the coefficients $c_{n,L}$ in the Gegenbauer decomposition of the residue to the coefficients $p_{n,k}$ appearing in (2.22), which are given in terms of the roots $x_{j,n}$ by

$$p_{n,n-k} = (-1)^k \sum_{i_1<i_2<\ldots<i_k} x_{i_1,n}\ldots x_{i_k,n}. \tag{2.26}$$

At fixed n, the $c_{n,L}$ coefficient only receives contributions from the $p_{n,k}$ coefficients with $k \geq L$ and with the same parity. Explicitly, for the scalar sector we have

$$c_{n,0} = p_{n,0} + \frac{p_{n,2}}{-1+d} + \frac{3p_{n,4}}{(-1+d)(1+d)} + \ldots \tag{2.27}$$

From the form of the roots $x_{j,n}$ one can see that the $p_{L,n}$ coefficients follow a well-defined pattern: when decreasing q starting from values where the amplitude is not unitary, the $p_{L,n}$ become positive in decreasing order of spin. In particular, at some point, all the $p_{n,k}$ coefficients will have become positive except $p_{n,0}$.

The important point is that right before $p_{n,0}$ turns positive (when $x_{n-1,n}$ becomes negative), $c_{n,0}$ will become positive by continuity, as only the first term in (2.27) remains negative. Thus, at large d, $c_{n,0}$ becomes positive when

$$d = \frac{p_{n,2}}{-p_{n,0}}. \tag{2.28}$$

Since $p_{n,0}$ is small and negative, d is large as expected. As all the other $c_{n,L}$ coefficients do not receive contributions from $p_{n,0}$, we see that the coefficient $c_{n,0}$ is the last one to become positive and thus the scalar ghosts are the ones defining the transition to the unitary regime in the large d limit.

Finally, similar arguments show that this ratio decreases as $n \to \infty$ and therefore the limit curves enveloppes the region of unitarity of the amplitude, and thus yields a lower bound for the critical dimension that matches nicely the numerical results at large d, as is shown in figure (2.4)

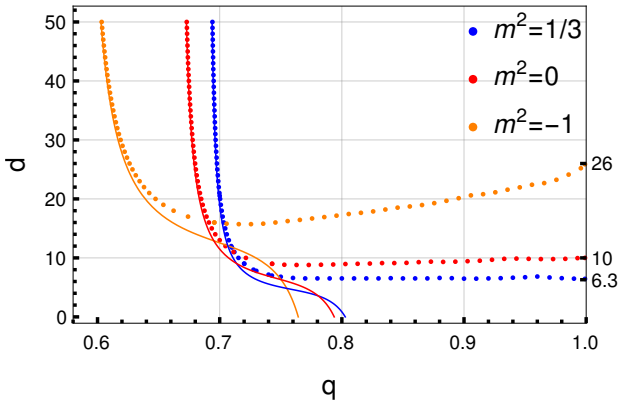


Figure 2.4.: Dots: Constant m^2 curves from the critical surface mapped in figure (2.4). Solid lines: Large d envelope given by $\lim_{n\to\infty} -p_{n,2}/p_{n,0}$.

While this analysis only holds at large d, our numerics show that this continues to be the case at finite values of the dimension. This evidence that the ghost sector is the one that determines the unitarity of the Coon amplitude could be a guide in finding an analytical proof of its positivity above $q_c(m^2)$, and therefore to prove the positivity of the Veneziano amplitude below the critical dimension in terms of the amplitude only, without reference to the worldsheet theory. This would complete recent the progress in this direction done in [136], where the positivity of the residues of the Veneziano amplitude was shown via other methods for $d \leq 6$.

2.2.2. Low energy expansion and EFT-hedron

As was mentioned in the previous chapter, recent times have witnessed a renewal of activity revolving around implications of dispersion relations, crossing symmetry and unitarity for low energy EFTs. Following the ideas of [138], various studies explored how the Wilson coefficients of weakly coupled EFTs are constrained and live inside a positive region in the space of Wilson coefficients sometimes dubbed "EFThedron" [59–63, 65–68, 101–112].

In this section, we compute the first few low energy couplings of the Coon amplitude. Because the Coon amplitude is well behaved at infinity, and respects analyticity and crossing, it admits dispersion relations and must fall in those positivity regions. We will see that the couplings indeed draw 1-dimensional varieties within those regions, parametrized by the value of q.

2.2.2.1. Wilson coefficients of the Coon amplitude

The first amplitude we consider is an (s,t,u) symmetric version of Coon, for external *massless* scalars ($m^2 = 0$) with no color indices:

$$M_q(s,t,u) = A_q(s,t) + A_q(t,u) + A_q(u,s) \tag{2.29}$$

The (s,t,u) symmetry allows to expand at small s,t,u thisfunction in terms of the variables $\sigma_2 = s^2+t^2+u^2$ and $\sigma_3 = stu$, as these two terms generate all the stu symmetric polynomials constrained to $s+t+u=0$. We therefore have that

$$M_q(s,t,u) = \frac{1}{s} + \frac{1}{t} + \frac{1}{u} + g_0(q) + g_2(q)\sigma_2 + g_3(q)\sigma_3 + g_4(q)(\sigma_2)^2 + \dots, \tag{2.30}$$

where the coefficients of this expansion are classically interpreted as low energy Wilson coefficients.

After a lengthy but straightforward explicit calculation involving Taylor expanding the factors in the infinite product in eq. (2.1) we obtained the first few Wilson coefficients up to $g_4(q)$. Trivially, $g_0(q) = 1-q$. The next ones are given by functions related to q-deformations of the values of the Riemann zeta function, referred to as q-zeta values [5]. For instance, $g_2(q)$

[5] A q-deformation or q-analog of a mathematical expression or theorem is simply a generalization involving a parameter q that returns the original object in the limit $q \to 1$. The simplest example are the q-integers $[n]_q \equiv \frac{1-q^n}{1-q}$, which satisfy $\lim_{q\to 1}[n]_q = n$, $n \in \mathbb{Z}$.

reads

$$g_2(q) = \frac{1}{2}(q-1)^3\left(3h_1(q) + 5h_2(q) + 2h_3(q)\right) - \frac{(q-1)^3}{\log(q)} \tag{2.31}$$

where

$$h_m(q) = \sum_{n=1}^{\infty} \frac{q^{nm}}{(1-q^n)^m} := \mathrm{Li}_m(q^m; q), \tag{2.32}$$

can be written in terms of q-deformed polylogarithms as defined for instance in [139] as

$$\mathrm{Li}_{n_1,\ldots,n_m}(z_1,\ldots,z_m;q) = \sum_{0<k_1<\cdots<k_m} \frac{z_1^{k_1}\ldots z_m^{k_m}}{(1-q^{n_1})^{k_1}\ldots(1-q^{n_m})^{k_m}}, \tag{2.33}$$

which yield the standard polylogarithms $\mathrm{Li}_{n_1,\ldots,n_m}(z_1,\ldots,z_m)$ as $q \to 1$ and whose values at $z_i = 1$ correspond to q-zeta values, i.e. q-deformations of the Riemman zeta values $\zeta(n_1,\ldots,n_m) = \mathrm{Li}_{n_1,\ldots,n_m}(1,\ldots,1)$. It is interesting to note that in contrast to the situation in string theory, in which only functions of the same transcendentality contribute at each given order of the low energy expansion, in the case of Coon different orders of q-transcendentality appear to be mixed. Similarly, the expressions for the higher orther couplings $g_3(q)$ and $g_4(q)$ are

$$\begin{aligned} g_3(q) =& -\frac{3}{2}(q-1)^4\left(h_1(q)^2 + 2\left(h_2(q)+1\right)h_1(q) + h_2(q)\left(h_2(q)+3\right) - h_4(q)\right) \\ &+ \frac{(q-1)^4\left(12\left(h_1(q)+h_2(q)\right)+7\right)}{4\log(q)} - \frac{3(q-1)^4}{2\log^2(q)}, \end{aligned} \tag{2.34}$$

and

$$\begin{aligned} g_4(q) =& \frac{1}{8}(q-1)^5\left(h_1(q)^2 + 2\left(h_2(q)+3\right)h_1(q) + h_2(q)\left(h_2(q)+21\right) + 28h_3(q)\right. \\ &\left. + 17h_4(q) + 4h_5(q)\right) + \frac{(q-1)^5\left(-12\left(h_1(q)+h_2(q)\right)-11\right)}{48\log(q)} + \frac{(q-1)^5}{8\log^2(q)}. \end{aligned} \tag{2.35}$$

We also verified that when $q \to 1$, they Wilson coefficients descend to the values given by the symmetrized sum $A^V(s,t) + A^V(t,u) + A^V(u,s)$:

$$g_2(1) = -\zeta_3,\ g_3(1) = 9/4\ \zeta_4,\ g_4(1) = -\zeta_5/2 \tag{2.36}$$

For the scattering of massless scalars in generic EFTs, the allowed range of coefficients g_2, g_3, g_4 was determined in [101], figure 8, in terms of dimensionless ratios $\tilde{g}_3 = g_3 M^2/g_2$ and $\tilde{g}_4 = g_4 M^4/g_2$ with M^2 given by the scale of the first massive mode, which in our conventions is $M^2 = 1$. We show in figure 2.5 the value of those ratios. They fall neatly in the domain determined in [101], albeit approaching tangentially the boundary at intermediate values of q.

One could also couple a massless scalar to a *massive* Coon amplitude by assuming that the external massless scalar does not self interact and thus does not correspond to any of the poles in the amplitude. As q goes from 1 to 0, these amplitudes reduce to the the extreme case of [101], coupling the massless scalar to a single massive scalar of mass $M^2 = m^2$. This was identified as the extremal amplitude located at tue upper right corner of their allowed region, and therefore simply accumulate to the upper right corner of figure (2.5).

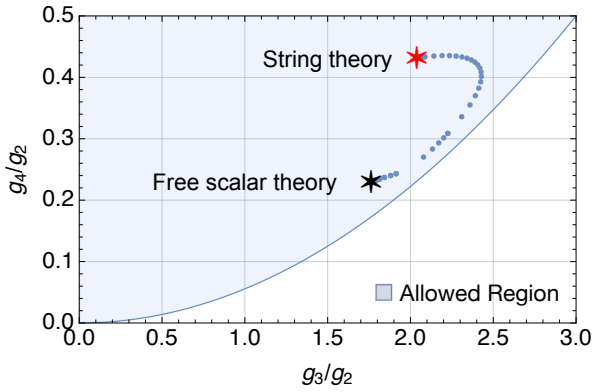


Figure 2.5.: Plot of Wilson coefficients with cut-off $M^2 = 1$, superposed with their allowed region determined in [101].

2.2.2.2. Low spin dominance

In the work [105], Bern, Kosmopoulos and Zhiboedov used dispersion relations and crossing symmetry to put bounds on the EFT coefficients for the $2 \to 2$ scattering of gravitons, and observed that the values of the coefficients corresponding to known, physical theories such as those arising from field and string theory live in a very small region of the in principle allowed space. Moreover, they identified a principle that allows to single out such region: The amplitudes residing in the small *theory island* satisfy the property of *low spin dominance* (LSD), meaning that their lowest-spin partial waves dominate the disperssive representation of their EFT coefficients. In [105] it was also shown that island determined by low spin dominance is almost one dimensional and extremely well approximated by a line in the space of Wilson coefficients, that we will referr to as the LSD line.

In this section we show how the Coon amplitude $A_q(s,t)$, together with its Veneziano limit, exhibit a form of low spin dominance, albeit weaker than that of [105]. In the case of the Coon amplitude not only the scalar state dominates the partial waves, but also the spin 1 state. Let us explain how this comes about.

Following the conventions of [105], we Taylor expand the amplitude as

$$A_q(t,-s-t) = \frac{1}{s} + \frac{1}{t} + \sum_{p<k} a_{k,p} s^{k-p} t^p. \tag{2.37}$$

Notice that we work again with the color-ordered amplitude $A_q(s,t)$, and not with the *stu*-symmetric version from last section. To compare to [105], we look at the Wilson coefficients $a_{k,p}$ in eq. (2.37) with $k = 2,4,6$, which we compare to those of amplitudes given by the exchange of a single spin J state at the cutoff mass M^2, with $J = 0,1$:

$$A^{(J)}(t,u) = (-1)^J \frac{\mathcal{P}_J(1+2s/M^2)}{t-M^2} + \frac{\mathcal{P}_J(1+2t/M^2)}{u-M^2}, \quad J = 0,1. \tag{2.38}$$

Consider a model in which only this two spins contribute to the amplitude as $A^{(\mathrm{LSD})}(t,u) = A^{(0)}(t,u) + q\, A^{(1)}(t,u)$, which satisfies pure low spin dominance at $q = 0$ but departs from it as q is turned on by recieving contributions from the spin 1 state. Since at $q = 0$ the Coon

amplitude represents the exchange of a single scalar, it will necessarily match this model (and pure LSD) for q=0.

Denoting by $a^{(J)}_{k,q}$, $J = 0, 1$, the low energy coefficients corresponding to expanding the $A^{(J)}(t, u)$ amplitudes in powers of s, t, this model will have $a_{k,p} = a^{(0)}_{k,p} + q\, a^{(1)}_{k,p}$. This linear dependence of the coefficients on q determines the straight yellow line in fig. 2.6, where different ratios of coefficients $a_{k,p}$ are shown. The blue dots correspond to the Wilson coefficients of the Coon amplitude for different values of q, starting from those of the Veneziano amplitude with $q = 1$ in the center of the plot, and moving towards the gray line corresponding to pure the pure low spin dominance when $q = 0$, as expected since only $J = 0$ contributes. We

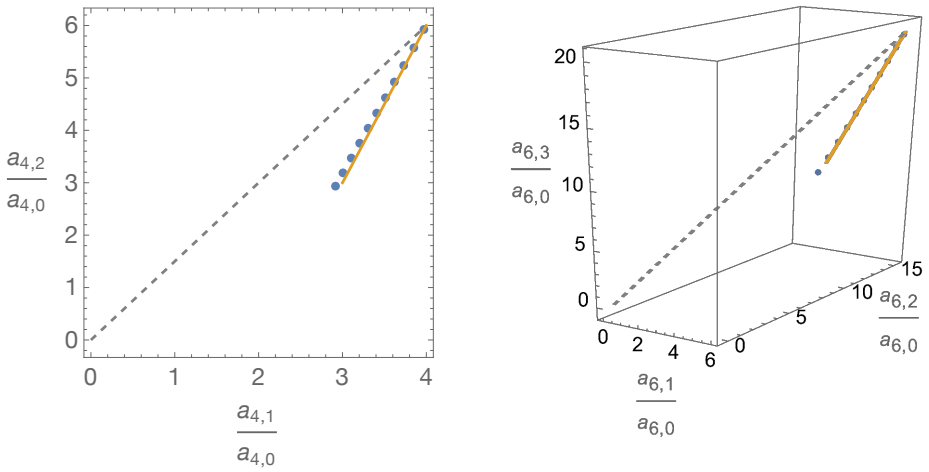


Figure 2.6.: Plots of a_4 and a_6. Gray dashed: LSD. Yellow: spin 0,1 model. Blue dots: actual points. Veneziano is in the middle of the graph ($q = 1$) and the scalar theory is at the intersection with LSD.

find that for intermediate values of q the EFT coefficients of the Coon amplitude are very well approximated by this spin 0-1 model, and thus satisfies the weaker form of low spin dominance alluded to previously.

This behavior is nothing but the well known property of Vector Meson Dominance satisfied by QCD, in which the largest contribution to the low energy dynamics comes from the spin 1 ρ meson. While it has been used very succesfully as an empirical observation since decades, it has recently been given a theoretical explanation in [62]. In this work the authors found that the standard bootstrap axioms imply that the couplings of higher spin states to an external scalar must decrease with spin, and therefore what we observe is a manifestation of this phenomenon.

Within this spin 0-1 model, it is immediate to verify that

$$\frac{a_{2,1}}{a_{2,0}} = \frac{2-2q}{1+q}, \tag{2.39}$$

$$\frac{a_{4,1}}{a_{4,0}} = \frac{2(q+2)}{q+1}, \quad \frac{a_{4,2}}{a_{4,0}} = \frac{6}{q+1}. \tag{2.40}$$

For $q \in [0, 1]$, this implies in particular that $0 \leq \frac{a_{2,1}}{a_{2,0}} \leq 1$ $3 \leq \frac{a_{4,1}}{a_{4,0}} \leq 4$ and $3 \leq \frac{a_{4,2}}{a_{4,0}} \leq 6$. The upper bound correspond to pure LSD, while the lower bound is pure spin-0 + spin-1 model.

While for the coefficients $a_{2,1}/a_{2,0}$, the bounds are exactly satisfied, at $k = 4$ it can be seen that string theory lies a bit away from that, at $(\frac{a_{4,1}}{a_{4,0}}, \frac{a_{4,2}}{a_{4,0}}) \simeq (2.9, 2.9)$.

The relative accuracy of the model is explained by the fact that as can be seen from the Gegenbauer expansion of the residues of the Coon amplitude, the spin J exchanges have coefficients proportional to $q^{J(J+1)/2}$, which clearly shows that away from $q = 1$ the higher spin contributions are strongly suppressed, and thus the linear approximation (spin 0 and 1) is a good approximation.

2.2.3. Impact parameter representation of the Coon amplitude

Continuing the characterization of the Coon amplitude, in this subsection we introduce its impact parameter representation.[6] The impact parameter representation of scattering amplitudes is defined as the Fourier transform of the amplitude $\mathcal{A}(s,t)$ with respect to the momentum transfer in the direction orthogonal to the scattering axis $\vec{k}_\perp$. In the small momentum transfer limit $\frac{-t}{s} \ll 1$, the momentum transfer $k = p_3 - p_1$ is almost perpendicular to the direction of motion of the scattered particles, and therefore we can approximate

$$t = -k^2 \sim -\vec{k}_\perp^2 \,.$$

For s fixed and $d = 4$ for simplicity we have

$$\mathcal{A}\left(s,b\right) = \frac{1}{2s}\int \frac{d^2k_\perp}{(2\pi)^2} e^{-ik_\perp b}\mathcal{A}\left(s, -\vec{k}_\perp^2\right), \tag{2.41}$$

where b is the impact parameter, i.e. the minimal distance between the scattered wave-packets.

The decay of the interaction as a function of b can give us an idea of the type of object that we are scattering. For example, the scattering of massive particles of mass m results in an Yukawa-like exponentially decaying amplitude in impact parameter space

$$\mathcal{A}_{\text{massive}}\left(s,b\right) \sim e^{-mb}, \tag{2.42}$$

while the scattering of strings at tree-level yields a Gaussian amplitude

$$\mathcal{A}_{\text{strings}}\left(s,b\right) \sim e^{\frac{-b^2}{4\alpha' \log s}}. \tag{2.43}$$

We obtained an analytic approximation to the impact parameter representation of the Coon amplitude at high energies by inserting its Regge limit in eq. (2.41) and evaluating the integral via a saddle point approximation in which the saddle point k_o is located at

$$k_o = -\frac{i\left(\sqrt{b^2 t_* \log^2 q + \log^2 s} - \log s\right)}{b \log q}, \tag{2.44}$$

where $\sqrt{t_*}$ corresponds to the accumulation point energy.

[6] Note that this results were not presented in [1].

Considering the large b limit of this result yields

$$\hat{A}_q(s,b) \sim \left(\frac{b}{\sqrt{t_*}}\right)^{-\frac{\log s}{\log q}} e^{-b\sqrt{t_*}}, \quad t_* = m^2 + \frac{1}{1-q}, \tag{2.45}$$

where $b \gg \frac{1}{\sqrt{t_*}}$. This result shows that for $0 < q < 1$, the Coon parton is seen at leading order in large impact parameter as a point-like particle with mass equal to the accumulation point energy $\sqrt{t_*}$, and the leading effect of the infinite number of energy levels below t_* causes a power law correction to this Yukawa term (at fixed energy).

It is important to notice that the asymptotic expression given in eq. (2.45) breaks down for $q = 1$ and $q = 0$, where we recover the Gaussian behaviour characteristic of string scattering amplitudes in the first case and a Yukawa potential associated to the mass of the external states in the last.

To extract the effective size of the Coon parton we cannot however make use of the expression given in eq. (2.45), as it is valid only for large b and therefore it does not provide a good description of the amplitude at the scales relevant for this purpose. More explicitly, defining the effective length of the Coon parton as the value $b_{\frac{1}{2}}$ at which the impact parameter amplitude reduces its size by half compared to its value at 0, one can verfy that $b_{\frac{1}{2}}$ always lies below t_*.

To have access to these length scales we solved numerically the equation

$$\hat{A}_q(s, b_{\frac{1}{2}}) = \frac{1}{2}\hat{A}_q(s,0), \tag{2.46}$$

obtaining $b_{\frac{1}{2}}$ for different values of q and s. The results are shown in the left panel of figure (2.7).

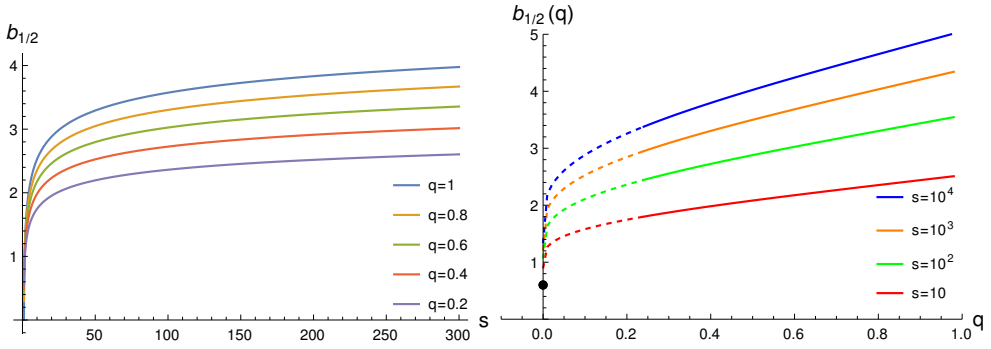


Figure 2.7.: **Left:** Position of the half maximum $b_{\frac{1}{2}}$ for $m^2 = 1/3$ and various values of q. The value of $b_{\frac{1}{2}}$ and thus the size of the Coon parton at a given s decreases as q goes from 1 to 0. **Right:** $b_{1/2}(q)$ for fixed values of s and $m^2 = 1/3$. The dashed lines signal the region where the saddle point approximation deviates significantly from the full impact parameter representation of the amplitude, and the solid black dot shows the $q \to 0$ limit of $b_{1/2}$ expected from eq. (2.42). The $q \to 0$ and $q \to 1$ limits give values consistent with eq. (2.42) and eq. (2.43), implying that varying q smoothly interpolates between particle and string behaviour and that even in the small q region the saddle point seems to provide a good qualitative description of the relevant physics.

One can already see from these results that the size of the Coon parton is a decreasing function of q. To study the dependence of $b_{\frac{1}{2}}$ on q we computed $b_{\frac{1}{2}}(q)$ for different fixed values of s. We show this explicitly for $m^2 = 1/3$ in the right panel of figure (2.7).

As $q \to 1$ the value of the half maximum scales increases linearly with q and matches that of string theory given in eq. (2.43) at $q = 1$. In particular, it grows with the energy as $\log s$ to some power, as obvious from the graph. It can be seen that $\sqrt{\log s}$ provides a good fit, and therefore the length $\ell_C$of the Coon parton is of the qualitative form

$$\ell_C \simeq \ell_0 + q\sqrt{\log(s)}. \tag{2.47}$$

The small q region of the plot is shown in dashed lines because below $q \sim 0.2$ the saddle point approximation ceases to accurately describe the amplitude. However, it still provides a good qualitative description, showing how when $q \to 0$ the s dependence disappears and all curves converge to the same limiting value of $b_{\frac{1}{2}}$ consistent with eq. (2.42), shown in black, as should be the case for the exchange of a single massive particle. This is in consonance with the previously stated idea that the Coon amplitude interpolates between strings and particles when varying q from 0 to 1 and shows that we can identify the q-deformation parameter with the size of the Coon parton. This gives a novel physical meaning to the mysterious deformation parameter q, and more generally a physical potential interpretation for the parameter q of q-deformed theories. It would be interesting to deepen this point further.

2.3. Attempting to extend Coon's method

As was alluded to before, Coon's original work had another interesting aspect besides the amplitude itself. In his paper, Coon came up with an interesting bootstrap method to build dual model amplitudes by writing an infinite product ansatz for a function with infinitely many zeros and poles and demanding that the residues have the features required to yield a local amplitude. In this section we briefly review Coon's method and explore possible extensions to bootstrap more general amplitudes. However, as will be explained, we find that using a more general ansatz still does not produce new solutions apart from the known Coon and Veneziano amplitudes.

2.3.1. Brief review of Coon's derivation of the Coon amplitude

We start by presenting Coon's method to obtain a generalization of the Veneziano amplitude. The basic idea is to use the fact that a meromorphic function (such as tree-level amplitudes) is characterized by its poles and zeros, and thus it is possible to write them as an infinite product of the form[7]

$$A(s,t) = \prod_{n=0}^{\infty} \frac{\text{zero}_n(s)\,\text{zero}_n(t)}{\text{pole}_n(s)\,\text{pole}_n(t)}, \tag{2.48}$$

[7] This is simply a consequence of the Weierstrass factorization theorem. See [44] for a recent short review of the theorem and its application to dual models.

where $\text{zero}_n(x)$, $\text{pole}_n(x)$, $n = 0, \ldots, \infty$ list all the zeros and poles of the amplitude in a given variable. Since both channels have the same functions for the zeros and poles this form is manifestly crossing symmetric and meromorphic by construction.

Based on this, Coon proposed an ansatz in which the zeros and poles only depended linearly on s and t:

$$A(s,t) = \prod_{n=0}^{\infty} \frac{\alpha_n s + \beta_n t + \gamma_n st - \lambda_n}{(s - m_n^2)(t - m_n^2)}, \tag{2.49}$$

where α_n, β_n, γ_n and λ_n are parameters that fix the location of the zeros of the amplitude and m_n^2 are the poles. Demanding crossing symmetry implies $\alpha_n = \beta_n$, and having only a finite number of intermediate states exchanged at each given pole requires the residues to be polynomials. The crucial point is that the polynomiality of the residues at a given pole requires the cancellation of an infinite number of terms between the numerator and the denominator of the infinite product. If one succeeds in building an amplitude this way then it is guaranteed by construction that the amplitude will satisfy the required constraints to be a good dual model amplitude.

The residue the amplitude at $s = m_k^2$ can be extracted to be (setting $\alpha = \beta$)

$$A(s,t) \propto \prod_{n=0}^{\infty} \frac{\alpha_n (m_k^2 + t) + \gamma_n m_k^2 t - \lambda_n}{(t - m_n^2)}. \tag{2.50}$$

One sufficient condition for this residue to be a polynomial of degree k in t is that the infinite product starting from $n = k$ in the numerator is exactly cancelled by all the t-channel poles in the denominator. This precisely happens for the Veneziano amplitude for instance.

To enforce this one, would be tempted to simply shift the n index in the numerator to get something like

$$A(s,t) \propto \prod_{n=0}^{k-1} \left(\alpha_n m_k^2 + \beta_n t + \gamma_n m_k^2 t - \lambda_n\right) \prod_{n=0}^{\infty} \frac{\alpha_{n+k}(m_k^2 + t) + \gamma_{n+k} m_k^2 t - \lambda_{n+k}}{t - m_n^2}. \tag{2.51}$$

However, one is only allowed to do this if both the numerator and the denominator are independently convergent infinite products. This has been a source of confusion in the literature, particularly with respect to the non-locality of the Coon amplitude in the regime with accumulation points, since it was this type of reasoning that led to the neglection of the non-meromorphic factor needed to render the amplitude local in the early works.

To fix this issue we simply write the amplitude in a manifestly convergent form that has the same zeros and poles:

$$A(s,t) = \prod_{n=0}^{\infty} \frac{1 - (s+t)a_n - stb_n}{(1 - s/m_n^2)(1 - t/m_n^2)}, \tag{2.52}$$

where a_n and b_n can be related to α_n, γ_n and λ_n and should go to zero as n goes to infinity fast enough to have a convergent product.

Now we are allowed to split the product evaluated at the pole as

$$A(s,t) \propto \prod_{n=0}^{k-1} \left(1-(m_k^2+t)a_n + m_k^2 b_n t\right) \prod_{n=0}^{\infty} \frac{1-(m_k^2+t)a_{n+k} + m_k^2 b_{n+k} t}{1-t/m_n^2}. \tag{2.53}$$

For eq. (2.53) to be a polynomial we need to cancel the t dependence on the infinite product on the right, which means that $t = m_n^2$ must be a zero of the numerator at each term, yielding the condition

$$1-(m_k^2+m_n^2)a_{n+k} + m_k^2 m_n^2 b_{n+k} = 0, \tag{2.54}$$

for each k and n. In other words, finding the non-trivial sequences $(a_n)_{n\geq 0}, (b_n)_{n\geq 0}, (m_n^2)_{n\geq 0}$ that satisfy the equation above provides a scattering amplitude with local residues.

With a bit of thought, this equation can be solved directly. Indeed one looks for relations between functions $p(n)p(k)$, $p(n)+p(k)$ and functions (a or b) $f(n+k)$. Linear relations alone select the Virasoro spectrum, and product relation select an exponential, Coon-like spectrum. The mixed case involves a combination of both, and for instance the tanh function satisfies the familiar identity

$$\tanh(x+y) = \frac{\tanh(x)+\tanh(y)}{1-\tanh(x)\tanh(y)} \tag{2.55}$$

so one could envisage that some combination of hyperbolic trigonometric functions should play a role in the solution. A few more lines of algebra should yield the Coon's solution. However, Coon's idea to solve it is more elegant and more systematic. He promotes a_n, b_n, and m_n^2 to functions of a continuous variable n, and makes use the fact that the coefficients a and b appear in this equation only depending on $k+n$ and not on k and n separately to obtain a differential equation on the poles *alone*.

To do so, he defines $u = k+n$ to get

$$1-(m_{u-n}^2+m_n^2)a_u + m_{u-n}^2 m_n^2 b_u = 0. \tag{2.56}$$

As the functions a_u and b_u don't depend on n, we can differentiate once and twice eq. 2.56 with respect to n to obtain new equations relating a_u and b_u to m^2 and its derivatives, given by

$$-(-p'_{u-n}+p'_n)a_u + (-p'_{u-n}p_n + p_{u-n}p'_n)b_u = 0. \tag{2.57}$$

$$-(p''_{u-n}+p''_n)a_u + (p''_{u-n}p_n + p_{u-n}p''_n)b_u = 0. \tag{2.58}$$

Solving for the coefficients and substituting them in 2.56 yields a differential equation for p_n as a function of n of the form

$$\mathcal{D}_k m_k^2 = \mathcal{D}_n m_n^2, \tag{2.59}$$

where $\mathcal{D}_x$ is the Schwarzian derivative, $\mathcal{D}_x f(x) = \frac{f'''(x)}{f'(x)} - \frac{3}{2}\left(\frac{f''(x)}{f'(x)}\right)^2$.

The separation between the independent variables k and n implies that each side of the equation must be constant. Solving the equation

$$\mathcal{D}_n p(n) = \text{constant}$$

yields the most general function m_n^2 compatible with the cancellation condition, which Coon found to be of the form

$$m_n^2 = c_1 + \frac{c_2}{1 - c_3 e^{kn}}, \tag{2.60}$$

with c_1, c_2, c_3 and k constants. This function is indeed related to the hyperbolic trigonometric functions mentioned above.

This solution for the location of the poles can be then substituted in the equations for the coefficients, and one is able to construct the full amplitude. Choosing the values of the constants appropriately, one recovers the Coon and Veneziano ($k = 0$ case) amplitudes.

One can easily show that this solution for m_n^2 contains the Coon and Veneziano spectrums for the appropriate choice of integration constants, and also from this procedure one concludes that this class of spectrums exhausts all the possible amplitudes that can be obtained from the ansataz (2.50), up to shifts in the pole cancellation condition.

2.3.2. Generalization to double-pole products

Given the success of Coon's method, it is natural to try to extend it to find new dual model amplitudes. One possible generalization, which we investigated, is to increase the degree of the polynomial factors in the numerator in (2.50). This produces more ansatz coefficients, and in principle could give more generic solutions. Since a tree-level amplitude must have single poles only as singularities, demanding polynomiality of the residues at each pole in s or t will still require various poles to cancel each factor in the numerator.

We therefore investigated the case where the factors in the numerator are quadratic in $s$and t. One immediate consequence is that, on a given pole, say in s, the residue is given by an infinite product of the form

$$\prod \frac{1 + b_n t + c_n t^2}{1 - t/p(n)} \tag{2.61}$$

The only way for this infinite product to reduce to a simple polynomial in t is to have a cancellation between each numerator factor and **two** denominator factors. By analogy to the linear case, we take the denominator factors to follow each other, so that the $2n$-th and $2n+1$-th poles cancel the n-th numerator.[8] We then arrive at what seems to be the most general crossing symmetric ansatz at quadratic order, given by

$$\prod_{n=0}^{\infty} \frac{\big(1 - stb(2n) - s^2t^2c(2n) - (s^2t + st^2)d(2n) - (s^2 + t^2)e(2n) - (s + t)f(2n)\big)}{(1 - s/p(2n))(1 - s/p(2n+1))(1 - t/p(2n))(1 - t/p(2n+1))}, \tag{2.62}$$

At this point, it is worth noting that instead of considering one family of poles $p(n)$ with cancelation through p_{2n}, p_{2n+1}, we also considered having two distinct families, $p_n, \tilde{p}_n$, but

[8] This does not seem to imply a loss of generality, as it appears to be a simple relabeling of the poles.

the residues conditions essentially force these families to obey exactly the same equations and it did not seem to us that new solutions could arise.

Now we proceed in an analogous way as before: we require that on a given pole $s = p(k)$, the residue of the amplitude is a polynomial of degree k in t. We extract the first k terms of the product and impose that the rest of the infinite product cancels in the same way as in the previous example. However for double poles there is a subtlety. When evaluating s at a pole, each term in the numerator is a polynomial of degree 2 in t, and so the product of any number of them will yield an even degree polynomial. At even poles, i.e. $s = p(2k)$, this poses no problem and the generalization of the single-pole to the double-pole case is straightforward, requiring both $t = p(2n)$ and $t = p(2n + 1)$ to be zeros of the numerator evaluated at $s = p(2k)$:

$$\begin{aligned} 1 - p(2k)p(2n)b(2n+2k) - p(2k)^2p(2n)^2c(2n+2k) \\ -(p(2k)^2p(2n) + p(2k)p(2n)^2)d(2n+2k) \\ -(p(2k)^2 + p(2n)^2)e(2n+2k) - (p(2k) + p(2n))f(2n+2k) = 0. \end{aligned} \tag{2.63}$$

$$\begin{aligned} 1 - p(2k)p(2n+1)b(2n+2k) - p(2k)^2p(2n+1)^2c(2n+2k) \\ -(p(2k)^2p(2n+1) + p(2k)p(2n+1)^2)d(2n+2k) \\ -(p(2k)^2 + p(2n+1)^2)e(2n+2k) - (p(2k) + p(2n+1))f(2n+2k) = 0. \end{aligned} \tag{2.64}$$

However, on an odd pole $s = p(2k + 1)$ the residue must be a polynomial of degree $2k + 1$, and therefore we need to "borrow" a power of t from the first left-over term in the infinite product in the numerator, causing a shift in the way in which the poles cancel the remaining terms. Equivalently, on $s = p(2k + 1)$, we extract from the quadratic polynomial in t the first root, and add it to the residue polynomial function.

Overall, for odd poles we get the following conditions:

$$\begin{aligned} 1 - p(2k+1)p(2n+1)b(2n+2k+2) - p(2k+1)^2p(2n+1)^2c(2n+2k+2) \\ -(p(2k+1)^2p(2n+1) + p(2k+1)p(2n+1)^2)d(2n+2k+2) \\ -(p(2k+1)^2 + p(2n+1)^2)e(2n+2k+2) - (p(2k+1) + p(2n+1))f(2n+2k) = 0, \end{aligned} \tag{2.65}$$

$$\begin{aligned} 1 - p(2k+1)p(2n+2)b(2n+2k+2) - p(2k+1)^2p(2n+2)^2c(2n+2k+2) \\ -(p(2k+1)^2p(2n+2) + p(2k+1)p(2n+2)^2)d(2n+2k+2) \\ -(p(2k+1)^2 + p(2n+2)^2)e(2n+2k+2) - (p(2k+1) + p(2n+2))f(2n+2k) = 0. \end{aligned} \tag{2.66}$$

It is easy to see that the first equation for the odd poles (eq. 2.65) is the same as the first equation for the even poles (eq. 2.63) with $n \to n + 1/2$, $k \to k + 1/2$, and therefore the polynomiality requirement enforces three independent constraints on the poles and the coefficients, namely equations 2.63, 2.64, 2.66.

While the equation (2.56) was simple enough and only required finding functions possessing functionnal relations between $f(x+y)$, $f(x)+f(y)$ and $f(x)f(y)$, which are easily realised to be related to the function $\tanh(x)$, we are now facing a much more complicated beast, which cannot be solved by naked eye. So we need to follow Coon's systematic strategy.

As we have six unknowns (the five coefficients in the numerator plus the poles) we need to find three extra independent equations. We'll follow the same strategy as before and take derivatives with respect to n upon performing the change of variables $k \to u - n$. Taking the first derivative of each constraint gives us enough equations to solve for the p's, arriving at a differential equation that the poles need to satisfy.

Before going into that, it is worth mentioning that if we restrict our ansatz by setting some of the coefficients to zero from the start, we need less independent equations and thus the system is more easily solved. In particular, if we only keep two non-zero coefficients the equations coming from the cancellation conditions are enough to solve the system, and one can check that in this case the only allowed solutions are Coon and Veneziano expressed in double-pole product form.

2.3.3. The differential equation in the double-pole product ansatz

Solving the system of equations given by equations 2.63, 2.64, 2.66 and their first derivative with respect to n, we arrive to the following differential equation for p:

$$\frac{(p(2k)-p(2k+1))(p(2k)-p(2n))p'(n)}{\mathcal{D}(p,p',n,k)}\mathcal{N}(p,p',n,k)=0, \tag{2.67}$$

with

$$\begin{aligned}
\mathcal{N}(p,p',n,k) &= p(2k)p(2n+1)(p(2k)-p(2n+1))\left(p'(2k+1)-p'(2n)\right)\\
&+p(2n)^2\left(p(2k)\left(p'(2k+1)+p'(2n+1)\right)-p(2n+1)\left(p'(2k)+p'(2k+1)\right)\right)\\
&+p(2n)\Big(p(2n+1)^2\left(p'(2k)+p'(2k+1)\right)-p(2k)^2\left(p'(2k+1)+p'(2n+1)\right)\Big)\\
&+p(2k+1)^2\left(p(2n+1)\left(p'(2k)+p'(2n)\right)+p(2n)\left(p'(2n+1)-p'(2k)\right)-p(2k)\left(p'(2n)+p'(2n+1)\right)\right)\\
&+p(2k+1)\Big(p(2k)^2\left(p'(2n)+p'(2n+1)\right)-p(2n+1)^2\left(p'(2k)+p'(2n)\right)+p(2n)^2\left(p'(2k)-p'(2n+1)\right)\Big),
\end{aligned}$$

and

$$\begin{aligned}
\mathcal{D}(p,p',n,k) &= p(2k+1)p(2n)^3p(2n+1)^2p'(2k)-p(2k)p(2n)^2p(2n+1)^2(p(2k+1)+p(2n))p'(2k)\\
&+p(2k)^4\Big((p(2k+1)p(2n)-p(2n+1)(p(2k+1)+p(2n)))p'(2n)-p(2n)^2p'(2n+1)\Big)\\
&+p(2k)^3(p(2k+1)+p(2n))\Big(p(2n)^2p'(2n+1)+p(2n+1)^2p'(2n)\Big)\\
&+p(2k)^2p(2n)\Big(p(2n+1)^2\left(p(2n)p'(2k)-p(2k+1)p'(2n)\right)-p(2k+1)p(2n)^2p'(2n+1)\Big).
\end{aligned}$$

From eq. (2.67), assuming that $p(x)$ is not constant, we can focus on finding solutions to the differential equation

$$\mathcal{N}(p,p',n,k)=0, \tag{2.68}$$

which will be solutions to the full differential equation as long as they are not solutions of

$$\mathcal{D}(p, p', n, k) = 0.$$

The differential equation $\mathcal{N}(p, p', n, k) = 0$ seems daunting at first sight. It is not at all obvious that it can be split into an n-independent and a k-independent part as it happened in the simpler case considered by Coon, and the shift induced by the even and odd pole cancellation conditions cause the differential equation to involve $p(n)$ and $p(k)$ at shifted values (i.e. it involves for example $p(2n)$ and $p(2n+1)$).

To deal with this last issue, we assume that the differential equation is valid for arbitrary shifts and not only when shifting $2n$ by 1.[9] We then perform the following replacement in eq. (2.68):

$$2n + 1 \to 2n + \epsilon, \quad 2k + 1 \to 2k + \epsilon,$$

followed by an expansion around $\epsilon = 0$ to obtain a differential equation without shifted variables by setting to zero the first non-zero term in the expansion.[10] Of course, one will then need to check that the solutions obtained under this assumption still satisfy the original differential equation.

Writing $2n = x$ and $2k = y$, this yields

$$\begin{aligned} -6p'(x)p'(y)\Big((p(x)+p(y))\left(p''(x)+p''(y)\right)+p'(x)^2-p'(y)^2\Big) \\ +(p(x)-p(y))^2\left(p^{(3)}(x)p'(y)-p^{(3)}(y)p'(x)\right)=0 \end{aligned} \tag{2.69}$$

Massaging eq. (2.69) by taking appropriate combinations of derivatives with respect to x and y and multiplying by the right factors at each step, we managed after several attemps to decouple the x and y dependence, arriving at our final and simplest differential equation:

$$\frac{p'''(x)}{p'(x)} = c_1 p(x) + c_2, \tag{2.70}$$

where c_1 and c_2 are arbitrary integration constants. The linear and exponential spectrums of the Veneziano and Coon amplitudes are obtained by setting $c_1 = 0$, $c_2 = 0$ for the linear case and and $c_1 = 0$, c_2 arbitrary for the exponential one.

Let's focus on the $c_1 \neq 0$, $c_2 \neq 0$ case. Shifting the argument and rescaling $p(x)$ we can bring eq. (2.70) to the following form:

$$\frac{p'''(x)}{p'(x)} = 12\, p(x). \tag{2.71}$$

This is the differential equation satisfied by the Weierstrass elliptic $\wp$-function, defined in the following way: Let $\omega_1, \omega_2 \in \mathbb{C}$ be two complex numbers that are linearly independent over $\mathbb{R}$ and let $\Lambda := \mathbb{Z}\omega_1 + \mathbb{Z}\omega_2 := \{m\omega_1 + n\omega_2 : m, n \in \mathbb{Z}\}$ be the lattice generated by them.

[9] Intuitively, on can think of n and k can be large. Furthermore, the relations of the form $\exp(x)\exp(y) = \exp(x+y)$ of the type we are after never depend on special properties of x and y, in particular y to does not have to be an integer.

[10] The first non-zero term happens at order ϵ^4.

Then the $\wp$-function is given by

$$\wp\left(z,\omega_1,\omega_2\right) := \wp(z,\Lambda) := \frac{1}{z^2} + \sum_{\lambda\in\Lambda\setminus\{0\}} \left(\frac{1}{(z-\lambda)^2} - \frac{1}{\lambda^2}\right). \tag{2.72}$$

Finally, undoing the shift and rescaling we arrive at a novel solution for the pole function:

$$p(x) = c_1\wp\left(x, g_2, g_3\right) + c_0, \tag{2.73}$$

where c_0, c_1, g_2 and g_3 are arbitrary integration constants. g_2 and g_3 are called lattice invariants and define the lattice over which the $\wp$-function is periodic. They are given in terms of the lattice sites by

$$g_2 = 60 \sum_{\lambda\in\Lambda\setminus\{0\}} \lambda^{-4},$$

$$g_3 = 140 \sum_{\lambda\in\Lambda\setminus\{0\}} \lambda^{-6}.$$

We checked that this function satisfies the original shift equation (2.67), which is a very non-trivial consistency check of the details of the procedure to reach the equation.

Note that one reason why the $\wp$ function is important here is that it satisfies a non-trivial addition identity involving quadratic terms given by

$$\wp(x+y) = \frac{1}{4}\left(\frac{\wp'(x)-\wp'(y)}{\wp(x)-\wp(y)}\right)^2 - (\wp(x)+\wp(y)) \tag{2.74}$$

This equation generalizes the relation (2.55) and it is therefore not surprising that it enters in our ansatz, which involves quadratic terms.

The physical meaning of an amplitude with such spectrum is intriguing. The $\wp$-function is a doubly periodic function with periods ω_1 and ω_2, and has one double pole in every cell defined by its periods. If one period is real, say ω_1, over the reals we therefore have a periodic pole function with a double pole at all $x \simeq x + \mathbb{N}\omega_1$.

If $\omega_1 = p/q \in \mathbb{Q}$ is rational, the periodicity of the function will yield a finite set of masses with an infinite degeneracy of states at each of them, because $p(x + q\mathbb{N}) = p(x)$.

On the other hand, for irrational periods, the pole function evaluated at integer arguments covers densely a half line given by $[\min(p(x)); +\infty]$.

At first sight, this sounds pathological. But in view of the obsveration by Mizera [140] on natural boundaries for scattering amplitudes, there exists situations with dense set of singularities (cuts, in his case). Yet, the Regge trajectories for this amplitude would be very exotic, unless some kind of reshuffling is done: two consecutive levels could have arbitrarily different spin content.

Finally, note that we recover the Veneziano spectrum from this Weierstrass spectrum by a decompactification limit of the torus. To see this we just need to use the integrated version of the differential equation for the $\wp$-function (2.71), given by

$$\wp''(x) = 6\wp\left(x\right) - \frac{1}{2}g_2. \tag{2.75}$$

We can study the decompactification limit of the torus by using the change of variables $x \to \frac{y}{\lambda}$ and sending λ to 0. In this limit the y variable zooms infinitely deep into the torus and is therefore blind to its periodicity. Naturally, the differential equation goes to

$$\wp''(y) = 0, \tag{2.76}$$

yielding the linear spectrum of the Veneziano amplitude.

2.3.4. Inconsistent numerator function

The previous section was a necessary condition on the spectrum. Once the most generic solution is obtained, it still needs to be re-injected in the coefficients. The crucial test that these coefficients need to pass is that, albeit being defined by a very complicated expression given in terms of $p(n)$ and $p(k)$, they have to depend only on $n+k$, e.g., schematically, we need to have

$$b(2n+2k) = \mathcal{F}\left(p(2n), p(2k), p'(2n), p(2k+1), ...\right).$$

This is not guaranteed by the procedure, and it turns out that it was somehow a lucky accident for the Coon amplitude.

When plugging the Weierstrass spectrum into the expressions for the coefficients, we obtain very complicated expressions that in general depend separately on n and k, as well on the constants of integration c_0, c_1, g_2, g_3.

We tried to search numerically values of these such that the coefficients $b_{n+k}, c_{n+k}, \ldots$ depend only on $n+k$, with no success, as the equations are somewhat involved. A more manageable and illuminating attempt is to evaluate the equations at $n+k=0$, as this would give a more trivial way to see if such values of the constants existed. We found that the coefficients, $b_{n+(-n)}, \ldots$ still depend on n on the right-hand side, in such a way that removing the dependence would make the solution trivial. Explicitly, we found that

$$b_{n+(-n)} = -\frac{4}{(c_0 + c_1 \wp(2n, g_2, g_3))^2}, \tag{2.77}$$

$$c_{n+(-n)} = -\frac{1}{(c_0 + c_1 \wp(2n, g_2, g_3))^4}, \tag{2.78}$$

$$d_{n+(-n)} = \frac{2}{(c_0 + c_1 \wp(2n, g_2, g_3))^3}, \tag{2.79}$$

$$e_{n+(-n)} = -\frac{1}{(c_0 + c_1 \wp(2n, g_2, g_3))^2}, \tag{2.80}$$

$$f_{n+(-n)} = \frac{2}{(c_0 + c_1 \wp(2n, g_2, g_3))}. \tag{2.81}$$

$$\tag{2.82}$$

It is clear from this case that the dependence on n, while simple, is not even identical between all the numerator coefficients and thus there is no set of values for the integration constants that can yield a consistent amplitude, except in the Coon and Veneziano limits.

2.3.5. Why can Coon's method can fail?

A priori it might sound like a paradox that we started from an equation in which the coefficients b_{n+k} etc were obvious functions of $n+k$ and ended with a class of solutions for which there coefficients are functions of n and k separately. So what happened?

Coon's method was used originally as a way to find which functions f, g, p satisfy the following functional relationship:

$$f(x+y)(p(x)+p(y)) + g(x+y)p(x)p(y) = 1 \tag{2.83}$$

It proceeds by taking derivatives **keeping $x+y$ fixed**, and obtain a necessary condition under the form of a differential equation that p must satisfy. It must then be verified *a posteriori* that the possible boundary conditions of this differential equation are compatible with the initial equation. Rather magically, this condition checks out for the non-trivial (non-linear) case of Coon.

In extending the ansatz to higher powers of p, somehow, the magic seems to stop and it seems that no non-trivial boundary conditions on the Weierstrass equations seem to give consistent solutions, leaving Coon and Veneziano as the only two solutions.

It is obvious but worth stressing that the faliure of this approach to obtain generalizations of the Coon amplitude does not mean that no other dual model amplitudes exist. In fact, since the moment in which this work was carried out and today, various groups have found more general dual model amplitudes via different methods [41, 43, 44, 47, 51, 54–57, 69]. The problem seems to be that the ansatz is just not flexible enough to capture them, since the precise pattern for the cancellations between the zeros and the poles is a strong assumption about the structure of the amplitude. It is not unthinkable that upgrading the ansatz to even higher orders in s and t or generalizing the pole-cancellation condition could yield new solutions, but given the complexity of the first non-trivial extension of the ansatz it does not seem that this is a reasonable avenue to explore the space of dual model amplitudes further.

2.4. Outlook and current status of the Coon amplitude

In the first sections of this chapter we presented the work first published in [1], where we provided the first characterization of the Coon amplitude, determining the range of (d, q, m^2) for which the amplitude is unitary as well as locating it in the allowed space of EFTs. This study opened many perspectives, and possibly most importantly brought the Coon amplitude into the attention of the community as a relevant object to be understood in greater detail.

When we presented this work, there were many natural questions to be followed up on. First of all, the connection between the Coon amplitude and string theory as its $q \to 1$ limit suggested strongly the possibility of a q-deformed worlsheet theory, from which higher point functions and a q-analog of the no-ghost theorem could be derived. Very few results existed in the literature on this topic (see [141, 142]), but in the last year there has been some progress in defining q-deformed worldsheet theories from which the Coon amplitude could potentially arise [49, 143], even though the second reference excluded the possibility of the Coon amplitude being obtainable from the class of q-deformed models they considered.

A related and also crucial question is that of the generalization of the Coon amplitude to higher points. While some early investigations had been carried in the 70s [122, 144–146], the results were not conclusive. In this respect, the recent work [51] showed that it is only possible to obtain a natural N-point generalization of the Coon amplitude in the $q > 1$ case, which corresponds to a 4-point Coon amplitude that exhibits ghosts among its intermediate states and thus violates unitarity. In the $q < 1$ case in which the Coon amplitude can be made ghost-free, the higher point functions do not factorize correctly when defined using the prescription that arises naturally from q-deformed calculus.

Moreover, the work [48] showed that even if in the $q < 1$ case the residues satisfy the constraints from unitarity, when considering the amplitude at energies above the accumulation point the discontinuity induced by the non-meromorphic factor violates positivity when expanded into partial waves, and thus even the $q < 1$ Coon amplitude is non-unitary if considered beyond its accumulation point. While the physical interptetation of the accumulation point is still not clear and it could be arguable that the Coon amplitude breaks down beyond this energy scale and thus should not be expected to respect unitarity in this region, this fact added to the seeming impossibility of obtaining higher point amplitudes that factorize correctly into the Coon 4-point amplitude make a bad case for the possibility of the Coon amplitude belonging to a fully consistent theory when $q \neq 1$.

This negative result, however, does not make the Coon amplitude unworthy of being fully understood. If seen as an effective field theory amplitude with a range of validity up to the accumuation point scale, the Coon amplitude satisfies all the bootstrap constraints for dual models and therefore constitutes an important example even if it can't be embedded in a complete theory. This is not unlike the case in the non-perturbative S-matrix bootstrap, where the constraints from higher point scattering amplitudes are expected to shrink the allowed regions obtained for $2 \to 2$ scattering, ruling out some regions of their boundary and implying that some extremal amplitudes are unphysical. Nevertheless, understanding the nature of the extremal amplitudes living at this boundary has been a central question in the S-matrix bootstrap.

Also, the presence of Coon-like amplitudes in certain contexts in string theory argued in [125], as well as the presence of accumulation point amplitudes in the allowed space of gravitational theories away from the small portion where usual theories seem to live reported in [124] make of the Coon amplitude a unique example to at least guide explorations in these directions.

Another point that can be made is that the Coon amplitude and its higher point ($q > 1$, non-unitary) generalizations provide a good avenue to studying String Theory itself in the $q \to 1$ limit. Since they possess additional structure with respect to string amplitudes by the presence of the deformation parameter q, it is not unthinkable that some questions can find easier answers for generic values of q, and then the result can be specialized to String Theory in the $q \to 1$ limit.

Finally, in the last section of this chapter we presented our (unpublished) attempt to generalize the original method by Coon to obtain the Coon amplitude, finding that even with this extended ansatz the Coon and Veneziano amplitudes are still the only consistent solutions. While it appears that the procedure of directly extending Coon's ansatz to higher order numerators is not an efficient way of obtaining new dual model amplitudes, other generalizations of this technique have provided new solutions with the same spectrum as the Coon amplitude but modified residues [44]. More generally, the large number of recent

works obtaining new classes of dual model amplitudes shows very clearly that the space of consistent dual model amplitudes is much larger than originally thought, with various families of novel amplitudes discovered in the last couple of years. Surely there are more surprises yet to come.

Chapter 3.

Regge Theory for Dual Models

In this chapter we return to the goal of constraining generic dual model amplitudes from a bootstrap perspective. It turns out that an extremely useful tool at our disposal is Regge theory, namely the analytic continuation of the partial wave coefficients (3.2) into complex angular momentum $J \in \mathbb{C}$. Introduced by Tulio Regge in the late 50s, it has been of fundamental importance in high energy physics since then [147], since it relates the high energy behavior of scattering amplitudes to their spectrum of resonances and their couplings, in a way that will be explained shortly.

To motivate its utility for our purposes, lets consider a dual model satisfying unsubtracted dispersion relations. In this case, as was explained in the first chapter around eq. (1.58), channel duality implies the following equation satisfied by the set of masses and couplings that defines the amplitude:

$$\sum_{n,J} c_{nJ} \left(\frac{P_J\left(1+\frac{2t}{m_{n,J}^2-4m_0^2}\right)}{s-m_{n,J}^2} - \frac{P_J\left(1+\frac{2s}{m_{n,J}^2-4m_0^2}\right)}{t-m_{n,J}^2} \right) = 0, \quad s,\, t < m_0^2, \quad c_{nJ} \geq 0, \quad (3.1)$$

where the P_J are Legendre polynomials and m_0^2 is the lightest mass in the spectrum participating in the poles of (3.1).

As was alluded to in that section, this crossing equation is extremely constraining and the question of which are the possible spectra $\{m_n^2\}$ that together with their couplings $\{c_{nJ}\}$ define consistent dual model amplitudes seems very natural. However, the possibility of exploiting this crossing equation to obtain information on the allowed dual model amplitudes is impeded by the slow convergence of this equation. To have a sense of how slow it converges, one can take the masses and couplings corresponding to the Veneziano amplitude and truncate the sum at $n = N_{\max}$, and verify that the speed at which the truncated sum approaches zero as a function of $N_{\max}$ is slower than logarithmic for some values of s and t [1].

Such slow convergence invites us to wonder if there might be a different representation of the amplitude that has better convergence properties, allowing us to use crossing symmetry to constrain dual model amplitudes as is done in [34] for instance. As it turns out, Regge theory is a good answer to this question, as it shows that the masses and couplings are not all independent, but rather they are grouped in infinite families, each of them defined by a single function. More precisely, Regge theory relates the spectrum and couplings to the poles of the

[1] An interesting remark is that the recent works [70,148] apply the technology of crossing symmetric dispersion relations to dual amplitudes, obtaining expansions over poles that converge faster. These are not the standard channel-duality equations considered here, but seem to yield a different, very powerful representation of dual model amplitudes

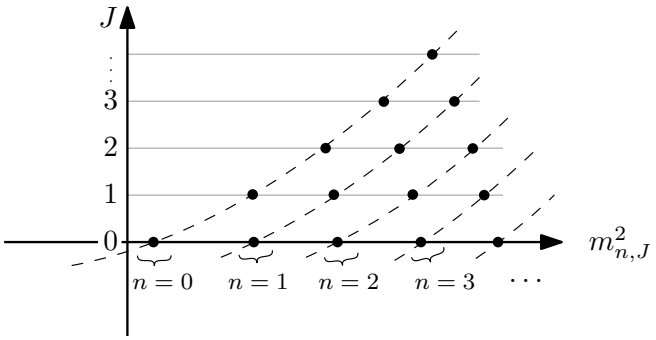


Figure 3.1.: Typical spectrum in a dual model amplitude, organized by Regge trajectories (dashes) and where the levels $n = 0, 1, 2, \ldots$ are explicitly shown.

partial wave coefficients as functions of complex J. If the partial wave coefficient behaves near a pole as $f_J(t) \sim \beta(t)/(J - \alpha(t))$, then the function $\alpha(t)$ determines the masses of all the particles belonging to a given Regge trajectory, while $\beta(t)$ determines their couplings. Therefore, Regge theory reorganizes the data characterizing a dual model amplitude in a different way, packaging the information of infinitely-many particles in a single function. Since the spectrum of dual model amplitudes is organized in Regge trajectories (see figure (3.1))t is reasonable to think that representing the amplitude in terms of its Regge poles might allow us to deal with the crossing equation in a more efficient way, and *this is indeed the case.*

In this chapter we will introduce the basics of Regge theory and give substance to the claims made in the previous paragraph as well as some tools required for this purpose, such as the Froissart-Gribov projection of the partial wave coefficients. Later, as a first application of Regge theory to the study of dual model amplitudes, we will use this technology to prove that dual model amplitudes require infinitely-many Regge trajectories to be compatible with crossing symmetry, analyticity and unitarity. This chapter is based partly on the results of [3]. Throughout it we restrict to $d = 4$ mostly for notational simplicity, as the generalization to arbitrary d is trivial in almost all the content. We provide the necessary details when differences arise between generic dimensions and the 4-dimensional case.

3.1. Froissart-Gribov projection of the partial wave coefficients

To be able to make use of Regge theory, we need first a representation of the partial wave coefficients that can be analytically continued to complex values of the angular momentum J. This can be achieved by a technique called the *Froissart-Gribov projection.* While this a standard technique that can be found in textbooks or in the review [72], to make the presentation self-contained we explain it in what follows.

The idea is simple: Consider for simplicity a color-ordered amplitude $A(s, t)$ corresponding to the scattering of identical scalars of mass μ^2, and start from the s-channel partial wave expansion of the scattering amplitude, defined in eq. (1.27) as

$$A(s,t) = 16\pi \sum_{J=0}^{\infty} (2J+1) f_J(s) P_J(z_s), \quad s > 4\mu^2,\, t < 0, \tag{3.2}$$

amd $z_s = 1 + \frac{2t}{s-4\mu^2}$ is the cosine of the scattering angle in the s channel. As explained in chapter 1, the partial-wave sum runs over all spins[2] and converges for all physical s for fixed t, $4\mu^2 - s < t < 0$. In the t plane it diverges at the first singularity, $t = 4\mu^2$ when there are no bound states, or at the first bound state $t = m_0^2$.

As in eq. (1.29), we can use the Legendre polynomial's orthogonality relation to project out the partial wave coefficients $f_J(s)$. Changing variables from z_s to t in the resulting integral, we get

$$f_J(s) = \frac{1}{16\pi}\frac{1}{s-4\mu^2}\int_{4\mu^2-s}^{0} P_J\left(1+\frac{2t}{s-4\mu^2}\right) A(s,t)\,\mathrm{d}t\,. \tag{3.3}$$

Now, the trick is to use the fact that the Legendre P polynomials are the discontinuity of the Legendre Q functions, which correspond to the family of solutions to the angular Laplace equation independent of the Legendre polynomials. They are singular at $z = \pm 1$, and in $d = 4$ are defined as [3]

$$Q_J(z) = \frac{\sqrt{\pi}}{(2z)^{J+1}}\frac{\Gamma(J+1)}{\Gamma(J+\frac{3}{2})}\,{}_2F_1\left(\frac{J+2}{2},\frac{J+1}{2};J+\frac{3}{2};\frac{1}{z^2}\right). \tag{3.4}$$

For integer $J \in \mathbb{Z}$, we have

$$\mathrm{Disc}_z\left(Q_J(z)\right) = -\frac{\pi}{2}P_J(z)\,, \quad z \in [-1;1] \tag{3.5}$$

where Disc is defined as

$$\mathrm{Disc}_z f(z) := \frac{1}{2i}(f(z+i\epsilon) - f(z-i\epsilon))\,. \tag{3.6}$$

Using this, the line integral in the partial wave transform can be turned into a contour integral encircling $[-1;1]$. This contour can then be extended to infinity and winds around the cut starting at the first singularity in the z-plane, as shown in fig. 3.2. Note that there is no cut on the left hand side because we consider a color-ordered amplitude without u-channel singularities, and that the right hand cut probes the high-energy t-channel region of the amplitude.

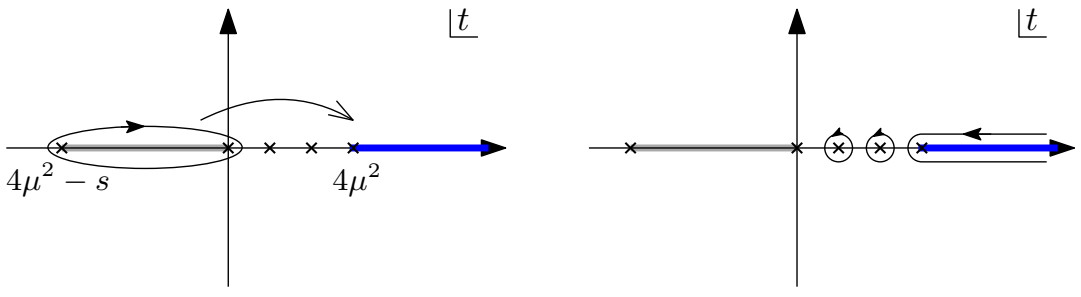


Figure 3.2.: Froissart-Gribov contour deformation in the presence of bound states below threshold. In our case, we have no threshold cut but only an infinite sequence of poles.

[2] Odd spins would drop out if we relaxed the "color-ordering" and had full $s-t-u$ symmetry.
[3] Their definition for arbitrary d can bedefined for instance in [72].

The condition under which the arc at infinity can be dropped depends on the spin J, and on the fall-off of the amplitude at infinity. A was mentioned in the introductory chapter and will be explained in greater detail in the following section, dual models exhibit one salient feature of non-perturbative behaviour: reggeization. At high energies $\sqrt{s}$ and fixed momentum transfer $\sqrt{-t}$, reggeizing amplitudes behave as $A(s,t) \sim s^{\alpha(t)}$, where the Regge trajectory function $\alpha(t)$ also determines the spectrum of the tower of resonances $m_0^2, m_1^2, \ldots$. Crossing symmetry implies that the same is true in the t-channel, and thus a reggeizing amplitude behaves as $t^{\alpha(s)}$ at large t.

Since the Q_J functions behave asymptotically as

$$Q_J(z) \sim \frac{1}{z^{J+1}}, \quad z \to \infty, \tag{3.7}$$

we have that the arc at infinity will dop if $J > \alpha(s)$.

Moreover, we will be interested in studying amplitudes satisfying one-subtracted dispersion relations. In this case, we know that the amplitude might approach a constant at infinity even if $\alpha(s)<0$, and thus we obtain analyticity in J for $J > \max[\,0, \alpha(\mathrm{s})\,]$.

Putting all these elements together we arrive at the Froissart-Gribov projection:

$$f_J(s) = \frac{1}{16\pi^2} \frac{2}{s-4\mu^2} \int_{t_0}^{\infty} \mathrm{d}z\, Q_J\left(1 + \frac{2t}{s-4\mu^2}\right) \mathrm{Disc}_t A(s,t)\,, \tag{3.8}$$

where t_0 is the location of the first singularity of the amplitude in the $t-$channel.

The greatest virtue of this formula is that while it is by construction equivalent to the representation of the partial wave coefficients in terms of Legendre polynomials for integer J, the Q_J functions have much better analytical properties as functions of complex J than the P_J's, and therefore allow to define a unique analytical continuation of the partial wave expansion into complex J.

To see this, note that the asymptotic behavior of the Q_J as $|J| \to \infty$ is given by

$$Q_J(z)\big|_{|J|\to\infty}\ e^{-J\zeta(z)}, \tag{3.9}$$

with $\zeta(z) = \log(z + \sqrt{z^2-1}) > 1$ if $z > 1$. A naive worry when analytically continuing the expression in eq. (3.8) to non-integer J is that there exist infinitely many ways of interpolating between the integers, and therefore in principle there is no meaningful, unique way of analytically continuing the partial wave coefficients beyond their physical, integer J values. However, the asymptotic behavior of the Q_J functions fixes this issue as a consequence of Carlson's theorem, which tells us that the f_J defined this way are the unique analytical continuation of the partial wave coefficients that yield the physical values at integer J and converge as $J \to \infty$.

To be precise, Carlson's theorem states that if a regular function $f(J)$ is bounded by $e^{\pi J}$ as $\mathrm{Re}J \to \infty$, and $f(l) = 0$ for an infinite sequence of integers $l = n, n+1, n+2, \ldots$, then $f(l)$ is identically zero. If we define a hypothetical alternative analytical continuation of the partial wave coefficients as

$$\tilde{f}_J(s) = f_J(s) + g(J,s), \tag{3.10}$$

with f_J defined by the Froissart-Gribov projection and $g(J,s)$ such that it vanishes at all non-negative integer values of J, then Carlson's theorem implies that either $g(J,s)$ is identically zero and $\tilde{f}_J(s) = f_J(s)$, or the alternative partial wave coefficients $\tilde{f}_J(s)$ diverge as $J \to \infty$, and therefore the definition given by the Froissart-Gribov projection yields the only convergent analytical continuation of the partial wave coefficients. This fact will allow us to analytically continue the partial wave expansion into complex values of J and relate the high energy behavior of the amplitude to the singularities of the f_J in complex J.

However, before going into that lets take a moment to specialize eq. (3.8) to the case of a dual model amplitude, where all the singularities are simple poles and the discontinuity reduces to an infinite sum of delta functions. In this case, we get a discrete sum over residues:

$$f_J(s) = \frac{1}{16\pi^2}\frac{2}{s-4\mu^2}\sum_{n=0}^{\infty}\oint_{|t-t_n|=\epsilon} \mathrm{d}t\, Q_J\left(1+\frac{2t}{s-4\mu^2}\right) A(s,t)\,, \tag{3.11}$$

When $t = m^2_{n,J'}$, we have that $z = z_{n,J'} = 1 + \frac{2m^2_{n,J'}}{s-4\mu^2}$. Expanding the residues of the amplitude at $t = m^2_{n,J'}$ in Legendre polynomials [4]:

$$f_J(s) = \frac{i}{4\pi}\frac{1}{s-4\mu^2}\sum_{n=0}^{\infty}\sum_{J'=0}^{n} c_{n,J'}\, Q_J\left(1+\frac{2m^2_{n,J'}}{s-4\mu^2}\right) P_{J'}\left(1+\frac{2s}{m^2_{n,J'}-4\mu^2}\right)\,. \tag{3.12}$$

This representation of the partial wave coefficients of dual model amplitudes will be crucial for proving the inconsistency of dual models with finitely many trajectories.

3.2. Regge Theory basics

We are now ready to introduce Regge theory as a way of exploiting the analytical structure of the partial waves as functions of complex J. This can be done by the means of a technique known as the *Sommerfeld-Watson transform* of the partial wave expansion of the amplitude, in which we replace the discrete sum over J in (3.2) with an integral along a contour C surrounding the non-negative real J axis shown in fig. 3.3 as follows:

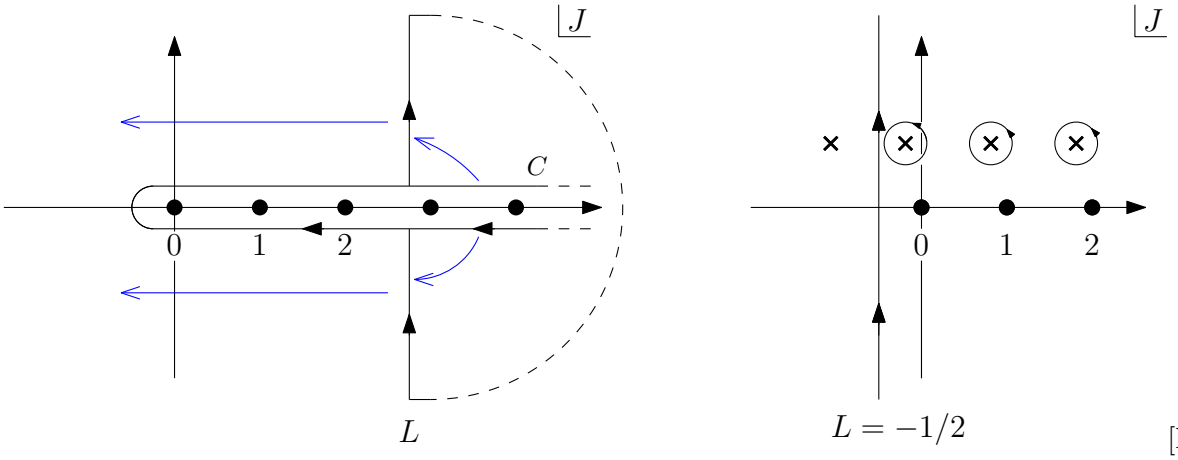
$$A(s,t) = -\frac{16\pi}{2i}\int_C \frac{\mathrm{d}J}{\sin\pi J}(2J+1) f_J(t) P_J(-z) \tag{3.13}$$

where the sine function in the denominator picks up the residues at non-negative integer values of J, and where we have used that $\oint_{|J-n|=\epsilon}\frac{\mathrm{d}J}{\sin(\pi J)} = 2i(-1)^n$ and that $P_J(-z) = (-1)^J P_J(z)$ for integer J. Note that here we are considering the t-channel partial wave expansion, and thus $z = \cos\theta = 1 + \frac{2s}{t-4\mu^2}$.

This integral representation of the amplitude allows us to deform the contour along the imaginary axis, as shown in fig. 3.3. The large J asymptotics of the Legendre P functions is given by

$$\begin{aligned} P_J(z)\big|_{J\to\infty} &\sim e^{iJ\theta} + e^{-iJ\theta}, \\ P_J(-z)\big|_{J\to\infty} &\sim e^{iJ(\theta-\pi)} + e^{-iJ(\theta-\pi)}, \end{aligned} \tag{3.14}$$

[4] Note that in the t-channel $\cos\theta = 1 + 2s/(t-4\mu^2)$, and thus the roles of s and t are reversed inside the P_J with respect to the Q_J.



[h]

Figure 3.3.: Sommerfeld-Watson transform. First we express the sum over discrete spins J as a continuous integral over contour C. Then we open up the contour (blue arrows) to obtain a vertical integral, picking up the contribution from the singularities of f_J in the complex J-plane. The vertical integral can be pushed to $L = -1/2$ where the Legendre P functions are the softest, which decreases the magnitude of the resulting vertical integral, called the background integral.

where $z = \cos(\theta)$ and $\mathrm{Re}J > 0$. Thus, in the physical region $-1 < \cos(\theta) < 1$, the factor $P_J(-z)/\sin(\pi J)$ decays exponentially as $\mathrm{Im}\, J \to \infty$ even if the P_J functions themselves are can grow exponentially. Given the asymptotic behavior of the Q_J functions at large J shown in eq. (3.9), using the Froissart-Gribov projection we see that for physical kinematics the partial waves decay exponentially on the right half J-plane and therefore we can drop the arc at infinity.

Once the contour at infinity is dropped, the representation of the amplitude in terms of the integral on the J-plane of eq. (3.13) is well defined in the full z-plane and not just for physical t-channel kinematics, as can be seen from the asymptotic behavior of the Legendre P and Q functions.

As we deform the contour along the complex J-plane, we may pick up singularities of the partial wave coefficients in J. Suppose that the rightmost singularity is a simple pole at $J = \alpha(t)$ with residue $\beta(t)$, such that

$$f_J(t) \simeq \frac{\beta(t)}{J - \alpha(t)}. \tag{3.15}$$

These types of partial wave singularities at analytically continued momenta are called *Regge poles*. They are crucial elements in Regge theory, as they are the ones that determine both the spectrum and the high energy asymptotics of the amplitude.

To see this, notice that once we pick up the Regge pole contribution, the Sommerfeld-Watson representation of the amplitude reads

$$A(s,t) = -16\pi^2(2\alpha(t)+1)\beta(t)\frac{P_{\alpha(t)}(-z)}{\sin(\pi\alpha(t))} - \frac{16\pi}{2i}\int_{C'}\frac{\mathrm{d}J}{\sin\pi J}(2J+1)f_J(t)P_J(-z), \tag{3.16}$$

where C' denotes the vertical contour once past the Regge pole and is usually referred to as the *background integral*.

The contribution from the Regge pole has remarkable features. On the one hand side, looking at the $z \to \infty$ limit of the amplitude, since $z \sim s$ we see that the contribution from the Regge pole grows as $s^{\alpha(t)}$. The background integral, being at a value of J to the left of $\alpha(t)$ in J-plane will yield a subleading contribution proportional to $s^{\mathrm{Re}J}$, and therefore it is the Regge pole the one that determines the large s, fixed t asymptotics of the amplitude. This is precisely the phenomenon of reggeization alluded to previously, and now we see that it is a direct consequence of the analytic structure of the partial wave coefficients in J.

Moreover, the factor of $(\sin \pi\alpha(t))^{-1}$ arising from the Regge pole implies that every time that t is such that $\alpha(t)$ is an integer, the amplitude exhibits a simple pole, signaling the exchange of an on-shell particle. Therefore, the function $\alpha(t)$ encodes the masses of infinitely-many particles defining a *Regge trajectory*, a family of particles that lie on the same curve when plotted in the (J, m^2) plane, giving an explanation to the presence of these structures in the hadronic spectrum that was mentioned in the introduction, when motivating dual models.

Analyzing the contribution from the Regge pole further, we see that the Regge residue function $\beta(t)$ completely determines the coefficient in the Legendre expansion of the residues at the poles when $\alpha(t)$ takes integer values. More explicitly, defining m_n^2 such that $\alpha(m_n^2) = n$, we see that the residue at the pole $t = m_n^2$ is given by

$$\operatorname*{Res}_{t=m_n^2} A(s,t) = -16\pi(2n+1)\beta(m_n^2)P_n(z), \tag{3.17}$$

signaling the exchange of a particle of spin n and mass m_n^2, whose coupling to the external particle is $g^2 \sim \beta(m_n^2)$, up to irrelevant, positive numerical factors. Therefore, we see that for each trajectory the pair of functions $\alpha(t)$ and $\beta(t)$ characterize completely the masses and couplings, and thus the information of infinitely-many contributions to the sum over poles in eq. (3.1) is contained in them. This is partly what makes Regge theory useful, and we will exploit this fact in the next chapter.

Going back to the Sommerfeld-Watson transform, as we continue to move the contour to the left we uncover new singularities of the partial wave coefficients. In general there can be other types of singularities apart from Regge poles, but these would give rise to non-meromorphicities on the scattering amplitude via the Sommerfeld-Watson transform, and since we are considering dual models we will assume that Regge poles are the only singularities in J.

Continuing this process, we obtain that in the case of meromorphic amplitudes the Sommerfeld-Watson transform gives

$$A(s,t) = -\frac{16\pi}{2i}\int_{-1/2-i\infty}^{-1/2+i\infty} \frac{\mathrm{d}J}{\sin \pi J}(2J+1)f_J(t)P_J(-z) + A_{\mathrm{Regge-poles}}(s,t), \tag{3.18}$$

where

$$A_{\mathrm{Regge-poles}}(s,t) = -16\pi^2 \sum_i (2\alpha_i(t)+1)\beta_i(t)\frac{P_{\alpha_i(t)}(-z)}{\sin(\pi\alpha_i(t))} \tag{3.19}$$

The choice to set the contour of the background integral at $\mathrm{Re}\, J = -1/2$ comes from the properties of the Legendre P_J function as a function of J, which changes behavior at the line $\mathrm{Re}J = -1/2$:

$$P_J(z) \sim_{z\to\infty} \pi^{-1/2}\frac{\Gamma(J+1/2)}{\Gamma(J+1)}(2z)^J \quad \mathrm{Re}\, J > -1/2 \tag{3.20}$$

$$\sim_{z\to\infty} \pi^{-1/2}\frac{\Gamma(-J-1/2)}{\Gamma(-J)}(2z)^{-J-1} \quad \mathrm{Re}\, J \leq -1/2\,, \tag{3.21}$$

hence this choice causes the contribution arising from the background integral to be as small as possible, with the amplitude being dominated by the Regge poles at large energies.

This obstruction to pushing the integration contour further to the left will be important in the next chapter. However, rather than going into that now, lets use these new tools to probe the structure of dual model amplitudes. As promised, now we have the necessary tools to show that only dual model amplitudes with infinitely many Regge trajectories are consistent, as we show in the next section.

3.3. Ruling out dual model amplitudes with finitely many trajectories

In this section we use the technology introduced in the first part of this chapter to explore the following question: *How simple can dual models be?*.

Arguably, the simplest dual model would be composed of exactly one Regge trajectory; it would make an elegant object, parameterized by its spectrum composed of particles of masses $m_n^2\big|_{n\in\mathbb{N}}$ and spin n. In the simplest case in which unsubtracted dispersion relations hold, the amplitude would read:

$$A(s,t) = -\sum_{n=0}^{\infty} c_n \frac{P_n\left(1+\frac{2t}{m_n^2-4\mu^2}\right)}{s-m_n^2} \tag{3.22}$$

where as before P_n are Legendre polynomials. The important point to notice is that in contrast to tree-level string theory for instance, at each level n there is only *one* state of spin n, instead of a sum over spins $J = 0, \ldots, n$. Thus, there is only one unknown per level, the residue c_n, required to be positive by the condition of unitarity $c_n \geq 0$. Therefore, such amplitudes would be parameterized by a *linearly growing* number of parameters; this is to be compared to the quadratic number of parameters seen in string theory, and thus could offer a good building block to study dual models numerically, provided such objects existed.

In addition to this simplicity, the question of the existence of meromorphic amplitudes with finitely many trajectories is timely given the recent works [59–61] where, through an elaborate bootstrap procedure, the authors have identified a special amplitude argued to potentially correspond to pion-pion scattering in large N QCD. In this case, the leading trajectory significantly dominates the sub-leading ones, raising the question of whether it could consist of a single trajectory.

In what follows, we prove that meromorphic scattering amplitudes of external scalars with finitely many Regge trajectories and satisfying unsubtracted or one-subtracted dispersion

relations cannot exist. Since the proof is slightly easier for the case with no subtractions, we present it first as a warm-up, even though this case is technically a sub-case of amplitudes with one subtraction (where the subtraction is trivially zero).

We also discuss how the presence of infinitely many trajectories allows to evade this no-go theorem as it should, since meromorphic amplitudes with infinitely many trajectories obviously exist. In particular, we observe that our argument yields no constraint on the size of the sub-leading trajectories: they can be as small as desired, as long as they come in an infinite number. This statement, therefore, suggests that the large N amplitude of [59–61] should have an infinite number of trajectories, but they might require extra numerical efforts to be detected. It would be interesting to study this point further.

Remark. After we had completed the proof presented in this chapter, we discovered that a few references had already considered the question of the number of Regge trajectories during the 60s. We discuss them in section. 4.5. Almost all of them[5] rely on the use of the so-called Finite Energy Sum Rules (FESRs), which involve making a certain number of assumptions which we discuss in an appendix. Our initial attempts to address the problem also relied on a version of FESRs, which we had independently re-discovered. However, we were unsatisfied with the assumptions going into their applicability. The argument presented in this chapter allows us to avoid any such assumptions, and also rules out the in principle possible case in which the dual model amplitude is not made up of Regge poles, but rather by infinitely many isolated poles in the Mandelstam variables[6]. Most importantly, we also work out the case with subtractions, which was not handled by these earlier papers, and which is relevant for the aforementioned pion amplitude at large N in particular, but also for the S-matrix program in general.

3.3.1. Case without subtractions

We present first the case of a dual model amplitude satisfying unsubtracted dispersion relations, since the procedure is slightly more straightforward. We begin ruling out the existence of amplitudes with a single trajectory, and then extend the result to any finite number.

The proof is rather simple: Channel duality imposes a very specific asymptotic behavior for the Legendre coefficients c_n at large n, which is incompatible with the existence of a Regge pole in the partial waves. Since a dual model amplitude comprised of a single trajectory as the one presented in eq. (3.22) would naturally arise in a scenario where the only singularity of the partial wave coefficients $f_J(s)$ as a function of $J \in \mathbb{C}$ is a simple pole at $J = \alpha(s)$, this strongly hints towards the inconsistency of these objects. However, we cannot exclude the possibility of an amplitude of the form of eq. (3.22) in which the poles in s are not related by a Regge pole. Nevertheless, since we consider meromorphic amplitudes, the only allowed singularities of the partial waves are simple poles, and thus this means that the partial waves in this putative model are entire functions. This will imply in turn an incompatibility between the finiteness of the partial wave coefficients and channel duality, rendering this objects inconsistent.

[5] In [149] there is an heuristic argument for the need of infinitely-many Regge poles based on the cancellation of unphysical spurious poles, but only applies for the scattering of particles with different masses and satisfying unsubtracted dispersion relations. We thank Aninda Sinha for showing us this reference.

[6] Isolated in the sense that they are not connected by a trajectory function $\alpha(t)$ that interpolates between them.

3.3.1.1. Decay of coefficients from channel duality

We start by deriving the asymptotic decay condition on the c_n coefficients required by channel duality. We saw in chapter 1 that for values of t such that fixed t unsubtracted dispersion are valid the amplitude can be expressed as a sum over s-channel poles as in eq. (3.22).

From the Sommerfeld-Watson transform restricted to the case in which the only singularities of the partial wave coefficients in J are simple poles, we see that the large s behavior of the amplitude for any given value of t must be controlled either by the leading Regge pole or by the background integral. Since the background integral depends on s only through $P_J(-z)$, $z = 1 + 2s/(t - 4\mu^2)$, closing the contour at $\mathrm{Re}J = -1/2$ as described in the previous section implies that its large s, fixed t growth is bounded by $s^{-1/2}$ for any t [150]. Therefore, the large s, fixed t behavior of the full amplitude is $A(s,t) \sim \max[\, \mathrm{s}^{-1/2}, \mathrm{s}^{\alpha(\mathrm{t})}\,]$.

By definition, $\alpha(t) = 0$ at $t = m_0^2$, and assuming that the trajectory functions are monotonic[7] this implies that $\alpha(t) < 0$, $\forall t < m_0^2$. Therefore, we see that $A(s,t) \to 0$ as $s \to \infty$ for $t < m_0^2$, while it goes to a constant when $t = m_0^2$, and thus unsubtracted dispersion relations hold for $t < m_0^2$.

For the s-channel pole expansion, this means

$$\forall t < m_0^2, \quad \sum_{n=0}^{\infty} c_n \frac{P_n\left(1 + \frac{2t}{m_n^2 - 4\mu^2}\right)}{m_n^2} < \infty, \tag{3.23}$$

whil it diverges *presicely* AT $t = m_0^2$.

To analyze the condition that this imposes on the c_n's, we need the asymptotic behaviour of the Legendre polynomials at large n, which will depend on the growth of m_n^2. Intuitively, near $\epsilon_n = 0$, $P_n(1 + \epsilon_n)$ grows like $(1 + \epsilon_n)^n$, and it can either diverge if ϵ_n does not decay fast enough, go to a constant or to 1.

It turns out that the limiting case is n^2. If m_n^2 grows slower than n^2 asymptotically, we get:

$$P_n\left(1 + \frac{2t}{m_n^2 - 4\mu^2}\right) \underset{n\to\infty}{\sim} \left(\frac{m_n^2}{t}\right)^{1/4} \frac{e^{2n\sqrt{t/m_n^2}}}{2\sqrt{n\pi}}. \tag{3.24}$$

This expression can be derived from the integral representation of the Legendre polynomials, $\frac{1}{\pi} P_n(\cos(\theta)) = \int_0^\pi (\cos(\theta) + i \sin(\theta)\cos(\phi))^n \, \mathrm{d}\phi$. The asymptotic behaviour of the $P_n(1 + 2t/(m_n^2 - 4m_0^2))$ is found by explicitly taking the limit $n \to \infty$, $m_n^2 \to \infty$.[8]

For $m_n^2 = n^2$, the series goes to a constant which depends on t:

$$P_n\left(1 + \frac{2t}{n^2 - 4\mu^2}\right) \underset{n\to\infty}{\to} {}_0F_1(1,t), \tag{3.25}$$

[7] This must be the case in general, as if $\alpha(t)$ was not monotonic it would either cross again the lines $J = 0$ or $J = 1$ at some value $t < m_0^2$, signaling the presence of a spin 0 or spin 1 state lighter than m_0^2 in the spectrum and thus violating the assumption that m_0^2 is the lightest state, or $\alpha(t)$ we would have $0 < \alpha(t) < 1\, \forall t < m_0^2$, which would imply that the amplitude doesn't decay at large s for any value of t and therefore contradict the assumption that it satisfies unsubtracted dispersion relations. The only way out would be for the Regge residues to vanish precisely every time the trajectory function crosses integer values at $t < m_0^2$, which is a very tuned-yet not impossible- scenario.

[8] See also [151].

where ${}_0F_1(a,z)$ is the confluent hyper-geometric function. Finally, for $m_n^2 > n^2$, they go to one.

From this asymptotic behaviour, we notice two different regimes, depending on whether the spectrum is bounded asymptotically by n^2 or not, which produces the exponential growth, or the flat trend of order unity.

Consider first the case $m_n^2 > n^2$ at large n. In this case, the Legendre polynomials simply go to 1 at large n independently of the value of t. This means that we can effectively decompose the series in eq. (3.23) into finitely many terms that depend on t (and are therefore regular in t), and an infinite $t-$independent tail of the form $\sum_n \frac{c_n}{m_n^2}$. Such a scenario can never yield a series which would be convergent for $t < m_0^2$ but diverge at $t = m_0^2$, and is thus inconsistent with crossing and channel duality.

If $m_n^2 \sim n^2$ at large n, the same argument can be made. Since the hypergeometric function is regular, it cannot blow up at $t = m_0^2$, nor the finite sum of terms that constitute the head of the series. We reach the same conclusion.

Now, let us focus on the nontrivial case $m_n^2 < n^2$ asymptotically. For $0 < t < m_0^2$ the Legendre polynomials grow exponentially as $e^{2n\sqrt{t/m_n^2}}$. Thus the only way for eq. (3.23) to be regular for $t < m_0^2$ is that the c_n coefficients decay exponentially:

$$c_n \leq \frac{e^{-2n\sqrt{m_0^2/m_n^2}}}{m_n^2}\,. \tag{3.26}$$

However, if the coefficients decay *strictly* faster than m_0^2, then the terms in the sum eq. (3.23) decay exponentially when $t = m_0^2$, and therefore the series is finite at this value contradicting channel duality, which predicts that the series should diverge as $1/(t - m_0^2)$. Therefore, it must be case that the c_n coefficients behave asymptotically as

$$c_n \sim \frac{e^{-2n\sqrt{m_0^2/m_n^2}}}{m_n^2}\left(1 + \mathcal{O}(n^{-k})\right), \tag{3.27}$$

for some number $k > 0$.

3.3.1.2. Decay of coefficients implies absence of Regge poles

As we will see, this decay condition is too strong to allow the formation of a Regge pole in the partial wave coefficients. For this we use the expression for the partial waves coefficients derived from the Froissart-Gribov projection specialized to the case of meromorphic amplitudes in eq. (3.12). In this expression, we can set $s = 0$ to get rid of the Legendre polynomials via $P_n(1) = 1$, to obtain

$$f_J(0) = -\frac{i}{16\pi\mu^2}\sum_{n=0}^{\infty} Q_J\left(1 - \frac{m_n^2}{2m_0^2}\right) c_n\,. \tag{3.28}$$

If the $f_J(s)$ possessed a Regge pole at some $J = \alpha(s)$, then naturally $f_J(0)$ would diverge at $J = \alpha(0)$. But an even more basic question that we can try to answer is: Can this series diverge as all?

As mentioned before, at fixed J the asymptotics of the Legendre Q functions is simply $Q_J(z) \sim z^{-J-1}$, and therefore the series in the right-hand side behaves as

$$\sum_{n=0}^{\infty} c_n \left(m_n^2\right)^{-J-1}. \tag{3.29}$$

Since the c_n's are exponentially decaying and $m_n^2 < n^2$ asymptotically, the above series does not diverge for *any* finite value of J. In particular, $f_J(0)$ is perfectly regular at $J = \alpha(0)$, which proves that, at least in the case without subtractions, scattering amplitudes with one trajectory cannot have a Regge pole. Since meromorphicity implies that these are the only allowed singularities in J of the partial wave coefficients, we conclude that in this case *partial wave coefficients are entire functions of* J.

As mentioned before, being this the case we lose the prediction from Regge behavior that relates the infinitely many particles in the spectrum to each other via the function α, and also the relation between the spectrum and the high energy behavior. While it seems unnatural that an amplitude made up of infinitely many disconnected poles not related by any underlying structure could be compatible with crossing, in principle we cannot yet discard the possibility that an amplitude as (3.22) could exist even in the absence of a Regge pole. However, we will see now that the absence of singularities in J fn the partial waves implies the non-existence of the single-trajectory amplitude.

3.3.1.3. Absence of Regge poles implies non-existence

If the partial waves have no singularities, we can deform the contour in the Sommerfeld-Watson transform without obstructions, and the amplitude will be given entirely by the background integral:

$$A(s,t) = -\frac{16\pi}{2i}\int_{-1/2-i\infty}^{-1/2+i\infty} \frac{\mathrm{d}J}{\sin \pi J}(2J+1) f_J(t) P_J\left(-1 - \frac{2s}{t-4\mu^2}\right), \tag{3.30}$$

which immediately implies that it decays at large s, fixed t at least as fast as $s^{-\frac{1}{2}}$ [150]. This ensures that the Froissart-Gribov projection for the partial waves can be defined for values of J all the way down to $J = 0$. Using this representation for the partial waves in terms of the residues derived in eq. (3.12), at least for generic s not corresponding to a mass in the spectrum, the partial waves are finite and therefore

$$f_J(s) = \frac{i}{4\pi}\frac{1}{s-4\mu^2}\sum_{n=0}^{\infty} c_n\, Q_J\left(1 + \frac{2m_n^2}{s-4\mu^2}\right) P_n\left(1 + \frac{2s}{m_n^2 - 4\mu^2}\right) < \infty, \quad J \geq 0. \tag{3.31}$$

However, this is incompatible with the decay condition eq. (3.27) imposed by channel duality on the c_n coefficients. Chosing a value of s larger than m_0^2 and using the asymptotic behavior of the Legendre polynomials from eq. (3.24) as well as the one for the Q-functions and inserting the asymptotic expression for the c_n's, we see that the series on the right hand side would go at large n as

$$\sum_n \frac{1}{\left(m_n^2\right)^{J+1}} \exp\left(2n\frac{\sqrt{s} - \sqrt{m_0^2}}{\sqrt{m_n^2}}\right). \tag{3.32}$$

Since m_n^2 is bounded by n^2, the J-dependent contribution coming from the Q-function is completely negligible, and the elements in the sum blow up exponentially as $c_n \sim e^{2(\sqrt{s}-m_0)}$. The only way in which the partial wave coefficients would be well defined would be if the c_n's satisfied

$$\lim_{n\to\infty} c_n\, e^{2n\sqrt{\frac{s}{m_n^2}}} = 0, \tag{3.33}$$

for positive s as large as we want. This is clearly in contradiction with the conditions imposed by crossing symmetry and channel duality on the c_n coefficients, which leads us to conclude that dual model amplitudes satisfying unsubtracted dispersion relations and composed of a single trajectory as in (3.22) are inconsistent with the bootstrap principles and therefore *are ruled out*.

3.3.1.4. Generalization to finitely-many trajectories

The generalization of the previous reasoning to finitely-many trajectories is straightforward. An amplitude consisting of $N+1$ Regge trajectories can be written as

$$A(s,t) = \sum_{i=0}^{N}\sum_{n=0}^{\infty} c_{n,n-i}\frac{P_{n-i}\left(1+\frac{2t}{m_{n,n-i}^2-4\mu^2}\right)}{s-m_{n,n-i}^2}, \tag{3.34}$$

where i indexes the different trajectories starting from the leading one at $i=0$, as in fig. 3.1.

Similarly, the equation for the partial wave coefficients in the case of $N+1$ trajectories is given by

$$f_J(s) = \frac{i}{4\pi}\frac{1}{s-4\mu^2}\sum_{i=0}^{N}\sum_{n=0}^{\infty} Q_J\left(1+\tfrac{2m_{n,n-i}^2}{s-4\mu^2}\right) c_{n,n-i} P_n\left(1+\frac{2s}{m_{n,n-i}^2-4\mu^2}\right). \tag{3.35}$$

It is important to note that despite of the fact that the partial wave coefficients should have poles at the values $J=\alpha_i(s)|_{i=0,\dots,N}$ corresponding to the different trajectories, the expression given in eq. (3.35) only makes sense until we hit the first singularity in J, and therefore we can only use it to probe the leading Regge pole at $J=\alpha_0(s)$, where the series is expected diverge. Beyond this value of J we are outside of the region of convergence of the series, and therefore we should not expect that the partial wave coefficients are correctly described by it.

The implications of channel duality are very similar to the previous, single trajectory case. The series should still convergent up to $t=m_{0,0}^2=:m_0^2$. As before, we need to distinguish the cases $m_{n,n}^2 \geq n^2$ and $m_{n,n}^2 < n^2$ when $n\to\infty$. The generalization for many trajectories with spectra growing faster than quadratically is trivial, as they fail for the same reason as in the single trajectory and the argument does not require any modifications.

For m_n^2 spectra growing slower than n^2, the argument generalizes easily. Along each trajectory, the coefficients must still decay so as to compensate the exponential growth of the

Legendre polynomials and ensure that

$$\sum_{n=0}^{\infty} c_{n,n-i} \frac{P_{n-i}\left(1+\frac{2t}{m^2_{n,n-i}-4m_0^2}\right)}{m^2_{n,n-i}} < \infty, \quad t < m_0^2, \quad i = 0, \ldots, N, \tag{3.36}$$

so that we get

$$c_{n,n-i} \leq e^{-2(n-i)\sqrt{m_0^2/m^2_{n,n-i}}}. \tag{3.37}$$

The main difference with the case of a single Regge trajectory is that now we don't get a strict decay condition as (3.27) on all the trajectories, but we find that an analog decay must be satisfied by at least one of them to generate the pole at $t = m_0^2$. To see this one simply needs to note that as $t \to m_0^2$, the sum of the contributions from each trajectory as the one in eq. (3.36) must diverge as $(t - m_0^2)^{-1}$. However, since the sum over trajectories has a finite number of terms, the full sum can only diverge if at least one of its constitutents diverges, although not necessarily all of them must do so. Therefore, the decay condition on the coefficients in the case of many trajectories is

$$c_{n,n-i} \leq e^{-2(n-i)\sqrt{m_0^2/m^2_{n,n-i}}}, \quad \forall i = 0, \ldots, N, \tag{3.38}$$

and

$$c_{n,n-k} \sim e^{-2(n-k)\sqrt{m_0^2/m^2_{n,n-k}}}, \quad \text{for at least one } k \in 0, \ldots, N. \tag{3.39}$$

A similar argument can be used to show that, as in the single-trajectory case, these decay conditions are to strong to allow the existence of Regge poles.

Imagine that there existed a Regge pole asociated to the leading trajectory. Then at least for $\mathrm{Re}(J) > \alpha_0(s)$ the series is convergent, and thus in this region we are free to re-organize the terms in the sum as we want, and we can express the partial wave coefficient as

$$f_J(s) = \sum_{i=0}^{N} f_J^{(i)}(s), \tag{3.40}$$

with

$$f_J^{(i)}(s) = \frac{i}{4\pi} \frac{1}{s-4\mu^2} \sum_{n=0}^{\infty} Q_J\left(1+\tfrac{2m^2_{n,n-i}}{s-4\mu^2}\right) c_{n,n-i} P_{n-i}\left(1+\tfrac{2s}{m^2_{n,n-i}-4\mu^2}\right), \tag{3.41}$$

being the contribution to the partial wave coefficient provided by the i^{th} trajectory. Again, given that the sum over trajectories has a finite number of terms, demanding that $f_J(s)$ diverges as $J \to \alpha_0(s)$ implies that at least one of the components $f_J^{(i)}(s)$ must diverge at this value of J. Repeating the argument used for the single-trajectory case, we see that at $s = 0$ the exponential damping of the $c_{n,n-i}$ coefficients yields partial wave trajectory coefficients $f_J^{(i)}$ that are regular and therefore the partial wave coefficients are free of poles also in this case.

The final step showing that this implies an inconsistency in the partial wave coefficients goes in the same way as in the single trajectory case. The absence of Regge poles in the case of finitely-many trajectories again implies that the Froissart-Gribov representation holds for $J \geq 0$, and in turn this implies that to have non-divergent partial wave coefficients the Legendre coefficients must satisfy a property analogous to eq. (3.42), namely

$$\lim_{n\to\infty} c_{n,n-i}\, e^{2(n-i)\sqrt{\frac{s}{m^2_{n,i}}}} = 0, \quad \forall i = 0, \ldots, N, \tag{3.42}$$

again for positive s as large as desired. Since this is in contradiction with the decay condition required to have channel duality, we conclude that the no-go also holds in the case of finitely many trajectories, and therefore these objects are ruled out too.

A crucial point is that the previous argument fails if we had an infinite number of Regge trajectories: in this case it would be possible that the contribution from each trajectory is finite, but the infinite sum over trajectories could give rise to the divergence of the partial wave coefficients. We will show later that this is precisely what happens for the Veneziano amplitude.

Importantly, this means that the residues corresponding to the subleading trajectories could in principle be arbitrarily small: this would not prevent the infinite sum to yield a pole in J in $f_J(s)$. Therefore, the argument we presented here does not put any constraint on the absolute size of the couplings $c_{n,J}$, and thus there is no immediate clash with the numerical results of [59–61]. The seemingly single-trajectory extremal amplitude that they observe could very well be a limiting case in which the couplings of the subleading trajectories are much smaller than those of the leading one, and therefore are not visible due to finite numerical precision.

3.3.1.5. Extension to higher dimensions

The extension of the previous result to higher dimensions can be proved as follows. In higher dimension $D = 4 + d$, Legendre polynomials get replaced by Gegenbauer polynomials with extremely similar properties. In order to rule out those cases as well, it is sufficient to observe that if meromorphic amplitudes with finitely many trajectories existed, they could be dimensionally reduced to $D = 4$ dimensions and would give rise to amplitudes with a larger number of Regge trajectories but still finitely many. Since these are excluded, they cannot have an ancestor in $4 + d$ dimensions and therefore these amplitudes cannot exist either, extending the previous results to $D \geq 4$.

3.3.1.6. How does the Veneziano amplitude evade the no-go?

As mentioned before, in the case of infinitely many Regge trajectories the exponential decay of the $c_{n,J}$ coefficients does not necessarily clash with the existence of Regge poles, as the divergence of the partial wave coefficients can be caused by the sum of the (finite) contributions of the infinitely many trajectories and not by the divergence of the contribution from a single trajectory. This is good news, as we would be in trouble if we found a constraint inconsistent with the existence of the Veneziano amplitude.

To check that this is the case, we use the fact that the residues of the Veneziano amplitude are given by

$$R_n^V(s) = \frac{(-1)^n}{n!}\frac{\Gamma(m_0^2 - s)}{\Gamma(m_0^2 - s - n)}. \tag{3.43}$$

Using Stirling's approximation for the Gamma function and the factorial as well as the Euler reflection formula of the Gamma function, it is simple to show that their asymptotic behaviour at large n is given by

$$R_n^V(s) \sim n^{s-m_0^2}, \quad n \to \infty. \tag{3.44}$$

Plugging this result for the residues and the asymptotic behaviour of the Q_J functions into eq. (3.12) we see that

$$f_J^V(s) \sim \sum_n n^{-J-1+s-m_0^2}, \tag{3.45}$$

which diverges as a simple pole precisely at the leading Regge pole $J = s - m_0^2$. To achieve this we used the full residue at each pole in s, and therefore all the infinitely many trajectories contributed to generating the divergence of the partial wave coefficient, as can be seen from decomposing the residues in Legendre polynomials. Note that the coefficients in the Legendre decomposition of the residues of the Veneziano amplitude are exponentially decaying at large n, meaning that the contributions of the form of eq. (3.41) are convergent when evaluated in the case of a linear spectrum. It is the infinite sum over trajectories that causes f_J to diverge.[9]

3.4. Discussion

In this chapter we have introduced some basic elements of Regge theory and then we have used them to prove that meromorphic amplitudes with finitely many Regge trajectories, with zero and one subtractions, are inconsistent with the standard bootstrap assumptions applied to dual models. To end we discuss how these results relate to older works and how they fit into the pool of knowledge regarding dual models, as well as possible new directions.

Relation to previous works: As noted in the introduction, we realized after completion of the proof presented here that the question of the consistencty of amplitudes with a finite number of Regge poles had been investigated in the literature before [151, 153–155]. These studies all rely on the use of the construction known as Finite Energy Sum Rules (FESRs) to attempt prove the non-existence of single-trajectory objects. We introduce FESRs in an appendix, and we mention the hidden assumptions that are required to employ them, for which no justification was given in the literature to the best of our knowledge. Basically, they assume that the speed at which the amplitude achieves Regge behavior is the same in all directions of the complex plane, and they rely on uncontrolled smoothing procedures to deal with the sum over poles. Moreover, while this works study the case of finitely many Regge poles, they do not consider the possibility of a meromorphic amplitude whose spectrum is not determined by Regge poles. In addition, they do not work out the case with subtractions,

[9] See some related comments in [152].

crucial to make contact with [59–61] and applications to large N QCD. Our work therefore supplements the existing body of literature with an argument directly tied to the amplitude's properties, with no extra assumptions, and extend it to the case with one subtraction.

Situation for Conformal Field Theories: Due to the higher amount of symmetry contained in the conformal group, the situation for conformal field theories (CFTs) is under better control. In particular, it is known that in $d \geq 2$ dimensions there exists infinitely many trajectories of double-trace operators which approach trajectories of constant twist [156, 157]. This has been proven rigorously recently in [158], and we refer to the references cited in there for a more thorough discussion of the question in CFTs.

Magnitude of daughter trajectories: In the last section we explained why our argument based on the regularity of the partial waves fails in the case of infinitely many trajectories. When showing how the Veneziano amplitude evades de no-go theorem, we saw explicitly that while each trajectory yields a finite contribution to $f_J(s)$, their infinite sum generates the divergence of $f_J(s)$ at $J = \alpha(s)$. This argument did not constrain the size of the trajectory.

The same argument can be made in the case with subtractions, and in particular, we are led to conjecture that the pion amplitude of [59–61] should possess infinitely many Regge trajectories, but we cannot give a lower bound on their size with the arguments of this work.

External spinning particles: We looked at the specific case of dual model amplitudes with external scalars. What if the external particles now have spin J_0? For instance, what about a four-vector boson or four-graviton amplitude? In this case, the spin-J_0–spin-J_0–spin-J vertex is comprised of more tensorial combinations, and we do not merely decompose on Legendre polynomials but on Wigner d-matrices, see e.g. [105]. For gravitons, we could also not keep the color-ordering assumption and should include explicitly the u-channel poles.

We have not studied this case in detail but we expect that it should be ruled out, too. This expectation derives from the similarity between adding more trajectories and adding tensor structures: any finite number should not allow for the existence of Regge pole for amplitudes with external spinning particles, and this should lead to their inconsistency in the same way as presented here. In particular, the crucial argument of our proof relies on the convergence of the s-channel pole expansion in t the cross channel, which forces the residue coefficients to be exponentially suppressed. Since Wigner d-matrices are also hyper-geometric functions, we would expect the same kind of exponential growth, forcing a similar exponential decay of the coefficients, which would then, in turn, give rise to regular partial waves. A more precise argument could be made using the results of [159], where it was shown how to decompose the spinning amplitudes on scalar amplitudes.

Regge cuts, relaxing narrow-width approximation: Finally, it would be very interesting to extend our work to the case of non-pure-meromorphic amplitudes and describe resonances with a non-vanishing width, amplitudes with cuts and Regge cuts, etc. Some remarks had been made in the past in [151, 160] and it would be interesting to revisit this story within the modern perspective of the S-matrix bootstrap. For instance, it is not obvious that a single Regge pole and a Regge cut is a disallowed configuration, but the techniques developed in this chapter would not allow us to say anything about this case.

Chapter 4.

Numerical bootstrap scheme for Dual Model Amplitudes

In this chapter we continue to put the Regge theory arsenal developed in the previous one in practice, and we present a numerical bootstrap framework based on linear programming to construct dual model amplitudes with customizable Regge trajectory functions. The results presented on this chapter are based on the article [2]. Throughout this chapter we work in units of $\alpha' = 1$.

Our main emphasis will be on the numerical construction of amplitudes with bending Regge trajectories as the ones shown in figure. (4.1). We focus on this case because this is the expected behavior for scattering amplitudes in QCD, and keeping the ultimate goal of finding the correct dual model amplitudes to describe hadronic scattering in large N QCD in mind, it is crucial to be able to produce meromorphic amplitudes with this feature. More precisely, it is a known general result from QCD [161] that scattering amplitudes at large energy and fixed angle exhibit a power-law decay of the form

$$A(s,t) \to s^{2-n_q/2} F(\theta), \tag{4.1}$$

where n_q corresponds to the total number of valence quarks involved in the process at hand ($n_q = 8$ for $2 \to 2$ pion scattering, for instance). Therefore, assuming that this prediction still holds in the large N limit, the expected fixed angle behavior of the dual model amplitudes describing these processes would differ sharply from the one of the available examples from string theory, which decay exponentially fast in this regime. Moreover, the exponential softness of stringy amplitudes can be traced to the fact that Regge trajectories are linear in t and therefore become infinitely negative as $t \to -\infty$. If we want to obtain power-law decay instead, they should rather bend and approach constant values in this region.

This makes the problem of constructing dual model amplitudes with bending Regge trajectories a very important one in the quest for a dual model-stringy description of large N QCD. However, this endeavour has proven to be notoriously difficult, and no models satisfying this behavior explicitly are known. Up to now, the only possibilities were to implement bending in an effective way by the superposition of linear trajectories, as we will elaborate on in what follows.

On the analytical side, even obtaining models departing from the linear (string-like) or logarithmic (Coon-like) spectra was out of reach until recently. However, a method to construct dual model amplitudes with non-linear spectra (and therefore non-linear trajectory functions) was proposed in [54]. Since the basic idea is beautifully simple we review it briefly.

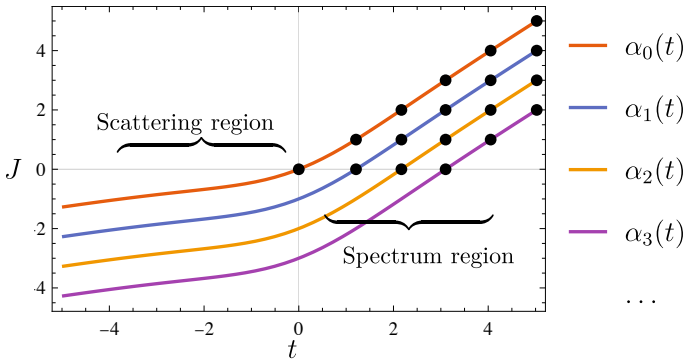


Figure 4.1.: Example of bent Regge trajectories for which we can construct amplitudes in dimensionless units $\alpha' = 1$.

Imagine one wants to construct a dual model amplitude with a spectrum that grows quadratically with the level, namely $m_n^2 = (n + m_0)^2$. A naive thing to do would be to simply take the Veneziano amplitude $A_V(s,t)$ and apply the non-linear map to s and t given by $s \mapsto \sqrt{s} - m_0$, and $t \mapsto \sqrt{t} - m_0$, yielding

$$A_V(s,t) = \frac{\Gamma(-s)\Gamma(-t)}{\Gamma(-s-t)} \mapsto A_V(\sqrt{s} - m_0, \sqrt{t} - m_0) = \frac{\Gamma(-\sqrt{s} + m_0)\Gamma(-\sqrt{t} + m_0)}{\Gamma(-\sqrt{s} - \sqrt{t} + 2m_0)}, \quad (4.2)$$

which obviously has poles at s, $t = (n + m_0)^2$ as desired. However, the square roots generate branch cut singularities inconsistent with meromorphicity, and moreover the residues at a given pole would be given in terms of non-integer powers of the Mandelstam variables, signaling a breakdown of locality.

It turns out that a simple fix exists, and the method proposed in [54] basically boils down to summing over all the branches induced by the square roots. The resulting amplitude is given by

$$A(s,t) = A_V(\sqrt{s} - m_0, \sqrt{t} - m_0) + A_V(-\sqrt{s} - m_0, \sqrt{t} - m_0) \quad (4.3)$$
$$+ A_V(\sqrt{s} - m_0, -\sqrt{t} - m_0) + A_V(-\sqrt{s} - m_0, -\sqrt{t} - m_0), \quad (4.4)$$

and it is such that all the branch cuts cancel out. Remarkably, it can be checked that this procedure also yields polynomial residues, and therefore allows to use the Veneziano amplitude as a starting point and then deform the spectra to obtain new meromorphic amplitudes. Naturally, the question of whether the resulting objects have positive residues or are compatible with higher-point factorization is not clear from this procedure, and it turns out that most of the amplitudes that can be generated this way cannot be embedded in consistent theories[1] However, it seems to be the case that there is still a non-trivial set of amplitudes generated by this method that are consistent with these properties.

Unfortunately, at least in its present form this method only allows to deal with spectra given by rational functions of the level, namely $m_n^2 = p(n)/q(n)$, with p and q polynomials. This limitation stems from the fact that in what we've done we had to invert the relation between n and m_n^2 to plug back into the Veneziano amplitude, and then summed over the

[1] In fact, the specific example with quadratic spectrum that we presented can be shown to posses negative residues for all values of m_0, and therefore doesn't yield a consistent amplitude.

branches arising from this procedure. In the case of non-rational spectra we cannot express the resulting amplitude as a finite sum over branches but rather we would need to consider infinitely many, and in general the required infinite sums would not be convergent. Since a rational function has the same growth at $\pm\infty$ (modulo a change of sign), it is clear that this method, while very interesting, cannont produce amplitudes with bending Regge trajectories.

This negative result seems to go in the direction of an old argument by Mandelstam for the linearity of Regge trajectories in dual models, which is a consequence of assuming that the trajectory functions $\alpha(t)$ are analytic and satisfy one-subtracted dispersion relations. Despite the fact that the reason to expect this requirements from the trajectory functions are unclear, this was the starting point taken in some existing works that attempted to build amplitudes with *effective* bending by summing over infinitely-many Veneziano amplitudes with decreasing slope [40, 162].

More explicitly, they consider constructions schematically of the form

$$A(s,t) = \sum_{k=1}^{\infty} a_k \, A_V\left(\frac{s}{k}, \frac{t}{k}\right). \tag{4.5}$$

While the contribution from each term has linear trajectories of the form $\alpha_k(t) \sim t/k$ and thus in the positive t region the one that dominates is simply the one with $k = 1$, we can see that for negative values of t the trajectories with larger k (and thus smaller slope) will become dominant, producing a bent effective leading trajectory as is shown in figure (4.2).

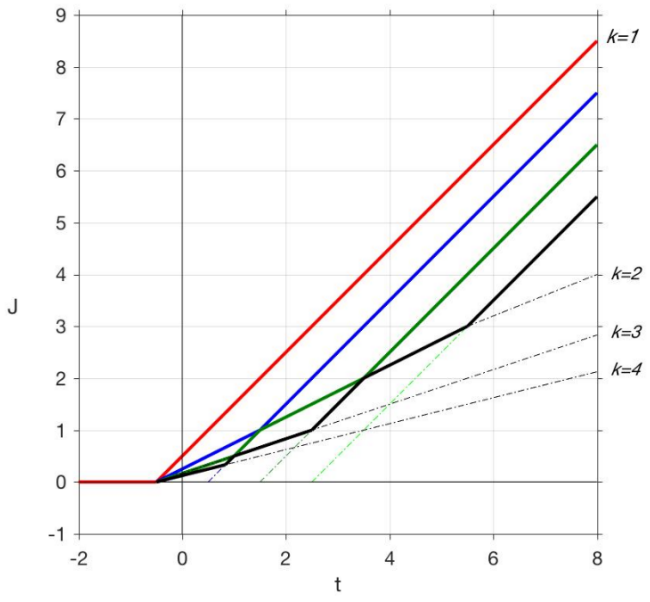


Figure 4.2.: Leading (in red) and next three subleading (in blue, green, black) Regge trajectories of a model of the kind of eq. (4.5) with intercept 1/2. The full lines represent the effective bending trajectories arising by combining the ones from different terms in the sum, while the dashed lines represent the individual contributions from each k. Image taken from [40].

This approach was quite succesful, and particularly in [40] the authors found some regions of parameter space[2] for which the resulting amplitudes had a power-law decay at fixed angles compatible with the one corresponding to pion scattering and where the residues were ghost-free, at least up to numerical truncation.

These two examples immediately lead to wonder if models with effective bending are indeed the only possibility to reconcile meromorphicity, channel duality and power-law decay at fixed angles, and if large N QCD is constrained to somehow realize this type of mechanism. This question partly motivates the work presented in this chapter. As we will explain shortly, our numerical method allows to construct seemingly consistent dual model amplitudes with explicit bending of the trajectories, hinting that there is more to this story yet to be understood.

On the numerical side, as has been mentioned in various parts of this text the task of creating numerical schemes to construct consistent, generic dual model amplitudes is a formidable one despite the recent remarkable progress on the understanding of dual models. The main reason why the problem is challenging is that the infinite sum over the resonances converges very slowly, and thus trying to impose the bootstrap constraints on the truncated amplitude doesn't yield meaningful, convergent results, at least for truncations that allow for a tractable numerical implementation.

Recently there has been advances in the numerical construction of dual amplitudes that manage to bypass this issue, but always restricted to the case of linear spectra. On the one hand, in [69], the authors used powerful primal and dual bootstrap tools to explore the space of amplitudes with linearly growing, stringy spectra. In the case of color-ordered (open string-like) amplitudes, they do so by using an ansatz of the form

$$A(s,t) = \sum_{i=0}^{\infty} \sum_{k=0}^{i} b_{ik} \frac{\Gamma(i-s)\Gamma(i-t)}{\Gamma(i+k-s-t)}, \tag{4.6}$$

in which each of the terms is individually crossing symmetric and where $i = k = 0$ yields the Veneziano amplitude. This expansion was originally studied by Khuri in [163], and it is expected that any amplitude with linear trajectories and equidistant spectrum can be written in this form. While the authors show that truncating this sum always leads to negative coefficients in the Gegenbauer decomposition of the residues and thus violates unitarity, they find a subset of amplitudes defined by three parameters (c_0, c_1, λ) that can be obtained by performing the sum (4.6) with a specific choice of coefficients $b_{ik}(c_0, c_1, \lambda)$ and can be expressed as an extension of the standard Koba Nielsen integral for open strings depending on these parameters. Therefore, they remove the need for truncations when restricting to this subspace of amplitudes, and they proceed to impose unitarity and explore the space of Wilson coefficients covered by this three-parameter family. However, despite the obvious advantages of this ansatz, it only allows to probe the space of amplitudes with linear spectra and parallel trajectories, as can be seen from the fact all the Veneziano blocks in the sum (4.6) have the same slope. Therefore, this family of models cannot produce bending, either explicitly nor effectively as was explained in the last section.

An even more recent attempt has been to use crossing symmetric dispersion relations to derive channel duality-like expressions for the amplitudes that have a much better speed of

[2] The parameter space is defined by the way in which they paramterized the coefficients a_k in the sum (4.5). They assumed an asymptotic decay of the coefficients $a_k \ k^{-\beta-1}(\log k)^{-\gamma}$ as $k \to \infty$, and explored the β, γ parameter space.

convergence, as was done for amplitudes with linear spectra in [148]. While this approach seems very powerful (and was not available at the time the results presented in this chapter were published), this technology has only been implemented for the case of linear spectra, and the generalization to non-linear trajectories remains unknown. Moreover, the data defining these expansions for the amplitudes are the locations of their poles and their corresponding residues, just as in the standard pole expansions that we have already seen. In both cases the amplitudes are written in terms of masses and couplings related to the "positive energy" region of the trajectories, namely the values of the trajectory functions $\alpha(t)$ and their residues $\beta(t)$ at positive values of t, while bending is a phenomenon intrinsically related to their behavior at large, negative t (see figure. (4.1)). Therefore, even if using crossing symmetric dispersion relations gives a fastly convergent expansion for the amplitude, it does not give direct access to the $\alpha(t)$ functions themselves but rather to their values in discrete set of points at positive t, and an approach allowing to deal directly with the behavior of these functions in the region $t < 0$ would be desirable.

All in all, neither the analytical nor the numerical approaches existing prior to the work presented in this chapter allowed to test the explicit bending of Regge trajectories in dual model amplitudes [3]. Contributing to this goal, in this chapter we present a numerical bootstrap scheme for dual models with linear and non-linear trajectories that combines the standard assumptions of analyticity, crossing and unitarity within a linear programming paradigm crucially granting us computational speed. It is based on an improvement by Mandelstam of the Sommerfeld-Watson transform presented in the previous chapter that allows to write an expansion for the amplitude as a sum of Regge poles that has much better convergence properties than the sum over poles in the Mandelstam variables, making a numerical treatment feasible, and that gives direct access to the shape of the Regge trajectories. We will refer to these improved techniques as the *Mandelstam-Sommerfeld-Watson* transform (MSW) and the *Mandelstam-Regge pole expansion* (MRPE), and we will introduce them shortly.

Our bootstrap takes as an *input* the set of Regge trajectory functions $\alpha_i(t)$, from the leading one $i = 0$ to a cut-off $i = N_{\text{traj}}$, and a tolerance ϵ which indicates by how much crossing is satisfied, as the truncated sum can never be completely crossing symmetric. It produces as an *output* the corresponding Regge residues $\beta_i(t)$, which allows us to fully reconstruct the amplitude.

To parametrize our input, we use a restricted but non-trivial polynomial ansatz which retains the general form of the Veneziano amplitude's Regge residues. To calibrate the bootstrap we start with the case of linear spectra, and we discover that the algorithm's tolerance drops significantly at the location of the Veneziano amplitude as we scan the space of amplitudes, showing that the Veneziano amplitude is a solution that maximizes crossing symmetry for the truncated ansatz.

This teaches us firstly that we can consistently detect the Veneziano amplitude. This self-consistency test alone is remarkable, and provides a solid proof of principle for our method. Moreover, this test also provides us with a guiding principle: When departing from Veneziano-like linear spectra, we can detect candidate physical amplitudes by searching for these special points that maximize crossing in the space of amplitudes.

[3] Note that we distinguish between *explicit* bending, which requires the trajectory functions to be non-linear, and *effective* bending, as the one in the models described previously.

Based on this observations, we proceed to deform the trajectories to ones exhibiting bending behavior at negative t defined by two different slopes for $t > 0$ and $t < 0$, and follow the location of the point in amplitude space maximizing crossing to identify physical amplitudes. We track and display various observables across the deformation. This constitutes a proof of principle that our method can firstly consistently generate meromorphic amplitudes, and provides compelling evidence that explicit bending of the trajectories is achievable within the realm of dual model amplitudes, at least at the level of the $2 \to 2$ scattering amplitudes. As an extra consistency check of our method, we show that it is sensitive to the fact that Regge trajectories growing faster than linearly at positive energies are expected to be inconsistent with the dual model bootstrap axioms [39, 69].

In what follows we introduce firstly the Mandelstam-Sommerfeld-Watson transform and then proceed to explain the bootstrap method in detail. Along the way, we derive the expressions for the first Regge trajectories and residues of the Veneziano amplitude using a trick based on the Froissart-Gribov projection of the partial wave coefficients. Since to the best of our knowledge these are not available anywhere in the literature, we briefly explain the computation and give their values on an appendix. In the discussion, we comment on the perspectives opened by our construction.

4.1. Mandelstam-Sommerfeld-Watson transform

We start by reviewing the improvement by Mandelstam to the Sommerfeld-Watson transform presented in last chapter. There we saw that the Sommerfeld-Watson transform induces a boundary in the complex J-plane at $\operatorname{Re} J = -1/2$, as continuing the contour past this point yields a background integral that grows increasingly faster at large energies and thus dominates over the contribution of the Regge poles. This limits the amount of Regge poles we can explicitly uncover and use for instance to determine the spectrum and couplings of the dual model. Therefore, if we want to use Regge theory to have access to trajectories beyond the few leading ones we need a way around this obstruction.

As often, fortunately the elders had come up with a solution to this, and in the early 60s Mandelstam gave a way of modifying the Sommerfeld-Watson transfom allowing to push the contour further to the left in the complex J-plane [150].

The basic idea is to replace the P_J function with a Q_J function, which has better convergence properties at infinity,[4] and the procedure boils down to Legendre function gymnastics.

Starting from the usual t-channel partial wave expansion for the amplitude we *add zero* in a smart way, by adding and subtracting the following terms

$$\begin{aligned} A(s,t) = 16\pi \sum_{J=0}^{\infty} \left\{ (2J+1) f_J(t) P_J(z) + \frac{1}{\pi}(2J) f_{J-1/2}(t) Q_{J-1/2}(z) \right\} \\ - 16\pi \sum_{J=1}^{\infty} \frac{1}{\pi}(2J) f_{J-1/2}(t) Q_{J-1/2}(z), \end{aligned} \tag{4.7}$$

[4] This feature is also what makes Froissart-Gribov powerful.

with

$$z = 1 + \frac{2s}{t - 4\mu^2}\,. \tag{4.8}$$

Notice that in eq. (4.7), the Q-term at $J = 0$ is absent because of the factor $2J$, thus $Q_{-1/2}$ does not belong to the sum.

As explained in last chapter when introducing the Froissart-Gribov projection, for integer J, Q_J has a cut on the $[-1;1]$ interval, with the discontinuity being the proportional P_J function. At non-integer J, Q_J also has a cut extending from -1 to $-\infty$ given by

$$\begin{aligned} \mathrm{Im} Q_J(z) &= \sin\pi J\, Q_J(-z), \quad -\infty < z < -1 &(4.9)\\ &= -\frac{\pi}{2} P_J(z), \qquad\quad -1 < z < 1. &(4.10)\end{aligned}$$

Now we perform a Sommerfeld-Watson transformation on the terms inside the curly brackets. For the first term we divide by $\sin\pi J$ as usual to replace the sum over integers by a contour integral in J, obtaining the standard Sommerfeld-Watson representation shown in eq. (3.13). For the second term, since the sum runs over half-integers we replace the usual $(\sin\pi J)^{-1}$ factor by $(\cos\pi J)^{-1}$ to get the correct poles at half-integers from the J-integral.

Using the following property relating the Q_J and P_J functions,

$$\frac{P_J(z)}{\sin\pi J} - \frac{1}{\pi}\frac{Q_J(z)}{\cos\pi J} = -\frac{1}{\pi}\frac{Q_{-J-1}(z)}{\cos\pi J},$$

we can we can combine both integrals to get that the term between curly brackets in eq. (4.7) can be expressed as

$$16\pi \sum_J \Big\{ \dots \Big\} = \frac{16}{2i} \int_{-i\infty-1/2+\epsilon}^{i\infty-1/2+\epsilon} (2J+1) f_J(t) \frac{Q_{-J-1}(-z_t)}{\cos\pi J}\, \mathrm{d}J. \tag{4.11}$$

We are now ready to push the contour to $\mathrm{Re}\, J < -1/2$. We will just pick up poles at every negative half-integer, apart from the possible singularities of f_J that we might cross. If we set the contour at $\mathrm{Re}\, J = -L$, we get:

$$\begin{aligned} 16\pi \sum_J \Big\{ \dots \Big\} = {} & \frac{16}{2i} \int_{-L-i\infty}^{-L+i\infty} (2J+1) f_J(t) \frac{Q_{-J-1}(-z_t)}{\cos\pi J}\, \mathrm{d}J \\ & - 16\pi \sum_{J=-L'}^{-1/2} \frac{(-1)^{J-1/2}}{\pi} (2J) f_J(t) Q_{-J-1}(-z_t) + \text{Regge poles and cuts}, \end{aligned} \tag{4.12}$$

where $L' = \lceil L \rceil$ is the closest half-integer to L greater than L. At half-integer points, the Q_J-functions possess a reflection symmetry around $J = 1/2$:

$$Q_J = Q_{-J-1} \quad J \in \mathbb{Z} + 1/2. \tag{4.13}$$

By means of the Froissart-Gribov projection, this symmetry is transmited to the partial wave coefficients f_J in the cases in which this representation is applicable, namely for J large enough for the integral along the discontinuity of the amplitude in eq. (3.8) to converge, and is sometimes called the "Mandelstam symmetry" of partial waves [164]. In his original

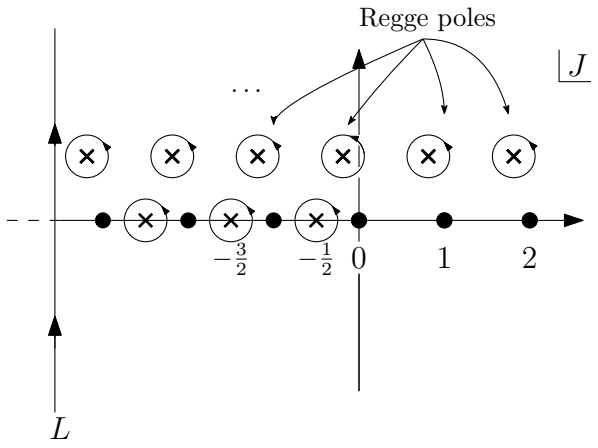


Figure 4.3.: Mandelstam-Sommerfeld-Watson contour.

paper [150], Mandelstam simply assumes that the same property holds for all partial waves and that we have that $f_J = f_{-J-1}$ at half-integer J. This seems reasonable from the Froissart-Gribov's perspective, but is still an assumption that we make in this derivation.

Assuming that the Mandelstam symmetry holds, it is easy to see that by changing $J \to -J - 1/2$ in the sum we will cancel the first $L' - 1/2$ terms in the infinite sum outside the curly brackets in eq. (4.7).

Under these conditions, we get

$$A(s,t) = \frac{16}{2i}\int_{L-i\infty}^{L+i\infty}(2J+1)f_J(t)\frac{Q_{-J-1}(-z)}{\cos\pi J}\,\mathrm{d}J - 16\pi\sum_{J=L'+1/2}^{\infty}\frac{(-1)^{J-1}}{\pi}(2J)f_{-J-1/2}(t)Q_{-J-1/2}(z) + \text{Regge poles and cuts.} \quad (4.14)$$

The important point that Mandelstam makes is that for z large, both the background integral and the infinite sum go like z^{-L} due to the asymptotic behaviour of the Q_J (see eq. (3.9), and thus we can suppress their contribution by pushing the contour to the left. This representation then allows us to express the amplitude exclusively in terms of the singularities of the analytical continuation of the partial waves into complex J in this regime to an extremely good approximation.

In the case of meromorphic amplitudes the only allowed singularities in J are Regge poles of the form $f_J(t) \sim \beta_i(t)/(J - \alpha_i(t))$, and their contribution is given by

$$-16\pi\sum_i(2\alpha_i(t)+1)\beta_i(t)\frac{Q_{-\alpha_i(t)-1}(-z)}{\cos\pi\alpha_i(t)}, \quad (4.15)$$

where i labels the Regge poles picked up by the Mandelstam-Sommerfeld-Watson integral. Note that while in the standard Sommerfeld-Watson case the Regge poles carried a factor of $(\sin\pi\alpha_i(t))^{-1}$ that produced the infinitely many poles in t defining the Regge trajectory, in this case this behavior is generated by the factor $Q_{-\alpha_i(t)-1}(z)$, as the Q_J functions have simple

poles at every negative integer J, and therefore diverge when $\alpha_i(t) = 0, 1, \ldots$, reproducing the expected poles in t.

The question of whether in some conditions this procedure can be continued indefinitely and the contour pushed arbitrarily to the left is an open question. This would require that the partial waves do not grow exponentially in the negative, imaginary J direction. If this were the case, the contribution from the background integral and the infinite sum would vanish, and the amplitude could be exactly expressed in terms of its singularities in complex J in the t-channel. An important point is that the terms associated with the singularities in J on the t-channel Mandelstam-Sommerfeld-Watson representation of the amplitude do not exhibit any of the s-channel singularities. Therefore, in the case in which the contour is closed at a finite value of J, they must be hidden in the background integral. Consequently, if we were allowed to drop this contribution this would imply a J-plane channel-duality, in which the s-channel singularities would be generated by the sum of the ones on the t-channel.

A clear counter-example to this procedure is the Veneziano amplitude. As is known and we checked explicitly, its expansion over Regge poles is only asymptotic, and therefore the effects of the background integral must be taken into account to recover the full amplitude. However, it might still be plausible to think that in some scenarios the situation could be different and that this sort of $J-$plane manipulations could be used to constrain amplitudes in a way analogous to channel duality.

The main source of uncertainty here is that we have a priori no control over the partial waves in the background integral at large $-L'$ and it is not even clear how to define them, as the Froissart-Gribov projection is not applicable there (remember the Mandelstam symmetry only works for *integer* J, on the complex line above the integer it no longer holds in general). Unfortunately, the rigorous definition of the partial wave coefficients at negative J would be needed to properly address this question is not available to us at the moment.

However, recall that the Q_J functions posses a branch cut extending between $z = 1$ and $-\infty$ which is not related to the physical cuts expected from unitarity. To make it worse, in the case of dual model amplitudes we do not expect branch cuts at all, and therefore if the amplitude could be expressed exclusively in terms of *Mandelstam-Regge poles* as those in eq. (4.15) we would need these branch cut singularities to somehow cancel each other out[5]. A similar phenomenon should happen with the spurious poles at half-integer values of the $\alpha_i(t)$ generated by the $(\cos \pi\alpha_i(t))^{-1}$ factors in eq. (4.15). For an expansion purely in terms of Mandelstam-Regge poles to be possible we need to require that the residues $\beta_i(t)$ have zeros at those precise values to cancel these infinitely-many spurious poles, which seems an unnatural restriction on the Regge residues when seen solely from the standard Sommerfeld-Watson transform.

These arguments together with the negative example of the Veneziano amplitude, while not a proof, are compelling evidence that in general the background terms cannot be neglected if one wants an exact representation for the amplitude, and the most reasonable scenario seems to be that at some point the behavior of the f_J for negative enough J is such that the background terms stop being under control and the approximation of the amplitude as a sum of Regge poles breaks down.

[5] Note that they are indeed canceled by the background terms by construction, the problem arises when these are sent to zero by pushing the contour infinitely to the left.

However, it is still the case that the expansion exclusively in terms of Mandelstam-Regge poles can approximate the amplitude to very large precision even when keeping only a few terms in the sum, at least away from the locations of the spurious singularities mentioned in the previous paragraph. Even if the background term would eventually come back to bite us if we increased the number of terms too much, the accuracy of the approximation with finitely many poles is such that one can still get a lot of information from it. As a concrete example, the Mandelstam-Regge pole expansion of the Veneziano amplitude including 8 poles matches the values of the full Veneziano amplitude to a precision higher than 10^{-10} away from the singular regions, as is shown in figure (4.5). As we will see, the large precision of the truncated Mandelstam-Regge expansion is at the center of the numerical appoach that will be presented in the following sections.

4.2. Lessons from the Veneziano amplitude

As explained in the previous section, we lack a rigorous understanding of the regions where the background terms in the Mandelstam-Sommerfeld-Watson are negligible, both in the Mandelstam variables and in the complex J-plane. While such an understanding is strongly desirable and developing it is definitely a question that should be addressed, for the moment we will take the more humble alternative of benchmarking and testing our assertions with the best available example: the Veneziano amplitude. Since after all our bootstrap method will be based on an ansatz inspired by the structure of the Veneziano amplitude, it seems reasonable to assume that the regions of applicability of this framework should not change dramatically in this more general setup.

However, to be able to compare the full Veneziano amplitude to its Mandelstam-Regge pole expansion we naturally need to first deal with the problem of extracting the corresponding Regge poles and their corresponding residues from the amplitude. A very efficient way of doing so is based on the Froissart-Gribov projection of the partial wave coefficients, which we will explain in what follows.

4.2.1. Extraction of the Regge poles

For simplicity, we set $m_0^2 = 0$, therefore the Regge poles will be located at values $J = \alpha_i(s) = s - i$, as dictated by the fact that the Veneziano amplitude has parallel, linear trajectories. As we saw, the Regge poles are defined by the values of J for which the partial wave coefficients have a simple pole, and therefore the strategy will be to extract this divergences from the Froissart-Gribov integral (see eq. (3.8)) of the Veneziano amplitude.

The first ingredient is to compute the discontinuity of the Veneziano amplitude, which can be readily done with some gamma function gymnastics. We start with the Veneziano amplitude

$$A_V(s,t) = -\frac{\Gamma(-s)\Gamma(-t)}{\Gamma(-s-t)} \tag{4.16}$$

Using Euler's reflection formula, $\Gamma(1-x)\Gamma(x) = \frac{\pi}{\sin(\pi x)}$, we can isolate the piece of the amplitude that generates the poles in the Mandelstam variables from the one generating the

residues:

$$-\frac{\Gamma(-s)\Gamma(-t)}{\Gamma(-s-t)} = \pi \frac{\sin(\pi(s+t))}{\sin(\pi s)\sin(\pi t)} \frac{\Gamma(s+t+1)}{\Gamma(s+1)\Gamma(t+1)} \tag{4.17}$$

where now the ratio of gamma functions in the right-hand-side allows to read directly the residues, while the poles in s and t are contained exclusively in the term with the sines. Note that the unphysical poles at the negative integers r are canceled by zeros of the ratio of gamma functions.

The virtue of this expression is that, while the discontinuity of the Veneziano is clearly given by a discrete sum over delta functions as it should for a meromorphic function, we are interested in extracting divergences for the Froissart-Gribov representation which will come from the large t region of the integral. Therefore it is legitimate to approximate the discrete sum by its averaged contribution, and we can use the ratio of gammas appearing on the right hand of eq. (4.17) to represent the discontinuity of the amplitude inside the integral.

More concretely, we look for divergences in J of the integral

$$f_J(s) = \frac{1}{16\pi^2}\frac{2}{s}\int_0^\infty \mathrm{d}z\, Q_J\left(1+\frac{2t}{s}\right) \mathrm{Disc}_t A(s,t)\,, \tag{4.18}$$

which must necessarily come from the large t tail, as truncating the integral at any finite value of t would yield a finite answer.

We proceed to expand both the discontinuity of the amplitude and the Q_J functions in powers of $\frac{1}{t}$. The asymptotic expansion of the Q_J function can be obtained by its definition in terms of hypergeometric functions given in eq. (3.4), and reads

$$Q_J\left(1+\frac{2t}{s}\right) = N(J)\left(\frac{s}{t}\right)^{J+1}\left(1-\left(\frac{s}{t}\right)\frac{1+J}{2}+\left(\frac{s}{t}\right)^2\frac{(1+J)(2+J)^2}{4(3+2J)}+\dots\right) \tag{4.19}$$

with

$$N(J) = \frac{\sqrt{\pi}\Gamma(J+1)}{2^{2(J+1)}\Gamma(J+\frac{3}{2})}, \tag{4.20}$$

while the discontinuity of the amplitude can be expanded asymptotically at large t as a simple application of the Stirling approximation of the gamma function:

$$\mathrm{Disc}A_V(s,t) = \frac{t^s}{\Gamma(s+1)}\left(1+\frac{s(s+1)}{2t}+\frac{(s-1)s(s+1)(3s+2)}{24t^2}+\dots\right). \tag{4.21}$$

The Regge residue $\beta_i(s)$ is the residue corresponding to pole in $f_J(s)$ at $J = s - i$. From the asymptotic expantions of the Q_J function and the discontinuity, it is clear that the integrand will be given by an expansion of the form

$$\sum_{k=0}^{\infty} \beta_k(J,s)\, t^{s-J-1-k}, \tag{4.22}$$

and upon integration the term that will yield a pole at $J = s - i$ is the term with $k = i$. Therefore, to obtain the Regge residue functions we simply need to extract the corresponding $\beta_k(J, s)$ term from the asymptotic expansion of the integrand, and set $J = s - i$.

Using this technique we can easily automatize this procedure and compute Regge residues up to very high trajectories. The first few residues are given by

$$\beta_0(t) = B(t), \quad \beta_1(t) = B(t)\frac{1+2t}{t}, \quad \beta_2(t) = B(t)\frac{(1+2t)(t(t+5)-t)}{6t^2}\ldots, \tag{4.23}$$

where

$$B(t) = \frac{t^t\Gamma(1+t)}{\Gamma(2+2t)}, \tag{4.24}$$

is a universal factor that is present in all the Veneziano Regge residues.

Using this method we computed the Regge residues of the Veneziano amplitude up to the 37^{th} trajectory. We display some more of them in the appendix.

4.2.2. Super-unitarity

The Veneziano amplitude's Regge residues have remarkable properties. They all follow the same pattern, given by the universal $B(t)$ function times a rational function of the form $p_i(t)/t^{d_i}$, namely

$$\beta_i(t) = B(t)\frac{p_i(t)}{t^{d_i}}. \tag{4.25}$$

Here the p_i's are polynomials of degree q_i, and the q_i and d_i are integers given by $q_0 = 0$, $q_1 = 1$, $q_i = 3\lfloor\frac{i}{2}\rfloor$ for $i \geq 2$, and $d_0 = 0$, $d_1 = 1$, $d_i = 2\lfloor\frac{i}{2}\rfloor$ for $i \geq 2$, where $\lfloor x\rfloor$ denotes the largest integer smaller than x.

As we mentioned in the previous chapter, the Regge residues are directly related to the coefficients in the Legendre expansion of the amplitude's residues. For arbitrary trajectories, the relation is the following:

$$-16\pi(2(n-i)+1)\beta_i(m_n^2) = c_{n,n-i}, \tag{4.26}$$

as is immediately implied by evaluating the standard Sommerfeld-Watson representation near a pole:

$$A(s,t) \sim -16\pi(2(n-i)+1)\frac{1}{t-m_n^2}\beta_i(m_n^2)P_{n-i}(1+2s/m_n^2), \quad t \to m_n^2, \tag{4.27}$$

where $\alpha_i(m_n^2) = n - i$ by definition and thus $\beta(m_n^2)$ is proportional to the Legendre coefficient of the spin $J = (n-i)$ state exchanged at mass m_n^2.

In the language above, unitarity demands that

$$\beta_i(m_n^2) \geq 0, \tag{4.28}$$

which for the Veneziano amplitude becomes

$$\beta_i(n) \geq 0. \tag{4.29}$$

Since for Veneziano the β_i always have the form described above, and the universal function $B(t)$ is positive for positive t, unitarity requires that the polynomials $p_i(t)$ are non-negative when evaluated on integers $n \geq i$, namely $p_i(n) \geq 0 \, \forall n \in \mathbb{N}$, $n \geq i$,, since the first state from the i^{th} in the spectrum is always the scalar of mass i.

However, we observe that for all the Regge residues we extracted the Veneziano residues obey a stronger property that we refer to as *super-unitarity*: not only the polynomials are positive on all such integers, but when expressed as functions of their shifted arguments $t = x + i$, all of the coefficients of these new polynomials are positive:

$$p_i(t) = p_i(x+i) = \sum_{k=0}^{\lfloor 3/2i \rfloor} x^k b_{ik}, \quad b_{ik} \geq 0 \tag{4.30}$$

Naturally, requiring the positivity of the b_{ik} coefficients guarantees the positivity of the residues, and while we haven't found a proof of this fact in general, we have checked that it holds for all the trajectories we have computed. In fact, we extracted the Regge residues for the Veneziano amplitude also in arbitrary dimension, and in this case we checked that this property fails precisely for $d > 10$, the critical dimension of the Veneziano amplitude when $m_0^2 = 0$. This suggests that for $d \leq 10$ this is a true property of the Veneziano amplitude, and we will work under this assumption in what follows.

4.2.3. Validity of the Mandelstam-Regge pole expansion

As explained before, we expect that generically the Mandelstam-Regge pole expansion should be asymptotic, and after enough poles have been included in the sum, it should stop yielding a good approximation for the amplitude. In the specific case of the Veneziano amplitude this is obviously true, as to extract the Regge residues we used the Stirling expansion of the gamma function, which is known to be an asymptoti expansion for large values of its argument.

What is surprising is that, as was claimed before, truncating the Mandelstam-Regge pole expansion to include only a few Regge poles in the sum gives an outstanding match to the full amplitude for large regions of s, t, far away from the high energy region where this asymptotic expansion is naturally expected to work.

Before showing this in the case of the Veneziano amplitude, lets analyze with more care the regions of $(s,t) \in \mathbb{C}^2$ where this expansion can work, for which we must look at the analytic structure of the $Q_J(z)$ functions.

As explained, for integer J the $Q_J(z)$ have a branch cut extending from $z = -1$ to $z = 1$, and allowing for non-integer J opens a new discontinuity from $z = -1$ to $-\infty$. In both cases, the Q_J's have logarithmic singularities at the branch points $z = \pm 1$. Moreover, as a function of complex J they have simple poles every time J hits a negative integer. This is shown in the s-channel (for fixed t) in the case of linear trajectories in fig. 4.4.

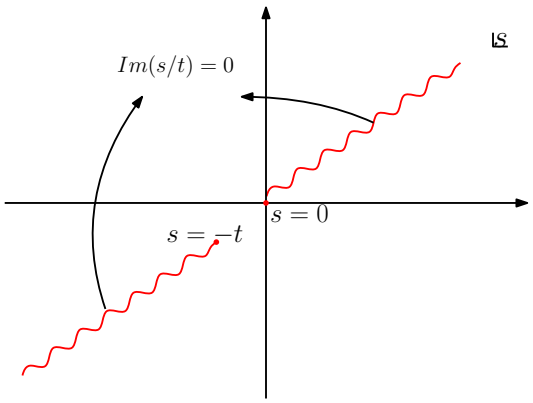


Figure 4.4.: Singularity structure of $Q_{-s-1}(-1-2t/s)$ in the complex s-plane for fixed t.

In the Mandelstam-Regge pole expansion, the Q_J's dependence on s and t is always of the form $Q_{-\alpha_i(s)-1}(-1-2t/s)$ (and the converse in the t-channel expansion), and thus we see that branch cuts are opening at $s=-t$ and $s=0$ and extending to infinity along the direction $\mathrm{Im}(s/t)=0$ [6].

As we have mentioned, this should raise some alarms. The objects we are trying to build are meromorphic functions, and thus they cannot have branch cuts or logarithmic singularities. In particular, we do not expect any discontinuity in the full amplitude when traversing these branch cuts, and therefore the Mandelstam-Regge expansion must stop being a good approximation for the full amplitude as one crosses them. One can indeed check this for the Veneziano amplitude: In terms of z the Mandelstam-Regge expansion can approximate the amplitude in the lower half plane $\mathrm{Im}z \leq 0$, and the match between the expansion and the full amplitude becomes better and better as one approaches $\mathrm{Im}z=0$ from below, where the Q_J's branch cut lies. However, as one crosses the real axis and passes into the $\mathrm{Im}z \geq 0$ region the discontinuity of the Q_J functions causes the Mandelstam-Regge expansion to completely break down. This teaches us that there is a *good side* of the branch cut where we need to stay, and that the Mandelstam-Regge expansion achieves its best convergence when approaching the branch cut on the real z axis from below. In the s-channel expansion the argument of the Q_J function is $-1-2t/s$, and therefore the above condition means that we need to restrict to values such that $\mathrm{Im}t/s \geq 0$, while the converse is true for the t-channel expansion. Moreover, naturally the convergence of the expansion worsens when $1+2t/s$ approaches ± 1 (or $1+2s/t$ approaches ± 1 for the t-channel) and one gets near the logarithmic singularities of the Q_J functions.

Finally, the $(\cos \pi\alpha_i)^{-1}$ terms in the Mandelstam-Regge expansion introduce an infinite number of spurious poles at half-integer values of the α_i's. This issue has been a matter of concern and some degree of confusion in the old days leading to efforts to find residue functions that vanish at every half-integer to cancel these poles. While this could be an extra constraint to impose on the β_i's. In the case of the Veneziano amplitude this is only realized half way as the residue functions have zeros at all negative half-integers and thus cancel the spurious poles at negative values. On the other hand, the poles caused by the cosines at positive values of the Mandelstam variables are still present, spoiling the validity of the

[6] Note that the singularity corresponding to $-1-2t/s=-1$ occurs at $s=\infty$, and therefore we will never deal with it in our numerics. However, the $z\to\infty$ singularity corresponds to $s=0$ for fixed t, and therefore we are sensitive to it.

expansion in the positive real axis. However, as one departs even a little from the real line the expansion quickly becomes spectacularly accurate again.

To sumarize, we expect the s-channel Mandelstam-Regge expansion to describe correctly the amplitude in regions of $(s,t) \in \mathbb{C}^2$ such that $\mathrm{Im}(t/s) \geq 0$, and sufficiently away from the positive real axis and the logarithmic singularities. To test this assertions, we can see how well the truncated Mandelstam-Regge expansion of the Veneziano amplitude approximates the full amplitude in in these values of (s,t). This is shown in figure (4.5), where we plot the ratio

$$\left|1 - \frac{A_{\mathrm{V}}^{N_{\mathrm{traj}}}(s,t)}{A_V(s,t)}\right|, \tag{4.31}$$

where $A_V(s,t)$ is the full Veneziano amplitude and $A_V^{N_{\mathrm{traj}}}$ is the truncated Mandelstam-Regge expansion:

$$A_V^{N_{\mathrm{traj}}}(s,t) = -16\pi \sum_{i=0}^{N_{\mathrm{traj}}} (2\alpha_i(s)+1)\beta_i(s)\frac{Q_{-\alpha_i(s)-1}(-z)}{\cos\pi\alpha_i(s)}. \tag{4.32}$$

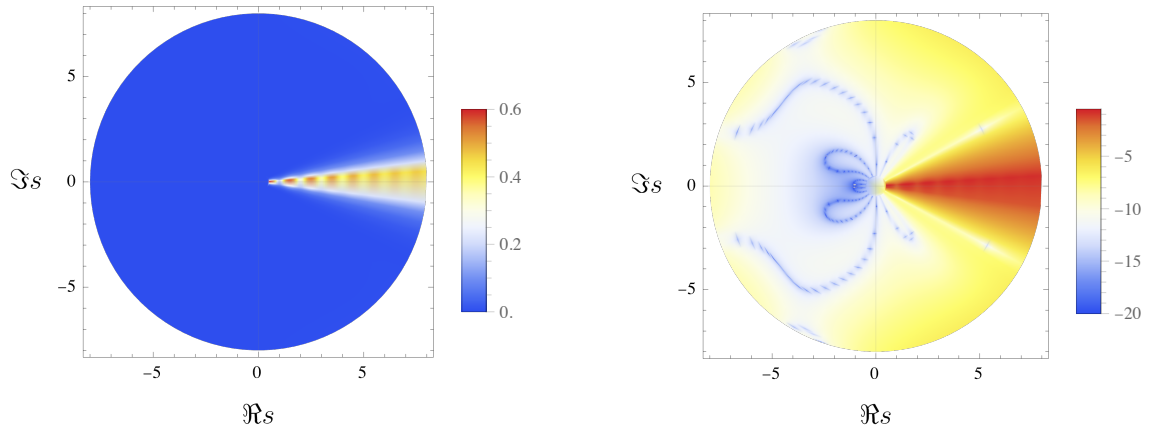


Figure 4.5.: (*Top*:) This displays $\left|1 - \frac{A_{\mathrm{Vene}}^{N_{\mathrm{traj}}=7}(s,t)}{A(s,t)}\right|$ over the complex plane for s, with $\Im(t/s) \to 0^+$ and $|t| = 2$, at $N_{\mathrm{traj}} = 7$ trajectories. (*Bottom*:) Logarithm of the same quantity.

In the plot we truncate the expansion at $N_{\mathrm{traj}} = 7$ over the complex s-plane, with $\mathrm{Im}(t/s) \to 0^+$ and $|t| = 2$. It shows that the Mandelstam-Regge expansion works extremely well away from the real axis, with the correct $i\epsilon$ prescription for $\mathrm{Im}t/s$, even when keeping only 8 terms in the sum [7]. This is in great contrast to what happens when trying to approximate the amplitude by a sum over poles in the Mandelstam variables: now the convergence is much faster, and the expansion is valid over a much larger region of $(s,t) \in \mathbb{C}^2$. Since the Regge trajectory functions and their respective residues characterize completely the amplitude, these considerations make it natural to choose this Regge basis as a starting point for a numerical bootstrap scheme. This will be the topic of the rest of the chapter.

[7] We have no interpretations for the features of super convergence (blue Rorschach curves on the right plot).

4.3. The Bootstrap method

By dissecting the Veneziano amplitude and the analytical structure of the Mandelstam-Regge expansion in the previous section we have learned various lessons. On the one hand, we found that there exist regions in complex s, t space where the Mandelstam-Regge expansion converges very fast. Moreover, the Regge poles $\alpha_i(s)$ contain all the information about the spectrum of the amplitude, each of them defining a Regge trajectory, and their respective residues $\beta_i(s)$ determine the coupling squared between the external particles that we scatter and all the particles lying in that trajectory. This last point allows us to turn the requirement of unitarity in the form of the reality of the couplings into a positivity condition on the $\beta_i(s)$.

These considerations motivate us to propose a bootstrap method for building dual amplitudes with customizable Regge trajectory functions which can be summarized in the following way:

- **Step 1:** Choose a set of $N_{\text{traj}} + 1$ trajectory functions (i.e. Regge Poles) $\alpha_i(s)$.
- **Step 2:** Write the truncated Mandelstam-Regge expansion for an amplitude with these trajectories and a priori arbitrary Regge residues $\beta_i(s)$, each of them parametrized by a set of coefficients a_{ij}.
- **Step 3:** Impose unitarity (as the positivity of the β_i's) and crossing over a grid of suitable points $(s, t) \in \mathbb{C}^2$. These become a set of linear constraints that the coefficients a_{ij} must satisfy.
- **Step 4:** Solve the linear program for the a_{ij}'s to obtain an amplitude with the desired Regge trajectories satisfying crossing and unitarity.
- **Step 5:** To explore the space of these amplitudes use linear programming to extremize a set of observables such as the value of the amplitude and its derivatives at a given point to find the regions in this space of observables compatible with the required constraints.

In what follows we provide the details of the method, defining the ansatz for the Regge residues and the specific way in which we impose unitarity crossing and the convergence with the number of trajectories to set up the optimization problem.

4.3.1. The truncated Mandelstam-Regge ansatz

The first ingredient to set up our Regge bootstrap is to write an ansatz for the amplitude on which we will enforce unitarity and crossing in a suitable way. To do this we use the Mandelstam-Regge expansion of the amplitude over Regge poles, truncated at some finite number of trajectories N_{traj} and neglecting the background integral contribution. In the s-channel this reads

$$A^{N_{\text{traj}}}(s,t) = -16\pi \sum_{i=0}^{N_{\text{traj}}} (2\alpha_i(s)+1)\beta_i(s)\frac{Q_{-\alpha_i(s)-1}(-z)}{\cos\pi\alpha_i(s)}. \tag{4.33}$$

From our analysis of the Mandelstam-Sommerfeld-Whatson transform we know that the contribution from the background integral becomes more and more suppressed the further

we push the integration contour to the left, exposing an increasing number of Regge poles. Thus, the truncated Mandelstam-Regge expansion approximates the full amplitude better the more trajectories we include. As explained before, a crucial point is that only a small number of trajectories is necessary to obtain a very good match to the full amplitude in some regions of s, t allowing for a numerically treatable setup. Of course, we expect that adding more trajectories improves the precision of the Mandelstam-Regge expansion only until a certain point, beyond which the asymptotic series diverges and the inclusion of trajectories causes new terms in the expansion to decrease the quality of the approximation. However, the number of trajectories for which this happens is generically very large, and given that our bootstrap attains good results using much fewer trajectories we can safely ignore this problem.

Moreover, once we fix the $\alpha_i(s)$ functions everything in eq. 4.33 is fixed by kinematics except for the Regge residues $\beta_i(s)$, and hence they define the amplitude. Our strategy is therefore to use an ansatz for the Regge residues mimicking the structure of those of the Veneziano amplitude shown in eq. (4.25), parametrizing the Regge residues as

$$\beta_i(s) = B(\alpha_0(s))\frac{1}{s^{d_i}}p_i(s), \qquad p_i(s) = \sum_{j=0}^{q_i} a_{ij}s^j \tag{4.34}$$

where the $p_i(s)$ are polynomials of the same degree as those in the corresponding Veneziano residue, but they are allowed to have arbitrary coefficients. We also keep the same power in the factor s^{-d_i}. The trajectory-independent function B is also the same as the one for Veneziano, but now composed with $\alpha_0(s)$, the leading trajectory. This will be important for the ansatz to be able to produce amplitudes with non-linear trajectories (note that for Veneziano, $\alpha_0(s) = s$ and therefore this is a natural generalization). Within this ansatz the amplitude is completely determined once setting the values of the coefficients a_{ij}.

4.3.2. Unitarity

Equipped with the ansatz 4.34 it is simple to recast unitarity as a condition on the a_{ij}. Recalling from the previous section, from eq. (4.27) we see that the $\beta_i(s)$ must be non-negative everytime s hits a mass in the i^{th} trajectory. Since we chose $B(s)$ to be positive in the spectrum region, this becomes just the condition that the polynomials $p_i(s)$ must be positive at this values of s.

A stronger but reasonable requirement is demanding that the polynomials are not just positive at these specific values but on the whole semi-infinite line starting at the mass $m_{i,0}^2 = \alpha_i^{-1}(0)$ of the lightest particle in the corresponding trajectory, namely

$$p_i(x + \alpha_i^{-1}(0)) \geq 0, \quad x \geq 0, \tag{4.35}$$

for $s = x + \alpha_i^{-1}(0)$. This type of constraint is amenable to semidefinite programming and could be incorporated to our bootstrap. However, borrowing inspiration from the case of the Veneziano amplitude described in the previous section, we will impose the stronger *super-unitarity* condition by demanding that all the coefficients in x of p_i are positive:

$$p_i(x + \alpha_i^{-1}(0)) = \sum_{j=0}^{q_i} b_{ij}x^j, \quad b_{ij} \geq 0. \tag{4.36}$$

This is a sufficient (albeit not necessary) condition for unitarity, and has the advantage that each b_{ij} is just a linear combination of the original a_{ij} coefficients. This way the positivity of the b_{ij}'s can be imposed as a set of linear constraints on the a_{ij}, allowing to restrict the optimization problem to a linear one. While this restricts the class of amplitudes that the ansatz can achieve, since the main goal is to build explicit examples of dual model amplitudes with specific features (bending trajectories in this case) and not to fully characterize the space of consistent dual models, this is not a problem.

4.3.3. Crossing

We arrive at one of the most delicate aspects of our bootstrap procedure, namely finding a way of imposing crossing consistently on our ansatz based on the Mandelstam-Regge expansions. One of the main challenges is the fact that crossing cannot be satisfied exactly with our ansatz, as each term in the finite sum is manifestly non-crossing symmetric, and hence we need a way of imposing crossing only *approximately*. Moreover, having determined the regions in s, t where the Mandelstam-Regge expansion in a given channel provides a good description of the amplitude, we must look for the intersection of these regions in both s and t-channels, as only there it is reasonable to impose (approximate) crossing on the ansatz.

We address the first issue by demanding that for a given number of trajectories N_{traj} the ansatz satisfies crossing up to a certain tolerance that we denote ϵ. To be more precise, we impose

$$\left| 1 - \frac{A^{N_{\text{traj}}}(t_j, s_j)}{A^{N_{\text{traj}}}(s_j, t_j)} \right| \leq \epsilon. \tag{4.37}$$

on a suitable set of N points $\{(s_j, t_j)\}_{j=1}^{N}$. Assuming a sign for $A^{N_{\text{traj}}}(s, t)$ allows to reformulate eq. (4.37) as a linear inequality involving the ansatz parameters a_{ij}, yielding

$$-\epsilon A^{N_{\text{traj}}}(s_j, t_j) \leq A^{N_{\text{traj}}}(s_j, t_j) - A^{N_{\text{traj}}}(t_j, s_j) \leq \epsilon A^{N_{\text{traj}}}(s_j, t_j), \tag{4.38}$$

if $A^{N_{\text{traj}}}(s_j, t_j) \geq 0$, while the inequality is reversed in the oposite case.

Sampling over the set of points $\{(s_j, t_j)\}_{j=1}^{N}$ generates the constraints that we use to impose crossing on the amplitude.

As we saw before, on a given channel the Mandelstam-Regge expansion is a good approximation for the amplitude whenever the argument of the Q_J functions is on the right side of the branch cut, which for the s-channel meant $\text{Im}(t/s) \geq 0$, while for the t-channel the reverse inequality $\text{Im}(s/t) \geq 0 \iff \text{Im}(t/s) \leq 0$. Therefore, the intersection of the two regions is precisely the branch cut located at $\text{Im}(t/s) = 0$, and this is where crossing can be imposed.

More precisely, at the branch cut the Q_J functions are ill defined and we should rather evaluate them using an $i\epsilon$ prescription to make sure we approach the cut from the right direction, evaluating the s- channel terms at points $(s_j - i\tilde{\epsilon}, t_j)$ and the t-channel terms at $(s_j + i\tilde{\epsilon}, t_j)$, with $\text{Im}(t_j/s_j) = 0$. Note that $\tilde{\epsilon}$ is just a small parameter to ensure the evaluation on the right branch of the Q_J functions, and has nothing to do with the parameter ϵ defining the tolerance up to which we impose crossing.

Taking these subtleties into account, we impose crossing along rays satisfying $\mathrm{Im}(t/s)$ in $(s,t) \in \mathbb{C}^2$, sufficiently far from the singularities of the Q_J functions and the positive, real axis and applying the mentioned prescription to deal with the branch cuts. We impose the constraints on $\mathcal{O}(10^3)$ points belonging to the regions shown in figure (4.6). The details on the grid of points we used are as follows: For R1 we used a set of 767 points from radius $\rho = 1$ to $\rho = 5$ and angle $\theta = 2/10$ to $\theta = \pi/4$ (using polar coordinates in the negative, real (s,t) quadrant given by $s = -\rho\cos\theta$, $t = -\rho\sin\theta$). For R2 we used a set of 270 points lying on rays $\Im(s/t) = 0$ (namely $s = |s|e^{i\theta}$, $t = |t|e^{i\theta}$, with $|s| \in [1,8]$ and fixing $|t| = 2$, and $\theta \in [2.9, 3.4]$; R3 = Point $(4e^{i/4}, 5e^{i/4})$; R4 = Point $(\frac{9}{2}e^{i6/5}, 2e^{i6/5})$. When s,t are complex, we restrict ourselves to applying crossing on the *real part* of $A^{N_{\mathrm{traj}}}(s_j,t_j)$ only.

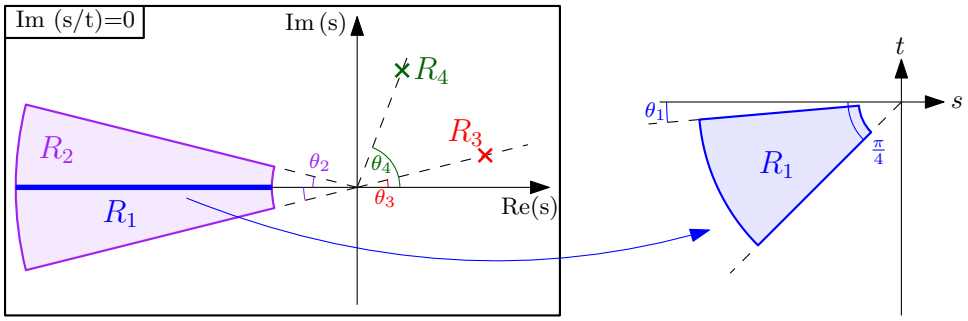


Figure 4.6.: Depiction of domains of $(s,t) \in \mathbb{C}^2$ where we enforce crossing. Left: complex plane for s, where t is constrained to lie on the same ray as s. Right: region $s,t < 0$. We have: $\theta_1 = 2/10 (\simeq \pi/15), \theta_2 \simeq \pi/12, \theta_3 = 1/4 \simeq \pi/12$, $\theta_4 = 6/5 \simeq 3\pi/8$.

These regions where chosen in such a way as to get results that are converged (namely, that are stable when adding more constraints by imposing crossing at extra points) with the lowest number of constraints possible. More details on the numerics are given in an appendix.

The question of the sign used to define (4.38) is important: as can be checked on the Mandelstam-Regge pole expansion of the Veneziano amplitude, in most parts of regions R1 and R2 the Mandelstam-Regge expansion is sufficiently dominated by the leading trajectory that the sign is determined by it. Since it depends only on the universal function as the leading Regge residue's polynomial is trivial, the ansatz itself fixes the sign of the amplitude at these points, and enforcing a sign different from the one of the leading trajectory causes the algorithm not to find solutions. Differently, in regions such as R_3 and R_4 in figure (4.6) the amplitude can change its sign and different sign choices will lead to different amplitudes.

In this work, we enforce the Veneziano sign for the few points which we take in the regions where the sign is free. As was the case when we imposed super-unitarity, this restricts the possible amplitudes that we can generate with our ansatz to a subclass, but since we are not insisting on exhaustively charting this space but rather building consistent examples of such amplitudes this is not a problem. The reason to prefer this approach is that it makes the numerics much more efficient, as the alternative would be to check at each point which sign convention allows for a better tolerance for crossing.

4.3.4. Setting up the optimization problem: Choosing observables to optimize

As is standard in the different bootstrap approaches, once that we have an ansatz for our amplitude depending on a collection of parameters and a set of constraints that we require it to satisfy, we can explore the space of consistent amplitudes in this class by extremizing a set of observables that characterize the amplitude and thus depend on the ansatz's parameters.

The choice of this set of observables is somewhat arbitrary and one can think of it as choosing a basis in which to reperesent the amplitude. A by now typical choice are the Wilson coefficients determining the low energy expansion of the amplitude, i.e. its Taylor expansion around $s = t = 0$. However, this choice is not convenient for our ansatz based on the Mandelstam-Regge expansion because the Q_J functions have logarithmic singularities around this point. Even if one tries to bypass this issue by computing the Wilson coefficients from the Mandelstam-Regge expansion usin dispersion relations, one finds that the double integration in s and t necessarily causes the integrand to pass by regions of $(s,t) \in \mathbb{C}^2$ where the expansion does not describe the amplitude correctly, obstructing this approach.

For these reasons we define a different set of observables given by the Taylor expansion of the amplitude around the point $s = t = -5/3$, namely

$$g_{ij} = \frac{\partial^i \partial^j}{\partial s^i \partial t^j} A(s,t)\Big|_{s=t=5/3}. \tag{4.39}$$

From equations (4.33) and (4.34) we see that the g_{ij} observables are nothing but linear functions of the parameters a_{ij}. This together with the fact that both crossing and unitarity are linear constraints on the ansatz parameters allows us to turn the problem of imposing crossing and unitarity on the ansatz given by eq. (4.33), and extremizing or fixing to specific values the observables g_{ij} into a linear optimization problem over the ansatz parameters a_{ij}.

It is important to notice that both unitarity and crossing are projective constraints on the parameters a_{ij}, meaning that if an amplitude defined by a given set of a_{ij} satisfies unitarity and crossing up to a certain tolerance ϵ, then rescaling them by a factor λ will yield an amplitude that also does. This stems from the fact that at weak coupling the amplitudes are not constrained by non-linear unitarity and then we can choose the normalization of the amplitude arbitrarily. To deal with this we fix the normalization of the amplitude as

$$g_{00} = A(-5/3, -5/3) = 1. \tag{4.40}$$

This is equivalent to obtaining projective bounds on the g_{ij} by extremizing the ratios $\frac{g_{ij}}{g_{00}}$.

4.3.5. Comment on the numerics

For the results presented in this work we chose to remain within the realm of linear programming, implementing the bootstrap scheme explained before with the powerful linear solver MOSEK [165]. We made this decision mainly on the grounds of speed, since MOSEK allows us to deal with optimization problems with very large number of constraints on time scales orders of magnitude smaller than those required by semidefinite solvers like SDPb. All the results shown in the next section can be reproduced in maximum a few hours of running time on a laptop. Since during the developing stages of this project it was necessary to test

and adjust the various aspects of the bootstrap, the speed granted by the linear optimization framework in general and MOSEK in particular were crucial.

One important drawback of MOSEK however is that it works with double point precision, and therefore there is a limit to the accuracy we can achieve with our results. In practical terms, since the contribution from subleading terms in the Mandelstam-Regge expansion are increasingly supressed, MOSEK is not able to work at the required precision to include trajectories beyond the 8^{th} one.

This seems to be a bottleneck for all available commercial linear solvers even those advertised as working with arbitrary precision. Therefore, to be able to push the accuracy of our numerics beyond the present point and obtain more detailed features of the constructed amplitudes we must implement our bootstrap in a different framework that allows for arbitrary precision. SDPb would be a natural choice, yet sub-optimal when dealing with linear optimization problems.

4.4. Results

We are now ready to put our bootstrap scheme in practice. To obtain the results presented in this work, we used the linear solver MOSEK [165]. Further details on the numerics are relegated to the appendix.

4.4.1. Linear trajectories

We start by considering amplitudes with Veneziano-like, linear, parallel Regge trajectories given by $\alpha_i(s) = s - i$. If one follows one's bootstrapper reflexes, the first thing one might attempt to do with a bootstrap scheme as the one presented above would be to try to analyze the space of amplitudes spanned by the ansatz given in eqs. (4.33) and (4.34) by extremizing one's favorite set of observables.

This can surely be done, and in figure (4.7) we show the result of extremizing the observables g_{11} and g_{20} subject to the unitarity and crossing constraints for various values of ϵ, with $N_{\text{traj}} = 4$ (Recall that the number of Regge trajectories is $N_{\text{traj}} + 1$).

At a first glance, the plot has the expected features of ths type of analysis. We can clearly see that for a fixed value of ϵ there is a finite region in the (g_{20}, g_{11}) plane where amplitudes satisfying unitarity and crossing up to ϵ can live. Naturally, as one pushes down the value of ϵ the size of these regions gets smaller, until one achieves the minimal value $\epsilon_{\text{min}}(N_{\text{traj}})$ beyond which no solutions to the constraints exist, as the Mandelstam-Regge expansion at given N_{traj} can only satisfy crossing up to a certain tolerance no matter how much we tune the ansatz's coefficients.

However, a second thought should raise some questions regarding this procedure coming from the fact that we impose crossing only approximately: How to know in this framework if an amplitude lying at a given location inside the allowed region for some value of ϵ actually corresponds to a physical object and not to some artifact of choosing ϵ arbitrarily that would get excluded when considering more trajectories and increasing the precision? The allowed regions depend on the value of ϵ, and thus the ellipses in figure (4.7), while compelling, do not

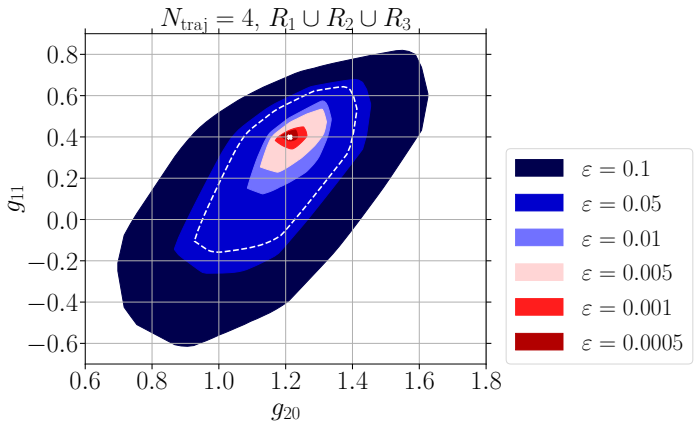


Figure 4.7.: Allowed regions in (g_{20}, g_{11}) space for amplitudes satisfying the bootstrap constraints generated with our ansatz for different values of the tolerance ϵ. The white point in the center of the ellipses marks the position of the Veneziano amplitude in these coordinates, at $g_{20} \simeq 1.212$, $g_{11} \simeq 0.399$.

allow to identify special physical objects like the Veneziano amplitude from other unphysical objects that just happen to not violate crossing more than the value of ϵ we impose.

Nevertheless, there is a remarkable feature from figure (4.7): The Veneziano amplitude, located at position $g_{20} \simeq 1.212$, $g_{11} \simeq 0.399$ in these coordinates, lies precisely at the center of the allowed region, in the location that manages to satisfy crossing up to the smallest value of ϵ for this given N_{traj} [8]. This suggests that despite the question of the fate of the allowed regions when increasing N_{traj} and decreasing ϵ, the Veneziano amplitude seems to be located at a special point where crossing is satisfied to a much better approximation, even when using the truncated Regge-Pole expansion.

This observation motivates our approach to make sense of imposing crossing approximately, which is the following: Instead of imposing crossing at a fixed value of ϵ and extremizing g_{20} and g_{11} to define allowed regions, we scan the space of observables by fixing the values of g_{20} and g_{11} to values $\hat{g}_{20}$ and $\hat{g}_{11}$ and decrease the tolerance ϵ until we find the minimal value ϵ_{min} for which the linear program corresponding to imposing unitarity and crossing subject to $g_{20} = \hat{g}_{20}$ and $g_{11} = \hat{g}_{11}$ has solutions. The results of applying these method over a line of values of g_{20} and g_{11} passing through the point corresponding to the Veneziano amplitude (taken as the origin) for different number of trajectories is shown in figure (4.8).

This analysis shows that for generic points in the (g_{20}, g_{11}) plane the minimal value of ϵ attainable does not depend much on the location but merely on the number of trajectories included in the ansatz. However, as one passes through the position of the Veneziano amplitude there is a very sharp decrease in ϵ_{min} for all values of N_{traj}, clearly indicating the presence of a special object in this location. Even if one might argue that we arrive a few decades too late to the discovery of the Veneziano amplitude, the fact that we can detect the existence of a physical amplitude with our bootstrap scheme constitutes an important proof of principle of the method. Most importantly, it provides a guiding principle that can be used to detect candidate physical amplitudes: one must look for points in parameter space where there is a sharp decrease in the minimal tolerance ϵ_{min}. Said differently, we conjecture

[8] To reader eager to recompute these values, remember we need normalize $g_{00} = 1$, so one needs to multiply by $1/A_V(-5/3, -5/3)$.

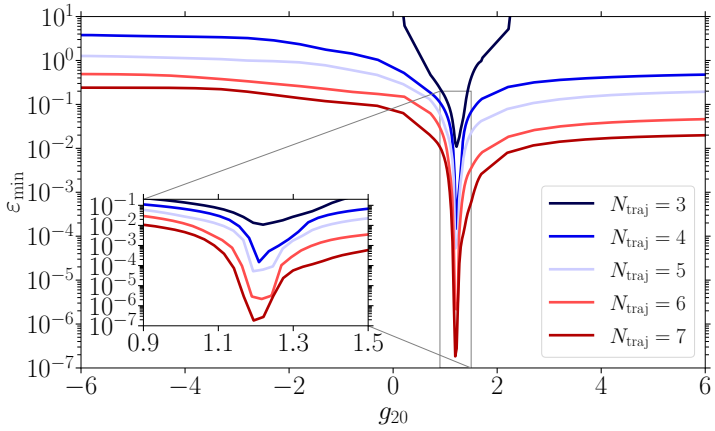


Figure 4.8.: Model with linear trajectories. Slices through the (g_{20}, g_{11})-plane at fixed g_{11} in terms of the minimal tolerance ϵ leading to the feasibility of (4.38). We fix g_{11} to the value attained for the global minimal ϵ. The inset plot zooms into the region around the Veneziano amplitude's position, $g_{2,0} \simeq 1.212$, $g_{1,1} \simeq 0.399$.

that physical amplitudes live on locations of parameter space where the Mandelstam-Regge expansion of the amplitude satisfies crossing maximally. This will be the approach that we will use to obtain amplitudes with non-linear Regge trajectories, as we will explain in the following section.

4.4.2. Bending trajectories

Having established how our bootstrap detects amplitudes, we move on to explore a class of models with bent trajectories. The idea is to take the linear case of the previous section where we can clearly identify the Veneziano in the space of amplitudes by a sharp dip in the value of the minimal tolerance $\epsilon_{\min}$ as a starting point, and then proceed to continuously deform the Regge trajectories. Following how the dip in $\epsilon_{\min}$ moves in the space of amplitudes we can identify objects that we conjecture correspond to consistent dual model amplitudes with the required Regge trajectory functions.

An heuristic way to justify this procedure is the following: Lets go back for a moment to the original channel-duality equation that we introduced at the begining of this thesis:

$$\sum_{n,J} c_{nJ} \left(\frac{P_J\left(1 + \frac{2t}{m_{n,J}^2 - 4m_0^2}\right)}{s - m_{n,J}^2} - \frac{P_J\left(1 + \frac{2s}{m_{n,J}^2 - 4m_0^2}\right)}{t - m_{n,J}^2} \right) = 0, \quad c_{nJ} \geq 0. \tag{4.41}$$

Starting from a set of masses and couplings that yield a solution to eq. (4.41), it is natural to expect the variation caused by a small deformation of the masses in the spectrum can be absorbed by a corresponding small variation of the coefficients $c_{n,J}$, in such a way as to remain inside the space of solutions to eq. (4.41). Following the flow generated by these small deformations we should be able to obtain new solutions to channel-duality that are at finite distance in amplitude space from the original amplitude that generated them. In fact, the Coon amplitude discussed previously can be seen as an example of this, with the

Veneziano amplitude playing the role of the original solution and the deformation parameter q implementing the flow.

In a sense, the strategy of continuously deforming the Regge trajectories and following the dip in ϵ_{min} is a way of implementing this flow in the space of solutions to channel duality. Of course, the analogy between our bootstrap scheme and the procedure described in the previous paragraph is only at the conceptual level, since we choose to expand the amplitude in the Mandelstam-Regge pole basis. However, we argue that not only these procedures are conceptually the analog to each other, but also that the Mandelstam-Regge pole expansion is better suited to implement bending: In eq.(4.41) the Regge trajectories only play a role in defining the masses in the spectrum, which corresponds to their behavior at positive values of their argument. Since bending requires controlling the asymptotic behavior of the trajectories both at negative and positive values, it is unclear how this feature can be imposed on the solutions to this equation. On the other hand, with our method we have direct access to the shape of the trajectory functions at all values of their argument and imposing bending trajectories is done trivially by selecting the desired α_i functions as the input for the bootstrap.

All this being said, we need a model for the Regge trajectories that allows to depart from the linear case in a smooth way. For this we use the following model for the leading trajectory:

$$\alpha_\lambda(s) = \lambda\, s + (1-\lambda) h(s) s, \tag{4.42}$$

where

$$h(s) = \frac{e^s}{e^s + 1}, \tag{4.43}$$

is a smooth step function that interpolates between 0 and 1 . In fact, this is the model used to generate figure (4.1). Since at $s \to \infty$ the function $h(s)$ goest to 1, the $s \to \infty$ behavior of $\alpha_\lambda(s)$ is $\alpha_\lambda(s) \to s$. On the other hand, when $s \to -\infty$, $h(s) \to 0$, and thus $\alpha_\lambda(s) \to \lambda\, s$. We see thus that this is model achieves the desired feature of yielding different slopes at $s > 0$ and $s < 0$, with λ being the continuous parameter that controls the amount of bending, and $\lambda = 1$ corresponding to the linear case considered before.

To sudy the bending of the trajectories we restricted to the case in which the non-linear trajectories remain parallel. Namely, the i^{th} trajectory can be determined in terms of the leading one $\alpha_\lambda(s)$ by

$$\alpha_i(\lambda; s) = \alpha_\lambda(s) - i. \tag{4.44}$$

The result of performing the minimal ϵ analysis described in the last section to models with different values of the bending parameter λ is shown in figure (4.9). To produce these plots we first obtain the value of g_{11} that allows for the smallest ϵ by maximizing g_{11} subject to the bootstrap constraints at fixed ϵ, and sequentially decreasing ϵ until the constraints cannot be satisfied. Then, we fix g_{11} to this value and scan in the g_{20} direction, finding the value of ϵ_{min} at each point.

As was the case for the linear trajectories, we find that for each value of λ there exists a point in parameter space for which the minimal tolerance ϵ_{min} exhibits a large dip, corresponding to

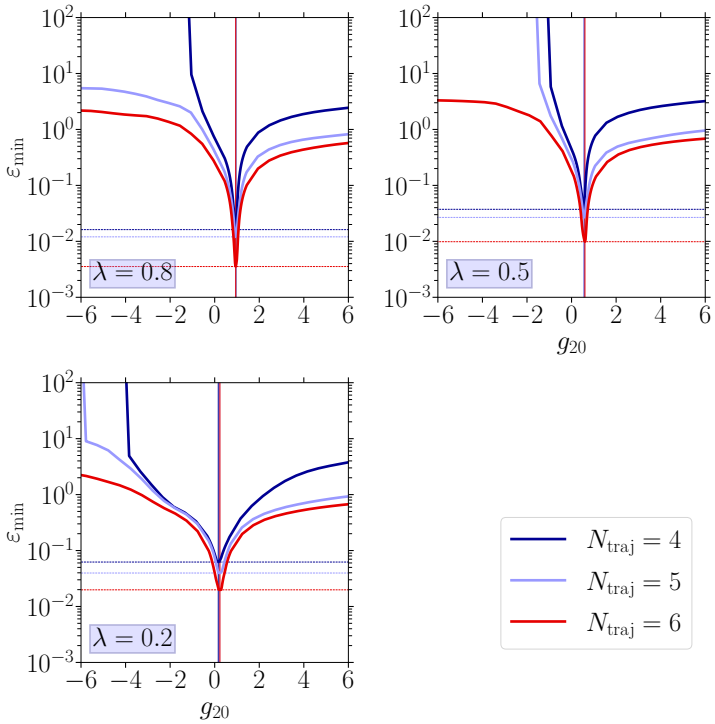


Figure 4.9.: Model with bent trajectories. Slices through the (g_{20}, g_{11})-plane at fixed g_{11} and an increasing number of sub-leading trajectories, showing the minimal tolerance $\epsilon_{\min}$ for values of $\lambda \in \{0.2, 0.5, 0.8\}$. For each λ and N_{traj}, g_{11} is fixed to the numerically derived value attained when imposing the global minimal tolerance ϵ before infeasibility. The vertical lines show the position of g_{20} corresponding to the lowest $\epsilon_{\min}$ while the colored horizontal lines refer to the value of $\epsilon_{\min}$ per N_{traj}.

the putative amplitude with bent trajectories obtained from deforming the linear-trajectory one.

To see the flow in parameter space defined by the bending parameter λ, in figure (4.10) we show the position of the global minimum of the tolerance in the (g_{20}, g_{11}) plane for different values of λ and N_{traj}.

For strong bending ($\lambda \simeq 0.2$) our algorithm starts to lack precision, and the position of the dips only converges to a reasonable degree of a few percent for smaller values of λ. While it is expected that convergence could be achieved by adding more trajectories, we are currently limited in our precision by the numerical implementation of the linear optimization problem using the solver MOSEK, which only works at finite precision and therefore eventually becomes insensitive to contributions from higher trajectories. More details on the numerics are given in the discussion and in the dedicated appendix. Nevertheless, the amplitudes follow an easily identifiable path, and we expect that with increasing precision we would be able to pinpoint their precise location on the (g_{20}, g_{11}) plane even at lower values of λ. The important point is that this continuous flow on amplitude space gives a strong hint that amplitudes with explicit Regge trajectory bending can be defined consistently.

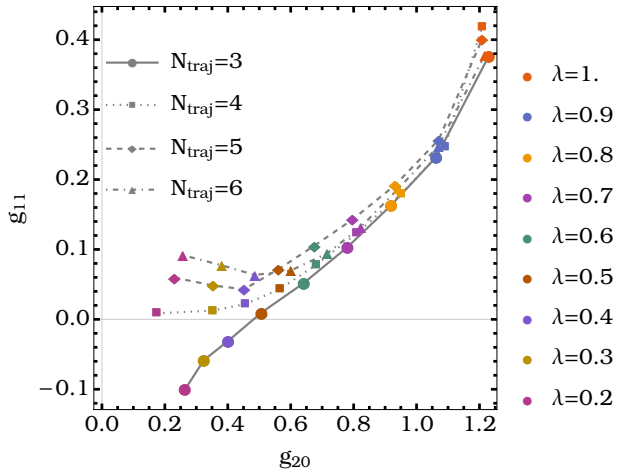


Figure 4.10.: Evolution of the position of the dip at different values of λ for N_{traj} from 3 to 6.

4.4.3. Asymptotic linearity

As an independent cross-check for our bootstrap scheme, we studied amplitudes with Regge trajectories $\alpha(s)$ exhibiting non-linear behavior at large, positive s. The motivation for this was to check the known fact that the Regge trajectories of dual model amplitudes cannot grow faster than linearly at large, positive values of their argument [39, 69]. Since amplitudes with this feature are not expected to exist, being able to obtain such amplitudes with our method would be a clearly bad sign. Conversely, finding that these models are not achievable with a reasonable tolerance ϵ with our framework would be a non-trivial check for the consistency of the approach.

More concretely, we considered models with the following parallel Regge trajectory functions $\alpha_i(s)$:

$$\alpha_i(s) = s - i, \quad \text{Re}(s) \leq 0, \tag{4.45}$$

$$\alpha_i(s) = s^{1+\gamma}, \quad \text{Re}(s) > 0, \tag{4.46}$$

with γ being a real parameter quantifying the deviations from linearity.

To be able to probe the positive, large energy region of the Regge trajectories, we added an extra set of points to the ones used to impose crossing in the previous section. Apart from the regions shown in figure (4.6) we imposed crossing on 40 extra points along rays $\text{Im}(s/t) = 0$ with $(s,t) = (|s|e^{i\theta}, |t|e^{i\theta})$, with $\theta = \{0.2,\ 1.17\}$, and $(|s|, |t|) = \{5, 6, \ldots 25\}$.

In figure (4.11) we show the value of the minimal ϵ for which the optimization algorithm manages to satisfy the constraints as a function of γ, for $N_{\text{traj}} = 6$.

As is clear from the plots, as soon as γ becomes larger than 0 the capacity of the ansatz to satisfy crossing worsens dramatically. For negative γ corresponding to sublinear behavior, we see that the situation is less spectacular but still crossing is maximally satisfied in the linear case $\gamma = 0$. While our method of imposing crossing approximately does not yield a sharp boundary between allowed and disallowed trajectories, this shows that super-linear trajectories are strongly disfavored, as expected from [39, 69]. This result is further evidence

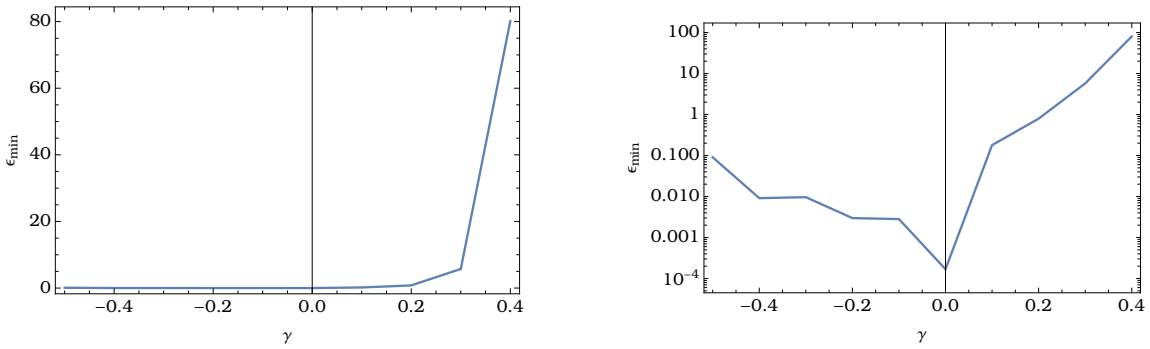


Figure 4.11.: (*Left*:) Minimal value of ϵ for which there exist solutions to the constraints as a function of the parameter γ characterizing the non-linearity of the trajectories. (*Right*:) Logarithm of the same quantity.

of the consistency of our bootstrap method, as it shows that not every trajectory function is accepted by the scheme, with it being sensitive to the fact that super-linear amplitudes are not allowed.

4.5. Discussion

In this chapter we presented our linear programming bootstrap and some results showing how is can be used to firstly detect known amplitudes such as the Veneziano amplitude, and then use this to build seemingly consistent deformations with customizable Regge trajectories. Let us now discuss various points related to the procedure and the results.

4.5.1. Numerics, precision and convergence of the results

The numerics in this work are based on a linear programming paradigm, implemented on the linear solver MOSEK. This technology is geared towards speed, but only allows to work at finite precision in all intermediate computations. This limitation puts a cutoff in the maximum accuracy we can expect from our results, as well on the number of Regge trajectories we can deal with in our ansatz.

Despite these facts, we reach a decent precision of order 1% for the location of the Veneziano g_{20}, g_{11} couplings. Convergence of other observables such as the $c_{n,J}$'s on subleading trajectories is less good. Some of them are shown in the appendix on numerics. To improve these results and be able to probe the finer details of the amplitudes generated by our bootstrap method we need to add more trajectories, which requires moving to arbitrary precision solvers. This is clearly a possible direction of improvement for this framework.

4.5.2. Scope of the method

In our results, we have presented compelling evidence that dual model amplitudes with explicit bending of the Regge trajectories exist, and we have done so by reaching them starting from the known position of the Veneziano amplitude in parameter space and continuously deforming

the Regge trajectories to go from the linear to the bending case. Even if for some values of the bending parameter λ the location of the bending amplitude is not yet converged and the limitations from the numerics prevent us from having access to the fine structure of the resulting amplitudes, the drop on the tolerance parameter and the flow of its position as λ is turned on shown in figures (4.9) and (4.10) are clear enough signs to argue that in those points in parameter space live consistent dual model amplitudes with Regge trajectories as (4.42).

However, there is a big leap between building a $2 \to 2$ amplitude consistent with the bootstrap axioms of dual models and claiming that it actually corresponds to an amplitude emerging from a phyisically relevant theory. More concretely, the model (4.42) that we used for bending is an arbitrary choice among many, and it is just supposed to capture the main features of this phenomenon. Thinking that the resulting amplitudes could belong to a physical theory such as large N QCD would be at best extremely naive. The utility of this approach is not to provide a definitive amplitude, but to generate classes of amplitudes that are consistent and satisfy customizable features. In this work we chose to use them to prove the fact that explicit bending of the Regge trajectories seems to be consistent with the bootstrap axioms, contrarily to what is suggested in the works proposing models with effective bending [40, 162]. It is possible that the dual model amplitudes corresponding to large N QCD realize this feature, or perhaps a mixture of explicit and effective bending. Similarly, other phenomenologically interesting features could be tested with this method, and then used as a guidance in the search for interesting dual models.

More generally, this framework could be used in combination to other bootstrap methods to isolate interesting theories. The reason for this is that our framework allows to directly input information about the UV of the amplitude in a very direct manner, while most availabe bootstrap approaches do not have access to it beyond requiring that it is compatible with the standard axioms. Therefore, if one could build amplitudes satisfying a given UV feature with our method and locate them in the space of couplings used by other approaches, it would be possible to guide their search to the regions of parameter space compatible with this property.

A very concrete example of this approach would be the investigation of the extremal amplitude found in [61] and discussed in the previous chapter. In this work, the authors set up a dual bootstrap program for scalar amplitudes whose IR properties are consistent with those from large N gauge theories in an attempt to bootstrap large N QCD pion scattering amplitudes, finding a remarkable amplitude living at a kink in the boundary of the allowed space that matches many features from real world QCD. A way in which our framework could help in understanding whether this kink could correspond to large N QCD or not could be to build generic models with known features of large N QCD (such as, but not limited to, bending trajectories) and locate them in the space of amplitudes using the same coordinates as the ones to locate the kink. If the regions are incompatible this would be strong evidence against the hypothesis that large N QCD resides at this kink. While it was explained that the Mandelstam-Regge expansion is not well suited to study the space of low energy Wilson coefficients that the authors use in the mentioned paper, it would be possible to find a set of mutually compatible observables in which to carry this analysis.

A different future direction would be to extend our ansatz for it to have access to a larger class of models with linear spectra, as our ansatz (4.34) does not describe the whole class of amplitudes with linear trajectories. The authors of [69] studied infinite shifted Veneziano sums [163] and argued that it is a complete basis of amplitudes with linear trajectories and equidistant spectrum. Among their examples there are amplitudes whose Regge poles don't

have the structure proposed in our ansatz, and therefore our residue function is restricted and can be improved. As a basic improvement, we have tried to enlarge the degree of the polynomials: This did not result in new dips nor changed their location, but it did make their bottoms more shallow, hinting at the possibility that more than one amplitude could be located in these regions. Similarly, it would be interesting to study possible Coon-like q-deformations of our ansatz.

Another important question related to the interpretation of our results is that of higher-point factorization. It is known that there exist $2 \to 2$ dual model amplitudes that satisfy all the consistency criteria but that fail when being extended to higher points. Probably the most famous example of this phenomenon is the Lovelace-Shapiro dual model for pion scattering, which defines a perfecly valid 4-point amplitude but propagates ghosts at higher points. As we discussed, this is also the case for the Coon amplitude in the unitary, $q < 1$ regime. Relatedly, in the introduction to this chapter we reviewed a method proposed recently to derive dual model amplitudes with rational spectra [54]. While in this work it was found that many of the obtained amplitudes (which are by construction meromorphic and crossing symmetric) were also consistent with unitarity, in a follow up paper it is shown that the allowed space shrinks dramatically when the constraints from higher-point factorization is imposed on these models [166].

The message coming from these works and from the fact that we are able to build seemingly consistent dual model amplitudes with an arbitrary choice of bending appears to be that the bootstrap constraints for dual models at the level of the 4-point amplitudes are hard, but maybe *not so hard* after all, and that finding a particular solution with some specific feature is not so complicated. It is when trying to make this concrete solution compatible with higher-point factorization that the situation becomes much more constraint. From this point of view, while the question of higher-point factorization was out of the scope of our work, it seems unlikely that the amplitudes we obtained will pass this criteria. Naturally, finding a way of adding higher-point constraints into the bootstrap method would be extremely useful.

Nevertheless, it is important to point out that while the constraints on the 4-point amplitudes might leave ample room for solutions, it is not the case that our bootstrap allows to construct amplitudes with any shape for the Regge trajectory. In particular, we attempted to obtain amplitudes with Regge trajectories growing faster than linearly at large energies parametrized as $\alpha(s) = s^{1+\gamma}$, and we observed that the minimum value of the tolerance ϵ shooted up for values of $\gamma > 0$, in perfect consonance with the known fact that dual model amplitudes must have trajectories that do not grow faster than linearly at large, positive values of their argument [39, 69]. This result is also a consistency check for our bootstrap, showing that not anything goes in what respects the shape of the trajectories, and indeed satisfying crossing becomes hard for amplitudes that should not be able to be realized.

A question that remains to be answered in this work is that of the analytic structure of the Regge trajectories. While we have shown that amplitudes with explicitly bending trajectories seem to be consistent, functions with asymptotically different growths at $\pm\infty$ always have non-analyticities somewhere in the complex plane. In particular, our bending function $h(t)$ has infinitely many poles in the complex plane. Thus, for a fixed t near one of these poles t_p, at large s the scattering amplitude would have a singularity of the form $A(s,t) \sim s^{1/(t-t_p)}$. This strongly singular behavior is in tension with having a well behaved meromorphic amplitude, and gives support to the alternative of effective bending developed in [40, 162]. However, mechanisms to cancel this type of singularities might exist, and it would be important to investigate this point further.

Finally, numerous recent works on the non-perturbative S-matrix bootstrap have seen the emergence of Regge trajectories of states [84, 90, 96, 97, 118, 167] and it would be intriguing to make contact with these fully non-perturbative objects with our approach.

Part II.

Three-point amplitudes in String Theory

Chapter 5.

String three-point amplitudes from the light-cone

The last part of this thesis is devoted to the study of the massive spectrum of String Theory and the interactions among its constutitents. In particular, we develop the technology to build one-particle physical states of arbitrary spin and mass from light-cone gauge oscillators, and then present a method to compute three-point amplitudes at tree-level using the light-cone gauge formalism.

What is presented in this chapter is based on work in progress with Bruno Bucciotti and Guilherme Pimentel, and while this project is yet not finished and therefore there are still various open questions and unexplored avenues, we have already achieved results that add a valuable new perspective to the ones presented in the first part of this thesis. In a sense, in the previous chapters we have focused on understanding the generic features of dual models as theories of weakly interacting higher spin states, gaining knowledge about their consistency requirements as well as developing methods to produce dual model amplitudes with desired features. Now, however, we concentrate on studying the original dual model: bosonic String Theory in 26 spacetime dimensions. This theory is arguably the massive higher spin theory of which we have the best handle on, and disecting its properties can teach us extremely valuable lessons on the universal features of these theories in general, as well as unveil new secrets of String Theory as a fundamental theory of quantum gravity in particular.

From this point of view, and despite the fact that String Theory will soon turn 60 years old, surprisingy little is known about the spectrum of the theory at high masses and their interactions. These highly excited states are nonetheless fundamental for the consistency of String Theory [1], and determine many of its most salient features, such as its extremely soft high energy behavior [129, 169–171]. A partial reason for this fact is that most studies have focused on the massless sector of the theory, since this is the one determining long range interactions as well as its low energy effective field theory. Another important reason is simply the sheer complexity of the task of excavating the spectrum of massive states, as the number of states grows exponentially fast at large mass levels [168]. Because of this, most of the available information about the massive string spectrum has come from level-by-level probes of the low lying levels [172–178]. While recently some efficient methods to have access to large families of states in the spectrum have been developed [179, 180], there is still much to be understood about the zoology of highly excited string states, and this question will occupy us later in this chapter.

Beyond understanding the structure of the spectrum itself, the interaction between highly excited string states is expected to probe very interesting physics, in particular connected to

[1] See [168] for instance for an introduction to String Theory

the emergence of black holes and their thermal properties in String Theory. The intuition for this is based on the correspondence between black holes and strings argued by Susskind, Horowitz and Polchinski [181, 182], which relates the value of the string coupling g_s at which a string collapses into a black hole[2] to its mass level N as $g_s \sim N^{-1/4}$, and therefore for highly excited string states one expects to be able to use weakly-coupled string theory to study these stringy black holes. Moreover, at the string-black hole transition point the entropy of the string and the one of the black hole computed with the Bekenstein-Hawking formula [3] are of the same order and scale with the same power of the mass of the black hole, suggesting that string microstates yield at least a large portion of the black hole entropy. This has lead various authors to consider the scattering of highly excited *coherent* string states [178, 185–190], which can be used as a way of obtaining information on black hole microstates and in particular test the assertion that black holes are chaotic quantum systems.

While the investigation of coherent state scattering has led to many new insights into the relation between the thermal and quantum properties of black holes and String Theory, in this project we opted for an in principle simpler yet much less studied basis for the massive sting spectrum: One-particle physical states, namely those satisfying the Virasoro constraints and transforming in irreducible representations of $SO(d-1)$, the *little group* of the Lorentz group, labeled by their mass and their spin.

One reason to be interested in this class of states is that these are the ones that allow to exploit the strong constraints that Lorentz symmetry imposes on scattering amplitudes most efficiently. In the last decades, a set of techniques collecively referred to as *on-shell methods* have revolutionized the way in which scattering amplitudes are computed in QFT, allowing to compute in a few lines amplitudes for processes that would be completely untractable using classic Feynman diagram calculus (see [191] for a modern, comprehensive review). In particular, the spinor-helicity formalism allows to take advantage of the Lorentz invariance of scattering processes between one-particle states by using kinematic variables that trivialize the mass-shell constraints and transform in the simplest representations of the Lorentz group: the chiral, spin 1/2 representations. This approach is most easily defined in the case of massless scattering in 4 dimensions, but it has been extended to higher dimensional [192–194] and massive [195] theories. It allows for drastic simplifications in the computation of scattering amplitudes, with the most famous example being the Parke-Taylor formula for tree-level n-gluon scattering [196].

Using this formalism it is simple to characterize *all* possible three-point amplitudes between particles of arbitrary mass and spin compatible with Lorentz symmetry, relegating all dynamical information to the coefficients in front of the straightforwardly computable structures that encode the kinematic dependence of the amplitude, which are completely fixed by Lorentz invariance. While this formalism has been applied extremely succesfully in particle physics and has become a standard tool in QFT, it has seldom been applied in String Theory, mostly because the optimality of the method decreases with the number of dimensions and requires additional structures to be useful in the $d = 10$ and $d = 26$ cases relevant for String Theory. However, in any case the spinor-helicity formalism shows that working with one-particle states one can uncover underlying structures and patterns that are not visible otherwise, and this alone provides a motivation to study their interactions in more detail.

[2] Note that the string coupling is related to Newton's constant G by $G \sim g_s^2 \alpha'$.

[3] The Bekenstein-Hawking formula states that the entropy of a black hole is given by the area of its horizon as $S = \frac{A}{4G}$ in $\bar{h} = c = 1$ units, and where G is Newton's constant [183, 184].

One concrete motivation to study one-particle, three-point scattering amplitudes that also relates to the link between black holes and String Theory is the discovery in [195] of a set of three-point amplitudes between two massive spin S particles and a massles spin J, with $J = 1, 2$. These amplitudes where simply postulated on the grounds of them satisfying interesting properties in the low energy limit, corresponding to the case of minimal coupling between the massive and massless states, but it was soon discovered that they were intimately connected to the Kerr black hole. More specifically, it was shown in [197, 198] that when taking the classical limit of these amplitudes by sending $\hbar \to 0$, $S \to \infty$ one recovers the linearized Kerr stress tensor, with its multipole expansion being reproduced term by term by the finite S, *minimally coupled* amplitudes of [195]. This surprising connection between Kerr black holes and three-point quantum scattering amplitudes between higher spin states naturally leads to wonder if such amplitudes can be realized within the spectrum of String Theory. Some first steps in this direction were taken in [199], where the authors considered the classical limit of the scattering amplitudes between a massles graviton and two states belonging to the leading Regge trajectory, obtaining instead the stress tensor corresponding to a classical rotating string. However, this negative result was the output of considering the simplest possible states to interact with the graviton, namely those in the leading trajectory, and it is very well possible that considering other families of one-particle states one could obtain Kerr as a classical limit.

Finally, from a more formal point of view, the three-point amplitudes between the one-particle states in the spectrum are a basic piece of information missing in the String Theory literature, and they constitute an elementary building block to have access to more complicated, multi-particle amplitudes. Increasing our understanding our understanding about these objects is clearly a relevant question.

As will be explained in more detail shortly, the main reason why computing amplitudes between excited states in String Theory, at least at tree-level, is actually specifying the excited string states corresponding to the physical Hilbert space. In the standard covariant formulation of String Theory, generic states created by acting on the vacuum with creation operators carry negative-norm excitations that need to be projected out of the Hilbert space by demanding that physical states satisfy the Virasoro constraints. This causes the different excitation modes of the string to not be independent, and while these constraints are simple enough at low levels, they become increasingly difficult to impose as one considers higher excitations of the string, with the problem quickly becoming untractable if one considers states whose mass level is large enough.

A way to go around this problem is to work directly with physical states by using the light-cone gauge formalism, which will be reviewed in what next. This is the approach that we choose to follow, as it allows to consider only oscillators corresponding to physical excitations, trivializing the Virasoro constraints and letting us focus on the computation of the amplitudes. However, this method makes the Lorentz invariance of scattering amplitudes not manifest, which naturally has its drawbacks. Specifically, it introduces the issue that light-cone gauge oscillators can only excite the transverse directions of the string, and thus carry indices transforming in representations of the group $SO(d-2)$, instead of the required $SO(d-1)$ to build one-particle states. Therefore, one needs to un- derstand how the different combinations of $SO(d-2)$ representations gather to form $SO(d-1)$ representations corresponding to the one-particle states we are interested in.

In this project we contribute to the analysis of one-particle states in bosonic String Theory by firsly developing a method to obtain the spectrum of one-particle states of a given mass

from the light-cone gauge formalism that can be systematically applied level by level. Since the method is completely algorithmic it is amenable to automatization, and in the course of this work we developed a code that performs this classification in Mathematica and Python automatically.

After understanding how to reconstruct one-particle states, we introduce the required formalism to compute three-point amplitudes in light-cone gauge. This is old, somewhat forgotten technology, and and in the course of this work we had to rediscover large portions of it. While this formalism is not convenient for higher-point or loop computations, it turns out that it allows to deal with three-point functions very efficiently, modulo some subtleties regarding excited vertex operators that we discuss in the text. We use these methods to compute three-point amplitudes between different classes of one-particle states. While we restrict to the open bosonic string for simplicity, all what is shown can be generalized to the closed string without obstructions.

In the rest of this chapter we briefly review some basic notions of bosonic String Theory and the light-cone gauge formalism. Then we devote a section to presenting the algorithm to classify the one-particle states in terms of light-cone gauge oscillators, as well as the bootstap scheme that allows to have access to infinite families of excited states. Next, we review the formalism to compute three-point amplitudes in light-cone gauge and apply it to various examples, including the one of a massless photon and two heavy spin S states that is relevant to make contact with the Kerr amplitudes described above via the double-copy. We end this chapter with a discussion of the methods presented and of possible future directions.

5.1. String Theory in the light-cone gauge

We start by providing a very quick review of String Theory basics and the light-cone gauge. The interested reader is referred to the standard introductory book on the topic [168].

5.1.1. The classical string

String Theory describes the quantum dynamics of fundamental one-dimensional objects, i.e. *strings*, rather than the zero-dimensional particles from Quantum Field Theory. When a classical particle propagates through spacetime, we can describe its dynamics by considering an action that extremizes the the propertime along the worldline swept by the particle. Analogously, a string propagating through spacetime will swipe a two-dimensional *worldsheet*, and its dynamics are dictated by an action that extremizes the area swept by it. We can consider two kinds of strings, open strings which have endpoints and closed string forming loops.

Denoting the string's spacetime coordinates as X^μ, $\mu = 0, \dots, d-1$, we can parametrize the worldsheet by a timelike coordinate τ and a spacelike coordinate σ, and the surface swept by the string defines a map from the worlsheet to d-dimensional Minkowski space $X^\mu(\sigma, \tau)$, as shown in figure (5.2).

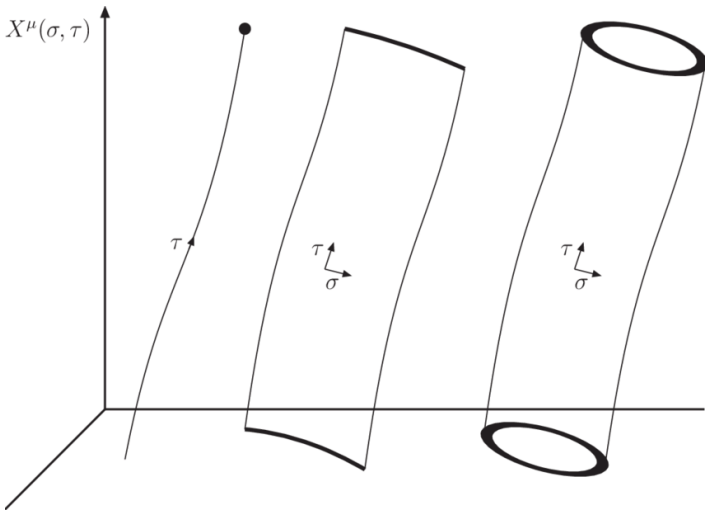


Figure 5.1.: Worldline swept by a point particle parametrized by the parameter τ (left), and worlsheets corresponding to the propagation of an open (center) string and closed (right) string, parametrized by (σ, τ).

The action that extremizes the area swept by the worldsheet is called the Nambu-Goto action, and it reads

$$S_{\text{NG}} = -T \int d\tau d\sigma \sqrt{-\det(\gamma_{ab})}, \tag{5.1}$$

where

$$\gamma_{\alpha\beta} = \frac{\partial X^\mu}{\partial \sigma^\alpha} \frac{\partial X^\nu}{\partial \sigma^\beta} \eta_{\mu\nu}, \tag{5.2}$$

is the induced metric on the worldsheet, $\sigma^\alpha = (\tau, \sigma)$, $\alpha = 0, 1$, and T is the string tension related to α' by $T = \frac{1}{2\pi\alpha'}$. Note that as can be seen from figure. (5.2), the closed string requires periodic boundary conditions in σ, namely

$$X^\mu(\sigma, \tau) = X^\mu(\sigma + 2\pi, \tau), \tag{5.3}$$

while for the open string we require $\sigma \in [0, \pi)$.

From the Nambu-Goto action we can see that we can describe the dynamics of the string moving in d dimensional spacetime by considering a 2-dimensional field theory living on the worldsheet, where the string coordinates $X^\mu(\sigma, \tau)$ are seen as scalar fields.

The Nambu-Goto action has two types of symmetry: Poincaré invariance of spacetime, which is seen from the point of view of the worlsheet as a global symmetry that mixes the X^μ among each other, and reparametrization invariance $\sigma^\alpha \mapsto \tilde{\sigma}^\alpha(\sigma)$, which reflects the fact that the worlsheet coordinates have no physical meaning and thus physics should be independent from them.

While its physical interpretation as the area swept by the worldsheet is very intuitive, the square-root in the Nambu-Goto action makes it very hard to quantize. However, we can introduce an auxiliary dynamical metric $h_{\alpha\beta}$ on the worldsheet to obtain an action that eliminates the square-root and has the same equations of motion as the Nambu-Goto action.

This is the Polyakov action, given by

$$S_P = -\frac{1}{4\pi\alpha'}\int d^2\sigma\,\sqrt{-h}\,h^{\alpha\beta}\partial_\alpha X^\mu \partial_\beta X^\nu \eta_{\mu\nu}, \tag{5.4}$$

with $h = \det h_{\alpha\beta}$, and simply solving the equations of motion for $h_{\alpha\beta}$ and plugging the solution back into the Polyakov action yields the Nambu-Goto action.

The Polyakov action has an extra symmetry with respect to the Nambu-Goto action. On top of Poincaré and reparametrization invariance, the Polyakov action is *Weyl invariant*, which means that the action is invariant under local rescalings of the form

$$h_{\alpha\beta}(\sigma) \to \Omega^2(\sigma) h_{\alpha\beta}(\sigma), \tag{5.5}$$

for an arbitrary function $\Omega(\sigma)$ and where the $X\mu(\sigma)$ are left unchanged.

Since both reparametrization and Weyl invariance are gauge symmetries of the worldsheet, we can use this extra freedom to fix the gauge to a convenient choice, choosing a flat metric for the worldsheet:

$$h_{\alpha\beta} = \begin{pmatrix} -1 & 0 \\ 0 & 1 \end{pmatrix} = \eta_{\alpha\beta}. \tag{5.6}$$

with this gauge choice the Polyakov action simplifies tremendously, simply becoming the action for d free scalars:

$$S_P = -\frac{1}{4\pi\alpha'}\int d^2\sigma\,\partial_\alpha X \cdot \partial^\alpha X, \tag{5.7}$$

with the equations of motion for X^μ given by the free wave equation.

$$\partial_\alpha \partial^\alpha X^\mu = 0. \tag{5.8}$$

The trick of adding a worlsheet metric has taken us very far, and we seem to have landed in the simplest action possible, a bunch of free scalars in $2d$, and we can readily proceed to its quantization. But there is a catch.

Even after gauge fixing, we must make sure that the equations of motion for $h_{\alpha\beta}$ are satisfied. Since there is no kinetic term for the worldsheet metric, its equation of motion simply reads

$$\frac{1}{\sqrt{-h}}\frac{\delta S}{\delta h^{\alpha\beta}} = 0. \tag{5.9}$$

Recalling that the variation of the action with respect to the metric defines the stress tensor $T_{\alpha\beta}$, we see that the equations of motion for $h_{\alpha\beta}$ imply that the worldsheet theory is constrained to have a vanishing stress tensor:

$$T_{\alpha\beta} = -2\pi\alpha'\frac{1}{\sqrt{-h}}\frac{\delta S}{\delta h^{\alpha\beta}} = 0. \tag{5.10}$$

As it turns out, enforcing this constraint at the quantum level will give rise to the complications that will lead us to choose to work on the light-cone gauge. But before getting there, we can have a better feel of the power of the constraints by looking at the mode expansion of the X^μ fields, which will also be a key ingredient in the quantization of the worldsheet theory.

To do this, recall that the most general solution to the freewave equation (5.8) is given by a superposition of left and right-moving waves:

$$X^\mu(\sigma,\tau) = X^\mu_L(\sigma^+) + X^\mu_R(\sigma^-), \quad \text{with } \sigma^\pm = \tau \pm \sigma, \tag{5.11}$$

as in these coordinates eq. (5.8) becomes $\partial_-\partial_+ X^\mu = 0$.

The most general solution can be expanded in Fourier modes. For closed strings, the periodicity condition $X^\mu(\sigma,\tau) = X^\mu(\sigma+2\pi,\tau)$ implies

$$X^\mu_L(\sigma^+) = \frac{1}{2}x^\mu + \frac{1}{2}\alpha' p^\mu \sigma^+ + i\sqrt{\frac{\alpha'}{2}}\sum_{n\neq 0}\frac{1}{n}\tilde{\alpha}^\mu_n\, e^{-in\sigma^+}, \tag{5.12}$$

$$X^\mu_R(\sigma^-) = \frac{1}{2}x^\mu + \frac{1}{2}\alpha' p^\mu \sigma^- + i\sqrt{\frac{\alpha'}{2}}\sum_{n\neq 0}\frac{1}{n}\alpha^\mu_n\, e^{-in\sigma^-}, \tag{5.13}$$

where x^μ and p^μ correspond to the position and momentum of the string's center of mass, and the reality of X^μ requires that the left and right-moving modes are related by

$$\alpha^\mu_n = (\alpha^\mu_{-n})^*, \quad \tilde{\alpha}^\mu_n = (\tilde{\alpha}^\mu_{-n})^*. \tag{5.14}$$

Note tha the periodicity condition is not satisfied by the left and right moving waves individually, but it is restored when they are combined to form X^μ.

In the case of the open string, we chose $\sigma \in [0,\pi]$, and therefore to specify a solution we need to give the boundary conditions at the endpoints of the string. Throughout this work we use Neumann boundary conditions:

$$\partial_\sigma X^\mu = 0 \quad \text{at } \sigma = 0,\pi, \tag{5.15}$$

which correspond to a string moving freely through spacetime. The open string mode expansion reads

$$X^\mu_L(\sigma^+) = \frac{1}{2}x^\mu + \alpha' p^\mu \sigma^+ + i\sqrt{\frac{\alpha'}{2}}\sum_{n\neq 0}\frac{1}{n}\tilde{\alpha}^\mu_n\, e^{-in\sigma^+}, \tag{5.16}$$

$$X^\mu_R(\sigma^-) = \frac{1}{2}x^\mu + \alpha' p^\mu \sigma^- + i\sqrt{\frac{\alpha'}{2}}\sum_{n\neq 0}\frac{1}{n}\alpha^\mu_n\, e^{-in\sigma^-}. \tag{5.17}$$

From this equations we see that Neumann boundary conditions relate the left and right-moving modes of the open string by

$$\alpha^\mu_n = \tilde{\alpha}^\mu_n, \tag{5.18}$$

and therefore the open string depends on a single set of oscillators. Combining the left and righ-moving waves in the case of the open string gives

$$X^\mu(\sigma,\tau) = x^\mu + 2\alpha' p^\mu \tau + i\sqrt{2\alpha'}\sum_{n\neq 0}\frac{1}{n}\alpha_n^\mu \cos n\sigma\, e^{-in\tau}. \tag{5.19}$$

Using the $\sigma^\pm$ worldsheet coordinates, the constraints from requiring a vanishing stress tensor become

$$(\partial_+ X)^2 = (\partial_- X)^2 = 0, \tag{5.20}$$

which can be expressed in terms of the oscillators α_n^μ, $\tilde{\alpha}_n^\mu$, as

$$(\partial_- X)^2 = \alpha' \sum_{n=-\infty}^{\infty} L_n\, e^{-in\sigma^-}, \quad L_n = \frac{1}{2}\sum_{m=\infty}^{\infty}\alpha_{n-m}\cdot\alpha_m, \tag{5.21}$$

where we have defined the *Virasoro generators* L_n corresponding to the Fourier modes of the T_{--} component of the stress tensor, and we identified the zero mode α_0^μ with the center of mass momentum as $\alpha_0^\mu \equiv \sqrt{\frac{\alpha'}{2}}p^\mu$ for the closed string, and $\alpha_0^\mu \equiv \sqrt{2\alpha'}p^\mu$ for the open string [4].

The analogous formula for the T_{++} component gives the corresponding relation for the left-moving modes:

$$(\partial_+ X)^2 = \alpha' \sum_{n=-\infty}^{\infty} \tilde{L}_n\, e^{-in\sigma^-}, \quad \tilde{L}_n = \frac{1}{2}\sum_{m=\infty}^{\infty}\tilde{\alpha}_{n-m}\cdot\tilde{\alpha}_m, \tag{5.22}$$

and $\tilde{\alpha}_0^\mu \equiv \sqrt{\frac{\alpha'}{2}}p^\mu$ for the closed string, and $\tilde{\alpha}_0^\mu \equiv \sqrt{2\alpha'}p^\mu$ for the open string.

The vanishing stress tensor constraint expressed in terms of its Fourier modes says that any classical solution of the string must obey the infinitely many constraints

$$L_n = \tilde{L}_n = 0, \quad \forall\, n \in \mathbb{Z}. \tag{5.23}$$

Expressed this way these are called the *Virasoro constraints*, and are the ones that we will enforce upon quantization. This constitutes the topic of the next section.

5.1.2. The quantum string

To quantize the string we will use the method of canonical quantization, in which we promote the Fourier modes of the string to creation and annihilation operators. There exist basically two approaches to canonically quantize a constrained theory as the one we are facing: either one quantizes the systen first, and then imposes the constraints as operator equations to define the physical states of the system, or one solves the constraints at the classical level to determine the space of physical solutions and then quantizes these. An example of the second

[4] Note the difference of a factor of 2 in the term proportional to p^μ in eqs. (5.12) and (5.16), which stems from requiring that the coefficient of τ in each mode expansion has the interpretation of the spacetime momentum of the string obtained by integrating the Noether current associated to translations of X^μ on the worldsheet. The missmatch comes from the fact that $\sigma \in [0, 2\pi]$ for the closed string, while $\sigma \in [0, \pi]$ for the open string.

approach is the method of light-cone quantization that we will use in this work. However, for illustrative purposes let us describe briefly what happens when using the first approach, usually called covariant quantization.

As standard, to canonically quantize a theory of d free scalar fields X^μ we promote them and their conjugate momenta $\pi^\mu = \partial L/\partial \dot{X}_\mu$ to field operators satisfying canonical equal-time commutation relations. Translating these into commutation relations for the Fourier modes using the mode expansion we obtain

$$[x^\mu, p_\nu] = i\delta^\mu_\nu, \quad [\alpha^\mu_n, \alpha^\nu_m] = [\tilde{\alpha}^\mu_n, \tilde{\alpha}^\nu_m] = n\eta^{\mu\nu}\delta_{n+m,0}, \tag{5.24}$$

with all other commutators being zero.

For eq. (5.24) we see that the Fourier modes α^μ_n and $\tilde{\alpha}^\mu_n$ are nothing but harmonic oscillators up to a rescaling, and therefore the scalar fields give rise to infinite towers of creation and annihilation operators, with $\alpha_{n>0}$ corresponding to creation operators and $\alpha_{n<0}$ to annihilation operators. Naturally, the left-moving modes satisfy identical properties.

Armed with these relations we can easily build the Fock space of the theory by acting on the vacuum with creation operators. From now on we will focus for simplicity on the case of the open string, so we will only deal with the α^μ_n oscillators.

The vacuum state of the theory corresponds to a string without excited modes and center of mass momentum p^μ, and is defined to obey

$$\alpha^\mu_n |0;p\rangle = 0 \quad \text{for } n > 0, \quad \hat{p}^\mu |0;p\rangle = p^\mu |0;p\rangle, \tag{5.25}$$

and a generic state corresponding to an excited state of the string is obtained by the action of oscillators with $n < 0$ on the vacuum as

$$\alpha^{\mu_1}_{n_1}\alpha^{\mu_2}_{n_2}\ldots|0;p\rangle, \quad n_1,\, n_2, \cdots < 0. \tag{5.26}$$

We immediately see that there is a problem with our Fock space. The fact that the commutation relations for the oscillators shown in eq. (5.24) depend on the metric gives rise to negative norm states when we excite the timelike oscillators. For instance, the norm of the state created by acting with α^0_{-1} on the vacuum is

$$|\alpha^0_{-1}|0;p\rangle|^2 = \langle 0;p|\alpha^0_1\,\alpha^0_{-1}|0;p\rangle = \langle 0;p|[\alpha^0_1, \alpha^0_{-1}]|0;p\rangle = -1, \tag{5.27}$$

explicitly showing the presence of ghosts in the Fock space generated by the string modes.

In covariant quantization, the way to get rid of the ghosts is to impose the Virasoro constraints, as demanding that the physical Hilbert space is the one annihilated by the Virasoro generators projects out the ghost excitations. More concretely, we demand that the matrix element of the Virasoro generators between physical states yield zero in the quantum theory. In fact, since $L^\dagger = L_n$, demanding that the constraints are satisfied inside matrix elements only requires that physical states are annihilated by half of the Virasoro generators, namely

$$L_n|\psi\rangle = 0, \quad \text{for } n > 0 \text{ and } |\psi\rangle \in \mathcal{H}_{\text{phys}}. \tag{5.28}$$

The constraint associated to L_0 is more delicate, as in this case each term in the sum is made of a pair of non-commuting oscillators, and therefore when going from the classical definition in terms of Fourier modes to the quantum mechanical one we face an ambiguity in the ordering of the oscillators. To deal with this ambiguity we simply define L_0 to be normal-ordered, and add an arbitrary constant a to the Virasoro constraint, namely

$$L_0 = \sum_{m=1}^{\infty} \alpha_{-m} \cdot \alpha_m + \frac{1}{2}\alpha_0^2, \quad (L_0 - a)|\psi\rangle = 0, \quad \text{for } |\psi\rangle \in \mathcal{H}_{\text{phys}}. \tag{5.29}$$

It turns out that the decoupling of the ghosts from the spectrum requires that the constant arising from the ordering ambiguity must be related to the spacetime dimension by $a = (d-2)/24$. While we refer the reader to the references mentioned at the beginning of the chapter for details, let us mention that this Virasoro constraint has a very important interpretation. Since α_0^μ is proportional to the momentum of the string, we find that the 0^{th} Virasoro constraint corresponds to the on-shell condition determining the mass of the physical string states. For the open string $\alpha_0^\mu = \sqrt{2\alpha'}p^\mu$, and therefore

$$M^2 = \frac{1}{\alpha'}\left(\sum_{m=1}^{\infty} \alpha_{-m} \cdot \alpha_m - \frac{d-2}{24}\right), \tag{5.30}$$

where the sum over oscillators sums the number of excited modes of the string weighted by their Virasoro index, defining the mass level N. In particular, by enforcing the L_0 constraint on the (level 0) vacuum we recover the known fact that the string's ground state is a tachyon, and since the vacuum is annihilated by all the Virasoro generators with $n > 0$ by construction we find that as expected it belongs to the physical Hilbert space.

To work with states at higher levels as was our original goal one needs to enforce an increasingly large number of Virasoro constraints. To see how this would work, lets consider the first non-trivial example of a state at the first level, given by

$$\mathcal{E} \cdot \alpha_{-1}|0;p\rangle, \tag{5.31}$$

where $\mathcal{E}$ is a d-dimensional polarization tensor.

The non-trivial Virasoro generators in this case are L_0 and L_1. Acting on it with L_0 we find that the mass of the state is $M^2 = 1 - (d-2)/24$, which already points to the fact that $d = 26$ is relevant, as in this case we have a massless spin 1 state in the spectrum. In fact, as is well known this is precisely the critical dimension of bosonic String Theory, which is the required one for the theory to be consistent when quantized in Minkowski space.

Acting on the level 1 state with L_1 we obtain

$$L_1\left(\mathcal{E} \cdot \alpha_{-1}|0;p\rangle\right) = \sqrt{2\alpha'}\mathcal{E} \cdot p\,|0;p\rangle \equiv 0, \tag{5.32}$$

which implies that the polarization vector must be transverse to the momentum for the state to be physical.

In principle, we could proceed the same way for states at higher levels. Consider an arbitrary state at level N of the form

$$\sum_i \mathcal{E}^{(i)}_{\mu_1^{(i)}\dots\mu_k^{(i)}} \alpha^{\mu_1^{(i)}}_{n_1^{(i)}} \dots \alpha^{\mu_k^{(i)}}_{n_k^{(i)}} |0;p\rangle, \quad n_1^{(i)} + \dots + n_k^{(i)} = N, \tag{5.33}$$

where i sums over all possible combinations of oscillators consistent with the level and $\mathcal{E}^{(i)}$ are arbitrary tensors of the required rank to contract all the indices at each given term. In this case we would need to act with the relevant Virasoro generators, $L_0, \dots, L_N$, to obtain the constraints that the polarization tensors $\mathcal{E}^{(i)}$ need to satisfy for the state to be physical.

However, while the above procedure is simple at low levels and allows to obtain the first few physical states in the spectrum, this way of imposing the constraints soon becomes untractable, as the mixing between all the different $\mathcal{E}^{(i)}$ tensors induced by the increasing number of relevant Virasoro constraints makes obtaining the conditions on the $\mathcal{E}^{(i)}$ to project out the negative norm states a daunting task. Even using the more modern path integral formulation, in which one removes unphysical states from the Hilbert space by requiring that they are annihilated by the BRST charge, this procedure is too cumbersome to be performed in practice for highly excited states creates by a large number of oscillators. This is the reason why in this work we chose to bypass this issue and directly quantize the space of physical solutions of the theory using the light-cone gauge, that we review in the following section.

5.1.3. Light-cone quantization

In light-cone quantization rather than imposing the Virasoro consraints as operator equations on the states, we solve the constraints at the classical level to find the physical phase space of the theory, and then we quantize it, keeping only the physical degrees of freedom by construction. The idea is to use the residual gauge freedom remaining after fixing the gauge to set the worldsheet metric to be $\eta_{\alpha\beta}$ to chose a gauge in which the constraints are simple to solve.

The residual gauge freedom is given by any transformation $\sigma \to \tilde{\sigma}$ that changes the flat metric by

$$\eta_{\alpha\beta} \to \Omega^2(\sigma)\eta_{\alpha\beta}, \tag{5.34}$$

as this can be compensated by a Weyl transformation. In terms of the $\sigma^{\pm}$ worlsheet coordinates, the gauge fixed metric on the worldsheet reads

$$ds^2 = -d\sigma^+ d\sigma^-, \tag{5.35}$$

and therefore any transformation of the form $\sigma^+ \to \tilde{\sigma}^+(\sigma^+)$, $\sigma^- \to \tilde{\sigma}^-(\sigma^-)$ is a remaining gauge freedom, as this would simply multiply the metric by a factor removable by a Weyl rescaling.

The way to best exploit this remaining freedom is to go to the light-cone gauge. For this, lets define the spacetime light-cone coordinates as

$$X^{\pm} = \frac{X^0 \pm X^{d-1}}{\sqrt{2}}, \tag{5.36}$$

in which the spacetime metric reads

$$ds^2 = -2dX^- dX^+ + \sum_{i=1}^{d-2} dX^i dX^i. \tag{5.37}$$

As in the last section we focus on the open string, but the story is completely analogous in the case of the closed string. The light-cone gauge is defined by using our remaining gauge freedom to impose

$$X^+ = x^+ + 2\alpha' p^+ \tau, \tag{5.38}$$

which fixes the residual reparametrization invariance.

The virtue of this gauge choice is that it makes solving the Virasoro constraints trivial. To see this, remember that the equations of motion are solved by a sum of right and left-moving waves. For X^- we have

$$X^- = X_L^-(\sigma^+) + X_R^-(\sigma^-). \tag{5.39}$$

We will see that X^- is completely fixed by the Virasoro constraints in this gauge. To see this, note that the constraint $(\partial_+ X)^2 = 0$ in light-cone coordinates reads

$$2\partial_+ X^- \partial_+ X^+ = \sum_{i=1}^{d-2} \partial_+ X^i \partial_+ X^i. \tag{5.40}$$

Since from our gauge choice (5.38) we have $\partial_+ X^+ = \alpha' p^+$, this constraint becomes

$$\partial_+ X^- = \frac{1}{2\alpha' p^+} \sum_{i=1}^{d-2} \partial_+ X^i \partial_+ X^i, \tag{5.41}$$

while the constraint $(\partial_- X)^2 = 0$ implies

$$\partial_- X^- = \frac{1}{2\alpha' p^+} \sum_{i=1}^{d-2} \partial_- X^i \partial_- X^i, \tag{5.42}$$

which shows that $X^-(\sigma^+, \sigma^-)$ is completely fixed by the other fields X^i, X^+, up to an integration constant. In terms of the mode expansion for X^-

$$X^- = x^- + 2\alpha' p^- \tau + i\sqrt{2\alpha'} \sum_{n \neq 0} \frac{1}{n} \alpha_n^- \cos n\sigma \, e^{-in\tau}, \tag{5.43}$$

x^- corresponds to the integration constant, and p^- and α_n^- are fixed by the constraints to

$$\alpha_n^- = \frac{1}{2\sqrt{2\alpha' p^+}} \sum_{m=-\infty}^{\infty} \sum_{i=1}^{d-2} \alpha_{n-m}^i \alpha_m^i, \quad p^- = \frac{1}{\sqrt{2\alpha'}} \alpha_0^-. \tag{5.44}$$

While as before p^- will suffer from an ordering ambiguity when we quantize, the important point is that now all the excitations of the string are expressed in terms of oscillators made up of indices pointing along the $i = 1, \ldots, d-2$, directions *only*, in contrast to the previous case

where the indices run from 0 to d and excited negative norm states in the quantum theory. The remaining oscillators are the transverse modes of the string, which correspond to the physical excitations solving the Virasoro constraints. This accomplishes our first objective of restricting to the physical phase space at the classical level. Now, the next step is quantizing.

As before, the way to canonically quantize is to take the mode expansions from the classical theory and replace the Poisson brackets by commutators. For the transverse oscillators this gives

$$[\alpha_n^i, \alpha_m^j] = [\tilde{\alpha}_n^i, \tilde{\alpha}_m^j] = n\delta^{ij}\delta_{n+m,0}, \tag{5.45}$$

and for the the zero-modes

$$[x^i, p_j] = i\delta^{ij}, \quad [x^-, p^+] = -i, \quad [x^+, p^-] = -i, \tag{5.46}$$

The Fock space is built in the same way as in covariant quantization except that now we only act on the vacuum with the transverse oscillators carrying spatial indices only, and therefore the Hilbert space is free of negative norm states by construction and the Virasoro constraints are automatically satisfied. This permits to bypass the cumbersome problem of determining the allowed polarization tensors for physical states that we described in the previous section, as any state of the form

$$\alpha_{n_1}^{i_1}\alpha_{n_2}^{i}\ldots|0;p\rangle, \quad n_1,\, n_2, \cdots < 0, \quad i_1, i_2, \cdots = 1, \ldots, d-2, \tag{5.47}$$

is physical in this setup, no matter the polarization tensor that comes with it[5].

To conclude this review of the light-cone gauge formalism, let us mention some subtleties that arise in quantization. As in the case of covariant quantization, the mass-shell constraint suffers also from an ordering ambiguity in the quantization of the operator p^- from its classical definition (5.45) that can be represented by an a priori unkwown constant a.

$$M^2 = \frac{1}{\alpha'}\left(\sum_{i=1}^{d-2}\sum_{n>0}\alpha_n^i\alpha_n^i - a\right), \tag{5.48}$$

as can be seen from inserting eq. (5.45) in p^2. Even more worrisome is the fact that by choosing the light-cone gauge we broke the manifest Lorentz invariance of the classical theory, and while at the classical level this is only a cosmetic change and the theory remains Lorentz invariant, upon quantization there is no guarantee that Lorentz symmetry does not become anomalous. It turns out that these two issues are related, and it can be seen that requiring that Lorentz invariance is mantained at the quantum level requires simultaneously that the normal ordering constant is $a = 1$ and that the spacetime dimension is $d = 26$, the critical dimension of the bosonic string [6].

[5] An arbitrary polarization tensor won't be necessarily an irreducible representation and therefore the state might not be a one-particle state, but it is still physical.

[6] We point the reader to the original reference [18] for details.

Finally, for completeness we provide the full table of commutators in the light-cone gauge:

$[\,,\,]$	p^+	p^-	p^j	x^+	x^-	x^j	α^j_m	α^-_m
p^+	0	0	0	0	i	0	0	0
p^-	0	0	0	i	$-i\frac{p^-}{p^+}$	$-i\frac{p^j}{p^+}$	$-\frac{1}{2\alpha' p^+}m\alpha^j_m$	$-\frac{1}{\alpha' p^+}m\alpha^-_m$
p^i	0	0	0	0	0	$-i\delta_{ij}$	0	0
x^+	0	$-i$	0	0	0	0	0	0
x^-	$-i$	$i\frac{p^-}{p^+}$	0	0	0	0	0	$i\frac{\alpha^-_m}{p^+}$
x^i	0	$i\frac{p^i}{p^+}$	$i\delta_{ij}$	0	0	0	$i\sqrt{2\alpha'}\delta_{ij}\delta_m$	$i\frac{\alpha^i_m}{p^+}$
α^i_n	0	$\frac{1}{2\alpha' p^+}n\alpha^i_n$	0	0	0	$-i\sqrt{2\alpha'}\delta_{ij}\delta_n$	$n\delta_{ij}\delta_{n+m}$	$\frac{1}{\sqrt{2\alpha' p^+}}n\alpha^i_{n+m}$
α^-_n	0	$\frac{1}{\alpha' p^+}n\alpha^-_n$	0	0	$-i\frac{\alpha^-_n}{p^+}$	$-i\frac{\alpha^j_n}{p^+}$	$-\frac{1}{\sqrt{2\alpha' p^+}}m\alpha^i_{n+m}$	$[\alpha^-_n,\alpha^-_m]$

with

$$[\alpha^-_n,\alpha^-_m]=\frac{2}{\sqrt{2\alpha' p^+}}(m-n)\alpha^-_{m+n}+\frac{1}{\alpha'(p^+)^2}m(m^2-1)\delta_{m+n}.$$

Note that the modes along the $-$ direction do not commute with the modes along the other directions nor with the center of mass degrees of freedom. This is the price to pay for working in a non-covariant framework.

5.2. Building one-particle states from light-cone oscillators

As advertised, by choosing the light-cone gauge we have managed to remove all the unphysical degrees of freedom, and every state created by the resulting transverse oscillators is physical by construction. However, as was also mentioned, these states do not correspond to the one-particle states that we are interested in, and understanding how to obtain them from the light-cone oscillators was the first challenge we faced in this project. In what follows, we present our approach to do so.

To begin, we recall that one-particle states are defined as irreducible, unitary representations of the Poincaré group, the isometry group of Minkowski spacetime, and are labeled by their mass and spin, which correspond to the eigenvalues of the Casimir operators of the corresponding algebra (for an introduction on these topics, see for instance [200, 201]). Using Wigner's method of induced representations [202] we can reduce the problem of finding all the irreducible representations of the full Poincaré group to determining the irreducible representations of its *litte group*, the subgroup of the Poincaré group that leaves the momentum k^μ of the particle invariant. Once the transformation properties of a given state under the little group are understood, we can reconstruct how it transforms under the full Poincaré group.

The relevant little group will depend on whether k^μ is spacelike, null, or timelike, corresponding to tachyonic, massless and massive particles respectively. In arbirtary dimensions, the corresponding little groups are $SO(d-2,1)$ for tachyons, $ISO(d-2)$ for massless particles and $SO(d-1)$ for massive particles, where $SO(d-2,1)$ is the homogeneous Lorentz group with one spatial dimension less, $ISO(d-2)$ corresponds to the isometry group of $(d-2)$-dimensional Euclidean space, and $SO(d-1)$ is simply the rotation group in $(d-1)$

spatial dimensions. In the massless case, the group $ISO(d-2)$ allows representations labeled by a continuous parameter, sometimes referred to as *continuous spin representations*. If one demands that the action of the little group generators that correspond to this continuous parameter is trivial, the little group becomes $SO(d-2)$.

In what follows we will work in the critical dimension of the bosonic string, $d = 26$, and since we will focus on massive states the relevant little group is $SO(25)$. However, the states obtained by exciting the vacuum with the oscillators obtained from the light-cone gauge quantization as (5.47) are labeled by indices i that run from $i = 1$ to $i = 24$, and therefore furnish representations of the group $SO(24)$. This means that states as eq. (5.47) are not one-particle states, and at a given level various combinations of light-cone oscillators will combine to create a given one-particle state corresponding to a representation of $SO(25)$. The only exception for this apart from the trivial case of the vacuum is the massless spin 1 state at level 1 created by α^i_{-1}, as in this case the transverse directions are enough to furnish an irreducible representation of the massless little group.

5.2.1. Some warm-up examples

Lets see an example of how this works in the case of the open string. The simplest case where this phenomenon plays a role is when considering the massive spin 2 paricle at level 2. It should be described by a rank 2, traceless, symmetric tensor $\mathcal{E}_{\mu\nu}$, and by choosing it to be at rest in the frame that we used to define the light-cone gauge in eq. (5.38) we can set to zero all its components involving the time direction in this frame. Denoting X^ℓ the spacetime coordinatate used to define $X^\pm$, we see that the non-trivial components of the tensor are $\mathcal{E}_{ij}$, $\mathcal{E}_{i\ell}$, $\mathcal{E}_{\ell\ell}$, where $i, j = 1, \ldots, 24$ correspond to transverse directions.

Now lets consider the states created from light-cone oscillators at level two. In terms of their transformation properties with respect to $SO(24)$, they are a symmetric-traceless rank 2 tensor, a vector and a scalar, given by

$$\alpha^{\langle i}_{-1}\alpha^{j\rangle}_{-1}|0\rangle, \quad \alpha^i_{-2}|0\rangle, \quad \sum_{i=1}^{24}\alpha^i_{-1}\alpha^i_{-1}|0\rangle, \tag{5.49}$$

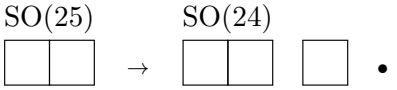
where $\langle ij\rangle$ denotes symmetrization in i, j and the removal of the trace.

It is not hard to imagine, and it is indeed the case, that each of these correspond to the different possible polarizations of the $SO(25)$, spin 2 particle. More specifically, the state $\alpha^{\langle i}_{-1}\alpha^{j\rangle}_{-1}|0\rangle$ corresponds to $\mathcal{E}_{ij}$, the case in which both polarizations are transverse, $\alpha^i_{-2}|0\rangle$ corresponds to choosing one transverse polarization and the other along ℓ, namely $\mathcal{E}_{i\ell}$, and finally the $\mathcal{E}_{\ell\ell}$ polarization is given by the $SO(24)$ scalar $\sum_{i=1}^{24}\alpha^i_{-1}\alpha^i_{-1}|0\rangle$.

Therefore, we see that the one-particle state is made up of a combination of different light-cone states. In mathematical terms, this is corresponds to the restriction of a representation the larger group $SO(25)$ into representations of its subgroup $SO(24)$, with the spin 2 representation of $SO(25)$ being decomposed into the direct sum of the spin 2, spin 1 and spin 0 $SO(24)$ representations. In general, the decomposition of the irreducible representations of a group G into irreducible representations of one of its subgroups H are described by the *branching rules* from G to H. For a review on branching rules as well as an extensive list of the branching rules between several groups, including the $SO(25) \to SO(24)$ case relevant for this work, see [203].

An efficient way of denoting the representations of $SO(N)$ groups is using Young tableaux. Each representation is encoded by a diagram called Young tableau composed by an arrangement of boxes encoding the symmetries of the representation. Each box corresponds to an index of the tensor characterizing the representation, and each (row/column) of boxes corresponds to (symmetrization/antisymmetrization) of the corresponding indices. For more details we refer the reader to any standard group theory textbook, such as [204, 205].

For the case at hand, the decomposition of the spin 2 particle at level 2 into light-cone states reads



However, knowing the branching rules $SO(25) \to SO(24)$ is not the end of the story. To see why, lets analyze one more example and consider the situation at level 3. From the light-cone oscillator point of view we have three possible structures acting on the vacuum which can be decomposed in the following $SO(24)$ irreducible representations:

$$(\alpha_{-1})^3 \to \square\!\square\!\square_{24} + \square_{24} \tag{5.50}$$

$$\alpha^i_{-2}\alpha^j_{-1} \to \square\!\square_{24} + \begin{array}{|c|}\hline\ \\ \hline\ \\ \hline\end{array}_{24} + \bullet_{24} \tag{5.51}$$

$$\alpha^i_{-3} \to \square_{24}, \tag{5.52}$$

where in the first row the $SO(24)$ rank 3 fully symmetric tensor corresponds to $\alpha^{\langle i}_{-1}\alpha^j_{-1}\alpha^{k\rangle}_{-1}$ and the vector to $(\alpha_{-1}\cdot\alpha_{-1})\alpha^i_{-1}$, and in the second row the different combinations are obtained by symmetrizing, antisymmetrizing and tracing over the indices respectively. Note that $\bullet_{24}$ denotes an $SO(24)$ scalar, in this case $\alpha_{-1}\cdot\alpha_{-2}$.

The situation at level 3 is already more involved, with various possible oscillator structures. To find out the $SO(25)$ irreducible representations at this level, we start by noting that the $SO(24)$ representations with the largest number of indices and a given symmetry pattern must trivially translate to the corresponding $SO(25)$ representation. In this case, the rank 3 tensor $\alpha^{\langle i}_{-1}\alpha^j_{-1}\alpha^{k\rangle}_{-1}$ necessarily implies the existence of a spin 3 one-particle state of which this oscillator combination gives the fully transverse part. Similarly, the antisymmetric rank 2 tensor $\alpha^{[i}_{-2}\alpha^{j]}_{-1}$[7] implies the existence of the corresponding $SO(25)$ representation, and we see that the one-particle states

$$\square\!\square\!\square_{25}, \quad \begin{array}{|c|}\hline\ \\ \hline\ \\ \hline\end{array}_{25}, \tag{5.53}$$

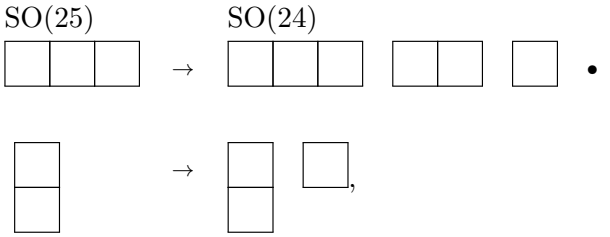
are part of the spectrum at level 3. These kind of $SO(24)$ irreducible representations that can be immediately matched with their corresponding $SO(25)$ representations will play an important role in what follows.

However, the situation is not so clear for the rest of the $SO(24)$ irreducible representations. We have two vectors and one scalar left, but we saw already in our level 2 example that the

[7] Square brackets denote antisymmetrization between a given set of indices

smaller $SO(24)$ representations can mix with the larger ones to provide the missing parts to complete the $SO(25)$ representations, and therefore at this point it is not clear if there can be a vector or a scalar particle at level three or if all these states will just be swallowed by the $\square\square\square_{25}$ and $\begin{smallmatrix}\square\\\square\end{smallmatrix}_{25}$ states.

In fact, it we look at the branching rules for $SO(25) \to SO(24)$ we find



exhausting all the $SO(24)$ structures, and therefore the one-particle states at level 3 are just the rank 3 fully symmetric and the rank 2 antisymmetric tensors.

This characterizes the spectrum at this level, but raises another question. If we want to find the combinations of oscillators that give the polarizations of the one-particle states along non-transverse directions as we did in the level 2 example, we need to understand which $SO(24)$ vector is inside each $SO(25)$ irreducible representation.

The way to proceed, which will be at the basis of our general method to obtain the spectrum at any given level, is to use the fact that $SO(24)$ states belonging to the same $SO(25)$ irreducible representation must mix exclusively among themselves under little group transformations. Therefore, we can start with the $SO(24)$ structures that can be trivially located inside an $SO(25)$ irreducible representation and rotate them by acting with the combinations of Lorentz generators spanning the little group to obtain the remaining $SO(24)$ structures. We will refer to these special $SO(24)$ states that map directly to one-particle states as *highest spinning states* or *highest spinning structures*, and they will play a crucial role in what comes. [8]

The Lorentz generators correspond to the conserved charges associated to Lorentz Transformations, and we can express them in terms of the oscillators by integrating the time component of the corresponding conserved current along the spatial direction of the worldsheet.

The conserved current associated to Lorentz transformations is

$$X^\mu P^{\nu,\alpha} - X^\nu P^{\mu,\alpha} \tag{5.54}$$

where

$$P^{\mu,\alpha} = \frac{1}{2\pi\alpha'}\partial_\alpha X^\mu, \tag{5.55}$$

[8] The name highest spinning structures makes reference to the fact that they are the $SO(24)$ structures that have the same number of indices as the $SO(25)$ irreducible representation where they are embedded, while all the other components have fewer. It does not necessarily mean that these are the objects with the highest number of indices at a specific level.

is the conserved current associated to translations. Integrating its τ component along the space direction of the worldsheet we get

$$J^{\mu\nu} = \int_0^\pi d\sigma\, X^\mu P^{\nu,\tau} - X^\nu P^{\mu,\tau} \tag{5.56}$$

which can be evaluated using the mode expansion (5.19) to give

$$J^{\mu\nu} = x^\mu p^\nu - p^\nu x^\mu + \frac{i}{2}\sum_{n\neq 0}\frac{\alpha_n^\mu \alpha_{-n}^\nu - \alpha_n^\nu \alpha_{-n}^\mu}{n}, \tag{5.57}$$

which is independent of τ as expected, and where the relevant part is the sum over oscillators, as this is the one that will mix the different $SO(24)$ structures, while the contribution from the center of mass variables must vanish if the transformation belongs to the little group. This point is more subtle than one would think in the light-cone gauge, as here the center of mass degrees of freedom do not commute with the α_n^-, but it can be checked with an explicit computation that the contribution from the center of mass terms drops.

To begin, lets prove the statement that the center of mass part of the angular momentum operators does not contribute. We will focus on the example of the light-cone state $\alpha_{-3}^i|0\rangle$, but the computation is analogous in every case.

In the rest frame, $p^+ = p^-$, which together with the mass shell condition fixes both of them to be

$$p^+ = p^- = \sqrt{\frac{N-1}{2\alpha'}}, \quad N = 3. \tag{5.58}$$

Since p^+ commutes with the oscillators, the value of p^+ of the excited state is the same as for the tachyonic vacum:

$$\hat{p}^+\alpha_{-3}^i\,|0\rangle = p^+\alpha_{-3}^i\,|0\rangle = \alpha_{-3}^i\hat{p}^+\,|0\rangle = \alpha_{-3}^i p_{tac}^+\,|0\rangle = p_{tac}^+\alpha_{-3}^i\,|0\rangle\,, \tag{5.59}$$

where we exceptionally use the hat notation to distinguish the operators from the eigenvalues.

While somewhat unintuitive, as naively one would expect a decoupling between the 4-momentum and the internal degrees of freedom, the case for p^- cannot be the same, as exciting internal degrees of freedom must turn the spacelike momentum of the tachyon into a timelike momentum.

Indeed, with essentially the same logic,

$$\hat{p}^-\alpha_{-3}^i\,|0\rangle = p^-\alpha_{-3}^i\,|0\rangle = \left(3\frac{\alpha_{-3}^i}{2\alpha' p^+} + \alpha_{-3}^i\hat{p}^-\right)|0\rangle \tag{5.60}$$

thus

$$\hat{p}^-\,|0\rangle = p^- - \frac{3}{2\alpha' p^+} = \frac{1}{\sqrt{\alpha'}}(1-\frac{3}{2}) = -\frac{1}{2\sqrt{\alpha'}}. \tag{5.61}$$

Since the particle is at rest, the little group is simply the $SO(25)$ corresponding to spatial rotations generated by the J^{ij} and $J^{\ell i}$, where the J^{ij} are rotations involving purely

transverse directions, and $J^{\ell i}$ includes the light-cone spatial direction, denoted X^ℓ. As the light-cone states are by construction representations of $SO(24)$ already, acting with the rotation generators J^{ij} along the transverse directions will not yield new information, and we must rather rotate them using the remaining little group element $J^{\ell i}$.

To express this operator in terms of transverse oscillators, note that since the light-cone coordinates are defined by

$$X^\pm = \frac{X^0 \pm X^\ell}{\sqrt{2}}, \tag{5.62}$$

we have that

$$J^{+i} = \frac{1}{\sqrt{2}}(J^{0i} + J^{\ell i}), \qquad J^{-i} = \frac{1}{\sqrt{2}}(J^{0i} - J^{\ell i}), \tag{5.63}$$

and therefore we can express $J^{\ell i}$ as

$$J^{\ell i} = \frac{J^{+i} - J^{-i}}{\sqrt{2}}. \tag{5.64}$$

Now we write these generators in light-cone gauge, where we have effectively set to zero all the oscillators along the + direction, as can be seen from eq. (5.38). A subtlety is that since p^- doesn't commute with x^i, to promote the classical expression for the rotation generators in eq. (5.57) to a hermitian operator we must symmetrize the term $x^i p^- \to (x^i p^- + p^- x^i)/2$. This yields

$$J^{+i} = x^+ p^i - x^i p^+, \qquad J^{-i} = x^- p^i - \frac{x^i p^- + p^- x^i}{2} + J^{-i}_{int} \tag{5.65}$$

where J_{int} is the part of (5.57) involving the oscillator internal degrees of freedom.

We are now ready act with $J^{\ell i}$ on $\alpha^j_{-3}\,|0\rangle$. In the rest frame, the action of the center of mass part $J^{\ell i}_{CoM}$ is

$$J^{\ell i}_{CoM}\,\alpha^j_{-3}\,|0\rangle = \frac{1}{\sqrt{2}}\left(-x^i p^+ + \frac{x^i p^- + p^- x^i}{2}\right)\alpha^j_{-3}\,|0\rangle\,, \tag{5.66}$$

Now $\dfrac{x^i p^- + p^- x^i}{2}\alpha^j_{-3}\,|0\rangle = \dfrac{x^i(\hat{N}-1)}{2\alpha' p^+}\alpha^j_{-3}\,|0\rangle$, and since $p^+ = \alpha'^{-1/2}$ the contribution from J_{CoM} vanishes as claimed.

From this computation we see that the relevant part of the generator $J^{\ell i}$ corresponding to the excitations of the string is proportional to the corresponding part of J^{-i}. Splitting the center of mass and the oscillator contributions as $J = J_{CoM} + J_{int}$, we have

$$J^{\ell i}_{int} = -\frac{1}{\sqrt{2}} J^{-i}_{int}, \tag{5.67}$$

and therefore we can equivalently act with J_{int}^{-i} on the $SO(24)$ structures to group them into $SO(25)$ representations. Explicitly, J_{int}^{-i} is given by

$$J_{int}^{-i} = \frac{i}{2}\sum_{n\neq 0}\frac{\alpha_n^-\alpha_{-n}^i - \alpha_n^i\alpha_{-n}^-}{n}. \tag{5.68}$$

From the definition of the α_n^- in eq. (5.45) we can obtain the commutators that we will need to act on the light-cone states:

$$[\alpha_n^-, \alpha_l^j] = \frac{1}{2\alpha' p^+}\sqrt{\frac{\alpha'}{2}}\sum_{m\in\mathbb{Z}}[\alpha_{n-m}^k\alpha_m^k, \alpha_l^j] = -\frac{l}{\sqrt{2\alpha' p^+}}\alpha_{n+l}^j, \tag{5.69}$$

and

$$[J_{int}^{-i}, \alpha_l^j] = \frac{i}{2}\sum_{n\neq 0}\frac{1}{n}[\alpha_n^-\alpha_{-n}^i, \alpha_l^j] - \frac{1}{n}[\alpha_n^i\alpha_{-n}^-, \alpha_l^j] = \tag{5.70}$$

$$-i\delta^{ij}\alpha_l^- - i\frac{l}{\sqrt{2\alpha' p^+}}\sum_{n\neq 0}\frac{1}{n}\left(\alpha_{-n}^i\alpha_{n+l}^j - \alpha_n^i\alpha_{l-n}^j\right). \tag{5.71}$$

Armed with these commutators, we can simply act with J_{int}^{-i} on the states $\alpha_{-1}^{\langle i}\alpha_{-1}^j\alpha_{-1}^{k\rangle}|0\rangle$ and $\alpha_{-2}^{[i}\alpha_{-1}^{j]}|0\rangle$ to find the $SO(24)$ vector belonging to each one-particle state. It turns out that it is linear combinations of both structures that go into each representation, namely

$$(-2\alpha_{-3}^i + \alpha_{-1}^i(\alpha_{-1}\cdot\alpha_{-1}))|0\rangle \in \begin{array}{|c|}\hline\\\hline\\\hline\end{array}_{25}\,, \tag{5.72}$$

$$(26\alpha_{-3}^i + 3\alpha_{-1}^i(\alpha_{-1}\cdot\alpha_{-1}))|0\rangle \in \begin{array}{|c|c|c|}\hline&&\\\hline\end{array}_{25}. \tag{5.73}$$

Note that the states are not normalized, as the relevant information is simply the relative weight of the two structures.

A point that will be crucial to generalize this strategy to arbitrary levels is the fact that if instead of acting on the highest spinning states $\alpha_{-1}^{\langle i}\alpha_{-1}^j\alpha_{-1}^{k\rangle}|0\rangle$ and $\alpha_{-2}^{[i}\alpha_{-1}^{j]}|0\rangle$ with J_{int}^{-i} we had used a little group element J_{int}^{-m} pointing along a direction m different from i, j and k we would necessarily get a vanishing result, as otherwise there would be a state with four indices at level 3, which is inconsistent with the mass-shell condition.

This is actually also true for the combinations of $SO(24)$ structures that yield the component of an $SO(25)$ one-particle state with the largest number of transverse polarizations, even if it does not correspond to the state with the highest number of indices at the given level. For example, we will see that at level 4 there is a rank 2, fully symmetric particle in the spectrum, and the combination of $SO(24)$ structures that yields its fully transverse polarizations in the rest frame is annihilated by J^{-i}.

This shows that the oscillator structures that form a given one-particle state behave in a way reminiscent of a highest weight representation, with J^{-i} acting similarly to a raising operator and the highest spinning states being the highest weights annihilated by it. Following this analogy, we see that at a given level we can find the highest spinning $SO(24)$ states that

map directly to one-particle states by looking at the kernel of J_{int}^{-i}. Since these characterize completely the spectrum at a given level, if we are only interested in knowing the one-particle content this would be enough. If moreover we want to understand how the remaining $SO(24)$ structures accomodate themselves inside the different particles, we proceed as in the example and act on the highest spinning states with J_{int}^{-i}, with i coinciding with one of the indices of the state, which in this analogy plays the role of the lowering operator.

It is important to remark that the analogy between J^{i-} and a lowering operator is not exact, as acting with J^{-i} with a repeated index on an $SO(24)$ structure with $n-k$ indices belonging to a rank n $SO(25)$ representation (that is, on a structure different from the highest spinning one), will yield not only $SO(24)$ structures in the same $SO(25)$ multiplet with $n-k-1$ indices but also ones with $n-k+1$ indices with two indices evaluated at equal values, which need to be disentangled in order to obtain the list of $SO(24)$ oscillator structures that furnish the given one-particle state. This is not a big problem, and starting from the highest spinning $SO(24)$ structure this procedure can always be carried out in a systematic way.

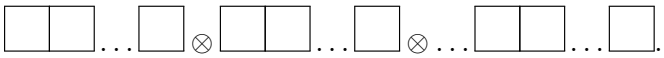
5.2.2. General method

After having understood the main features and difficulties of the problem of organizing the $SO(24)$ states into one-particle states with a few examples, let us generalize the approach to find the one-particle content at an arbitrary level N.

- The first step is to find all the possible light-cone oscillator structures that contribute at level N. Since the sum of all the Virasoro indices of the oscillators at level N must be N, this is simply given by all the partitions of N, namely all the different combinations of integers that give N when summed. For example, at level 4 we would have $\{4,\, 3+1,\, 2+2,\, 2+1+1,\, 1+1+1+1\}$, corresponding to the structures α_{-4}, $\alpha_{-3}\,\alpha_{-1}$, $(\alpha_{-2})^2$, $\alpha_{-2}\,(\alpha_{-1})^2$, $(\alpha_{-1})^4$, were we have ommited the transverse indices.

- For each structure, consider all possible non-equivalent pairings of oscillators, where two pairings are equivalent if they group oscillators with the same Virasoro index. These pairings will correspond to $SO(24)$ traces in the light-cone structures. For example, the $\alpha_{-2}\,(\alpha_{-1})^2$ structure at level 4 can be paired as $\alpha^i_{-2}\,\alpha_{-1}\cdot\alpha_{-1}$, in which corresponds to tracing over the -1 oscillators, as $\alpha_{-2}\cdot\alpha_{-1}\,\alpha^i_{-1}$, where the trace is taken between a -1 and the -2 oscillators, and $\alpha^i_{-2} j \alpha^k_{-1}$, where no traces are taken. Note that the second trace is counted only once, even if there are two possible -1 oscillators. The transverse indices are just dummy variables at this stage, so either option corresponds to the same state.

- For each pairing write all the possible symmetry structures that can be built up with the remaining free transverse indices. The most efficient way to characterize them is using Young tableaux as before. Each group of oscillators of the same Virasoro index will form a fully symmetric substructure, and therefore we can obtain all the possible Young tableaux by taking tensor products of fully symmetric, one-row Young tableaux as



In the previous example, the trivial pairing without traces will produce the Young tableaux given by the tensor product

$$\begin{array}{|c|c|}\hline 1&1\\\hline\end{array}\otimes\begin{array}{|c|}\hline 2\\\hline\end{array}=\begin{array}{|c|c|c|}\hline 2&1&1\\\hline\end{array}\oplus\begin{array}{|c|c|}\hline 1&1\\\hline 2\\\cline{1-1}\end{array},$$

where the numbers inside the Young tableaux show the Virasoro index of the corresponding oscillator.[9] The set of all Young tableaux obtained this way yields all the $SO(24)$ irreducible representations at level N

- After getting all the Young tableaux correspwith Virasoro indices placed, we must turn these blueprints to actual symmetrized structures of oscillators with transverse Lorentz indices. The way we do this is to place Lorentz indices in each box of a given Young tableau, and then first antisymmetrize columns and, for each possibility, we then symmetrize rows. In the previous example, the $\begin{array}{|c|c|c|}\hline 2&1&1\\\hline\end{array}$ tableau corresponds to the oscillator structure $\alpha^i_{-2}j\alpha^k_{-1}+\alpha^i_{-1}j\alpha^k_{-2}+\alpha^i_{-1}j\alpha^k_{-2}$, while $\begin{array}{|c|c|}\hline 1&1\\\hline 2\\\cline{1-1}\end{array}$ corresponds to $(\alpha^i_{-2}-\alpha^j_{-1})\alpha^k_{-1}$.

- To find the one-particle content at the required level, we must obtain the highest spinning $SO(24)$ structures that map to one-particle states. This is done by writing an arbitrary linear combination of all the $SO(24)$ structures corresponding to a given Young tableau, and demanding that it is annihilated by the action of J^{-i}, where i is different from all the indices of the $SO(24)$ structures. These yields a linear system on the coefficients, and if it has solutions then they correspond to one-particle states furnishing $SO(25)$ representations with the same Young tableau as the $SO(24)$ structures. If no solutions are found, then this specific Young tableau is not present in the spectrum, and all the $SO(24)$ structures with this symmetry must be embedded in a larger representation. Performing this procedure for all the $SO(24)$ Young tableaux determined in the previous step we completely characterize the one-particle content at the required level.

- If apart from the spectrum one is interested in understanding how the different $SO(24)$ structures that do not correspond to highest spinning structures fill the remaining polarizations in the rest frame, one can proceed to act on the highest spinning structures with J^{-i}, with i repeated in the structures, to climb down the ladder and find the different components of the representation

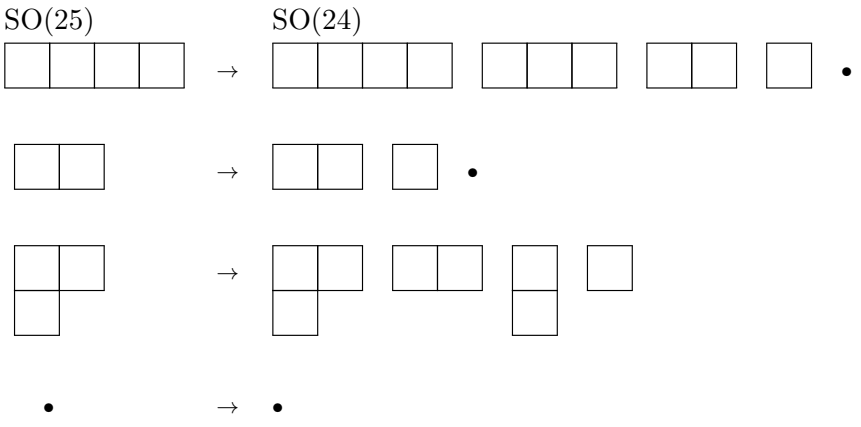
The procedure that we just introduced can be automatized in a straightforward way, and we implemented this algorithm both in MATHEMATICA and Python to obtain the one-particle content and its oscillator representations at high levels. The method is very efficient and allows to excavate the one-particle states from the spectrum up to levels that were not accesible before. As a reference, the authors of [178] very recently used a method somewhat similar to ours -discovered independently- to build all the one-particle states up to

[9] Note that while the relevant group for us is $SO(24)$, we can use the simpler tensor product rules of $SU(24)$, as the (anti)symmetrization patterns are the same. The difference is that in orthogonal groups we need to remove the traces from the irreducible representations, but his can be dealt with after the oscillator structures with their given symmetry are obtained.

level 10, also using light-cone gauge technology. With our method we match all their results, and the computation up to level 10 takes only a few seconds.[10]

As an example we present the data at level 4, and we include higher levels in an appendix.

The one-particle content at level 4 in terms of Young tableaux together with its decomosition into $SO(24)$ states is the following:



It is given by a spin 4 state, namely a fully symmetric, traceless rank 4 tensor, a rank 3 tensor with mixed symmetry, a spin 2 state and a scalar. While the highest spinning $SO(24)$ structures that yield the spin 4 and the mixed symmetry tensor are trivially $\alpha^i_{-1}\alpha^j_{-1}\alpha^k_{-1}\alpha^\ell_{-1}$ and $(\alpha^i_{-2}-\alpha^j_{-1})\alpha^k_{-1}$ respectively, as they are the only structures having this $SO(24)$ Young tableaux, the spin 2 and the scalar are not obvious.

It turns out that the linear combination of light-cone oscillators that gives the scalar is

$$\overset{\bullet}{}_{25} = \Big(((\alpha_{-1}\cdot\alpha_{-1}))^2 + 7(\alpha_{-2}\cdot\alpha_{-2}) - 10(\alpha_{-1}\cdot\alpha_{-3})\Big)\,|0\rangle\,, \tag{5.74}$$

while the $SO(24)$ structures associated to the spin 2 state are

$$\square\!\square_{24} = \Big(\alpha^i_{-1}\alpha^j_{-1}(\alpha_{-1}\cdot\alpha_{-1}) + 7\alpha^i_{-2}\alpha^j_{-2} - 4(\alpha^i_{-1}\alpha^j_{-3}+\alpha^j_{-1}\alpha^i_{-3})\Big)\,|0\rangle\,, \tag{5.75}$$

$$\square_{24} = \Big(4\alpha^i_{-4} + 4\alpha^i_{-1}(\alpha_{-1}\cdot\alpha_{-2}) - 9\alpha^i_{-2}(\alpha_{-1}\cdot\alpha_{-1})\Big)\,|0\rangle\,, \tag{5.76}$$

$$\overset{\bullet}{}_{24} = \Big(8((\alpha_{-1}\cdot\alpha_{-1}))^2 - 19(\alpha_{-2}\cdot\alpha_{-2}) + 20(\alpha_{-1}\cdot\alpha_{-3})\Big)\,|0\rangle\,, \tag{5.77}$$

with $\square\!\square_{24}$ corresponding to the massive spin 2 state at rest and polarized along the i,j directions, $\square_{24}$ to the state polarized along the i,ℓ directions, with ℓ still corresponding to the spatial light-cone component, and $\overset{\bullet}{}_{24}$ to the state with both indices polarized along ℓ.

[10] This is the case for the one-particle determination by looking for the kernel of J^{-i} to obtain the highest spinning component. Finding all the oscillators that build the rest of the polarization is less optimal.

5.2.3. Validity of the results in arbitrary frames

Up to now we have worked a lot to provide the spectrum and its decomposition into oscillators. However, all the computations were carried in the reference frame in which the massive particles are at rest, and this might lead to wonder if the results we obtained are general or their validity is restricted to this specific frame. While the particle content cannot depend on the reference frame and therefore the set of Young tableaux characterizing the $SO(25)$ irreducible representations at a given level is on solid ground already, it could be that the specific oscillator structures furnishing the highest spinning structures corresponding to each one-particle, as well as the subleading components providing the missing polarizations, are frame-dependent. After all, we computed them by assuming that the little group corresponded to spatial rotations, but this is only true in the rest frame of the particle. For states with non-trivial spatial momentum, the little group will be generated by some linear combination of the Lorentz generators that annihilate the momentum of the state[11] that will obviously be momentum dependent, so it is not trivial to show that the above structures will pass through to the generic momentum case.

In this section we bridge this gap, and show that indeed the oscillator structures obtained in the rest frame are generic, and the same combinations of oscillators create the same particles when acting on a vacuum state with arbitrary momentum. The proof is as follows:

We want to show that the same oscillator structures that define one-particle states in the rest frame, obtained by demanding that they mix exclusively among themselves under the action of the relevant little group element $J^{\ell i}$ also define one-particle states in boosted reference frames.

To perform this analysis when considering a generic state at level N given by light-cone oscillators acting on a vacuum state with arbitrary momentum k^μ, we would proceed analogously as in the case in which the state is at rest. We would write down the most general linear combination of oscillator structures at this level, and demand it rotates into itself under the action of the little group elements. In this case, however, the little group that leaves k^μ invariant is not simply the one of spatial rotations anymore, but its generators can be written in terms of the angular momentum generators as

$$J^a(k) \equiv \mathcal{E}^a_{\mu\nu}(k) J^{\mu\nu}, \quad a = 1, \ldots, \mathcal{N} \tag{5.78}$$

where the $\mathcal{E}^a_{\mu\nu}(k)$ are such that the $J^a(k)$ annihilate the momentum k, and $\mathcal{N} = \dfrac{25 \times 24}{2}$ is the dimension of the little group.

An important point to notice is that, identically as in the rest frame case, splitting $J^a(k)$ into center of mass and an oscillator contributions $J^a_{CoM}(k)$ and $J^a_{int}(k)$ we find that $J^a_{CoM}(k)$ must act trivially by definition, as this is the only term that can change the momentum of the state. This is non-trivial, as the non-commutativity of the p^- with the oscillators causes the appearance of momentum dependent terms when commuting $J^a_{CoM}(k)$ through them, which are precisely cancelled by the ones arising from acting with $J^a_{CoM}(k)$ on the vacuum (note that this is exactly the mechanism that took place in the explicit computation in the rest frame shown in the last section), and we see that as before the relevant piece to classify the one-particle states is $J^a_{int}(k)$.

[11] So as to leave it invariant when exponentiating the Lie algebra elements to form an element of the litte group.

Now comes the punchline. A smart way of choosing a basis for the algebra of the little group for arbitrary momentum k^μ is to pick basis elements of the form

$$J^{ij} + a_{ij}(k)J^{i+} + b_{ij}(k)J^{j+}, \quad i,j \text{ transverse}, \tag{5.79}$$

and

$$J^{i-} + a_{i-}(k)J^{i+} + b_{i-}(k)J^{-+}, \tag{5.80}$$

where the $a(k)$ and $b(k)$ are functions of the momentum of the state that are fixed by demanding that these are indeed elements of the little group algebra and thus annihilate k. *Note that there is no summation over the i and j indices.* They are given by

$$a_{ij}(k^\mu) = -\frac{k^j}{k^+}, \quad b_{ij}(k^\mu) = \frac{k^i}{k^+}, \tag{5.81}$$

$$a_{i-}(k^\mu) = -\frac{N}{2\alpha'(k^+)^2}, \quad b_{i-}(k^\mu) = \frac{k^i}{k^+}, \tag{5.82}$$

where N is the level of the state. This set of generators has obviously the right dimensionality to span the little group and maps to the set $\{J^{ij}, J^{i-}\}$ in the rest frame, and has the advantage that when using them to classify particles, the parts containing + directions don't contribute (as all α_n^+ oscillators are zero) and therefore they act on the oscillators in exactly the same way as in the rest frame case. In particular, the only little group element that has a non-trivial action is J^{i-} and therefore the one-particle states are still classified by it, showing that the oscillator structures that we identified with $SO(25)$ representations in the rest frame also constitute one-particle states when acting on a vacuum state with non-trivial spatial momentum.

5.3. Amplitudes in the light-cone gauge formalism

After having presented a method to systematically obtain the one-particle states in the bosonic string spectrum and their expression in terms of light-cone gauge oscillators, we move on to our ultimate goal: computing three-point scattering amplitudes between them.

Before the advent of the modern path integral formalism to compute string scattering amplitudes in terms of worldsheet CFT correlators in a covariant way, there existed various non-covariant approaches based on the light-cone gauge construction or similar methods to compute scattering amplitudes. Examples of these are the functional methods pioneered by Sakita and Gervais and developed by Mandelstam [206–208], Kaku and Kikkawa's light-cone string field theory [209,210] and methods based on DDF operators (by Del Giudice, Di Vecchia and Fubini) [211, 212], in which vertex operators for excited physical states are obtained by bombarding a tachyon vertex operators with photons. It is worth mentioning again that DDF method's have recieved renewed interest recently in the context of coherent state scattering and emergent caos in string theory amplitudes, as was mentioned in the introduction to this chapter [185–190, 213].

However, we would like to make use of the oscillator structures that we derived in the last section, and therefore a framework for computing amplitudes directly in terms of them would serve our purposes better. This technology indeed existed, and the method we use to compute scattering amplitudes is based on the one used by Green and Schwars in their

classical papers [214–216]. While these methods are less powerful than the CFT path integral methods to compute higher-point amplitudes or loop corrections, they are very efficient and simple to apply to the case of three-point functions at tree-level.

5.3.1. The tachyon vertex operator

The idea to compute the amplitudes is very simple: We will compute the scattering amplitude between three states by implementing at the level of the oscillators the spacetime picture of a string three-point scattering, in which a string in a given state is prepared in the asymptotic past, it emits or absorbs another string state at time τ and comes out in the asymptotic future.

In String Theory, the emission or absorption of an on-shell state is represented by the insertion of a local *vertex operator* $V(\sigma, \tau)$ for the corresponding state on the string worldsheet. This operator acts on an initial state $|in\rangle$ and maps it into the outgoing state upon emission of the corresponding state at worlsheet time τ and position σ. Therefore, we will compute three-point amplitudes between states a, b and c by creating two of them by the action of light-cone oscillators on the vacuum and representing the third by the corresponding vertex operator. The three-point amplitude is obtained by simply sandwiching the vertex operator between the other two states, namely

$$A(a, b, c) = \langle a | \, V_b(\tau, \sigma) \, | c \rangle \, . \tag{5.83}$$

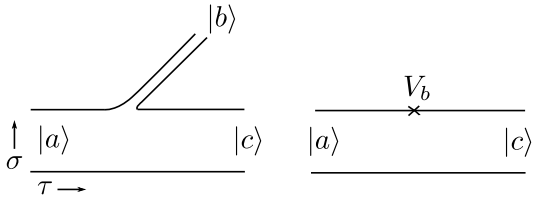


Figure 5.2.: Emission of an open string on-shell state represented by the insertion of a vertex operator.

For open strings, the emission of an on-shell state always happens at the boundary of the worldsheet, which we can take as $\sigma = 0$. Moreover, due to reparametrization invariance, the amplitudes will not depend on τ, and we can simply evaluate the vertex operators at $\tau = 0$. In all computations we will assume that the external states transform in the adjoint representation of a group and we will consider color-ordered amplitudes, with an overall color factor $\mathrm{Tr}(\lambda_a \lambda_b \lambda_c)$ that we always leave implicit. Similarly, all amplitudes will be proportional to the open-string coupling, which we also omit.

While the bra and the ket are readily obtained for any desired state using the formalism presented in the last section, it turns out that light-cone gauge vertex operators are complicated beasts. To see this, lets revert for a moment to covariant quantization, and consider the vertex operator corresponding to the emission of a tachyon in this context:

$$V(p) =: e^{ip \cdot X} :, \quad X^\mu = x^\mu + i\sqrt{2\alpha'} \sum_{n \neq 0} \frac{\alpha_n^\mu}{n}, \tag{5.84}$$

where p^μ is the momentum of the tachyon and we have set $\tau = \sigma = 0$.

If we naively try to evaluate this formula in light-cone gauge formalism, we run into the problem that X^- contains α^- oscillators. As we saw in the previous section, they do not commute with the oscillators corresponding to the transverse directions, and neither with the center of mass variables. This renders the exponential ill-defined even inside the normal ordering symbol, as in each term there is an ordering ambiguity related to the positions of the α^- oscillators.

However, there is a quick fix: if we choose a reference frame in which the p^+ component of the momentum of the tachyon vanishes, then there are no α^- oscillators involved and the vertex operator is in principle well defined. As it turns out, this prescription is correct and gives the correct result when computing amplitudes in these restricted kinematics. If eventually one wishes to compute an amplitude in completely generic kinematics, one can do so by applying the necessary Lorentz transformation $U(k)$ mapping $p^\mu = (0, p^-, p^i)$ to the desired momentum k^μ to the vertex operator:

$$U(k) = e^{i\theta \cdot J} \tag{5.85}$$

where J are the Lorentz generators written in terms of oscillators in the last section and θ is the set of coefficients needed to define the required element of the Lorentz group. Applying this transformation to the well-defined vertex operator we obtain the expression for the tachyon vertex operator with arbitrary momentum k^μ in light-cone gauge:

$$V(k) = U(k)V(p)U^\dagger(k) = U(k) : e^{ip^j X^j} : U^\dagger(k) =: e^{ip^j U(k) X^j U^\dagger(k)} :, \tag{5.86}$$

where we arrived at the last term by repeated insertions of $U(k)U^\dagger(k)$ in the expansion of the exponential. The crucial point is that while in covariant gauges $UX^jU^\dagger = \Lambda^j_k X^k$, where Λ is the usual matrix in the vector representation of the Lorentz group corresponding to the required Lorentz transformation, in light-cone gauge we can check that

$$UX^jU^\dagger \neq \Lambda^j_k X^k. \tag{5.87}$$

This is precisely the meaning of working in a non-covariant gauge, and is the reason why rotating the vertex operator with a Lorentz transformation is not equivalent to simply choosing the desired momentum from the start.

While this procedure is in principle doable, applying the required Lorentz transformation in terms of oscillators is very involved. However, we will see that for our purposes it will always be enough to choose a frame with $p^+ = 0$ for the vertex operator and perform the computations in this setup. The results for the amplitudes can be covariantized *a posteriori* quite straightforwardly.

Let us look at the structure of the tachyon vertex operator in more detail. We can implement the normal ordering by splitting the exponential in three factors, one containing the creation operators, one the zero-modes corresponding to the center of mass variables, and one containing the annihilation operators. This reads

$$V(p) = e^{-\sqrt{2\alpha'}\sum_{n<0}\frac{p\cdot\alpha_n}{n}}\, e^{ip\cdot\hat{x}}\, e^{-\sqrt{2\alpha'}\sum_{n>0}\frac{p\cdot\alpha_n}{n}}, \tag{5.88}$$

and in amplitude computations it will always be placed inside inner products of the form

$$\langle p_b|\, \alpha_{m_1}^{i_1} \dots \alpha_{m_k}^{i_k}\, V(p)\, \alpha_{n_1}^{j_1} \dots \alpha_{n_\ell}^{j_\ell}\, |p_k\rangle\,, \tag{5.89}$$

where p_b^μ is the momentum of the bra, p_k^μ the momentum of the ket, and the oscillators acting on the bra have always Virasoro index $m > 0$ and thus act as creation operators when acting on the left, while the ones acting on the ket have Virasoro index $n < 0$ and act as creation operators when acting on the right.

The simplest recipe to compute any specific scattering amplitude involving a tachyon vertex operator is simply to expand the exponentials carrying the oscillators and term by term perform all the necessary commutations until no oscillators are left. This can always be done with a finite amount of work, as when the exponentials are expanded to orders higher than the number of oscillators in the external states, there will always be uncontracted oscillators remaining which will annihilate the vacum and therefore the process truncates. The term $e^{ip\cdot\hat{x}}$ in the vertex operator corresponding to the center of mass variables ensures momentum conservation, as it commutes with the oscillators and acts as a translation in momentum space, adding momentum p to the vacuum state on the right such that it has a non-zero overlap with the vacuum on the left.

In order to perform explicit computations, it will be useful to compute once and for all the commutator between the tachyon vertex operator and a light-cone oscillator. This way, rather than expanding the exponential we can proceed by simply commuting the oscillators from one side of the vertex operator to the other, where they will either annihilate among themselves and yield a non-zero contribution, or commute through and annihilate the vacuum, yielding a zero contribution.

The commutator reads:

$$[\alpha_m^i, V(p)] = [\alpha_m^i, e^{-\sqrt{2\alpha'}\sum_{n<0}\frac{p\cdot\alpha_n}{n}}]\, e^{ip\cdot\hat{x}}\, e^{-\sqrt{2\alpha'}\sum_{n>0}\frac{p\cdot\alpha_n}{n}}, \tag{5.90}$$

where we assumed $m > 0$ and therefore only has non-trivial commutators with the annihilation operators coming from the exponential on the left. Focusing on the relevant part, we have:

$$[\alpha_m^i, e^{-\sqrt{2\alpha'}\sum_{n<0}\frac{p\cdot\alpha_n}{n}}] = \sum_{k=1}^{\infty}\frac{(-\sqrt{2\alpha'})^k}{k!}\sum_{n_1,\dots n_k<0}\left[\alpha_m^i, \frac{(p\cdot\alpha_{n_1})}{n_1}\dots\frac{(p\cdot\alpha_{n_k})}{n_k}\right]$$
$$= \sum_{k=1}^{\infty}\frac{(-\sqrt{2\alpha'})^k}{k!}\sum_{n_1,\dots n_{k-1}<0}(-k\,p^i)\frac{(p\cdot\alpha_{n_1})}{n_1}\dots\frac{(p\cdot\alpha_{n_{k-1}})}{n_k} = \sqrt{2\alpha'}\,p^i\, e^{-\sqrt{2\alpha'}\sum_{n<0}\frac{p\cdot\alpha_n}{n}},$$

where in the last step we shifted the index k in the sum to recover the exponential. Putting everything together, we arrive at the simple commutation relation between an oscillator and a tachyon vertex:

$$[\alpha_m^i, V(p)] = \sqrt{2\alpha'}\,p^i\,V(p), \tag{5.91}$$

and while we assumed $m > 0$ for the computation, it is easy to check that the same result holds for $m < 0$.

Armed with this technology, we are able to compute any amplitude involving two arbitrary light-cone states and a tachyon. If we wish to consider amplitudes between one-particle

states, we only need to build the necessary state with the combination of $SO(24)$ pieces as we explained in the previous section. Let us see an example in detail.

5.3.2. Covariantizing the amplitudes: The case of the massive spin 2 state at level 4 to two tachyons

As an example, let us compute the scattering amplitude between two tachyons and the massive, spin 2 one-particle state at level 4 that we mentioned in the previous section, where we gave its decomposition into light-cone oscillators in eq. (5.75).

Beyond being a concrete application of the light-cone gauge oscillator methods explained above, it will teach us a very important lesson that will guide us into a recipe to obtain covariant expressions for the amplitudes we compute. The idea is simply to note that at least for particles with polarization tensors of rank smaller than 25, one can always choose a reference frame in which the polarization is aligned along the transverse directions (and the vertex operator still satisfies $p^+ = 0$). In this case, the state will be given in terms of $SO(24)$ structures corresponding to the highest spinning structure of this multiplet *only*, and therefore one can perform the identification

$$\mathcal{E}^{\text{non-cov}}_{i_1\ldots i_n} A^{i_1\ldots i_n}_{\text{non-cov}} \mapsto \mathcal{E}^{\text{cov}}_{\mu_1\ldots\mu_n} A^{\mu_1\ldots\mu_n}_{\text{cov}}, \tag{5.92}$$

between the non-covariant amplitude corresponding to the highest spinning $SO(24)$ structure and the covariant expression for the full one-particle state, where $\mathcal{E}^{\text{non-cov}}$ and $\mathcal{E}^{\text{cov}}$ are the corresponding non-covariant and covariant polarization tensors.

Clearly, if this prescription is correct then the covariant amplitude obtained from the highest spinning structure should know about the other polarizations and predict correctly the rest of the non-covariant amplitudes corresponding to the other $SO(24)$ representations inside the one-particle state when evaluated along the appropriate directions. This example gives a very non-trivial check that this is indeed the case, providing a straightforward way of obtaining covariant results from light-cone computations.

Lets proceed to the computation of the amplitude between two tachyons and the maximally spinning structure of the spin 2 state at level 4. From eq (5.75) we see that the oscillator structures involved are the following:

$$s_1 = \alpha^i_{-3}\alpha^j_{-1} + \alpha^i_{-1}\alpha^j_{-3}, \tag{5.93}$$

$$s_2 = \alpha^i_{-2}\alpha^j_{-2}, \tag{5.94}$$

$$s_3 = \alpha_{-1}\cdot\alpha_{-1}\,\alpha^i_{-1}\alpha^j_{-1}. \tag{5.95}$$

The highest spinning structure of the representation is obtained by acting on the vacuum with these structures with the following weights:

$$\begin{array}{|c|c|}\hline & \\ \hline \end{array}_{24} = \left(-4s_1 + 7s_2 + s_3\right)|0;k\rangle\,. \tag{5.96}$$

To compute amplitudes involving this state we must first normalize it correctly. The square of the norm of a generic state created by a string of light-cone oscillators acting on

the vacuum is easily seen to be

$$\langle 0|\,(\alpha_1)^{n_1}(\alpha_2)^{n_2}\dots(\alpha_{-1})^{n_1}(\alpha_{-2})^{n_2}\,|0\rangle = \prod_k k^{n_k}, \tag{5.97}$$

where k runs over the Virasoro indices of the oscillators creating the state, and n_k is the number of oscillators of Virasoro index $-k$ in the state.

Carefully dealing with the trace in the case of s_3, we can use this to compute the norms of each individual structure. They are given by

$$||s_1||^2 = 6, \qquad ||s_2||^2 = 4, \qquad ||s_3||^2 = 56. \tag{5.98}$$

To obtain the non-covariant amplitude for the highest spinning structures we simply compute the non-covariant amplitudes between two tachyons and s_1, s_2 and s_3 individually, and then combine them with the required weights and normalization.

Let's start by s_1, assuming it corresponds to the bra with momentum p_b. The momentum of the tachyon vertex is p, and the momentum of the ket is p_k, such that $p_b = p + p_k$. Since the momentum conservation is ensured by the center of mass degrees of freedom in the tachyon vertex operator, we will simply omit the momentum references on the vacuum states.

We must compute:

$$\langle 0|\,(\alpha^i_{-3}\alpha^j_{-1} + \alpha^i_{-1}\alpha^j_{-3})V(p)\,|0\rangle\,. \tag{5.99}$$

Simply applying the commutation relation between the vertex operator and the oscillators (5.91) twice we find that each term yields $2\alpha' p^i p^j$, and therefore we obtain

$$\langle 0|\,s_1\,V(p)\,|0\rangle = 4\alpha' p^i p^j. \tag{5.100}$$

Doing the same type of simple computations we can see that the other structures give

$$\langle 0|\,s_2\,V(p)\,|0\rangle = 2\alpha' p^i p^j, \quad \langle 0|\,s_3\,V(p)\,|0\rangle = 4\alpha' p^i p^j, \tag{5.101}$$

and therefore the non-covariant amplitude for the highest spinning state is

$$A^{\text{non-cov}} = \frac{1}{\sqrt{4^2||s_1||^2 + 7^2||s_2||^2 + ||s_3||^2}}\,\langle 0|(-4s_1 + 7s_2 + s_3)V(p)|0\rangle = \tag{5.102}$$

$$= \frac{2\alpha'}{\sqrt{348}} p^i p^j(-4\times 2 + 7\times 1 + 1\times 2) = \frac{2\alpha'}{\sqrt{348}} p^i p^j. \tag{5.103}$$

Now, as explained above we will try to build a covariant amplitude that reduces to the value we have just computed when choosing a purely transverese polarization tensor. From the above result, it is clear that the only possible form of the covariant amplitude is

$$A^{\text{cov}} = \frac{\epsilon_{\mu\nu}}{\sqrt{2}} p^\mu p^\nu \kappa \tag{5.104}$$

where κ is a constant to be determined, the polarization tensor is normalized as $\epsilon_{\mu\nu}\epsilon^{\mu\nu} = 1$, and the factor of $1/\sqrt{2}$ was chosen for future convenience.

When exciting the directions i, j, $\epsilon_{\mu\nu}$ is normalized $\epsilon_{\mu\nu}\epsilon^{\mu\nu} = 1$ if it is

$$\epsilon_{\mu\nu} = \frac{1}{\sqrt{2}} \begin{pmatrix} 0 & 1 \\ 1 & 0 \end{pmatrix}. \tag{5.105}$$

Thus the covariant amplitude, when exciting the i, j directions, is

$$A^{\rm cov} = p^i p^j \kappa \tag{5.106}$$

and, comparing with the non-covariant amplitude from earlier, we get $\kappa = \frac{2\alpha'}{\sqrt{348}}$, and we claim that the covariant amplitude between the spin 2 state at level 4 and two tachyons is

$$A^{\rm cov} = \frac{1}{\sqrt{2}} \frac{2\alpha'}{\sqrt{348}} \epsilon_{\mu\nu} p^\mu p^\nu. \tag{5.107}$$

To test this claim, we must check if we are able to predict the amplitudes for other polarization configurations with this formula. To do this we go back to the rest frame, where the polarization tensors are simple to identify.

If we excite the directions i, ℓ where ℓ is the light-cone spatial direction, the prediction from our candidate covariant amplitude is

$$A^{i\ell}_{\rm cov} = \frac{2\alpha'}{\sqrt{348}} p^i p^\ell = \frac{2\alpha'}{\sqrt{348}} p^i \left(-\frac{1}{\sqrt{2}} p^- \right) = -\sqrt{\frac{3}{2}} \frac{\sqrt{2\alpha'}}{\sqrt{348}} p^i = -\frac{\sqrt{2\alpha'} p^i}{2\sqrt{58}} \tag{5.108}$$

where we used $p^\ell = (p^+ - p^-)/\sqrt{2}$ and $p^+ = 0$ for the tachyon vertex, and $p^- = \sqrt{3}/\sqrt{2\alpha'}$ from the mass-shell conditions.

Now we check with a direct computation using light-cone oscillators. In the rest frame for the massive spin 2, the $SO(24)$ structures furnishing the transverse-lightcone polarization can be read from eq (5.75) to be

$$\tilde{s}_1 = \alpha^i_{-4}, \quad \tilde{s}_2 = (\alpha_{-1} \cdot \alpha_{-2}) \alpha^i_{-1}, \quad \tilde{s}_3 = (\alpha_{-1} \cdot \alpha_{-1}) \alpha^i_{-2}, \tag{5.109}$$

corresponding to the $SO(24)$ vector representation inside this $SO(25)$ multiplet when combined with the following weights:

$$\square_{24} = (4\tilde{s}_1 + 4\tilde{s}_2 - 9\tilde{s}_3) \, |0; k\rangle \, . \tag{5.110}$$

Their norms are

$$||\tilde{s}_1||^2 = 4, \quad ||\tilde{s}_2||^2 = 50, \quad ||\tilde{s}_3||^2 = 96. \tag{5.111}$$

Note the crucial non-zero overlap between the second and third structures

$$\langle (\alpha_1 \cdot \alpha_2) \alpha^i_1 | (\alpha_{-1} \cdot \alpha_{-1}) \alpha^i_{-2} \rangle = 4 \quad \text{NO sum over } i. \tag{5.112}$$

The amplitudes $\langle 0 | \tilde{s}_i V(p) | 0 \rangle$ can be readily computed with the above techinques, yielding

$$\langle 0 | \tilde{s}_1 V(p) | 0 \rangle = \sqrt{2\alpha'} p^i, \quad \langle 0 | \tilde{s}_2 V(p) | 0 \rangle = 2\sqrt{2\alpha'} p^i, \quad \langle 0 | \tilde{s}_3 V(p) | 0 \rangle = 2\sqrt{2\alpha'} p^i. \tag{5.113}$$

Finally, we combine the $\tilde{s}_i$ with the appropriate weights to obtain the non-covariant amplitude:

$$A^{i\ell}_{\text{non-cov}} = \frac{1}{\sqrt{4^2||\tilde{s}_1||^2 + 4^2||\tilde{s}_2||^2 + 9^2||\tilde{s}_3||^2 + 2(4)(-9)4}} \langle 0|(4\tilde{s}_1 + 4\tilde{s}_2 - 9\tilde{s}_3)V(p)|0\rangle = \tag{5.114}$$

$$= \frac{\sqrt{2\alpha'}}{\sqrt{8352}} p^i (4 \times 1 + 4 \times 2 - 9 \times 2) = -\frac{6\sqrt{2\alpha'}}{\sqrt{8352}} p^i = -\frac{\sqrt{2\alpha'}p^i}{2\sqrt{58}} \tag{5.115}$$

where the norm of the state accounts for the cross product between $4s_2$ and $-9s_3$.

We see that the computation lands on its feet, and the result matches the one we predicted by directly covariantizing the non-covariant amplitude involving the highest spinning $SO(24)$ structure. Proceeding in exactly the same way it can be seen that the polarization ℓ, ℓ predicted by the covariant amplitude matches the non-covariant amplitude for the remaining piece of the $SO(25)$ multiplet, the $SO(24)$ scalar shown in eq. (5.75). This is an extremely non-trivial check for the consistency of the framework in general and of the prescription for covariantizing in particular.

We claim that this recipe can be applied in general, and that to compute the covariant amplitude for a given $SO(25)$ one-particle state, it suffices to compute the non-covariant amplitude between the relevant highest spinning $SO(24)$ structures and then map the non-covariant tensors to covariant ones in the same way as discussed above. In more complicated reference frames, it might be that the mapping between the different subleading $SO(24)$ structures and the polarizations is less trivial, with coefficients in principle depending on the momentum of the states, but the prescription for the full covariant amplitude computed this way is correct nonetheless.

This not only gives a way to obtain covariant results, but is also a great simplification of the framework in general. For computing amplitudes we only need to consider the highest spinning structures, and the obtained object knows about all the remaining components of the $SO(25)$ multiplet. All these extra pieces may be computed as a cross-check for the result, but do not carry new information. This in turn means that when we scan the spectrum of states applying the procedure explained in the previous section, it is indeed only the highest spinning structures annihilated by J^{i-} that we care about. Happily, these are the ones we can obtain with the least amount of work, and they capture all the information we need.

Finally, let us comment on the fate of this covariantization recipe when the rank of the involved tensors is larger than 24, and therefore we cannot choose a frame in which all the non-trivial polarizations are along the transverse directions. One might fear that in this scenario the recipe we provided to compute the amplitude simply in terms of the highest-spinning structure would break down. While we do not have yet a full understanding of what happens in generic cases and this issue definitely falls inside the *work in progress* part of the project, we have checked in some examples that it is possible to formally work in arbitrary dimensions to compute the amplitude assuming that the highest-spinning structure prescription holds. One obtains then a result in terms of the different momenta involved pointing along the $d-2$ "transverse" directions, that can be covariantized by contracting it with an appropriate tensor and lifting the contractions between transverse indices to contractions including all $SO(d)$ indices. Then, evaluating the amplitude including the polarization tensor in 26 dimensions, one obtains the correct result. While this is somewhat mysterious, as in arbitrary dimensions the Lorentz symmetry becomes anomalous in the light-cone gauge construction, it provides the correct expressions for amplitudes such as the one between a leading Regge trajectory

state and two tachyons, and two leading Regge states and a tachyon, that we present in the next section. Understanding this point further is definitely an important step to move forward with this framework.

5.3.3. Covariant tachyon-leading Regge trajectory amplitudes

In this section we provide some more results for three-point amplitudes as another example of the application of the method presented previously. In particular, we focus on amplitudes involving leading trajectory states, namely fully symmetric, rank N tensors, i.e. spin N particles at level N.

Lets consider first the case of two tachyons and one leading trajectory state. In this case, the highest spinning $SO(24)$ structure is given by only one term, namely a string of N α_{-1} oscillators with free indices:

$$\underbrace{\square\square\ldots\square_{24}}_{N} = \alpha_{-1}^{i_1}\ldots\alpha_{-1}^{i_N}|0\rangle\,. \tag{5.116}$$

Performing the necessary commutations, it is easy to compute the non-covariant amplitude between this state and two tachyons:

$$\langle 0|\alpha_1^{i_1}\ldots\alpha_1^{i_N}V(p)|0\rangle = (2\alpha')^{\frac{N}{2}}p^{i_1}\ldots p^{i_N}. \tag{5.117}$$

The covariant amplitude can be easily obtained by requiring that it yields the above result in the case of a polarization tensor with only transverse components. Requiring that the covariant polarization tensor is normalized as $\epsilon_{\mu_1\ldots\mu_N}\epsilon^{\mu_1\ldots\mu_N}=1$, we find that the covariant amplitude between a state in the leading Regge trajectory and two tachyons is

$$\mathcal{A}_{cov}^{LR-T-T} = \frac{(2\alpha')^{N/2}}{\sqrt{N!}}p^{\mu_1}\ldots p^{\mu_N}\epsilon^{cov}_{\mu_1\ldots\mu_N}, \tag{5.118}$$

which matches the result already known in the literature, see for instance [179, 217]. Note that while quite sofisticated methods are needed to compute these amplitude with covariant methods, in the light-cone gauge formalism it can be done in two lines by performing simple Wick contractions!

The same kind of computation can be performed in the case of two leading trajectory states and a tachyon. For two leading Regge states of spins a and b, momenta p_a^μ and p_b^ν and polarizations $\epsilon^a_{\mu_1\mu_2\ldots\mu_a}$ and $\epsilon^b_{\nu_1\nu_2\ldots\nu_b}$, the covariant amplitude reads

$$\mathcal{A}_{cov}^{LR-LR-T} = \sum_{k=0}^{\min(a,b)}\frac{(2\alpha')^{\frac{a+b}{2}-k}\sqrt{a!b!}}{(a-k)!(b-k)!k!}\epsilon^a_{\mu_1\mu_2\ldots\mu_a}\epsilon^b_{\nu_1\nu_2\ldots\nu_b}\delta^{\mu_1,\nu_1}\ldots\delta^{\mu_k,\nu_k}p_b^{\mu_{k+1}}\ldots p_b^{\mu_a}p_a^{\nu_{k+1}}\ldots p_a^{\nu_b}, \tag{5.119}$$

where the sum occurs because now the polarization tensors can contract either with the momenta or among themselves, and where this expression also matches the known result for the amplitude.

Let us comment that as mentioned in the last section, in these examples there is no limitation for the validity of these expressions to the case in which the number of indices is smaller than 24 and one can embed the full polarization tensors in the transverse directions. While not a proof, this is encouraging evidence that this framework can be pushed further to arbitrarily spinning states.

5.3.4. Excited vertex operators

Up to now we have only presented amplitudes in which the vertex operator corresponded to an emitted tachyon. In this section we remediate this omission and address the issue of defining excited vertex operators in the light-cone gauge formalism. As we did for the tachyon vertex operator, the strategy will be to try to adapt the covariant expression for the excited vertex operator to the light-cone gauge, and deal with the problems caused by the behavior of the α^- oscillators.

In the covariant formulation of string theory, we associate a vertex operator to a state created by a particular string of oscillators acting on the vacuum in the following way:

$$\alpha^{\mu_1}_{-n_1} \dots \alpha^{\mu_k}_{-n_k} |0;p\rangle \leftrightarrow : \partial^{n_1} X^{\mu_1} \dots \partial^{n_k} X^{\mu_k} e^{ip\cdot X} :, \tag{5.120}$$

where we map a given oscillator α^μ_n, $n > 0$ to $\partial^n X^\mu$, where the derivatives are taken with respect to the worldsheet variables. For simplicity, let us focus on the case of the gluon, namely the massless vector at level 1. For the massless vector with polarization vector ζ^μ and momentum k^μ, the covariant vertex operator reads

$$V^{\text{cov}}(\zeta,k,\tau) =: \zeta \cdot P(\tau) e^{ik\cdot X(\tau)} :, \quad P^\mu(\tau) = \frac{\partial}{\partial\tau} X^\mu(\tau), \tag{5.121}$$

where $X^\mu(\tau)$ means $X^\mu(\tau, \sigma = 0)$.

If we naively try to evaluate this formula in light-cone gauge formalism, we run into the same problem as in the case of the tachyon: X^- does not commute with the other components and thus the exponential is not well defined, and now we have the extra issue that α^- oscillators can also come from the factor P^μ dressing the exponential.

As we did for the tachyon vertex operator, we will deal with this issue by restricting to kinematics that do not excite the problematic $(-)$ components and choose $k^+ = 0$ as before to get rid of the X^- in the exponential, and likewise $\zeta^+(k) = 0$ to avoid the presence of P^-. In fact, things simplify further if we also demand k and ζ to point along the $SO(24)$ transverse directions exclusively. In this case we have a well defined expression for the massless vector vertex operator in terms of oscillators that reads

$$V(\zeta,k,\tau) = \zeta^i \ : P^i(\tau) e^{ik^j X^j(\tau)} :, \quad P^i(\tau) = \sqrt{2\alpha'} \sum_{n=-\infty}^{\infty} \alpha^i_n \, e^{-in\tau}, \tag{5.122}$$

where we wrote $P^i(\tau)$ in terms of oscillators by simply derivating eq. (5.19), and where the normal ordering effectively splits the operator in two terms. Setting τ to zero as before, this reads

$$V(\zeta,k) = \zeta^i \ : P^i(0) e^{ik^j X^j(0)} := g\sqrt{2\alpha'}\zeta^i \left(\sum_{m<0} \alpha^i_m V_{tac}(k) + V_{tac}(k) \sum_{m\geq 0} \alpha^i_m \right), \tag{5.123}$$

where $V(\zeta, k) = V(\zeta, k, \tau = 0)$, and $V_{tac}(k)$ is the normal-ordered exponential that yields the tachyon vertex operator in eq (5.88), albeit with $k^2 = 0$ rather than $-1/\alpha'$ as in the tachyon case.

This prescription allows to compute three-point amplitudes between two arbitrary states and a gluon using exactly the same techniques as in the previous cases. As for the tachyon vertex operator, it is useful to compute the commutator between an oscillator and the gluon vertex operator. Using the derived result for the commutator between an oscillator and $V_{tac}(k)$ and carefully handling the normal ordering one obtains

$$[\alpha_m^i, V^j(k)] = \sqrt{2\alpha'}\left(k^i V^j(k) + m\delta^{ij} V_{tac}(k)\right), \tag{5.124}$$

where $V^j(k)$ denotes the j^{th} component of the gluon vertex operator, stripped its polarization vector.

Using this commutation relation it is a simple exercise to compute the three-point amplitude between three gluons of momenta k_1, k_2 and k_3. The relevant non-covariant amplitude is

$$\langle 0; k_1 |\, \alpha_1^i\, V^j(k_2)\, \alpha_{-1}^k \,|0; k_3\rangle\,, \tag{5.125}$$

which upon performing the necessary commutations is readily seen to give

$$2\alpha'\left(\delta^{ik}k_3^j + \delta^{jk}k_2^i - \delta^{ij}k_2^k\right) - (2\alpha')^2 k_2^i k_3^j k_2^k. \tag{5.126}$$

Dotting back the polarization vectors for each gluon and using the fact that each polarization vector is transverse to its corresponding momentum and momentum conservation, we obtain an expression in terms of contractions between the momenta and polarization vectors that can be uniquely extended to a covariant expression by mapping the dot products $a^i b^i \mapsto a_\mu b^\mu$. Denoting $|\zeta_i\rangle = \zeta_i^j\, \alpha_{-1}^j\, |0\rangle$, the covariant three-point amplitude between gluons reads

$$\langle \zeta_1, k_1 | V(\zeta_2, k_2) | \zeta_3, k_3 \rangle = 2\alpha'\,(\zeta_1\cdot\zeta_2\,\zeta_3\cdot k_1 + \zeta_1\cdot\zeta_3\,\zeta_2\cdot k_3 + \zeta_2\cdot\zeta_3\,\zeta_1\cdot k_2) \tag{5.127}$$

$$+ (2\alpha')^2(\zeta_1\cdot k_2\,\zeta_2\cdot k_3\,\zeta_3\cdot k_1), \tag{5.128}$$

which perfectly reproduces the known result that the three-gluon amplitude in tree-level string theory corresponds to the Yang-Mills three-gluon amplitude plus a stringy correction at higher orders in α'.

This procedure can be generalized to vertex operators associated to states created by many oscillators. Each oscillator will add an extra sum $\sum_n \alpha_n$ dressing the exponential, and one simply needs to compute the non-covariant amplitudes in kinematical regimes such that the α^- modes are not excited, and then covariantize. We have checked this in some computations considering level 2 and level 3 states and computing scattering amplitudes among them using alternatively an excited vertex operator or a bra/ket to represent a given state, obtaining consistent results.

The limitation of this approach is when it comes to dealing with states involving traces of oscillators, such as the massive spin 2 state we considered as an example previously. Terms such as $\alpha_{-1}\cdot\alpha_{-1}$ would imply contributions to the excited vertex operator corresponding to this state of the form $\partial X\cdot\partial X$, which unavoidably bring contributions from the α^- modes

that can't be removed by choosing specific kinematics. While it is possible that a prescription to deal with this class of states can be found, at the moment this is a limitation of the framework. We can consider arbitrarily complicated states for the bra and the ket, but the vertex operator is constrained to states without index contractions between their oscillators.

5.4. Discussion and future directions

In this chapter we have presented techniques based on the light-cone gauge formalism to systematically obtain the one-particle states and their realization in terms of light-cone oscillators at any given level in an efficient way, as well as to compute three-point amplitudes among them. While these results are part of an on going project and therefore there are still various things to be done to fully exploit their potential, the framework has already given some fruits worth showing.

An immediate advantage of these methods is their simplicity and algorithmic nature, which makes them easily automatizable. The operations required both to obtain the one-particle states and to compute three-point amplitudes in light-cone gauge are easily implemented using any symbolic programming language, and in the course of this project we have implemented codes in MATHEMATICA and Python that automatize both procedures. As was mentioned, this allows us to obtain the $SO(25)$ irreducible representations making up the open bosonic string spectrum up to high levels very efficiently, reproducing the state of the art level by level state classification in just a few seconds of running time.

Similarly, with respect to the amplitude computations we have implemented a code that automatically performs the required commutations and inner products to compute three-point amplitudes for arbitrary bra/ket and tachyonic and gluonic vertex operators. This allows to compute very efficiently amplitudes between a gluon or tachyon and any desired pair of states for the first few levels[12], making the data of literally hundreds of excited state three-point amplitudes easily available, possibly giving access to statistical information about the spectrum and its couplings.

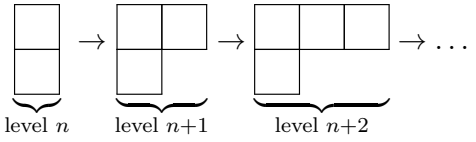
While in this chapter we have focused on open strings, everything we have done can be extended to the case of closed strings. This only implies an increase of complexity due to the larger number of oscillators in the states at a given level, but does not pose neither conceptual nor significant practical complications, and the framework could be generalized to compute three-point amplitudes in the closed string sector. This would be particularly relevant for the study of black hole physics, since as was mentioned in the introduction there exists a connection between the Kerr black hole and the classical limit of a specific set of three-point amplitudes between a graviton and two massive higher spin states. This avenue is certainly interesting, and we plan to apply this framework to study this specific problem. Let us mention in any case that it would even be possible to attack this problem with the present tools by considering the scattering amplitudes between a massless vector and two massive higher spin states and then access the gravitational analog amplitudes via the double copy, as done for instance in [199].

A very interesting future direction for this approach in which we are currently working on is on the determination of closed formulas for the highest-spinning $SO(24)$ structures

[12] We have currently pushed it to compute amplitudes including states up to level 10, but there is room for improvement and we expect to be able to do better.

at arbitrary level. As was explained, these are the relevant components of the full $SO(25)$ irreducible representations at the time of classifying the spectrum and computing three-point amplitudes, and having analytical control over them for arbitrary levels would open the door to many possibilities, starting with closed formulas for amplitudes between any state of a full trajectory, generalizing the ones for one leading trajectory state and two tachyons and two leading trajectory states and one tachyon shown in eqs. (5.118) and (5.119).

While this idea is still in development and for this reason was not included in the body of this chapter, let us sketch it to give a sense of how one could profit from this formalism beyond brute force computations. In terms of the Young tableaux representing the one-particle states there is a sense of "Regge trajectories" given by states belonging to contiguous levels corresponding to Young tableaux that differ by one box in the first row. In this way, we can say that the state at the bottom of the trajectory generates the higher states on the same trajectory by addition of a box in the first row of the Young tableau as one goes up one level, with the scalar tachyon generating the leading trajectory for example. For instance, we could consider a trajectory generated by an antisymmetric rank 2 state at the bottom:



In terms of oscillators, the operation of adding a box in the top row to a diagram when going up one level corresponds to adding an α^i_{-1} oscillator and symmetrizing i with the Lorentz indices corresponding to the top row of the original Young tableau. For a given state in the desired trajectory, we can find the highest-spinning $SO(24)$ structure associated to it by considering a linear combination of all the $SO(24)$ structures corresponding to the same Young tableau as the desired state at this level, and demand that the linear combination is annihilated by the action of J^{i-}, as was explained in the text. Since in general the action of J^{i-} on a set of $SO(24)$ structures will give another set of $SO(24)$ structures at the same level, the action of J^{i-} can be written in matrix form upon choosing a basis for these structures, and the determination of the highest-spinning combinations that directly map to one-particle states corresponds to finding the kernel of this matrix.

Now, the crucial observation is that when comparing the coefficients of the matrix associated to states on the same trajectory at different levels, we see that in all cases they scale linearly with the level. While we have not a general proof of this fact for the moment, we have substantial evidence that this is always the case. Therefore, this allows to compute the matrix associated to the action of J^{i-} for a *full trajectory* by simply determining the matrix at two levels and performing a linear fit of the coefficients. Once this is done, we can find the kernel of the matrix as a function of the level and this way obtain the coefficients of the highest-spinning structures corresponding to the full trajectory. This would allow to obtain closed form expressions for the three-point amplitudes between the elements of full Regge trajectories, giving access to a wealth of information. While this approach is still under test, we have managed to obtain encouraging preliminary results using this technique that make us confident about its validity, and we hope to implement it consistently soon.

Finally, there are various open questions regarding the computation of the three point amplitudes that require addressing. On the first place, it would be important to understand rigurously the regime of validity of the method we use to covariantize the results obtained in

light-cone gauge in the case of tensors of rank larger than the number of transverse directions. Moreover, to be able to apply the light-cone gauge techniques to arbitrary states it would be necessary to develop a consistent way of defining excited vertex operators for states containing traces of oscillators, which are currently out of reach for this framework.

Conclusions

The overarching theme unifying the research presented in this thesis is the study of Dual Models, a class of consistent theories of weakly interacting higher spin states of which tree-level String Theory is the prime example, from a modern bootstrap point of view. In the first and largest part of this thesis we have presented new results concerning their general structure and consistency requirements, which we obtained by adapting tools and ideas developed in the context of the modern S-matrix bootstrap and Regge theory to the case of dual model amplitudes. Moreover, we analyzed specific models as concrete realizations of these conditions, and introduced a numerical framework to genereate consistent dual model amplitudes with customizable features. In the last part of this thesis we have concentrated on *the* Dual Model for excellence, tree-level String Theory, and presented novel tools that allow to better understand its particle content and interactions. In summary, this work has increased our knowledge on the allowed space of weakly interacting higher spin theories, as well as provided new insights into the structure of String Theory as arguably their most relevant realization.

In chapter 2 we presented the first characterization of the Coon amplitude, a dual model whose properties were poorly known. We found the parameter range in which it is free of ghosts, obtained its low energy Wilson coefficients and located them in the space of coefficients allowed by the bootstrap axioms, and provided an interpretation for its defining parameter q in terms of the size of a putative Coon parton. Moreover, we provided an extension of the original method to construct the amplitude, finding that the Coon and Veneziano amplitudes still yield the only consistent solutions achievable with this approach.

In chapter 3 we adapted tools from Regge theory to the analysis of dual model amplitudes, and applied these techniques to prove that dual model amplitudes require infinitely many trajectories to have a well defined partial wave expansion and be consistent with crossing.

In chapter 4 we use the aformentioned tools from Regge theory to construct a primal numerical bootstrap framework that allows to obtain consistent dual model amplitudes with customizable Regge trajectories. As an application of this method we built amplitudes with bending Regge trajectories, an expected feature of QCD amplitudes whose implementation in dual models had remained elusive.

Finally, in chapter 5 we used the light-cone quantization formalism to develop a novel approach to systematically obtain the one-particle content of the open bosonic string at each given level in terms of light-cone gauge oscillators, and presented an efficient way to compute three-point amplitudes between these states.

A central motivation when starting the work that gave birth to this thesis was to understand how restrictive the constraints of analyticity, unitarity, crossing symmetry and channel duality are when imposed on weakly interacting theories of higher spins at the level of the $2 \to 2$ amplitudes. A clear answer emerging from this thesis is that, while these conditions definitely impose restrictions on the structure of the amplitudes and the theories in which they are embedded, with the necessity for infinitely many Regge trajectories as a powerful

example, they are not constraining enough to isolate physical theories only. Often we find amplitudes that cannot be uplifted to a full theory, even when passing all the constraints to be consistent at the $2 \to 2$ level.

Already in the first results presented in this work we found evidence of this. When discussing the Coon amplitude we found that at, least when restricted to energies below its accumulation point, it yields a dual model amplitude consistent with all the required constraint. However, the evidence against the possibility of Coon being realized in a consistent theory has accumulated since then, and it seems that the main obstruction comes from the impossibility of extending it to higher points [48, 49, 51].

Our numerical framework allowing to obtain consistent amplitudes with customizable trajectories also points along this direction, as the fact that we are able to obtain consistent amplitudes for somewhat arbitrary choices of the Regge trajectory functions -albeit not violating any known requirement, such as their asymptotic linearity- is a strong hint that the resulting objects, while consistent at the level of $2 \to 2$ scattering, should not correspond to amplitudes of a fully consistent theory. Physical theories, one expects, should be harder to find than this. These observations also go in line with the recent proliferation of new dual model amplitudes in the literature which are consistent at the $2 \to 2$ level but fail to satisfy the required higher-point factorization properties [54, 166].

The fact that dual model amplitudes arising from physical theories exhibit more structure than the minimal one required to satisfy the bootstrap axioms resonates also with our observations about the open bosonic string spectrum. As was mentioned in the discussion of chapter 5, while our explorations are still preliminary we observe patterns among the oscillator combinations defining the one-particle states that are a hint of a deep structure going beyond the simple requirements of tree-level unitarity, crossing and channel-duality. This is no surprise, as string theory is full of amazing features and underlying structures, and being one of the very few fully consistent theories of weakly interacting higher spin particles that we know, it is not possible to rule out that these features could simply be a particularity of this specific realization of a consistent higher spin theory. However, it seems sensible to believe that this is a general feature of consistent theories that the restriction to $2 \to 2$ amplitudes only does not allow to capture.

The inability of $2 \to 2$ constraints to fully identify physical theories does not, however, diminish the utility of a better understanding of dual model amplitudes. Focusing on the results of this thesis, the no-go theorem ruling out the existence of dual model amplitudes with finitely many trajectories provides information on the minimal requirements for weakly coupled amplitudes involving higher spins, showing that consistent, weakly coupled higher spin theories must have a spectrum consisting of infinitely many Regge trajectories as is famously the case for String Theory, except in the degenerate case in which all states lie the same mass. This information is timely, as single-trajectory-like amplitudes have been found recently as extremal solutions to the bootstrap constraints, whose nature and properties are still to be understood [61, 65]. Being able to rule out the absence of subleading trajectories is a useful tool for interpreting these results and assess their viability as physical objects. With this aim it would be very valuable to extend this result and put a bound on the relative size of subleading trajectories with respect to the leading one, which is not provided by the present form of our proof. This constitutes a clear future direction for this research line. More generically, various recent non-perturbative bootstrap works have seen Regge trajectories emerge as solutions living at the boundary of the allowed space of amplitudes [84, 90, 96, 97, 118, 167], and it would

be important to extend our analysis beyond meromorphic amplitudes to be able to apply it to this scenario.

Relatedly, our Regge theory-based numerical approach to build customizable dual model amplitudes can help answer the question of whether a concrete feature is admisible by consistent dual model amplitudes or not. In this thesis we used this method to explicitly construct consistent amplitudes with non-linear, bending Regge trajectories, proving -within the limits of numerical approaches- that this feature is accessible to dual model amplitudes, despite the fact that only models achieving effective bending trajectories by the superposition of many amplitudes with linear trajectories were known in the literature until our work [40, 162]. Immediate avenues of improvement for this framework are going beyond finite precision numerics to be able to capture the contibution from higher trajectories, as well as having a more flexible ansatz for the Regge residues to be able to scan over a larger class of models. Connecting to the highly constraining restrictions coming from higher point factorization that we alluded to in the previous paragraphs, a more long term goal would be to extend this framework to include higher-point amplitudes and their factorization constraints. It would also be very interesting to implement our Regge-based method in sinergy with other bootstrap approaches, along the lines described in the discussion of chapter 4.

Focalizing on String Theory as the ultimate dual model, the methods we have presented in chapter 5 open the door to the efficient exploration of the string particle spectrum and their interactions. While still a work in progress, the light-cone framework introduced in the last chapter of this thesis allows to classify all one-particle states level by level in a very methodic way that can be easily automatized, as well as to compute the three-point amplitudes between these states written in terms of light-cone gauge oscillators. While the methods used are non-covariant, we gave a prescription to covariantize the resulting amplitudes that actually makes computations less costly, bypassing the need to deal with most of the oscillator structures inside a given one-particle state. Remarkably, we observe that within this framework there exist patterns between the oscillator composition of infinite families of states that could allow to bootstrap the three-point amplitudes between full generic Regge trajectories. While this is still speculative and constitutes a line of ongoing research, achieving this goal could have interesting applications to study the emergence of black holes from string theory along the lines of [198, 199], as well as providing valuable information on the structure of String Theory itself.

In conclusion, this thesis has provided numerous qualitative and quantitative data on Dual Models that will help guide future S-matrix bootstrap studies interested in weakly coupled higher spin theories, such as large N QCD and String Theory. We have set up the framework to study them from different angles, with an emphasis on techniques coming from Regge theory as well as non-covariant approaches. These results, combined with other bootstrap methods, will surely collaborate in shining new light on the structure of physical theories in future research.

Appendix A.

Finite Energy Sum Rules (FESRs)

In this appendix, we briefly explain the notion of Finite energy sum rules (FESRs). FESRs are a consequence of the analyticity of the scattering amplitude in the Mandelstam variables. The idea is as follows: Consider the amplitude as a function of s for fixed t and the following contour integral in the complex s-plane:

$$\mathcal{I}_k(t,R) = \int_{\mathcal{C}} \frac{\mathrm{d}s'}{2\pi i} s'^k A(s',t), \tag{A.1}$$

where $\mathcal{C}$ is a circle of radius R.

This contour integral can be shrunk to the poles inside the circle. If the largest mass in the spectrum such that $m_n^2 < R$ is $m_{N_{\max}}^2$, we have

$$\mathcal{I}_k(t,R) = \sum_{n=0}^{N_{\max}} (m_n^2)^k P_n(t), \tag{A.2}$$

where $P_n(t)$ is the residue of the amplitude at $s = m_n^2$.

On the other hand, if R is sufficiently large we might be able to approximate $\mathcal{I}_k(t,R)$ by the integral of the Regge limit of the amplitude along this contour. If we consider only one trajectory we have in this limit

$$A(s,t) \sim \frac{f(t)e^{-i\pi\alpha(t)}}{\Gamma(\alpha(t)+1)\sin(\pi\alpha(t))} s^{\alpha(t)}, \tag{A.3}$$

where $f(t)$ is a residue function solely depending on t (an important fact exploited in some of the past works on single-trajectory dual amplitudes). The integral along the contour $\mathcal{C}$ can be performed explicitly to yield

$$\mathcal{I}_k(t,R) = \frac{f(t)R^{\alpha(t)+k+1}}{\pi\Gamma(\alpha(t)+1)(\alpha(t)+1+k)}, \tag{A.4}$$

assuming that $R \gg t$, such that corrections to (A.4) can be neglected.

Two main difficulties emerge in this context. The first one, which is not addressed in any piece of the literature, is the question of the speed of reggeization at arguments of complex s along the integration contour $\mathcal{C}$ in (A.1). While it is conceivable that this speed does not depend on the angle, this is an unproven assumption, and our method prevents having to assume anything of the sort. Another difficulty is that the integration contour varies discontinuously as it jumps from one pole to the next and picks up a new residue when we

increase the radius R. However, the approximation in terms of the reggeized amplitude from eq. (A.4) is a continuous function of R. This incompatibility led previous works to employ smoothing procedures that are plausible but to our understanding not rigorous even though they were fundamental for the previous attempts to study the reggeization of single-trajectory dual amplitudes.

Appendix B.

Regge residues of the Veneziano amplitude

In this appendix we give the Regge residues of the Veneziano amplitude up to the 10^{th} Regge pole. We set $m_0^2 = 0$, but we keep the spacetime dimension d general. In arbitrary dimension, the function multiplying all the Regge residues is

$$B^{(d)}(s) = \frac{\pi^{\frac{1}{2}-\frac{d}{2}} s^s 2^{-2d-2s+3}}{\Gamma\left(\frac{d-1}{2}+s\right)}. \tag{B.1}$$

On top of the $B^{(d)}(s)$, we factorize from the i^{th} Regge residue $\beta_i(s)$ corresponding to the pole $\alpha_i(s) = s - i$ the factor $f_i(s) = (-3+d+2s)(-5+d+2s)\dots(-2\lfloor\frac{i+1}{2}\rfloor - 1 + d + 2s)$ for $i \geq 2$, and $f_0 = f_1 = 1$. Defining $\tilde{\beta}_i = \frac{\beta_i}{f_i(s)\, B^{(d)}(s)}$, we have:

$$\tilde{\beta}_0(s) = 1,$$
$$\tilde{\beta}_1(s) = \frac{d+2s-3}{s},$$
$$\tilde{\beta}_2(s) = \frac{-ds+2d+s^2+9s-10}{6s^2},$$
$$\tilde{\beta}_3(s) = \frac{-d+s+7}{6s^2},$$
$$\tilde{\beta}_4(s) = \frac{5d^2s^2-18d^2s-8d^2-10ds^3-92ds^2+256ds+128d+5s^4+98s^3+439s^2-878s-504}{360s^4},$$
$$\tilde{\beta}_5(s) = \frac{5d^2s+2d^2-10ds^2-92ds-40d+5s^3+78s^2+415s+198}{360s^4},$$
$$\tilde{\beta}_6(s) = \frac{1}{45360s^6}(-123552+34464d-3168d^2+96d^3-234804s+72052ds-7212d^2s$$
$$+236d^3s-109336s^2+40392ds^2-4632d^2s^2+168d^3s^2+43179s^3-11245ds^3$$
$$+1029d^2s^3-35d^3s^3+12101s^4-2310ds^4+105d^2s^4+1113s^5-105ds^5+35s^6),$$
$$\tilde{\beta}_7(s) = \frac{1}{45360s^6}(34320-8048d+624d^2-16d^3+73994s-18630ds+1542d^2s-42d^3s+53337s^2$$
$$s^2-14269ds^2+1239d^2s^2-35d^3s^2+10211s^3-2100ds^3+105d^2s^3+903s^4-105ds^4+35s^5),$$
$$\tilde{\beta}_8(s) = \frac{1}{5443200s^8}(-42007680+12321792d-1343232d^2+64512d^3-1152d^4-87960336s+27656320ds$$
$$-3213536d^2s+163712d^3s-3088d^4s-59460172s^2+20886368ds^2-2661416d^2s^2+146592d^3s^2$$
$$-2956d^4s^2-10965924s^3+4957488ds^3-741256d^2s^3+45392d^3s^3-980d^4s^3+4486383s^4-1261624ds^4$$
$$+139106d^2s^4-7560d^3s^4+175d^4s^4+1303560s^5-322692ds^5+26040d^2s^5$$

$$
\begin{aligned}
&- 700d^3s^5 + 144174s^6 - 25480ds^6 + 1050d^2s^6 + 7980s^7 - 700ds^7 + 175s^8),\\
&\tilde{\beta}_9(s) = \frac{1}{5443200s^8}(9069840 - 2313216d + 219744d^2 - 9216d^3 + 144d^4 + 20819508s\\
&- 5610880ds + 561208d^2s - 24704d^3s + 404d^4s + 17535364s^2 - 5035616ds^2\\
&s^2 + 532440d^2s^2 - 24608d^3s^2 + 420d^4s^2 + 6986383s^3 - 2071304ds^3 + 223106d^2s^3\\
&- 10360d^3s^3 + 175d^4s^3 + 1226296s^4 - 314292ds^4 + 26040d^2s^4 - 700d^3s^4\\
&+ 118414s^5 - 22680ds^5 + 1050d^2s^5 + 6580s^6 - 700ds^6 + 175s^7).
\end{aligned}
$$

Appendix C.

Details on the numerics of chapter 4

For the results presented in this chapter, we chose to remain within the realm of linear programming, for which we employ the commercial solver MOSEK, under free academic license, utilizing its implementation in MATHEMATICA and a `python` interface provided by the CVXPY package [218, 219]. As an alternative, we explored and used the functionalities of "SoPlex" [220]; in particular, its capability to derive exact solutions based on rational numbers.

During the development, we tried many numerical strategies, including quadratic/conic optimization. The quadratic/conic problems corresponded to a class of problems where we minimize crossing, instead of mini-/maximizing observables. For instance, we would define an objective function as $\mathcal{O} = \sum_{i\in\text{points}}(A^N(s_i,t_i) - A^N(t_i,s_i))^2$ and minimize it.

Compared to the current implementation based on uniform ratios as in eq. (4.38), minimizing the crossing equation itself turned out to come with major drawbacks: *(i)* Even though a conic formulation of a quadratic problem improves the numerical performance of the solver, round-off errors can prevent the algorithm from initializing properly (spurious negative eigenvalues); *(ii)* Imposing crossing in terms of the objective function above with measure 1 introduces many useless constraints whenever and wherever the MR ansatz decays exponentially. In particular, the region R_1 for large $|s|, |t|$ does not add much information to the problem; *(iii)* Along the same lines, adding points in R_3 is very delicate since the MR ansatz grows exponentially with s and t. Picking suitable points leads to a very tailored problem without sufficient flexibility. Eventually, our strategy does essentially the same thing, while remaining within linear programming, hence being much faster.

The main limitation of MOSEK is that it only works with double point precision, which for us means that $N_{\text{traj}} = 7$ is the last reliable number of trajectories. SoPlex allows us to extend this limitation to an even larger number of trajectories of $N_{\text{traj}} \sim 10$. In contrast to MOSEK, SoPlex exhibits a substantial increase in computation time for such numbers of trajectories ($\sim$ 8h for ten trajectories) rendering quick exploratory work nearly infeasible. While it technically enables us to work with arbitrary precision via rationalizing the constraints, we experienced SoPlex to struggle with either a large number of parameters or small tolerances $\epsilon < 10^{-7}$ that both inevitably occur for large N_{traj}. The problem seems to be connected to the fact that some internal computations are still based on floating point numbers, which are rationalized in each iteration step.

Finally, we routinely used SDPb during the development of the project, but the large number of constraints which we processed induced a slowdown in speed not adapted to the exploratory work. For the future, if we want to bootstrap more precisely specific amplitudes,

we will need to include more trajectories and hence work with arbitrary precision. For this, and given the issues with SoPlex, SDPB will be a very serious option.

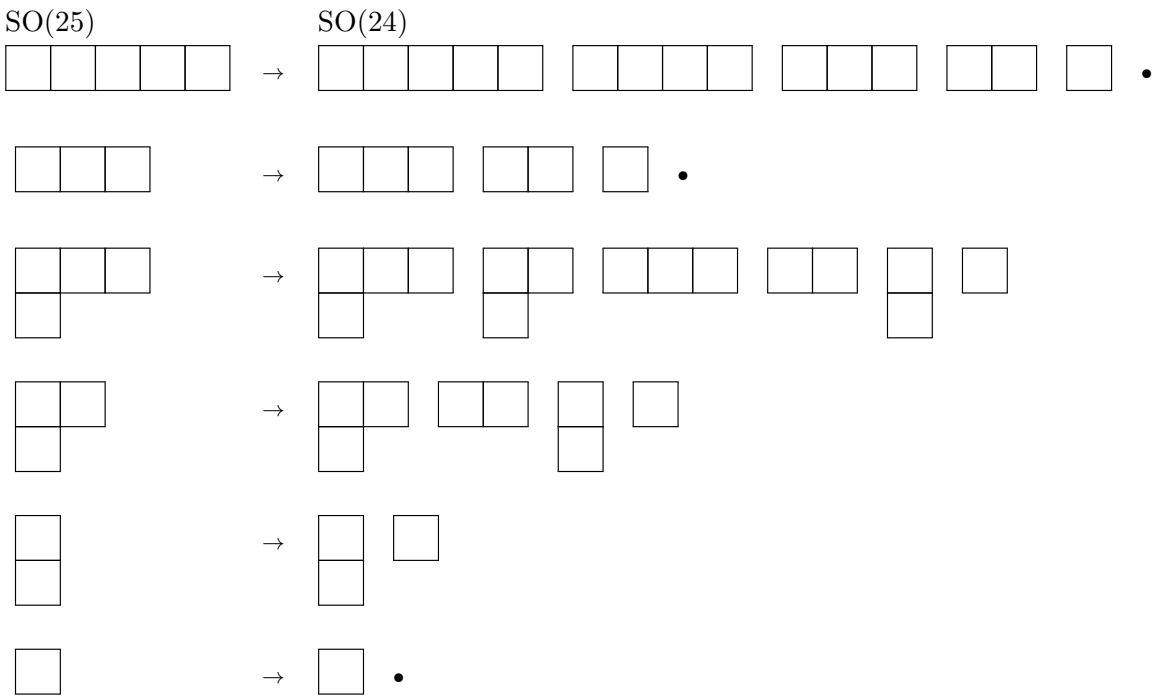
Appendix D.

Open string one-particle states

In this appendix we provide the one-particle states in the first eight levels for the open bosonic string.

D.1. Level 5

At level five we also provide how each one-particle state decomposes in $SO(24)$ representations, and give explicitly the oscillator structures forming the different components of the fully symmetric, rank 5 tensor state in the leading trajectory as an example of oscillator decompositions.



The $SO(24)$ structures forming the leading Regge $SO(25)$ multiplets are the following:


$= \alpha^i_{-1}\alpha^j_{-1}\alpha^k_{-1}\alpha^l_{-1}\alpha^m_{-1},$


$= \alpha^{(i}_{-2}\alpha^j_{-1}\alpha^k_{-1}\alpha^{l)}_{-1},$

$$\square\square\square_{24} = \alpha^i_{-1}\alpha^j_{-1}\alpha^k_{-1}\,\mathrm{Tr}(\alpha_{-1}\cdot\alpha_{-1}) + \frac{60}{7}\alpha^i_{-1}\alpha^j_{-2}\alpha^k_{-2} + \frac{90}{7}\alpha^i_{-3}\alpha^j_{-1}\alpha^k_{-1},$$

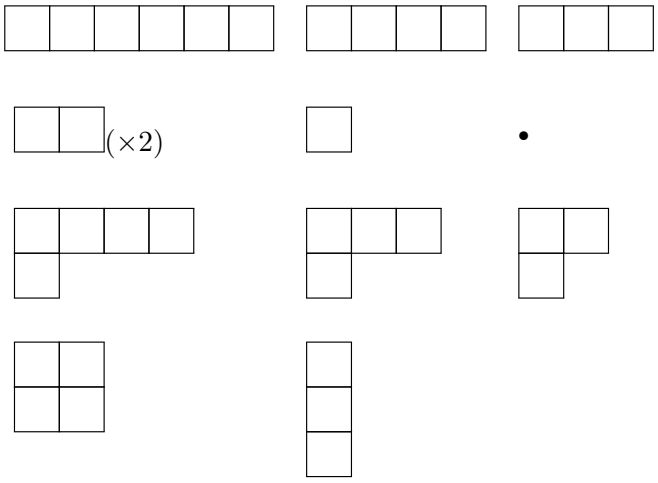
$$\square\square_{24} = \alpha^i_{-1}\alpha^j_{-1}\,\mathrm{Tr}(\alpha_{-1}\cdot\alpha_{-2}) + \frac{9}{32}\alpha^{(i}_{-2}\alpha^{j)}_{-1}\,\mathrm{Tr}(\alpha_{-1}\cdot\alpha_{-1}) + \frac{63}{13}\alpha^{(i}_{-3}\alpha^{j)}_{-2} + 7\alpha^{(i}_{-4}\alpha^{j)}_{-1},$$

$$\square_{24} = \alpha^i_{-1}(\mathrm{Tr}(\alpha_{-1}\cdot\alpha_{-1}))^2 + \frac{1008}{11}\alpha^i_{-1}\,\mathrm{Tr}(\alpha_{-2}\cdot\alpha_{-2}) + \frac{3136}{33}\alpha^i_{-2}\,\mathrm{Tr}(\alpha_{-2}\cdot\alpha_{-1}) +$$
$$\frac{1932}{11}\alpha^i_{-1}\,\mathrm{Tr}(\alpha_{-3}\cdot\alpha_{-1}) + \frac{420}{11}\alpha^i_{-3}\,\mathrm{Tr}(\alpha_{-1}\cdot\alpha_{-1}) + \frac{45500}{33}\alpha^i_{-5},$$

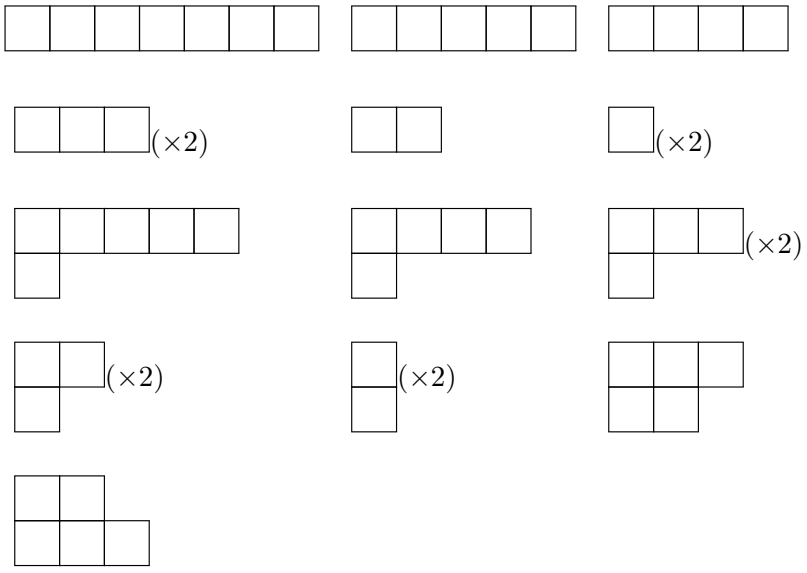
$$\bullet_{24} = \mathrm{Tr}(\alpha_{-2}\cdot\alpha_{-1})\,\mathrm{Tr}(\alpha_{-1}\cdot\alpha_{-1}) + \frac{3042}{55}\,\mathrm{Tr}(\alpha_{-3}\cdot\alpha_{-2}) + \frac{2912}{55}\,\mathrm{Tr}(\alpha_{-4}\cdot\alpha_{-1}).$$

D.2. Level 6

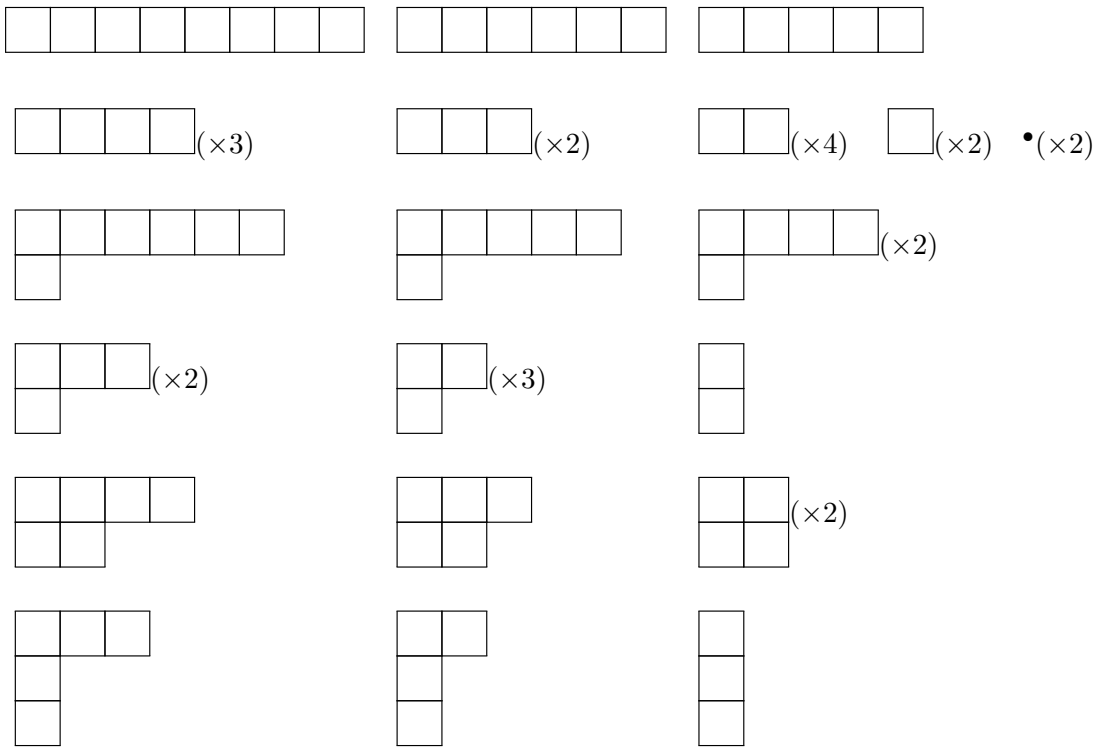
From now on we restrict to showing only the one-particle states at each given level, namely the irreducible representations of $SO(25)$.



D.3. Level 7



D.4. Level 8



Bibliography

[1] F. Figueroa and P. Tourkine, *Unitarity and Low Energy Expansion of the Coon Amplitude*, *Phys. Rev. Lett.* **129** (2022) 121602, [2201.12331].

[2] C. Eckner, F. Figueroa and P. Tourkine, *The Regge bootstrap, from linear to non-linear trajectories*, 2401.08736.

[3] C. Eckner, F. Figueroa and P. Tourkine, *On the number of Regge trajectories for dual amplitudes*, 2405.21057.

[4] G. F. Chew, *S-Matrix Theory of Strong Interactions without Elementary Particles*, *Rev. Mod. Phys.* **34** (1962) 394–401.

[5] G. Breit and E. Wigner, *Capture of slow neutrons*, *Phys. Rev.* **49** (Apr, 1936) 519–531.

[6] A. Cappelli, E. Castellani, F. Colomo and P. Di Vecchia, eds., *The birth of string theory*. Cambridge Univ. Press, Cambridge, UK, 5, 2012.

[7] R. Dolen, D. Horn and C. Schmid, *Finite energy sum rules and their application to pi N charge exchange*, *Phys. Rev.* **166** (1968) 1768–1781.

[8] G. Veneziano, *Construction of a crossing - symmetric, Regge behaved amplitude for linearly rising trajectories*, *Nuovo Cim. A* **57** (1968) 190–197.

[9] H.-M. Chan, *A generalised veneziano model for the n-point function*, *Phys. Lett. B* **28** (1969) 425–428.

[10] Z. Koba and H. B. Nielsen, *Reaction amplitude for n mesons: A Generalization of the Veneziano-Bardakci-Ruegg-Virasora model*, *Nucl. Phys. B* **10** (1969) 633–655.

[11] J. A. Shapiro, *Narrow-resonance model with regge behavior for pi pi scattering*, *Phys. Rev.* **179** (1969) 1345–1353.

[12] J. A. Shapiro, *Electrostatic analog for the virasoro model*, *Phys. Lett. B* **33** (1970) 361–362.

[13] C. Lovelace, *A novel application of regge trajectories*, *Phys. Lett. B* **28** (1968) 264–268.

[14] M. A. Virasoro, *Alternative constructions of crossing-symmetric amplitudes with regge behavior*, *Phys. Rev.* **177** (1969) 2309–2311.

[15] L. Susskind, *Dual symmetric theory of hadrons. 1.*, *Nuovo Cim. A* **69** (1970) 457–496.

[16] T. Goto, *Relativistic quantum mechanics of one-dimensional mechanical continuum and subsidiary condition of dual resonance model*, *Prog. Theor. Phys.* **46** (1971) 1560–1569.

[17] A. Neveu and J. H. Schwarz, *Factorizable dual model of pions*, *Nucl. Phys. B* **31** (1971) 86–112.

[18] P. Goddard, J. Goldstone, C. Rebbi and C. B. Thorn, *Quantum dynamics of a massless relativistic string*, *Nucl. Phys. B* **56** (1973) 109–135.

[19] M. Breidenbach, J. I. Friedman, H. W. Kendall, E. D. Bloom, D. H. Coward, H. DeStaebler et al., *Observed behavior of highly inelastic electron-proton scattering*, *Phys. Rev. Lett.* **23** (Oct, 1969) 935–939.

[20] H. Fritzsch, M. Gell-Mann and H. Leutwyler, *Advantages of the Color Octet Gluon Picture*, *Phys. Lett. B* **47** (1973) 365–368.

[21] H. D. Politzer, *Reliable Perturbative Results for Strong Interactions?*, *Phys. Rev. Lett.* **30** (1973) 1346–1349.

[22] D. J. Gross and F. Wilczek, *Ultraviolet behavior of non-abelian gauge theories*, *Phys. Rev. Lett.* **30** (Jun, 1973) 1343–1346.

[23] J. Scherk and J. H. Schwarz, *Dual Models for Nonhadrons*, *Nucl. Phys. B* **81** (1974) 118–144.

[24] G. 't Hooft, *A Planar Diagram Theory for Strong Interactions*, *Nucl. Phys. B* **72** (1974) 461.

[25] J. M. Maldacena, *The Large N limit of superconformal field theories and supergravity*, *Adv. Theor. Math. Phys.* **2** (1998) 231–252, [hep-th/9711200].

[26] S. S. Gubser, I. R. Klebanov and A. M. Polyakov, *Gauge theory correlators from noncritical string theory*, *Phys. Lett. B* **428** (1998) 105–114, [hep-th/9802109].

[27] D. J. Gross and H. Ooguri, *Aspects of large N gauge theory dynamics as seen by string theory*, *Phys. Rev. D* **58** (1998) 106002, [hep-th/9805129].

[28] J. Polchinski and M. J. Strassler, *The String dual of a confining four-dimensional gauge theory*, hep-th/0003136.

[29] J. Polchinski and M. J. Strassler, *Hard scattering and gauge / string duality*, *Phys. Rev. Lett.* **88** (2002) 031601, [hep-th/0109174].

[30] M. F. Paulos, J. Penedones, J. Toledo, B. C. van Rees and P. Vieira, *The S-matrix bootstrap. Part I: QFT in AdS*, *JHEP* **11** (2017) 133, [1607.06109].

[31] M. F. Paulos, J. Penedones, J. Toledo, B. C. van Rees and P. Vieira, *The S-matrix bootstrap II: two dimensional amplitudes*, *JHEP* **11** (2017) 143, [1607.06110].

[32] M. F. Paulos, J. Penedones, J. Toledo, B. C. van Rees and P. Vieira, *The S-matrix bootstrap. Part III: higher dimensional amplitudes*, *JHEP* **12** (2019) 040, [1708.06765].

[33] A. Homrich, J. a. Penedones, J. Toledo, B. C. van Rees and P. Vieira, *The S-matrix Bootstrap IV: Multiple Amplitudes*, *JHEP* **11** (2019) 076, [1905.06905].

[34] R. Rattazzi, V. S. Rychkov, E. Tonni and A. Vichi, *Bounding scalar operator dimensions in 4D CFT*, *JHEP* **12** (2008) 031, [0807.0004].

[35] R. Rattazzi, S. Rychkov and A. Vichi, *Bounds in 4D Conformal Field Theories with Global Symmetry*, *J. Phys. A* **44** (2011) 035402, [1009.5985].

[36] S. El-Showk, M. F. Paulos, D. Poland, S. Rychkov, D. Simmons-Duffin and A. Vichi,

Solving the 3D Ising Model with the Conformal Bootstrap, *Phys. Rev. D* **86** (2012) 025022, [1203.6064].

[37] S. El-Showk and M. F. Paulos, *Bootstrapping Conformal Field Theories with the Extremal Functional Method*, *Phys. Rev. Lett.* **111** (2013) 241601, [1211.2810].

[38] F. Kos, D. Poland and D. Simmons-Duffin, *Bootstrapping Mixed Correlators in the 3D Ising Model*, *JHEP* **11** (2014) 109, [1406.4858].

[39] S. Caron-Huot, Z. Komargodski, A. Sever and A. Zhiboedov, *Strings from Massive Higher Spins: The Asymptotic Uniqueness of the Veneziano Amplitude*, *JHEP* **10** (2017) 026, [1607.04253].

[40] G. Veneziano, S. Yankielowicz and E. Onofri, *A model for pion-pion scattering in large-N QCD*, *JHEP* **04** (2017) 151, [1701.06315].

[41] N. Geiser and L. W. Lindwasser, *Properties of infinite product amplitudes: Veneziano, Virasoro, and Coon*, *JHEP* **12** (2022) 112, [2207.08855].

[42] J. Chakravarty, P. Maity and A. Mishra, *On the positivity of Coon amplitude in $D = 4$*, *JHEP* **10** (2022) 043, [2208.02735].

[43] C. Cheung and G. N. Remmen, *Veneziano variations: how unique are string amplitudes?*, *JHEP* **01** (2023) 122, [2210.12163].

[44] N. Geiser and L. W. Lindwasser, *Generalized Veneziano and Virasoro amplitudes*, *JHEP* **04** (2023) 031, [2210.14920].

[45] C. B. Jepsen, *Adelic amplitudes and intricacies of infinite products*, *Nucl. Phys. B* **987** (2023) 116094, [2211.01611].

[46] R. Bhardwaj, S. De, M. Spradlin and A. Volovich, *On unitarity of the Coon amplitude*, *JHEP* **08** (2023) 082, [2212.00764].

[47] C. Cheung and G. N. Remmen, *Stringy dynamics from an amplitudes bootstrap*, *Phys. Rev. D* **108** (2023) 026011, [2302.12263].

[48] C. B. Jepsen, *Cutting the Coon amplitude*, *JHEP* **06** (2023) 114, [2303.02149].

[49] R. Bhardwaj and S. De, *Dual resonant amplitudes from Drinfel'd twists*, 2309.07214.

[50] K. C. Rigatos, *Positivity of the hypergeometric Veneziano amplitude*, *Phys. Rev. D* **109** (2024) 086008, [2310.12207].

[51] N. Geiser, *The Baker-Coon-Romans N-point amplitude and an exact field theory limit of the Coon amplitude*, 2311.04130.

[52] K. C. Rigatos and B. Wang, *Coon unitarity via partial waves or: how I learned to stop worrying and love the harmonic numbers*, 2401.13031.

[53] B. Wang, *Positivity of the hypergeometric Coon amplitude*, *JHEP* **04** (2024) 143, [2403.00906].

[54] C. Cheung and G. N. Remmen, *Bespoke dual resonance*, *Phys. Rev. D* **108** (2023) 086009, [2308.03833].

[55] R. Bhardwaj, M. Spradlin, A. Volovich and H.-C. Weng, *On Unitarity of Bespoke Amplitudes*, 2406.04410.

[56] C. Cheung, A. Hillman and G. N. Remmen, *A Bootstrap Principle for the Spectrum and Scattering of Strings*, 2406.02665.

[57] C. Cheung, A. Hillman and G. N. Remmen, *Uniqueness Criteria for the Virasoro-Shapiro Amplitude*, 2408.03362.

[58] G. Mansfield and M. Spradlin, *On Unitarity of the Hypergeometric Amplitude*, 2409.09561.

[59] J. Albert and L. Rastelli, *Bootstrapping pions at large N*, *JHEP* **08** (2022) 151, [2203.11950].

[60] J. Albert and L. Rastelli, *Bootstrapping pions at large N. Part II. Background gauge fields and the chiral anomaly*, *JHEP* **09** (2024) 039, [2307.01246].

[61] J. Albert, J. Henriksson, L. Rastelli and A. Vichi, *Bootstrapping mesons at large N: Regge trajectory from spin-two maximization*, 2312.15013.

[62] C. Fernandez, A. Pomarol, F. Riva and F. Sciotti, *Cornering large-N_c QCD with positivity bounds*, *JHEP* **06** (2023) 094, [2211.12488].

[63] T. Ma, A. Pomarol and F. Sciotti, *Bootstrapping the chiral anomaly at large N_c*, *JHEP* **11** (2023) 176, [2307.04729].

[64] Y.-Z. Li, *Effective field theory bootstrap, large-N χPT and holographic QCD*, *JHEP* **01** (2024) 072, [2310.09698].

[65] J. Albert, W. Knop and L. Rastelli, *Where is tree-level string theory?*, 2406.12959.

[66] J. Berman and H. Elvang, *Corners and islands in the S-matrix bootstrap of the open superstring*, *JHEP* **09** (2024) 076, [2406.03543].

[67] J. Berman, H. Elvang and A. Herderschee, *Flattening of the EFT-hedron: supersymmetric positivity bounds and the search for string theory*, *JHEP* **03** (2024) 021, [2310.10729].

[68] L.-Y. Chiang, Y.-t. Huang and H.-C. Weng, *Bootstrapping string theory EFT*, *JHEP* **05** (2024) 289, [2310.10710].

[69] K. Häring and A. Zhiboedov, *The Stringy S-matrix Bootstrap: Maximal Spin and Superpolynomial Softness*, 2311.13631.

[70] A. P. Saha and A. Sinha, *Field Theory Expansions of String Theory Amplitudes*, *Phys. Rev. Lett.* **132** (2024) 221601, [2401.05733].

[71] R. J. Eden, P. V. Landshoff, D. I. Olive and J. C. Polkinghorne, *The analytic S-matrix*. Cambridge Univ. Press, Cambridge, 1966.

[72] M. Correia, A. Sever and A. Zhiboedov, *An analytical toolkit for the S-matrix bootstrap*, *JHEP* **03** (2021) 013, [2006.08221].

[73] G. Sommer, *Present state of rigorous analytic properties of scattering amplitudes*, *Fortsch. Phys.* **18** (1970) 577–688.

[74] H. Lehmann, *Analytic properties of scattering amplitudes in two variables in general quantum field theory*, *Commun. Math. Phys.* **2** (1966) 375–383.

[75] J. Bros, H. Epstein and V. J. Glaser, *Some rigorous analyticity properties of the four-point function in momentum space*, *Nuovo Cim.* **31** (1964) 1265–1302.

[76] S. Mandelstam, *Some rigorous analytic properties of transition amplitudes*, *Il Nuovo Cimento (1955-1965)* **15** (1960) 658–685.

[77] A. Martin, *Extension of the axiomatic analyticity domain of scattering amplitudes by unitarity. 1.*, *Nuovo Cim. A* **42** (1965) 930–953.

[78] M. Froissart, *Asymptotic behavior and subtractions in the Mandelstam representation*, *Phys. Rev.* **123** (1961) 1053–1057.

[79] K. Häring and A. Zhiboedov, *Gravitational Regge bounds*, *SciPost Phys.* **16** (2024) 034, [2202.08280].

[80] D. Simmons-Duffin, *A Semidefinite Program Solver for the Conformal Bootstrap*, *JHEP* **06** (2015) 174, [1502.02033].

[81] L. Córdova and P. Vieira, *Adding flavour to the S-matrix bootstrap*, *JHEP* **12** (2018) 063, [1805.11143].

[82] L. Córdova, Y. He, M. Kruczenski and P. Vieira, *The O(N) S-matrix Monolith*, *JHEP* **04** (2020) 142, [1909.06495].

[83] Y. He, A. Irrgang and M. Kruczenski, *A note on the S-matrix bootstrap for the 2d O(N) bosonic model*, *JHEP* **11** (2018) 093, [1805.02812].

[84] J. Elias Miro, A. Guerrieri and M. A. Gumus, *Bridging positivity and S-matrix bootstrap bounds*, *JHEP* **05** (2023) 001, [2210.01502].

[85] H. Chen, A. L. Fitzpatrick and D. Karateev, *Nonperturbative bounds on scattering of massive scalar particles in $d \geq 2$*, *JHEP* **12** (2022) 092, [2207.12448].

[86] A. Hebbar, D. Karateev and J. Penedones, *Spinning S-matrix bootstrap in 4d*, *JHEP* **01** (2022) 060, [2011.11708].

[87] P. Tourkine and A. Zhiboedov, *Scattering from production in 2d*, *JHEP* **07** (2021) 228, [2101.05211].

[88] P. Tourkine and A. Zhiboedov, *Scattering amplitudes from dispersive iterations of unitarity*, *JHEP* **11** (2023) 005, [2303.08839].

[89] J. Elias Miró, A. L. Guerrieri, A. Hebbar, J. a. Penedones and P. Vieira, *Flux Tube S-matrix Bootstrap*, *Phys. Rev. Lett.* **123** (2019) 221602, [1906.08098].

[90] F. Acanfora, A. Guerrieri, K. Häring and D. Karateev, *Bounds on scattering of neutral Goldstones*, *JHEP* **03** (2024) 028, [2310.06027].

[91] K. Häring, A. Hebbar, D. Karateev, M. Meineri and J. a. Penedones, *Bounds on photon scattering*, 2211.05795.

[92] A. Gaikwad, V. Gorbenko and A. L. Guerrieri, *QCD worldsheet axion from the bootstrap*, *JHEP* **01** (2024) 090, [2310.20698].

[93] A. L. Guerrieri, J. Penedones and P. Vieira, *S-matrix bootstrap for effective field theories: massless pions*, *JHEP* **06** (2021) 088, [2011.02802].

[94] A. L. Guerrieri, J. Penedones and P. Vieira, *Bootstrapping QCD Using Pion Scattering Amplitudes*, *Phys. Rev. Lett.* **122** (2019) 241604, [1810.12849].

[95] Y. He and M. Kruczenski, *Gauge Theory Bootstrap: Pion amplitudes and low energy parameters*, 2403.10772.

[96] A. Guerrieri, J. Penedones and P. Vieira, *Where Is String Theory in the Space of Scattering Amplitudes?*, *Phys. Rev. Lett.* **127** (2021) 081601, [2102.02847].

[97] A. Guerrieri, H. Murali, J. Penedones and P. Vieira, *Where is M-theory in the space of scattering amplitudes?*, *JHEP* **06** (2023) 064, [2212.00151].

[98] D. Karateev, S. Kuhn and J. a. Penedones, *Bootstrapping Massive Quantum Field Theories*, *JHEP* **07** (2020) 035, [1912.08940].

[99] Y. He and M. Kruczenski, *Bootstrapping gauge theories*, 2309.12402.

[100] L. Cordova, M. Correia, A. Georgoudis and A. Vuignier, *The O(N) monolith reloaded: sum rules and Form Factor Bootstrap*, *JHEP* **01** (2024) 093, [2311.03031].

[101] S. Caron-Huot and V. Van Duong, *Extremal Effective Field Theories*, *JHEP* **05** (2021) 280, [2011.02957].

[102] L. Alberte, C. de Rham, S. Jaitly and A. J. Tolley, *QED positivity bounds*, *Phys. Rev. D* **103** (2021) 125020, [2012.05798].

[103] N. Arkani-Hamed, T.-C. Huang and Y.-t. Huang, *The EFT-Hedron*, *JHEP* **05** (2021) 259, [2012.15849].

[104] S. Caron-Huot, D. Mazac, L. Rastelli and D. Simmons-Duffin, *Sharp boundaries for the swampland*, *JHEP* **07** (2021) 110, [2102.08951].

[105] Z. Bern, D. Kosmopoulos and A. Zhiboedov, *Gravitational effective field theory islands, low-spin dominance, and the four-graviton amplitude*, *J. Phys. A* **54** (2021) 344002, [2103.12728].

[106] J. Henriksson, B. McPeak, F. Russo and A. Vichi, *Rigorous bounds on light-by-light scattering*, *JHEP* **06** (2022) 158, [2107.13009].

[107] S. D. Chowdhury, K. Ghosh, P. Haldar, P. Raman and A. Sinha, *Crossing Symmetric Spinning S-matrix Bootstrap: EFT bounds*, *SciPost Phys.* **13** (2022) 051, [2112.11755].

[108] B. Bellazzini, M. Riembau and F. Riva, *IR side of positivity bounds*, *Phys. Rev. D* **106** (2022) 105008, [2112.12561].

[109] S. Caron-Huot, Y.-Z. Li, J. Parra-Martinez and D. Simmons-Duffin, *Causality constraints on corrections to Einstein gravity*, *JHEP* **05** (2023) 122, [2201.06602].

[110] B. Bellazzini, G. Isabella, S. Ricossa and F. Riva, *Massive gravity is not positive*, *Phys. Rev. D* **109** (2024) 024051, [2304.02550].

[111] C. Beadle, G. Isabella, D. Perrone, S. Ricossa, F. Riva and F. Serra, *Non-Forward UV/IR Relations*, 2407.02346.

[112] F. Bertucci, J. Henriksson, B. McPeak, S. Ricossa, F. Riva and A. Vichi, *Positivity Bounds on Massive Vectors*, 2402.13327.

[113] S. Boyd and L. Vandenberghe, *Convex Optimization*. Cambridge University Press, 3, 2004, 10.1017/cbo9780511804441.

[114] Y. He and M. Kruczenski, *S-matrix bootstrap in 3+1 dimensions: regularization and dual convex problem*, *JHEP* **08** (2021) 125, [2103.11484].

[115] A. L. Guerrieri, A. Homrich and P. Vieira, *Dual S-matrix bootstrap. Part I. 2D theory*, *JHEP* **11** (2020) 084, [2008.02770].

[116] A. Guerrieri and A. Sever, *Rigorous Bounds on the Analytic S Matrix*, *Phys. Rev. Lett.* **127** (2021) 251601, [2106.10257].

[117] J. Elias Miró and A. Guerrieri, *Dual EFT bootstrap: QCD flux tubes*, *JHEP* **10** (2021) 126, [2106.07957].

[118] A. L. Guerrieri, A. Hebbar and B. C. van Rees, *Constraining Glueball Couplings*, 2312.00127.

[119] J. Elias Miro, A. L. Guerrieri and M. A. Gumus, *Extremal Higgs couplings*, *Phys. Rev. D* **110** (2024) 016007, [2311.09283].

[120] G. Veneziano, *An Introduction to Dual Models of Strong Interactions and Their Physical Motivations*, *Phys. Rept.* **9** (1974) 199–242.

[121] D. D. Coon, *Uniqueness of the veneziano representation*, *Phys. Lett. B* **29** (1969) 669–672.

[122] M. Baker and D. D. Coon, *Dual resonance theory with nonlinear trajectories*, *Phys. Rev. D* **2** (1970) 2349–2358.

[123] D. D. Coon, U. P. Sukhatme and J. Tran Thanh Van, *DUALITY AND PROTON PROTON SCATTERING AT ALL ANGLES*, *Phys. Lett. B* **45** (1973) 287–291.

[124] L.-Y. Chiang, Y.-t. Huang, W. Li, L. Rodina and H.-C. Weng, *(Non)-projective bounds on gravitational EFT*, 2201.07177.

[125] J. Maldacena and G. N. Remmen, *Accumulation-point amplitudes in string theory*, *JHEP* **08** (2022) 152, [2207.06426].

[126] I. R. Klebanov, J. M. Maldacena and C. B. Thorn, III, *Dynamics of flux tubes in large N gauge theories*, *JHEP* **04** (2006) 024, [hep-th/0602255].

[127] M. Arik and D. D. Coon, *ABSORPTIVE PARTS AND DOUBLE SPECTRAL FUNCTIONS ASSOCIATED WITH DUAL AMPLITUDES*, *Phys. Lett. B* **48** (1974) 141–144.

[128] D. B. Fairlie and J. Nuyts, *A fresh look at generalized Veneziano amplitudes*, *Nucl. Phys. B* **433** (1995) 26–40, [hep-th/9406043].

[129] D. Amati, M. Ciafaloni and G. Veneziano, *Can Space-Time Be Probed Below the String Size?*, *Phys. Lett. B* **216** (1989) 41–47.

[130] J. Gamboa, C. Ramirez and M. Ruiz-Altaba, *NULL SPINNING STRINGS*, *Nucl.*

Phys. B **338** (1990) 143–187.

[131] F. Lizzi, B. Rai, G. Sparano and A. Srivastava, *Quantization of the Null String and Absence of Critical Dimensions*, *Phys. Lett. B* **182** (1986) 326–330.

[132] A. Karlhede and U. Lindstrom, *The Classical Bosonic String in the Zero Tension Limit*, *Class. Quant. Grav.* **3** (1986) L73–L75.

[133] A. Schild, *Classical Null Strings*, *Phys. Rev. D* **16** (1977) 1722.

[134] E. Casali and P. Tourkine, *On the null origin of the ambitwistor string*, *JHEP* **11** (2016) 036, [1606.05636].

[135] P. Goddard and C. B. Thorn, *Compatibility of the Dual Pomeron with Unitarity and the Absence of Ghosts in the Dual Resonance Model*, *Phys. Lett. B* **40** (1972) 235–238.

[136] N. Arkani-Hamed, L. Eberhardt, Y.-t. Huang and S. Mizera, *On unitarity of tree-level string amplitudes*, *JHEP* **02** (2022) 197, [2201.11575].

[137] D. D. Coon and S. Yu, *Dual Four Point Functions with No Negative Residues*, *Phys. Rev. D* **10** (1974) 3780.

[138] A. Adams, N. Arkani-Hamed, S. Dubovsky, A. Nicolis and R. Rattazzi, *Causality, analyticity and an IR obstruction to UV completion*, *JHEP* **10** (2006) 014, [hep-th/0602178].

[139] K.-G. Schlesinger, *Some remarks on q-deformed multiple polylogarithms*, *arXiv preprint math/0111022* (2001) .

[140] S. Mizera, *Natural boundaries for scattering amplitudes*, *SciPost Phys.* **14** (2023) 101, [2210.11448].

[141] M. Chaichian, J. F. Gomes and P. Kulish, *Operator formalism of q deformed dual string model*, *Phys. Lett. B* **311** (1993) 93–97, [hep-th/9211029].

[142] L. L. Jenkovszky, M. Kibler and A. Mishchenko, *Two parametric quantum deformed dual amplitude*, *Mod. Phys. Lett. A* **10** (1995) 51–60, [hep-th/9407071].

[143] Y. Li and H.-Y. Sun, *Towards α'-finiteness: q-deformed open string amplitude*, 2307.13117.

[144] L. Gonzalez Mestres and R. Hong Tuan, *New Dual n-Point Amplitudes with Logarithmic Trajectories*, *Phys. Rev. D* **13** (1976) 3460.

[145] S. Yu, M. Baker and D. D. Coon, *First and second factorization in a dual multiparticle theory with nonlinear trajectories*, *Phys. Rev. D* **5** (1972) 3108–3121.

[146] D. D. Coon, S. Yu and M. Baker, *Operator formulation of a dual multiparticle theory with nonlinear trajectories*, *Phys. Rev. D* **5** (1972) 1429–1433.

[147] T. Regge, *Introduction to complex orbital momenta*, *Nuovo Cim.* **14** (1959) 951.

[148] F. Bhat, D. Chowdhury, A. P. Saha and A. Sinha, *Bootstrapping string models with entanglement minimization and Machine-Learning*, 2409.18259.

[149] O. Nachtmann, *Pomeron physics and QCD*, in *Ringberg Workshop on New Trends in*

HERA Physics 2003, pp. 253–267, 2004, hep-ph/0312279, DOI.

[150] S. Mandelstam, *An extension of the regge formula*, *Annals of Physics* **19** (1962) 254–261.

[151] D. Atkinson, K. Dietz and J. Honerkamp, *Conditions that must be satisfied by crossing-symmetric finite-energy sum-rules*, *European Physical Journal A* **216** (jun, 1968) 281–292.

[152] P. Nayak, R. R. Poojary and R. M. Soni, *A Note on S-Matrix Bootstrap for Amplitudes with Linear Spectrum*, 1707.08135.

[153] J. E. Mandula and R. C. Slansky, *Misuses of the finite-energy sum rules*, *Phys. Rev. Lett.* **20** (Jun, 1968) 1402–1405.

[154] M. Ademollo, H. R. Rubinstein, G. Veneziano and M. A. Virasoro, *Bootstrap of meson trajectories from superconvergence*, *Phys. Rev.* **176** (1968) 1904–1925.

[155] H. Fujisaki, *Rising regge trajectories and finite energy sum rules*, *Prog. Theor. Phys.* **43** (1970) 101–113.

[156] Z. Komargodski and A. Zhiboedov, *Convexity and Liberation at Large Spin*, *JHEP* **11** (2013) 140, [1212.4103].

[157] A. L. Fitzpatrick, J. Kaplan, D. Poland and D. Simmons-Duffin, *The Analytic Bootstrap and AdS Superhorizon Locality*, *JHEP* **12** (2013) 004, [1212.3616].

[158] S. Pal, J. Qiao and S. Rychkov, *Twist Accumulation in Conformal Field Theory: A Rigorous Approach to the Lightcone Bootstrap*, *Commun. Math. Phys.* **402** (2023) 2169–2214, [2212.04893].

[159] M. K. N. Balasubramanian, R. Patil and A. Rudra, *Spinning amplitudes from scalar amplitudes*, *JHEP* **11** (2021) 151, [2106.05301].

[160] D. Atkinson and K. Dietz, *Infinitely rising regge trajectories and crossing symmetry*, *Phys. Rev.* **177** (1969) 2579–2581.

[161] S. J. Brodsky and G. R. Farrar, *Scaling Laws at Large Transverse Momentum*, *Phys. Rev. Lett.* **31** (1973) 1153–1156.

[162] O. Andreev and W. Siegel, *Quantized tension: Stringy amplitudes with Regge poles and parton behavior*, *Phys. Rev. D* **71** (2005) 086001, [hep-th/0410131].

[163] N. N. Khuri, *Derivation of a veneziano series from the regge representation*, *Phys. Rev.* **185** (1969) 1876–1887.

[164] P. D. B. Collins, *An Introduction to Regge Theory and High Energy Physics*. Cambridge Monographs on Mathematical Physics. Cambridge University Press, 7, 2023, 10.1017/9781009403269.

[165] E. D. Andersen and K. D. Andersen, *The Mosek Interior Point Optimizer for Linear Programming: An Implementation of the Homogeneous Algorithm*, pp. 197–232. Springer US, Boston, MA, 2000.

[166] N. Arkani-Hamed, C. Cheung, C. Figueiredo and G. N. Remmen, *Multiparticle*

Factorization and the Rigidity of String Theory, *Phys. Rev. Lett.* **132** (2024) 091601, [2312.07652].

[167] A. Bose, A. Sinha and S. S. Tiwari, *Selection rules for the S-Matrix bootstrap*, *SciPost Phys.* **10** (2021) 122, [2011.07944].

[168] M. B. Green, J. H. Schwarz and E. Witten, *SUPERSTRING THEORY. VOL. 1: INTRODUCTION*. Cambridge Monographs on Mathematical Physics. 7, 1988.

[169] D. Amati, M. Ciafaloni and G. Veneziano, *Superstring Collisions at Planckian Energies*, *Phys. Lett. B* **197** (1987) 81.

[170] D. J. Gross and P. F. Mende, *String Theory Beyond the Planck Scale*, *Nucl. Phys. B* **303** (1988) 407–454.

[171] D. J. Gross and P. F. Mende, *The High-Energy Behavior of String Scattering Amplitudes*, *Phys. Lett. B* **197** (1987) 129–134.

[172] I. Koh, W. Troost and A. Van Proeyen, *Covariant higher spin vertex operators in the ramond sector*, *Nuclear Physics B* **292** (1987) 201–221.

[173] W.-Z. Feng, D. Lust, O. Schlotterer, S. Stieberger and T. R. Taylor, *Direct Production of Lightest Regge Resonances*, *Nucl. Phys. B* **843** (2011) 570–601, [1007.5254].

[174] M. Bianchi, L. Lopez and R. Richter, *On stable higher spin states in heterotic string theories*, *Journal of High Energy Physics* **2011** (10, 2010) .

[175] W.-Z. Feng and T. R. Taylor, *Higher level string resonances in four dimensions*, *Nuclear Physics B* **856** (2012) 247–277.

[176] K. Benakli, N. Berkovits, C. Daniel and M. Lize, *Higher-spin states of the superstring in an electromagnetic background*, .

[177] D. Lust, C. Markou, P. Mazloumi and S. Stieberger, *A stringy massive double copy*, .

[178] I. Pesando, *The bosonic string spectrum and the explicit states up to level* 10 *from the lightcone and the chaotic behavior of certain string amplitudes*, 2405.09987.

[179] C. Markou and E. Skvortsov, *An excursion into the string spectrum*, *JHEP* **12** (2023) 055, [2309.15988].

[180] T. Basile and C. Markou, *On the deep superstring spectrum*, *JHEP* **07** (2024) 184, [2405.18467].

[181] G. T. Horowitz and J. Polchinski, *A Correspondence principle for black holes and strings*, *Phys. Rev. D* **55** (1997) 6189–6197, [hep-th/9612146].

[182] L. Susskind, *Some speculations about black hole entropy in string theory*, hep-th/9309145.

[183] S. W. Hawking, *Black Holes and Thermodynamics*, *Phys. Rev. D* **13** (1976) 191–197.

[184] J. D. Bekenstein, *Black holes and entropy*, *Phys. Rev. D* **7** (1973) 2333–2346.

[185] M. Firrotta, *The chaotic emergence of thermalization in highly excited string decays*, *JHEP* **04** (2023) 052, [2301.04069].

[186] M. Bianchi, M. Firrotta, J. Sonnenschein and D. Weissman, *Measuring chaos in string scattering processes*, *Phys. Rev. D* **108** (2023) 066006, [2303.17233].

[187] M. Firrotta, *Veneziano and Shapiro-Virasoro amplitudes of arbitrarily excited strings*, *JHEP* **06** (2024) 115, [2402.16183].

[188] M. Bianchi, M. Firrotta, J. Sonnenschein and D. Weissman, *From spectral to scattering form factor*, *JHEP* **06** (2024) 189, [2403.00713].

[189] M. Firrotta, E. Kiritsis and V. Niarchos, *Scattering, Absorption and Emission of Highly Excited Strings*, 2407.16476.

[190] D. J. Gross and V. Rosenhaus, *Chaotic scattering of highly excited strings*, *JHEP* **05** (2021) 048, [2103.15301].

[191] H. Elvang and Y.-t. Huang, *Scattering Amplitudes in Gauge Theory and Gravity*. Cambridge University Press, 4, 2015.

[192] C. Cheung and D. O'Connell, *Amplitudes and Spinor-Helicity in Six Dimensions*, *JHEP* **07** (2009) 075, [0902.0981].

[193] S. Caron-Huot and D. O'Connell, *Spinor Helicity and Dual Conformal Symmetry in Ten Dimensions*, *JHEP* **08** (2011) 014, [1010.5487].

[194] R. H. Boels and D. O'Connell, *Simple superamplitudes in higher dimensions*, *JHEP* **06** (2012) 163, [1201.2653].

[195] N. Arkani-Hamed, T.-C. Huang and Y.-t. Huang, *Scattering amplitudes for all masses and spins*, *JHEP* **11** (2021) 070, [1709.04891].

[196] S. J. Parke and T. R. Taylor, *An Amplitude for n Gluon Scattering*, *Phys. Rev. Lett.* **56** (1986) 2459.

[197] A. Guevara, A. Ochirov and J. Vines, *Black-hole scattering with general spin directions from minimal-coupling amplitudes*, *Phys. Rev. D* **100** (2019) 104024, [1906.10071].

[198] N. Arkani-Hamed, Y.-t. Huang and D. O'Connell, *Kerr black holes as elementary particles*, *JHEP* **01** (2020) 046, [1906.10100].

[199] L. Cangemi and P. Pichini, *Classical limit of higher-spin string amplitudes*, *JHEP* **06** (2023) 167, [2207.03947].

[200] S. Weinberg, *The Quantum theory of fields. Vol. 1: Foundations*. Cambridge University Press, 6, 2005, 10.1017/CBO9781139644167.

[201] X. Bekaert and N. Boulanger, *The unitary representations of the Poincar\'e group in any spacetime dimension*, *SciPost Phys. Lect. Notes* **30** (2021) 1, [hep-th/0611263].

[202] E. P. Wigner, *On Unitary Representations of the Inhomogeneous Lorentz Group*, *Annals Math.* **40** (1939) 149–204.

[203] N. Yamatsu, *Finite-Dimensional Lie Algebras and Their Representations for Unified Model Building*, 1511.08771.

[204] W. Fulton and J. Harris, *Representation Theory*. Graduate Texts in Mathematics. Springer, New York, 2004, 10.1007/978-1-4612-0979-9.

[205] A. Zee, *Group Theory in a Nutshell for Physicists*. Princeton University Press, USA, 3, 2016.

[206] J.-L. Gervais and B. Sakita, *Functional integral approach to dual resonance theory*, *Phys. Rev. D* **4** (1971) 2291–2308.

[207] C. S. Hsue, B. Sakita and M. A. Virasoro, *Formulation of dual theory in terms of functional integrations*, *Phys. Rev. D* **2** (1970) 2857–2868.

[208] S. Mandelstam, *Interacting String Picture of Dual Resonance Models*, *Nucl. Phys. B* **64** (1973) 205–235.

[209] M. Kaku and K. Kikkawa, *The Field Theory of Relativistic Strings. I. Trees*, *Phys. Rev. D* **10** (1974) 1110.

[210] M. Kaku and K. Kikkawa, *The Field Theory of Relativistic Strings. II. Loops and Pomerons*, *Phys. Rev. D* **10** (1974) 1823–1843.

[211] E. Del Giudice, P. Di Vecchia and S. Fubini, *General properties of the dual resonance model*, *Annals Phys.* **70** (1972) 378–398.

[212] M. Ademollo, E. Del Giudice, P. Di Vecchia and S. Fubini, *Couplings of three excited particles in the dual-resonance model*, *Nuovo Cim. A* **19** (1974) 181–203.

[213] D. Skliros and M. Hindmarsh, *String Vertex Operators and Cosmic Strings*, *Phys. Rev. D* **84** (2011) 126001, [1107.0730].

[214] M. B. Green and J. H. Schwarz, *Supersymmetrical Dual String Theory*, *Nucl. Phys. B* **181** (1981) 502–530.

[215] M. B. Green and J. H. Schwarz, *Supersymmetrical Dual String Theory. 2. Vertices and Trees*, *Nucl. Phys. B* **198** (1982) 252–268.

[216] M. B. Green and J. H. Schwarz, *Supersymmetrical Dual String Theory. 3. Loops and Renormalization*, *Nucl. Phys. B* **198** (1982) 441–460.

[217] A. Sagnotti and M. Taronna, *String Lessons for Higher-Spin Interactions*, *Nucl. Phys. B* **842** (2011) 299–361, [1006.5242].

[218] S. Diamond and S. Boyd, *Cvxpy: A python-embedded modeling language for convex optimization*, *Journal of Machine Learning Research* **17** (2016) 1–5.

[219] A. Agrawal, R. Verschueren, S. Diamond and S. Boyd, *A rewriting system for convex optimization problems*, *Journal of Control and Decision* **5** (09, 2017) .

[220] S. Bolusani, M. Besançon, K. Bestuzheva, A. Chmiela, J. Dionísio, T. Donkiewicz et al., *The scip optimization suite 9.0*, 2024.